UNIVERSITY OF CAPE TOWN

THE RHEOLOGICAL CHARACTERISATION OF NON-NEWTONIAN SLURRIES USING A NOVEL BALANCED BEAM TUBE VISCOMETER

by

PAUL THOMAS SLATTER
B.Sc. (CIV. ENG.) NATAL

A thesis submitted in partial fulfilment of the requirement for the degree of Master of Science in the Department of Civil Engineering, University of Cape Town.

CAPE TOWN
SOUTH AFRICA
September 1986

DECLARATION

I hereby declare that this is my own work except where specific acknowledgement is made, and that it has not been submitted for a degree at any other University.

Signed by candidate

P. T. SLATTER

30 September 1986

DEDICATION

To my parents

who inspired and guided my first thoughts on Nature

ABSTRACT

The novel Balanced Beam Tube Viscometer (BBTV), developed at the University of Cape Town, has been further developed and refined.

Extensive Work has been done in the following areas:

(i) The effective length of the BBTV tubes.

(ii) Interpretation of the data obtained using the BBTV in both the laminar and turbulent flow regimes.

(iii) Comparison with the rotary type viscometer.

Kaolin clay and uranium tailings slimes slurries of different particle size range and concentration have been successfully characterised by yield-pseudoplastic rheologies using the BBTV.

The BBTV is in fact a miniature pipeline and it has been shown that it is capable of producing valid turbulent flow data and indicating the laminar/turbulent transition region in the two tube sizes.

ACKNOWLEDGEMENTS

Associate Professor J.H. Lazarus, for his leadership, enthusiasm and encouragement.

Associate Prof. F.A. Kilner, for his helpful discussions and advice.

Mr A.W. Sive and Mr. M. Hurworth for laying the foundations for this work.

Associate Prof. R.O. Heckroodt and Mr G. Evans for the electron microscope micrographs.

Dr. L. Bayvel and Mr J. Knight for the particle size analyses.

Mrs P. Jordaan for typing this thesis.

My family for their support, encouragement and sacrifices.

Rössing Uranium for material and funds.

Serina Kaolin for material.

The Council of the Cape Technikon for the privilege of study leave.

CONTENTS

Chapter		Page
1	INTRODUCTION	
	1.1 The Hydraulic Transportation of Solids	1.1
	1.2 The Role of Rheology	1.1
	1.3 Rheological Characterisation	1.2
	1.4 The Balanced Beam Tube Viscometer (BBTV)	1.3
2	LITERATURE REVIEW AND THEORY	
	2.1 Introduction	2.1
	2.2 The Newtonian Model	2.1
	2.2.1 Viscosity	2.1
	2.2.2 Limits of applicability of the laws of viscous (laminar) flow	2.2
	2.2.3 The flow of Newtonian fluids in tubes	2.4
	2.3 The Power Law Model	2.6
	2.4 The Yield-Pseudoplastic Model	2.7
	2.5 The Bingham Plastic Model	2.8
	2.6 The Metzner and Reed Generalised Approach	2.9
	2.7 Turbulent Flow of Newtonian Fluids	2.10
	2.8 Turbulent Flow of Non-Newtonian Fluids	2.11
	2.8.1 Torrance	2.11
	2.8.2 Metzner and Reed	2.11
	2.8.3 Nikuradse	2.12
	2.8.4 Hydraulic gradient	2.12
	2.9 Viscometry	2.12
	2.9.1 Tube viscometry	2.13
	2.9.2 Rotational viscometry	2.15
	2.10 Use of Viscometers in Non-Newtonian Slurry Rheology	2.18
	2.10.1 The advantages and disadvantages of each type	2.18
	2.10.2 Previous use of viscometers in non-Newtonian slurry rheology	2.18
	2.11 Conclusion	2.20
3	APPARATUS AND EXPERIMENTAL PROCEDURE	
	3.1 Description of the BBTV	3.1
	3.2 Instrumentation	3.2
	3.2.1 Transducers	3.2
	3.2.2 Data Acquisition Unit	3.3
	3.2.3 HP-75C Computer	3.4
	3.2.4 HP 86 Computer	3.4
	3.3 Calibration Procedure	3.4
	3.3.1 Calibration of load cell	3.5
	3.3.2 Calibration of DP cell	3.6
	3.4 Experimental Procedure	3.7
	3.4.1 Preparation	3.7
	3.4.2 Run	3.8
	3.5 Dumping Procedure	3.11
	3.6 Processing	3.12

4 END EFFECTS IN THE BBTV
- 4.1 Introduction 4.1
- 4.2 Previous Work 4.2
- 4.3 Gravity Head Laminar Flow of Clear Water 4.2
  - 4.3.1 Theory 4.2
  - 4.3.2 Experimental procedure 4.3
  - 4.3.3 Analysis 4.4
  - 4.3.4 Discussion 4.4
- 4.4 Steady State Laminar Flow of Clear Water 4.4
  - 4.4.1 Experimental procedure 4.4
  - 4.4.2 Results 4.5
  - 4.4.3 Discussion 4.5
- 4.5 Correlation of Clear Water Laminar Flow Results 4.5
  - 4.5.1 Estimation of energy losses in the developing flow region 4.5
  - 4.5.2 Correlation using a velocity energy head correction factor 4.6
- 4.6 Kaolin Clay Slurry BBTV Tests 4.6
  - 4.6.1 Experimental procedure 4.6
  - 4.6.2 Results 4.7
  - 4.6.3 Correlation using a velocity energy head correction factor 4.7
- 4.7 Discussion 4.7
- 4.8 Conclusions 4.8

5 RHEOLOGICAL CHARACTERISATION PROCEDURE
- 5.1 Introduction 5.1
- 5.2 Synthetic Data 5.2
- 5.3 Reduction Technique and Results 5.2
- 5.4 Discussion of Reduction Technique 5.3
- 5.5 New Technique 5.4
- 5.6 Illustration of the New Technique 5.5
- 5.7 Conclusion 5.6

6 DESCRIPTION OF MATERIAL TESTED
- 6.1 Test Procedure 6.1
- 6.2 Kaolin 6.1
- 6.3 Uranium Mining Tailings Slimes 6.1
  - 6.3.1 Particle size separation (Uranium tailings) 6.2
  - 6.3.2 Material tested in the BBTV (Uranium tailings) 6.2
  - 6.3.3 Results of solids relative density tests 6.3
  - 6.3.4 Micrographs 6.4

7 EXPERIMENTAL RESULTS AND ANALYSIS
- 7.1 Detailed Experimental Results 7.1
- 7.2 Rheological Characterisation 7.1
- 7.3 Turbulent Flow Data and Predictions 7.1
- 7.4 Critical Reynolds Numbers 7.1

8 ROTARY VISCOMETER
8.1 Introduction 8.1
8.2 The Haake Rotovisco Viscometer 8.2
8.2.1 Physical description 8.2
8.2.2 Operating procedure 8.2
8.2.3 Determination of rheograms for non-Newtonian slurries using a Haake Rotovisco viscometer 8.3
8.3 Experimental Results 8.4
8.4 Rheograms 8.4
8.5 Comparative Rheograms 8.5
8.6 Pipe Flow Predictions 8.5
8.7 Discussion 8.5
8.7.1 Rheological comparisons 8.5
8.7.2 Comparative rheograms 8.5
8.7.3 Pipe Flow predictions 8.6
8.7.4 Thixotropy 8.6
8.8 Conclusion 8.8

9 DISCUSSION OF BBTV EXPERIMENTAL RESULTS AND ANALYSIS
9.1 Observations During Tests - Flow Visualisation 9.1
9.2 Observations from the Pseudo-Shear Diagrams 9.1
9.3 Laminar Flow Predictions 9.2
9.4 Turbulent Flow Predictions 9.2
9.5 Laminar/Turbulent Transition 9.2

10 CONCLUSIONS

REFERENCES

Figures

1.1 Rheological models 1.2
3.1 BBTV Diagrammatic Layout 3.13
3.2 BBTV Photograph 3.13
3.3 Assembly Drawing 3.14
3.4 Load Cell 3.15
3.5 Wheatstone Bridge Circuit 3.15
3.6 DP Cell 3.16
3.7 DP Cell Circuit Diagram 3.16
3.8 DAU and HP-75C Photograph 3.17
3.9 HP-75C Connection Diagram 3.17
3.10 Load Cell Calibration Output 3.18
3.11 DP Cell Calibration Connections 3.19
3.12 DP Cell Calibration Output 3.20
3.13 Tapping Lengths 3.21
3.14 Data File Format 3.22
3.15 A READING in Graphical Form 3.22
3.16 Print Out from a "VISCOPX" Run 3.23
3.17 Processed Data Output as a Pseudo Shear Diagram 3.23
4.1 The hydraulic gradient in a BBTV tube 4.10
4.2 Apparatus for gravity head laminar flow of clear water 4.10
4.3 Experimental results for gravity head laminar flow of clear water 4.11

4.4	Apparatus for steady state laminar flow of clear water	4.12
4.5	Experimental results for steady state laminar flow of clear water	4.12
4.6	The velocity distributions in the inlet of a BBTV tube	4.13
4.7	Correlation using the theory from Goldstein (Ref. 17)	4.13
4.8	Experimental results and correlation for clear water	4.14
4.9	Experimental results for kaolin	4.14
4.10	Velocity energy head correction factor for kaolin plotted on logarithmic axes	4.15
4.11	Velocity energy head correction factor for kaolin plotted on linear axes	4.16
5.1	Tube Flow for a Bingham Plastic - Eq. 5.1 (Logarithmic Axes)	5.7
5.2	Tube Flow for a Yield Pseudo-Plastic - Eq. 5.2 (Logarithmic)	5.7
5.3	Synthetic Data	5.8
5.4	Data Reduction using a First Order Fit	5.9
5.5	Data Reduction using a Second Order Fit	5.10
5.6	Data Reduction using a Third Order Fit	5.11
5.7	Data Reduction using a Fourth Order Fit	5.12
5.8	Data Reduction using a Fifth Order Fit	5.13
5.9	Summary of Errors	5.14
5.10	Best line drawn by hand	5.15
5.11	Results of procedure in graphical form	5.15
6.1	Particle size distribution of the kaolin slurries	6.5
6.2	Micrograph of kaolin particles	6.5
6.3	Particle size distribution of uranium slurries: Slurry 1	6.6
6.4	Particle size distribution of uranium slurries : Slurries 2 & 3	6.6
6.5	Particle size distribution of uranium slurries : Slurry 4	6.7
6.6	Micrographs of uranium particle	6.8
7.1	Rheological Characterisation of Kaolin	7.3
7.2	Rheological Characterisation of Uranium Tailings	7.4
7.3	The rheological constants for kaolin as a function of volumetric concentration	7.5
7.4	The rheological constants for uranium tailings as a function of C_v with maximum particle size as parameter	7.6
7.5	The rheological constants for uranium tailings as a function of maximum particle size with C_v as parameter	7.7
7.6	Flow Predictions : Kaolin	7.8
7.7	Flow Predictions : Uranium Tailings	7.9
8.1	Absolute calibration of the measuring head	8.10
8.2	Spread of rotary viscometer readings on linear axes	8.11
8.3	Spread of rotary viscometer readings on logarithmic axes	8.11
8.4	Rotary viscometer rheograms : kaolin	8.12
8.5	Rotary viscometer rheograms : uranium tailings	8.13
8.6	Comparative rheograms for kaolin	8.14
8.7	Comparative rheograms for uranium tailings	8.15

8.8 Pipe flow predictions for kaolin 8.16
8.9 Pipe flow predictions for uranium tailings 8.17
8.10 Kaolin BBTV Log Standard Error Plots 8.18
8.11 Kaolin Rotary Viscometer Log Standard Error Plots 8.19
8.12 Uranium BBTV Log Standard Error Plots 8.20
8.13 Uranium Rotary Viscometer Log Standard Error Plots 8.21
8.14 Particle size distribution at the inner and outer surface 8.22

Tables

7.1 : Summary of Results 7.2
7.2 : Critical Flow Values 7.2
8.1 : Summary and comparison of viscometer results 8.9
8.2 : Log Standard Error Comparison - BBTV vs. Rotary Viscometer 8.10

NOMENCLATURE

Symbol	Description	Unit
A	cross sectional area	m^2
A'	shear stress constant	Pa/div
C	concentration	%
d	particle diameter	μm
D	internal tube diameter	m
f	Fanning friction factor	
F	factor, function	
h	effective bob height	m
H	height, head	m
i	hydraulic gradient	m/m
k	constant	
K	fluid consistency index	
K'	apparent fluid consistency index	
L	tube length	m
M	mass	kg
n	flow behaviour index	
n'	apparent flow behaviour index	
N	speed of rotation	1/s
p	pressure	Pa
P	static pressure	Pa
Q	volumetric flow rate	m^3/s
r	radius at a point in the tube	m
R	radius	m
Re	Newtonian Reynolds number	
Re_{nn}	non-Newtonian Reynolds number	

s	radius ratio	
S	relative density	
S'	rotary viscometer torque reading	
t	time	s
T	torque	N m
U	rotary viscometer speed setting	
u	point velocity	m/s
v	volume	m^3
V	average slurry velocity	m/s
x	horizontal distance	m
X	abscissa	
Y	ordinate	
α	shear stress ratio	
η_p	plastic viscosity	Pa s
Δ	increment	
θ	angular displacement	radian
μ	dynamic viscosity	Pa s
ρ	density	kg/m^3
τ	shear stress	Pa
τ_y	yield stress	Pa

Subscripts

o	at the tube wall
b	bob
c	cup
m	mixture (slurry)
s	solids
v	volumetric
vess	vessel
w	weight

CHAPTER 1

INTRODUCTION

1.1 THE HYDRAULIC TRANSPORTATION OF SOLIDS

The hydraulic transportation of solids with solids relative density (S_g) significantly greater than unity is a proven technology, with a large number of pipelines in operation today.

However, this technology remains, as yet, relatively unresearched and much refinement of existing design techniques is possible.

Research in this area is extremely complex when compared with ordinary Newtonian pipeline flow. The number of variables rises from five to fourteen (Ref. 1). This may be considered conservative since non-Newtonian rheology requires three variables and these can be affected by other factors such as pH, zeta potential and solids surface texture, in addition to the other fourteen independent parameters.

1.2 THE ROLE OF RHEOLOGY

Rheology (rheos - flow; logos - knowledge) encompasses the science of flow phenomena. Within the context of this thesis, rheology means the viscous characterisation of a fluid.

A relatively simple form of hydraulic transportation would involve the transportation of coarse solids ($d > 1$ mm) turbulently suspended in water. The vehicle portion (carrier fluid) is thus water and the vehicle rheology is that of water.

However, when fine particles ($d < 100$ μm) are present, they modify the vehicle rheology and are not considered part of the suspended "load".

In order to determine the specific power consumption of a hydro-transport application, the vehicle rheology must be known (Ref. 2), and is therefore a fundamental design parameter.

1.3 RHEOLOGICAL CHARACTERISATION

Rheological characterisation involves firstly the measurement of shear stress in a fluid at various shear rates. These results may be plotted as shear stress versus shear rate, called a rheogram.

The rheological model which best fits the data points gives the fluid its rheological character.

Various rheological models are available. The more common ones are shown in Fig. 1.1.

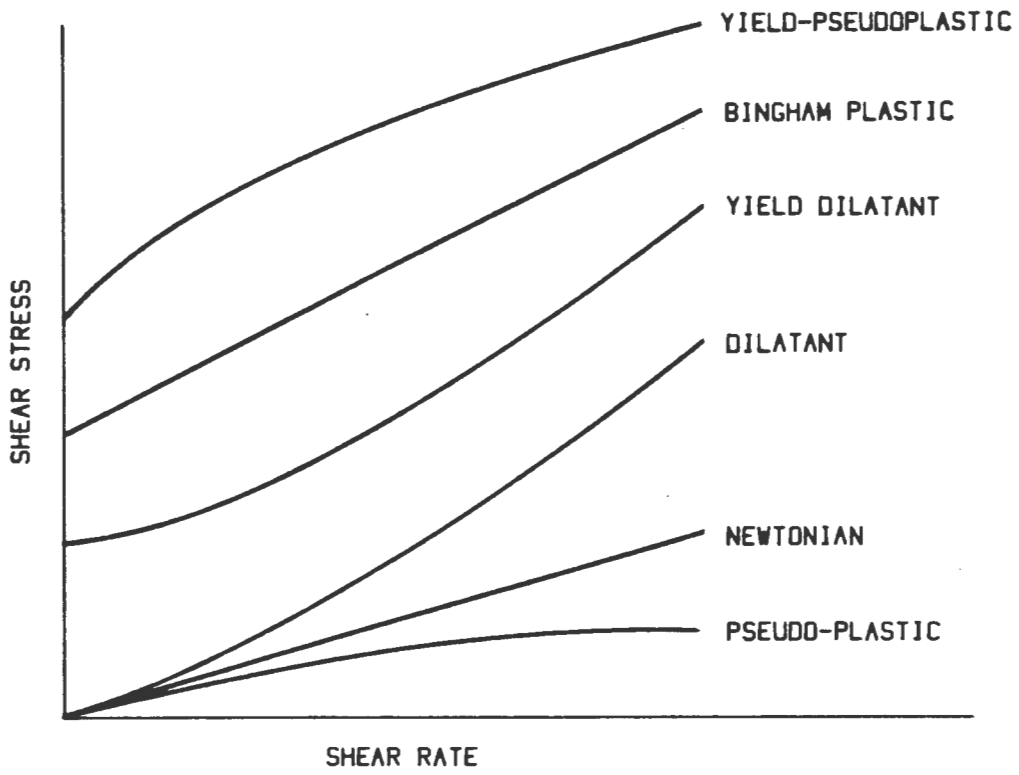

Fig. 1.1 : Rheological Models

The instrument used to measure the shear stress at various shear rates is called a viscometer. There are two types commonly in use, viz. rotational viscometers and tube viscometers.

In the rotational viscometer, the fluid to be tested is introduced into the annular gap between a beaker and a spindle, one of which rotates. The rheology of the fluid can be determined from the resistance to rotation caused by the fluid.

In the tube viscometer, the fluid is forced through a tube. The velocity of the fluid and the pressure drop across a known length of the tube are measured. From this, the shear rate and the accompanying shear stress can be determined.

1.4 THE BALANCED BEAM TUBE VISCOMETER (BBTV)

The BBTV is of the second type and is unique, having been developed at UCT. Detailed descriptions are given in Chapter 3 and Reference 20.

This instrument and its operation has been refined to the point where it yields meaningful and accurate results. The BBTV is, in fact, a miniature pipeline, and its use extends beyond viscometry.

In this thesis, the BBTV has been used to rheologically characterise kaolin clay and uranium mining tailings slurries of various concentrations and particle size distributions, capture turbulent flow data and indicate the laminar/turbulent transition.

Further, the BBTV results have been compared with the results obtained using a conventional rotary type viscometer and an investigation was undertaken into the effective length of the BBTV tubes.

CHAPTER 2

LITERATURE REVIEW AND THEORY

2.1 INTRODUCTION

In its simplest (Newtonian) form, the rheology of a fluid requires only one independent variable which is called viscosity and common liquids such as water and oil fall into this category.

Unfortunately, many fluids used industrially do not fall into this fundamentally simple category, thus necessitating the formulation of the rather more complex rheological models which are shown in Fig. 1.1.

2.2 THE NEWTONIAN MODEL (Ref. 3)

2.2.1 Viscosity

In his Principia of 1687, Sir Isaac Newton made the following hypothesis:

"The resistance which arises from the lack of slipperiness originating in a fluid - other things being equal - is proportional to the velocity by which the parts of the fluid are being separated from each other."

The mathematical formulation of Newton's hypothesis is

$$\tau = \mu \frac{du}{dy} \tag{2.1}$$

where τ is the force exerted by the fluid per unit area of a plane parallel to the direction of motion when the velocity is increasing with the distance y, measured normally to the plane, at the rate $\frac{du}{dy}$. For tube flow, this becomes

$$\tau = \mu\left(-\frac{du}{dr}\right) \tag{2.2}$$

The constant of proportionality, μ, is the coefficient of dynamic viscosity, and was defined by Maxwell (in Ref. 3):

"The coefficient of viscosity of a fluid is the numerical value of the tangential force on unit area of either of two parallel planes at unit distance apart when the space between these planes is filled with the fluid in question and one of the planes moves with unit velocity in its own plane relatively to the other."

2.2.2 Limits of applicability of the laws of viscous (laminar) flow.

The laws of viscous flow deduced from Newton's hypothesis have provided a foundation for the viscometry of the most diverse materials, from gases and mobile liquids like ether to substances like pitch and glass which, though apparently solid, may be shown to flow under very minute shearing forces. It is thus possible to measure and to define in absolute and reproducible units the viscous properties of any system, subject to the conditions laid out below.

2.2.2.1 Reynolds Number and Flow Regimes (Ref. 4)

It is a well known and important fact that the relationship between friction loss and velocity for flow in a pipe depends upon the velocity of flow. For a given pipeline and fluid, when the velocity is below a certain critical value, the flow in the pipe is found to be laminar; when the velocity is above another critical value, the flow is found to be turbulent. The change from laminar to turbulent flow results in a large increase in the flow resistance and also in a change in the way friction loss varies with mean velocity.

These facts came to light as a result of a systematic study of the head losses associated with the flow of water through pipes which was conducted by Osborne Reynolds in 1883. He applied dimensional analysis to this phenomenon of transi-

tion from laminar to turbulent flow and concluded that it occurred at a fixed, critical value (2320) of a dimensionless group, now termed the Reynolds number in his honour, defined as:

$$Re = \frac{\rho VD}{\mu} = \frac{\text{inertial forces}}{\text{viscous forces}}$$

The critical Reynolds number of 2320, however, represents the lower bound, which is obtained when maximum mechanical disturbance occurs upstream from the measured section.

Under ideal conditions, critical Reynolds numbers in the range 30000 to 50000 can be obtained in the metastable laminar regime (Ref. 3).

2.2.2.2 Low Reynolds number effects

Stokes remarked in 1845 (in Ref. 3):

"A fluid admits of a finite but exceedingly small amount of constraint before it will be released from its state of tension by its molecules assuming new positions of equilibrium", but he regarded the constraint as "probably insensible". No evidence of this phenomenon has yet been reported.

2.2.2.3 Application to viscometry

Clearly, turbulent flow is unsuitable for the determination of viscosity, since the resistance offered by the fluid is more nearly proportional to the density than to the viscosity.

Viscosity measurements must therefore be performed at Reynolds numbers less than 2320 in order to ensure laminar flow. In practice this is not possible since the Reynolds number can only be computed once the viscosity is known.

The practical procedure is to obtain readings over a large velocity range, identify the transition region (if any) by the large increase in flow resistance which accompanies the onset of turbulence and then reject turbulent flow readings for viscosity determination purposes.

Low Reynolds number effects may or may not be observed.

2.2.3 The flow of Newtonian Fluids in Tubes (Ref. 3)

The flow of liquids and gases in pipes and channels is an occurrence so common in daily life and of such importance in engineering design that it could hardly fail to engage the attention of scientists as soon as the cardinal principles of physics began to be studied by experiment and analysis. Hydrodynamics attracted the most eminent mathematicians of the eighteenth century, and much careful and practical investigation of the flow of water in pipes was carried out before the middle of the nineteenth century. But the laws governing the large-scale movements of water are of a very complicated nature (turbulent flow) and it was only when attention was directed to the flow of liquids through tubes of very small cross-section that the relatively simple laws of viscous flow could be discovered.

2.2.3.1 Viscous or laminar flow

Although biophysics has made many valuable contributions to general physical science in recent years, it has provided no discovery so fruitful as that announced in 1840 by Poiseuille, professor of physics in the Paris medical schools. With a view to obtaining some understanding of the laws governing the passage of blood through the capillaries by which it is distributed through the body, he instituted a series of researches on the simplest analogue of which he could conceive, namely, the flow of pure water through the fine bores of thermometer tubing. By this simplification, made in accordance with the principles which have so often been adopted in modern experimental science, he was led to discover definite relationships between the rate of flow Q

and (i) the pressure difference Δp between the ends of the tube, (ii) the length L and (iii) the radius R of the tube. The results are summarised in the formula

$$Q = k \frac{R^4 \Delta p}{L} \qquad (2.3)$$

where k is a constant; this empirical result, expressed in this and other forms, is known as Poiseuille's Law. It may be remarked, parenthetically, that the flow of blood through fine capillaries has since been found not to obey this law.

The concept of viscosity had scarcely been developed at this time and Poiseuille went no further than to show that k was a property of the liquid at a given temperature.

The first published deduction of Poiseuille's Law was by Weidemann in 1856, but was given in a more precise form by Hagenbach in 1860.

Using the initial mathematics from Appendix A, assuming no slip at the tube wall and performing the integration in Equation A6 with equation 2.2, it can be shown that

$$Q = \frac{\pi R^4 \Delta p}{8 \mu L} \qquad (2.4)$$

Thus the constant k of Poiseuille's empirical formula is

$$k = \frac{\pi}{8\mu} \qquad (2.5)$$

Poiseuille's Law may be rewritten making use of conventional hydraulic design parameters.

The Fanning friction factor, f, is defined by the Fanning equation (Ref. 5)

$$-\frac{dp}{dL} = \frac{2 f \rho V^2}{D} \qquad (2.6)$$

$$\text{also} \quad f = \frac{2\tau_o}{\rho V^2} \tag{2.7}$$

From (2.6) it can be shown that for laminar flow

$$f = \frac{16}{Re} \tag{2.8}$$

2.3 THE POWER LAW MODEL (Ref, 5, 6 and 7)

In place of the Newtonian hypothesis (Equation 2.2), this model uses the following initial rheological assumption:

$$\tau = K\left(-\frac{du}{dr}\right)^n \tag{2.9}$$

Depending on the value of n, the following rheological models can be described by the power law model

(i)	Pseudo-plastic	$(n < 1)$
(ii)	Newtonian	$(n = 1)$
(iii)	Dilatant	$(n > 1)$

The equations for laminar tube flow may be derived in a manner analogous to the derivation of Poiseuille's Law. A force balance on a cylindrical element of radius r and length dL yields

$$\tau = -\frac{rdp}{2dL} \tag{2.10}$$

Substituting in equation (2.9), we obtain

$$-\frac{du}{dr} = \left(-\frac{1}{2K}\frac{dp}{dL}\right)^{1/n} r^{1/n} \tag{2.11}$$

Integrating this equation and substituting $u = 0$ at $r = R$, we obtain the velocity profile

$$u = \left[\left(-\frac{1}{2K}\frac{dp}{dL}\right)^{1/n}\frac{n}{1+n}\right]\left(R^{(1+n)/n} - r^{(1+n)/n}\right) \tag{2.12}$$

Now $$Q = 2\pi \int_0^R urdr \tag{2.13}$$

from which the equation for the total flow rate is

$$Q = \pi\left(-\frac{1}{2K}\frac{dp}{dL}\right)^{1/n}\left(\frac{n}{1+3n}\right)R^{(1+3n)/n} \tag{2.14}$$

and the average velocity is given by

$$V = \left(-\frac{1}{2K}\frac{dp}{dL}\right)^{1/n}\left(\frac{n}{1+3n}\right)R^{(1+n)/n} \tag{2.15}$$

2.4 THE YIELD-PSEUDOPLASTIC MODEL (Ref. 5)

In order to take account of a yield stress, the following initial rheological assumption applies:

$$\tau - \tau_y = K\left(-\frac{du}{dr}\right)^n \tag{2.16}$$

This is, in fact, a yield power law model (compare with equation (2.9)) and depending on the value of n, the following rheological models can be described by the yield-pseudoplastic model

(i) Yield-pseudoplastic ($n < 1$)
(ii) Bingham plastic ($n = 1$)
(iii) Yield dilatant ($n > 1$)

The equations for laminar tube flow are derived as before:

The velocity gradient is given by

$$-\frac{du}{dr} = \left(\frac{1}{K}\right)^{1/n}\left(-\frac{r}{2}\frac{dp}{dL} - \tau_y\right)^{1/n} \tag{2.17}$$

In this case we observe that, when $\tau = -rdp/2dL \leq \tau_y$, the fluid does not shear and adjacent laminae are stationary relative to one another. This occurs for values of $r \leq r_{plug}$, where

$$r_{plug} = \frac{2\tau_y}{\left(-\frac{dp}{dL}\right)} \tag{2.18}$$

For $R > r > r_{plug}$ the laminae of the fluid are in relative motion and we may integrate equation (2.17). Inserting $u = 0$ when $r = R$, we obtain

$$u = \frac{\left(\frac{1}{K}\right)}{\left(-\frac{dp}{2dL}\right)} \frac{n}{1+n}\left[\left(-\frac{R}{2}\frac{dp}{dL} - \tau_y\right)^{(1+n)/n} - \left(-\frac{r}{2}\frac{dp}{dL} - \tau_y\right)^{(1+n)/n}\right] \tag{2.19}$$

When $0 < r < r_{plug}$ the fluid moves as a plug at a uniform velocity u_{plug}.

We obtain the discharge as the sum of the flow through the sheared region ($R > r > r_{plug}$) and the plug ($r < r_{plug}$) as follows:

$$Q = \int_{r_{plug}}^{R} 2\pi r u dr + \pi r_{plug}^2 u_{plug} \tag{2.20}$$

Setting $\tau_o = \frac{D\Delta p}{4L}$ and integrating to obtain the volumetric discharge and average velocity, we have

$$\frac{16Q}{\pi D^3} = \frac{8V}{D} = \frac{4n}{K^{1/n}\tau_o^3}(\tau_o - \tau_y)^{\frac{1+n}{n}}\left[\frac{(\tau_o-\tau_y)^2}{1+3n} + \frac{2\tau_y(\tau_o-\tau_y)}{1+2n} + \frac{\tau_y^2}{1+n}\right] \tag{2.21}$$

2.5 THE BINGHAM PLASTIC MODEL

The Bingham plastic model is a special (ideal) case of the yield-pseudoplastic model. Setting n=1 and substituting η_p for K

$$\tau - \tau_y = \eta_p\left(-\frac{du}{dr}\right) \tag{2.22}$$

The velocity profile in the sheared region is

$$u = \frac{1}{\eta_p}\left[-\frac{dp}{4dL}\left(R^2 - r^2\right) - \tau_y\left(R - r\right)\right] \tag{2.23}$$

Let $$\alpha = \frac{\tau_y}{\tau_o} \qquad (2.24)$$

Then the average velocity and discharge can be computed using

$$\tau_o = \frac{8V}{D} \cdot \eta_p \cdot \left[\frac{1}{1 - \frac{4}{3}\alpha + \frac{\alpha^4}{3}}\right] \qquad (2.25)$$

This equation was developed by Buckingham in 1921 (Ref. 5).

2.6 THE METZNER AND REED GENERALISED APPROACH

Metzner and Reed (Ref. 8) have developed a generalised approach applicable to the laminar pipe flow of any time-independent fluid, based upon the Rabinowitsch-Mooney relation (see Appendix A).

i.e. $$\left[-\frac{du}{dr}\right]_o = \frac{8V}{D}\left[\frac{3n' + 1}{4n'}\right] \qquad (A1)$$

where $$n' = \frac{d\,(\ell n\, \tau_o)}{d\,(\ell n\, \frac{8V}{D})} \qquad (A2)$$

The coefficient n' is determinable from the slope of a log-log plot of $D\Delta p/4L$ versus $8V/D$ where $\Delta p/L$ is the pressure gradient at a flow velocity V in a pipe or capillary tube of diameter D under laminar flow conditions. The log-log plot itself characterises the rheological properties of the non-Newtonian fluid and may be used directly for pipe scale up or design purposes.

Metzner and Reed carry the approach further by writing the equation

$$\frac{D\Delta p}{4L} = K' \left(\frac{8V}{D}\right)^{n'} \qquad (2.26)$$

which represents the tangent to the logarithmic plot of $D\Delta p/4L$ versus $8V/D$ at any particular value of $D\Delta p/4L$ or $8V/D$. (If the plot is a straight line, then Equation 2.26 is the equation of the line.)

Now if we recall that

$$f = \frac{D\Delta p}{2\rho V^2 L} \tag{2.27}$$

and define a non-Newtonian Reynolds number, Re_{nn} such that

$$f = 16/Re_{nn} \tag{2.28}$$

we may combine Equations (2.27) and (2.28) and substitute $D\Delta p/4L$ from Equation (2.26) to obtain the following solution for Re_{nn}

$$Re_{nn} = \frac{8\rho V^2}{K' \left(\frac{8V}{D}\right)^{n'}} \tag{2.29}$$

2.7 TURBULENT FLOW OF NEWTONIAN FLUIDS (Ref. 5)

From the time of the earliest suggestion by Blasius in 1913, pressure gradient data have been expressed in terms of a friction factor, as defined by equation (2.6) and correlated with the Reynolds number. Over the years the evidence supporting the existence of a single line correlation has mounted; and empirical, graphical representations of data covering a limited range of variables have given way to well confirmed relations applicable to a wide or the full range of the variable. A few of the best such relations are mentioned. The Balsius equation (Blasius, 1913)

$$f = 0{,}079\ Re^{-0{,}25} \tag{2.30}$$

is simple and entirely empirical, but it fits the reliable data to a good degree of accuracy in the range $3\ 000 < Re < 100\ 000$. A number of equations of this type with different values of the constants are in use, such as the following (Knudsen and Katz, 1958):

$$f = 0{,}046\ Re^{-0{,}2} \tag{2.31}$$

These equations are often referrred to as Blasius-type equations.

For the full practical range of turbulent flow, say
3 000<Re<3 000 000, the more complex equation due to Nikuradse (1932) provides an excellent fit to essentially all reliable data.

$$\frac{1}{\sqrt{f}} = 4{,}0 \log (Re \sqrt{f}) - 0{,}40 \qquad (2.32)$$

2.8 TURBULENT FLOW OF NON-NEWTONIAN FLUIDS

Several methods for predicting the energy loss of non-Newtonian fluids in turbulent flow are presented below.

2.8.1 Torrance

According to Torrance (Ref. 9), for a yield-pseudoplastic fluid in turbulent flow, the friction factor (f) can be expressed in terms of the non-Newtonian Reynolds number:

$$(2/f)^{0,5} = \left(\frac{3{,}8}{n} - 4{,}17\right) + \frac{2{,}78}{n} \ell n \left[1 - \frac{\tau_y}{\tau_o}\right]$$

$$+ \frac{2{,}78}{n} \ell n \left[Re_{nn} \sqrt{f^{2-n}}\right] + 0{,}965 \left(5n - \frac{8}{n}\right) \qquad (2.33)$$

where $$Re_{nn} = \frac{8 \rho_m V^2}{K \left(\frac{8V}{D}\right)^n} \qquad (2.34)$$

Note that equation (2.34) is similar to equation (2.29) with K and n substituted for K' and n'.

This equation can be used for power law fluids ($\tau_y = 0$) and Bingham plastics (n = 1).

2.8.2 Metzner and Reed

Using the generalised approach of Metzner and Reed, Dodge and Metzner (in Ref. 5) developed the following

$$\frac{1}{\sqrt{f}} = \frac{4{,}0}{n'^{0,75}} \log \left[Re_{nn} f \left(1 - \frac{n'}{2}\right)\right] - \frac{0{,}40}{n'^{1,2}} \qquad (2.35)$$

with Re_{nn} using K' and n' (equation 2.29).

It is important to note that K' and n' must be evaluated at a stress corresponding with the wall shear stress.

2.8.3 Nikuradse

For comparison, a simple approach was adopted by fitting a straight line to laminar flow data from the BBTV on the relevant pseudo-shear diagram. For the rotary viscometer, the line was fitted to the data points on the rheogram.

The slope of these lines was taken as the dynamic viscosity (μ) and turbulent predictions were made using Newtonian theory. Yield stress and rheogram curvature are therefore neglected.

2.8.4 Hydraulic Gradient

Hydraulic gradient calculations are performed using the following equations:

$$i_m = \frac{4\,\tau_o}{D\,\rho_w\,g} \qquad (2.36)$$

or

$$i_m = \frac{2\,f\,V^2\,S_m}{D\,g} \qquad (2.37)$$

2.9 VISCOMETRY

Barr (Ref. 3) lists four qualitative tests for viscosity used by craftsmen:

"(a) he may rock the container and see or feel how large a surge of liquid is produced or how rapidly the wave dies down; (b) he may note the resistance offered to the motion of a stirrer; (c) he may observe the form of the falling column which results when he pours the liquid over an edge or allows it to drain from a rod; (d) he may place a quantity of the liquid on a smooth surface and notice how it 'runs'"

Unfortunately each of these qualitative tests involves another property (surface tension or density) which makes them unsuitable for elaboration into a precise method of viscometry.

Newton's hypothesis, upon which the whole theory and practice of viscometry are based, paved the way for the formulation of qualitative methods for measuring the phenomenon of viscosity.

Stokes (in Ref. 3) found that pipe discharge data (in turbulent flow) did not agree with the laminar hypothesis, and suggested experiments with rotating cylinders (made later by Couette). Poiseuille's experiments using thermometer tubing did, however, confirm Stokes' formulae.

Thus developed the two main branches of viscometry, viz. tube viscometry and rotational viscometry, which are discussed below.

2.9.1 Tube Viscometry

2.9.1.1 Definition and description

A capillary (tube) viscometer is defined (Ref. 5) as "a device that causes a sample of fluid to flow at a measured rate in laminar motion under a measured pressure gradient through a precision bore capillary tube of known diameter and length".

The first tube viscometer was therefore that of Poiseuille (1840). The diameter varied between 0,013 mm and 0,65 mm, the pressure range from 5 mm to 10 m of mercury (670 Pa to 1,3 MPa) and the length varied up to one metre.

Tube viscometers are inherently simple, and the fundamentals have remained unchanged after 146 years. From Poiseuille's Law it can be seen that viscosity is directly proportional to the fourth power of the diameter. It is therefore essential to make accurate diameter determinations, normally done by first weighing the tube empty and then filled with liquid of known density, as did Poiseuille.

The other area of attention for the tube viscometer is the end effects of the tube. Poiseuille noticed these effects in his early experiments, and tabulated critical L/D ratios, below which his law ceases to hold.

Many different types of tube viscometer are described in the literature (Ref. 3, 4, 5, 6, 7 and others). The largest diameter tube reported is 6 mm (Ref. 6) but most tubes are less than 1,5 mm diameter.

2.9.1.2 Interpretation of Rheological Measurements (Ref. 5)

With the capillary instrument, the measured data related to the viscous properties, after application of any appropriate corrections, are:

Q = volumetric flow rate,
D = inside diameter of capillary,
L = effective length of capillary, and
Δp = pressure drop due to laminar friction.

The average fluid velocity is

$$V = \frac{4Q}{\pi D^2} \tag{2.38}$$

and the wall shear stress is

$$\tau_o = \frac{D\Delta p}{4L} \tag{2.39}$$

where τ_o is the shearing stress at the wall of the capillary. The rate of shear at the capillary wall may be determined from the general equation of Rabinowitsch (1929) and Mooney (1931), which is (see Appendix A)

$$\left(-\frac{du}{dr}\right)_o = \left(\frac{3n' + 1}{4n'}\right)\frac{8V}{D} \tag{A1}$$

where

$$n' = \frac{d\ \ell n \frac{D\Delta p}{4L}}{d\ \ell n \frac{8V}{D}} \qquad (A2)$$

n' is the slope of the logarithmic plot of $D\Delta p/4L$ versus $8V/D$. The slope, n', may vary and the applicable value should be used for each value of $8V/D$. For Newtonian fluids $n' = 1$.

The interpretive procedure is, therefore,

a. to calculate τ_o from the data after any appropriate corrections, and equation (2.39);

b. to plot τ_o versus $8V/D$ on logarithmic co-ordinates and determine n' as a function of $8V/D$;

c. to calculate $\left(-\frac{du}{dr}\right)_o$ from equation A1;

d. to plot τ_o versus $\left(-\frac{du}{dr}\right)_o$ on arithmetic or logarithmic co-ordinates as preferred, and

e. if desired, to fit an appropriate constitutive equations to the data.

2.9.2 Rotational Viscometry

2.9.2.1 Description

A rotational viscometer (Ref. 5) permits a sample of fluid placed in the annular space between a stationary and a rotating cylinder to be subjected to shear, and the torque acting upon the stationary cylinder to be measured. The rate of shear is determinable from the geometry of the system and the speed of the rotating cylinder. The shear stress is obtained from the measured torque.

2.9.2.2 Interpretation of Rheological Measurements (Ref. 5)

The data obtained with a concentric cylinder instrument are:

D_b = diameter of the inner cylinder (bob),
D_c = diameter of the outer cylinder (cup),
θ = spring deflection being a measure of the torque on the stationary cylinder,
h = height of stationary cylinder immersed in fluid, corrected for end effect,
N = speed of rotating cylinder, sec^{-1}.

From a simple force balance, the following equation is obtained

$$\tau_b (\pi D_b h) \frac{D_b}{2} = T = k\theta \qquad (2.40)$$

or
$$\tau_b = \frac{2k\theta}{\pi D_b^2 h} \qquad (2.41)$$

where T is the torque on the stationary cylinder, and k is a suitable spring constant.

The relationship between the rate of shear and the geometry of the system is given by an equation due to Krieger and Maron (1954)(in Ref. 5):

$$\left(\frac{du}{dr}\right)_b = \frac{4\pi N}{1 - s^{-2}} F_{KM} \qquad (2.42)$$

where $s = D_c/D_b$
F_{KM} = the Krieger-Maron correction factor,

$$F_{KM} = 1 + \frac{s^2 - 1}{2s^2}\left(1 + \frac{2}{3}\ell n\, s\right)\left(\frac{1}{n''} - 1\right)$$

$$+ \frac{s^2 - 1}{6s^2}\ell n\, s\left(\left(\frac{1}{n''} - 1\right)^2 + \frac{d\left(\frac{1}{n''} - 1\right)}{d \log T}\right) \qquad (2.43)$$

n'' = d ℓn T/d ℓn N is the slope of a logarithmic plot of T versus N.

If the annular gap is made very small ($s \approx 1$) then

$$\left(\frac{du}{dr}\right)_b = \frac{2 \pi D_b N}{D_c - D_b}$$

When n" is constant, or nearly so, the equation simplifies somewhat and may be approximated by a series expansion.

For Newtonian fluids, $n'' = 1$ and $F_{KM} = 1$.

The procedure for interpreting data from the concentric cylinder viscometer is, therefore,

a. to calculate τ_b from θ, Equation (2.41) and the appropriate value of k;

b. to plot θ versus N on logaarithmic co-ordinates and determine n" as a function of N;

c. to calculate F_{KM} for the values of s and N of interest from equation (2.43);

d. to calculate $\left(\frac{du}{dr}\right)_b$ from equation (2.42) with the appropriate values of N, s, and F_{KM};

e. to plot τ_b versus $\left(\frac{du}{dr}\right)_b$ on arithmetic or logarithmic co-ordinates as preferred, and

f. if desired, to fit an appropriate one of the constitutive equations to the data.

2.10 USE OF VISCOMETERS IN NON-NEWTONIAN SLURRY RHEOLOGY

2.10.1 The advantages and disadvantages of each type

2.10.1.1 The tube viscometer

Advantages	Disadvantages
1. Mechanically simple.	1. Sample is subjected to a varying rate of shear over the tube cross-section.
2. Geometric similarity (i.e. miniature pipeline).	2. The same sample of fluid cannot be subjected to sus tained flow for measuring time-dependent fluids.
3. Can attain high shear rates.	

2.10.1.2 The rotational viscometer

Advantages	Disadvantages
1. Time dependency can be measured.	1. The annular gap must be much larger than the largest particles, where-as this gap is usually made as small as possible to minimise the correction factor.
2. Many minor advantages (see Chapter 8).	2. Non-Newtonian end effects are difficult to account for.

These attributes (advantages) are not typical of most capillary (tube) viscometers. For these reasons rotational viscometers have become the single most widely used class of instruments for rheological determinations (Ref. 6).

2.10.2 Previous use of Viscometers in Non-Newtonian Slurry Rheology

Barr (Ref. 3) mentions the study of "anomolous systems" (now known as non-Newtonian fluids) undertaken by Bingham and Green using a clay slurry in a capillary (tube) viscometer. This was the first significant work in the field of non-Newtonian slurry rheology and led to the formulation of the Bingham plastic constitutive equation (equation 2.22).

Barr goes on to say that, due to cost and lack of familiarity, rotational viscometers were not preferred (C 1931) for non-Newtonian work.

However, with work such as that by Krieger and Maron (Ref. 10), many of the problems associated with the rotational viscometer were solved, allowing it to develop into the versatile and accurate instrument that it is today.

Metzner and Reed (Ref. 8) correlated all useful tube (pipe) flow data available up to 1953, with diameters ranging in size from 3 mm to 300 mm (1/8" to 12"), all of which correlated well in the laminar region using their theoretical method.

Iwanami and Tachibana (Ref. 11) developed a short-tube viscometer and used it to determine the viscosity of flyash slurries for concentrations up to C_v = 30% and C_w = 40%.

Faddick (Ref. 12) used Brookfield and Stormer rotational viscometers to characterise coal-water slurries of various concentrations and particle size range. He concludes that pipeline energy requirements can be predicted from rheology data obtained from these rotational viscometers.

Shook et al (Ref. 13) developed a vertical tube viscometer with a diameter of 1,56 cm and lengths of 2,98 m and 4,88 m. Metallurgical coal of -14 mesh size was tested in this viscometer and in 5, 11 and 31 cm diameter pipes. They conclude that although reliable rheological data were obtained, a satisfactory correlation of pipeline pressure drops could not be obtained.

Yamagata et al (Ref. 14) used capillary (tube) and rotational viscometers to predict the rheological properties of coal-oil mixtures. Viscometer results agreed well with pipe flow data.

Lazarus (Ref. 15) used a Brookfield rotational viscometer to characterise a phosphate ore slurry in the range C_w = 20 to 35%. The viscometer tests agreed with large scale pipeline tests.

Duckworth et al (Ref. 16) tested a fine coal slurry at various concentrations in a Haake rotary viscometer with three bobs, a 16,07 mm diam x 3.5 m long tube viscometer and a 150 mm pipeline. In the laminar regime for the 150 mm pipeline, "reasonable" agreement was obtained with the tube viscometer and the largest rotary bob. Agreement with the two smaller bobs was not good.

Hanks and Hanks (Ref. 17) developed a Direct Measurement Tube Viscometer with horizontal and vertical test sections, for accurate rheological determinations of fine coal slurries (-325 mesh) at concentrations ranging from C_w = 6,3% to 33,9%.

Horsely (Ref. 18) conducted a detailed investigation into the rheological properties of a gold slime slurry, using a Haake rotary viscometer and a 40 mm diameter pipeline. The results show that rotary viscometers can be used to predict pressure gradients in slurry pipelines as long as the concentration by weight is kept high.

Want et al (Ref. 19) used a "capillary rheometer" (tube viscometer) to obtain data to establish rheological models to determine head loss and power requirements for full scale pipelines. The slurry was a high density Bauxite residue in the concentration range C_w = 36% to 67%.

Lazarus and Sive (Ref. 20) developed a novel Balanced Beam Tube Viscometer (BBTV) for the rheological characterisation of high concentration flyash slurries. Scaled up predictions using the Bingham plastic rheological model and a modified Torrance equation correlated well with pipeline tests.

2.11 CONCLUSION

The fundamental background and theory of viscometry and rheology have been presented.

The record of previous use of both types of viscometer show that, apparently, both have been used successfully in the past to characterise non-Newtonian slurries and predict full scale pipeline energy requirements.

This thesis is a continuation and development of the work presented by Lazarus and Sive (Ref. 20).

CHAPTER 3

APPARATUS AND EXPERIMENTAL PROCEDURE

3.1 DESCRIPTION OF THE BBTV

Fig. 3.1 shows a diagrammatic layout, Fig. 3.2 shows a photograph and Fig. 3.3 shows an assembly drawing of the novel Balanced Beam Tube Viscometer, which has been developed at UCT. The viscometer consists of two pressure vessels (1 and 2) mounted on a steel joist and supported at two points L and F. A load cell is located at point L and point F is the system fulcrum (supported on a knife edge). Figs. 3.2 and 3.3 show that the pressure vessels are connected by two transparent plastic tubes of 13mm and 32mm nominal diameter.

The precise internal diameters are 13,37mm and 32,625mm and were determined to this precision by weighing sections of the tubes with and without water. This precision is required since a rheogram point inherently contains the fourth power of the diameter. Each tube has valves at either end and only one tube is used at a time. Each pressure vessel has a nest of stirrers (inside), driven by motors (on top) connected via shafts through gland seals in the vessel cover plate. Air pressure is supplied to either of the vessels through pressure regulation and a 3-way valve. When a vessel is pressurised, the other is vented to atmosphere, via the vent valve, in order to develop the driving force necessary to cause the slurry to flow from the one vessel to the other.

The BBTV has pressure tappings in the tubes, allowing direct measurement of wall friction loss. This avoids the inclusion of entrance losses, exit losses and hydraulic grade line curvature due to developing flow.

There are four pressure tappings in each tube, allowing the operator flexibility of pressure range. The pressure tappings are water filled and connected to the differential pressure transducer (DP cell) via solids collecting pods, and a flushing/bleeding facility.

The pressure tappings are located so that fully developed flow exists between them. The hydraulic effective length is thus equal to the physical distance between tappings (L).

The output from the BBTV consist of successive voltage readings representing load cell input (power supply voltage), load cell output and DP cell output.

3.2 INSTRUMENTATION

3.2.1 Transducers

3.2.1.1 Load Cell (Fig. 3.4)

The load cell is located at point L (Fig. 3.1), and is used to determine the slurry mass distribution between the two vessels. It can operate in both tension and compression.

Four strain gauges are located at positions A, B, C and D (Fig. 3.4) because these are positions of maximum strain. The strain gauges are connected as a Wheatstone Bridge (Fig. 3.5).

The output voltage of the bridge varies linearly with applied force, and is proportional to the input voltage. The output voltage is divided by the input voltage, giving a non-dimensional load cell reading which is independent of input voltage.

The input voltage is derived from an HP 6214A Power Supply. This unit was set at a nominal 5V for calibration and operation.

The load cell used has a resolution of 0,3N and a range of ±800N.

The load cell is a sensitive device and should not be installed until the BBTV has been charged with equal amounts of slurry in each vessel. Under these conditions, the BBTV balances on its knife edge, and the load cell can be care-fully installed. The stirrer motors should be off.

A typical response characteristic is shown in Fig. 3.10.

The load cell is located by two bolts and should be removed and replaced with the blank when not in use.

3.2.1.2 Differential Pressure Transducer
(DP cell - Fig. 3.6)

The DP cell used is a Gould PDH 3000 series. It is located on the computer stand (which is located near the BBTV fulcrum) and is connected to the BBTV via flexible reinforced tubing. The DP cell is used to measure the pressure drop across the pressure tappings in the selected viscometer tube. Because the DP cell cannot read in reverse, high-low selectors are provided so that the pressure differential can be reversed.

The DP cell is connected as shown in Fig. 3.7 to a constant voltage 24V supply. The output is 4-20 mA in the supply leads which is linear with pressure differential across the two halves of the cell. This current output is converted to a 40-200 mV voltage output by a 10 Ω series resistor.

The DP cell has an accuracy of 0,25% and a maximum range of 200 kPa.

The range and span are adjustable. A typical response characteristic is shown in Fig. 3.12.

3.2.2 Data Acquisition Unit (DAU)

The Data Acquisition Unit is an HP 3421A model.

Essentially it consists of a digital voltmeter which can be software controlled to connect to the various analogue input channels. It is battery operated and can be used remote from the electrical mains.

The DAU is used to digitise the transducer voltages, and is connected as shown in Fig. 3.9.

The DAU is controlled by an HP-75C computer via the HP-IL serial interface loop.

3.2.3 HP-75C Computer

The HP-75C is a battery powered computer which is programmed in BASIC.

By means of the various programmes, it captures the transducer outputs in digital form from the DAU. A limited amount of processing is performed before the transducer outputs are stored in internal data files.

The HP-75C has an internal timer which is used to record the time at which the transducer readings are taken. This timer is accurate to 1 ppm and has a resolution of 1 ms.

When sufficient data has been collected, these data files are transferred to the HP 86 computer via the HP-IL serial interface loop.

3.2.4 HP 86 Computer

The HP 86 is a 128k RAM BASIC micro-computer with a floppy disk drive, printer and plotter.

It is used to store the tranducer readings as data files on a floppy diskette, and then process this data and output the results either as another data file, or in printed or graphical form.

3.3 CALIBRATION PROCEDURE

Five computer programmes are used for calibration. "READCHAN" runs on the HP-75C and reads the voltage on any DAU channel. The two calibration programmes "LOADCAL" and "PRESCAL" are run on the HP-75C (See section 3.2.3). The data files thus generated can be dumped to the HP 86 and then plotted using "LCALPLOT" and "PCALPLOT". (See section 3.5)

3.3.1 Calibration of Load Cell

The following steps are followed for load cell calibration:

1. The programme "READCHAN" is run to check that the transducer is operating properly. The reading should remain constant and change only when the operator applies upward or downward force on the beam.

2. The programme "LOADCAL" is then run. This programme will prompt the operator for information, as follows:

   a. Standard weights are placed above the centroids of each vessel (i.e. on top of the centre of the stirrer motors). Downward force on the LH vessel is considered as positive and downward force on the RH vessel is considered as negative.

   b. Enter the force value in newtons when prompted by the programme.

   c. Repeat Steps a and b with different loads, normally nine times.

   d. To exit the programme and complete the calibration, enter "N" when prompted "ANOTHER LOAD?"

   Note that zero load is valid and desirable for calibration purposes.

The program will take ten transducer readings for each applied force, and do a least squares linear regression which yields the calibration equation:

$$\text{(Applied load)} = m \times \text{(Transducer output)} + c$$

where m = gradient of the calibration line

c = ordinate intercept of the calibration line

A load cell calibration can be performed again at any time during a test.

A typical load cell calibration output is shown in Fig. 3.10.

3.3.2. Calibration of the DP Cell

1. Connect the pods to the mercury/water manometer as shown in Fig. 3.11.

2. Open the manometer relief valve.

3. Bleed the DP cell system and manometer of all air and solids by flushing supply water via the bleed valve through the various components.

4. Close the manometer relief valve.

5. Run the programme "READCHAN" to check that the transducer is operating properly. The reading should remain constant at approximately 0,04V for zero pressure differential, and should increase with increasing pressure differential to a maximum of 0,2V.

6. Run the programme "PRESCAL" which will prompt the operator for information.

7. Using the main bleed tap, or the manometer relief valve, a pressure differential is set up. The lefthand pod is the high pressure side and the high-low selectors are set to run from Left to Right.

8. When the manometer levels have settled, the levels in mm Hg are entered and the computer will take ten transducer readings and then prompt with "ANOTHER PRESSURE?".

9. Repeat steps 7 and 8 using different pressure differentials, normally nine times.

10. To exit the programme and complete the calibration, enter "N" when prompted "ANOTHER PRESSURE?"

    Note that zero pressure differential is valid and desirable for calibration purposes.

A least squares linear regression is then performed by the computer, yielding the calibration equation.

A DP cell calibration can be performed at any time.

A typical DP cell calibration output is shown in Fig. 3.12.

3.4 EXPERIMENTAL PROCEDURE

The final product of the BBTV is a set of rheological constants (i.e. τ_y, K and n) which characterise the particular slurry being tested.

The following definitions shall apply.

A READING consists of ten consecutive BBTV transducer outputs (load cell, DP cell and time) yielding one point on a rheogram.

A RUN consists of enough readings to fill the memory of the HP-75C - usually 16 readings.

A TEST consists of 30 to 40 readings from each diameter tube, yielding one rheogram (i.e. one set of rheological constants).

3.4.1 Preparation

Before a TEST can be executed, the BBTV must be prepared, and certain tests must be performed on the slurry. The power supplies (located in the computer hut) must be switched on and allowed to warm up (about half an hour). The pods should be disconnected and the load cell replaced with the blank. Connect up the data logger. The slurry should be prepared and each vessel approximately half filled.

At this stage, the operator should pump the slurry from vessel to vessel a few times in order to mix it thoroughly. This is done by following the READING procedure in section 3.4.2, without using the computer (i.e. without steps 6 and 8). The operator should begin to get a qualitative "feel" for the slurry rheology.

A one litre sample should be taken (4 x 250mℓ sample bottles) for record purposes (for pH, S_m, S_s and particle size distribution tests), using the sample valve.

The solids and slurry relative densities (S_s and S_m) must be determined (See Appendix). The pH and the temperature of the slurry must be recorded.

Remove the pods and bleed the pressure system of air and flush any solids from the pods using the bleed valve. Connect the pods to the selected tube and record the length (see Fig. 3.13). Close the other viscometer tube at both ends.

Both fill port covers should be on. A calibration (3.3) is normally done at this stage. The BBTV is now ready for a RUN.

3.4.2 RUN

In order to do a RUN, load and run the "VISCORUN" programme on the HP-75C. The operator will then be prompted:-

PIPE SIZE L/S?

Enter either L (for large) or S (for small).

MIXTURE TEMP?

Enter the slurry temperature in °C

LENGTH BETWEEN TAPS?

Enter the correct length (Fig. 3.13)

TYPE OF MATERIAL?

Enter a single identity character (i.e. K for kaolin or U for uranium tailings).

SOLIDS RELATIVE DENSITY?

Enter the S_s value

MIXTURE RELATIVE DENSITY?

Enter the S_m value.

The programme then names the DATA FILE as follows

A B X X D D M M

where: A is the identity character
B is the tube size (L or S)
XX is the C_v value as a percentage
DDMM is the date.

PRESS CONT WHEN READY M9 = __

The BBTV is now ready to take a READING. The value of M9 is the number of seconds that the computer will wait between capturing consecutive transducer outputs. One vessel should be full and the other empty.

The READING procedure is as follows:-

1. Close the vent valve on the full vessel and close the tube valve on that side. Replace the fill port cover if removed.

2. Open the vent valve on the empty vessel and open the tube valve on that side. When a very thick slurry is being tested, the viewing window cannot be used. The fill port cover should then be removed.

3. Select the correct direction on the high-low selectors (see Fig. 3.3).

4. Switch the 3-way valve so that the full vessel is pressurised (see Fig. 3.3).

5. Set the pressure regulator to the desired pressure.

6. Change M9 if necessary by typing e.g.

   M9 = 5 if a 5 second wait between READINGS is required
   Press RET

   Type CONT

7. Open the tube valve on the pressurised vessel side.

8. Quickly press the RET key on the computer and move to the vented vessel.

9. Gently close the tube valve on the vented vessel side when that vessel has filled. This terminates the READING.

A number of READINGS are taken using steps 1 to 9 above, each with a different pressure regulator setting.

The M9 values should be chosen so that the ten transducer outputs for each READING are evenly spaced over the flow time. For high V_m READINGS, M9 = 0. Determining the correct value of M9 is a matter of skill and experience and trial and error procedure is normally followed.

The stirrer motors should be used when necessary (i.e. if the slurry begins to settle in the vessels. If in doubt, leave the stirrer motors on).

When the RUN is complete, the data is dumped from the HP-75C to the HP 86 using the "TRANSMIT" and "RECEIVE" programmes (see section 3.5).

The data file should be scrutinised to ensure that the DP cell is not limiting (i.e. DP cell output < 0,2 V).

The data file format is shown in Fig. 3.14.

3.5 DUMPING PROCEDURE

After each RUN, the data file should be dumped from the HP-75C to the HP 86.

1. Switch off the HP-75C and disconnect it from the DAU.

2. Connect the HP-75C to the HP 86 using the HP-IL connectors.

3. Switch both machines on.

4. CREATE a data file on the HP 86 to accept the data.

5. Type LOAD "RECEIVE" and press END LINE on the HP 86 and type EDIT "TRANSMIT" and press RTN on the HP-75C.

6. Press the RUN key on both machines at the same time.

7. Type the file name on the HP-75C when prompted. Both machines will display FINISHED when the dump operation has terminated.

A hard copy of a programme or data file on the HP-75C can be obtained using the programmes "PROGPRINT" (HP 86) and "PSEND" (HP-75C) and the procedure outlined above, without step 4.

3.6 PROCESSING

The processing is done on the HP 86, using the programme "VISCOPX".

A typical READING is shown in graphical form in Fig. 3.15 as a plot of mass in RH vessel vs. time and pressure drop vs. time. Each READING is analysed, as explained below, to yield a co-ordinate (V_m; Δp). The programme shows these two graphs on the screen and the operator must select the FIRST and LAST points to be used for the analysis (usually 1 and 10).

A least squares linear regression is performed on the (time; mass) co-ordinates from FIRST to LAST. This yields the mass flow rate [dM/dt] from which V_m can be calculated:

$$Q_m = \frac{dM/dt}{\rho_m} \qquad (3.1)$$

$$V_m = \frac{Q_m}{A} \qquad (3.2)$$

The Δp value is calculated as the arithmetic mean of all the pressure drop ordinates from FIRST to LAST.

The programme produces a print-out (Fig. 3.16) and stores the co-ordinates and file data in a processed data file.

This processed data is output in graphical form using "GRAPH 21" (Fig. 3.17) called a "Pseudo-shear Diagram".

For laminar flow, the pseudo-shear diagram is independent of tube diameter. Thus the laminar, transition and turbulent regions can be identified using a pseudo-shear diagram.

Only the laminar flow data is used for rheological characterisation.

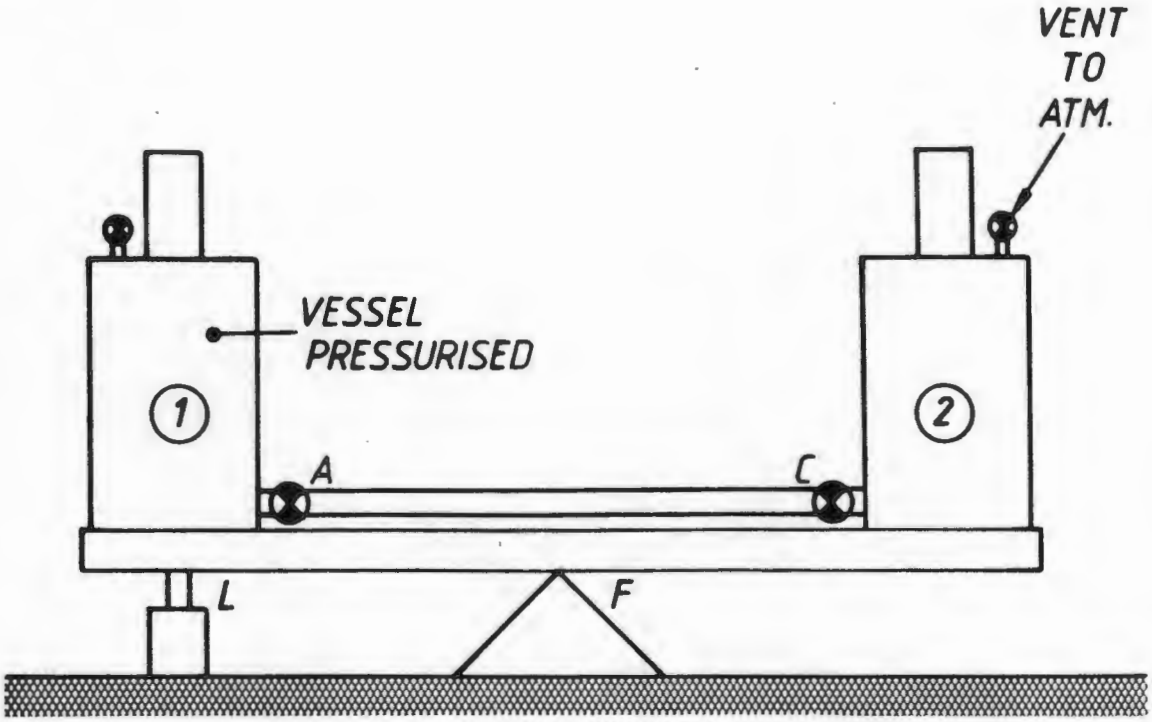

Fig. 3.1 : BBTV Diagrammatic Layout

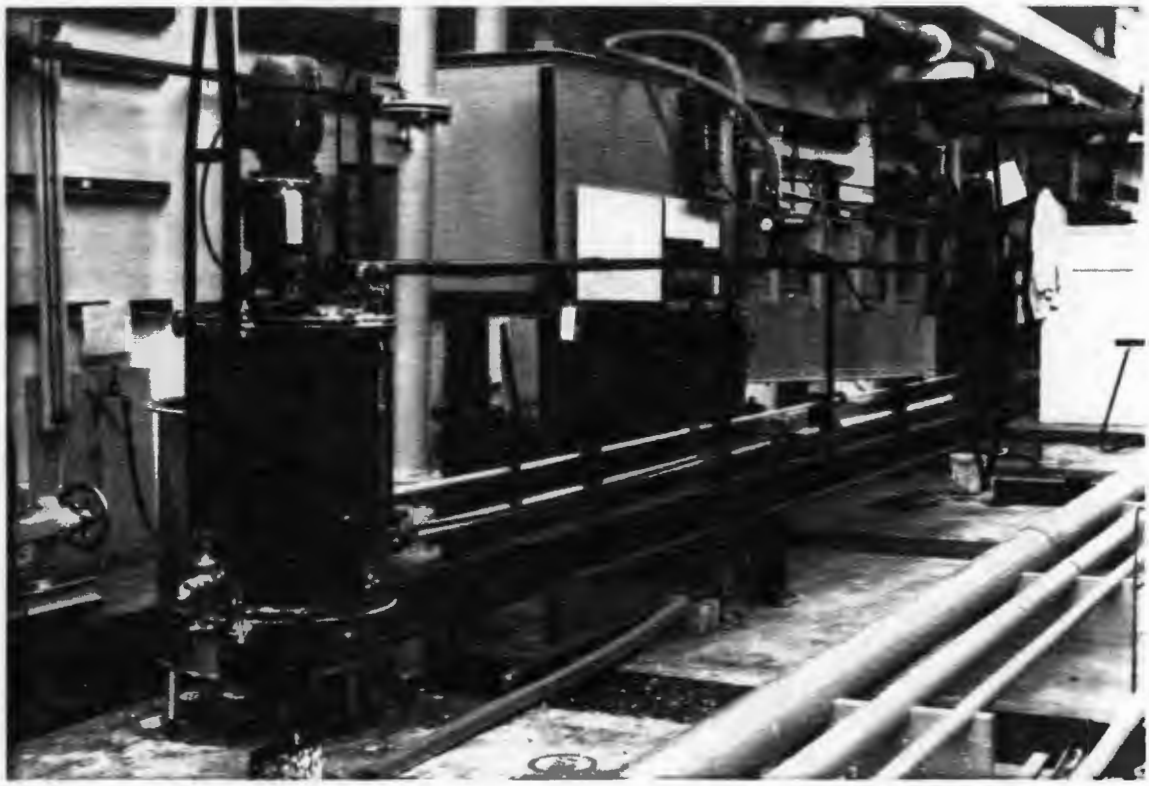

Fig. 3.2 : BBTV Photograph

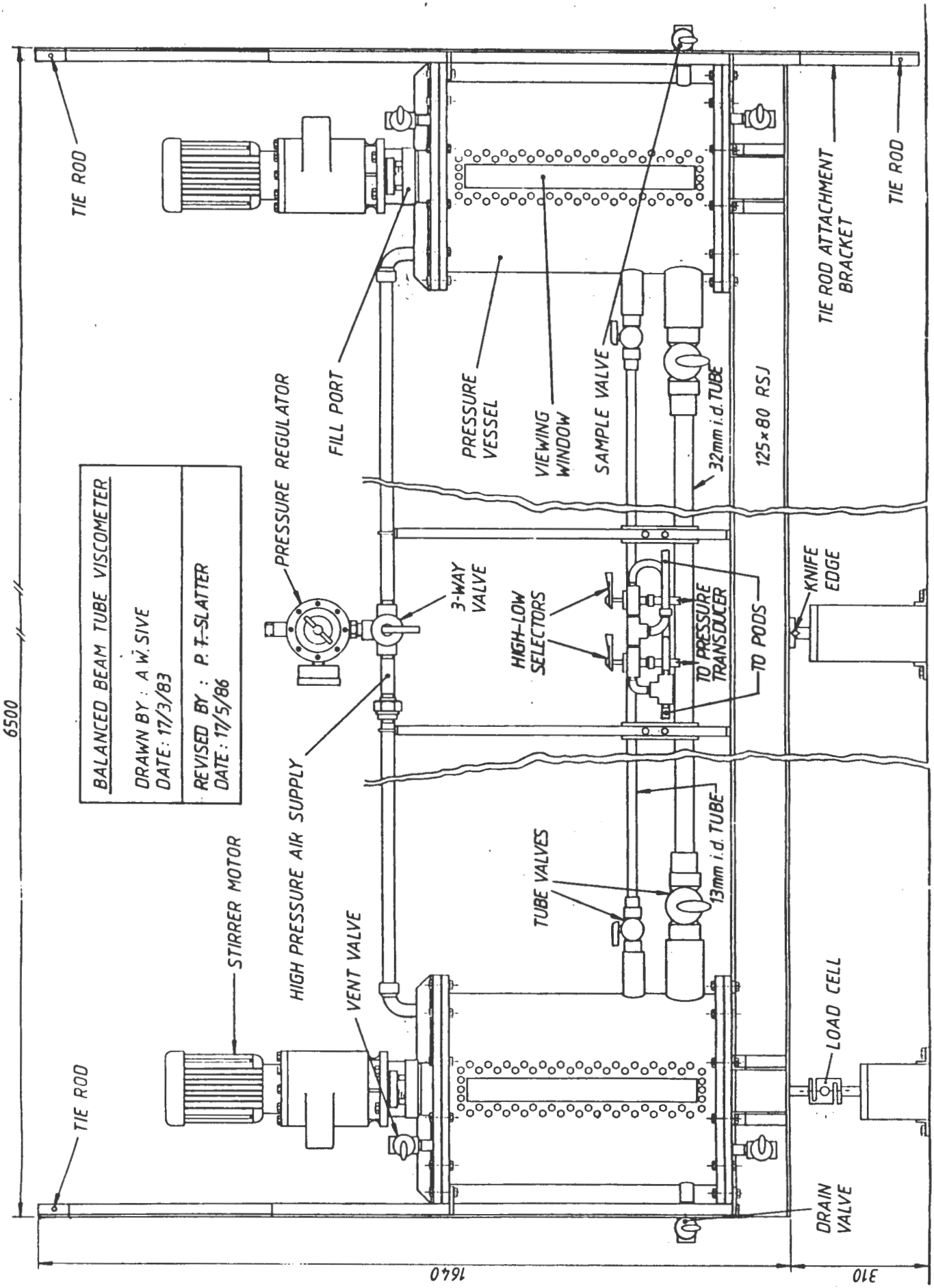

Fig. 3.3 : Assembly Drawing

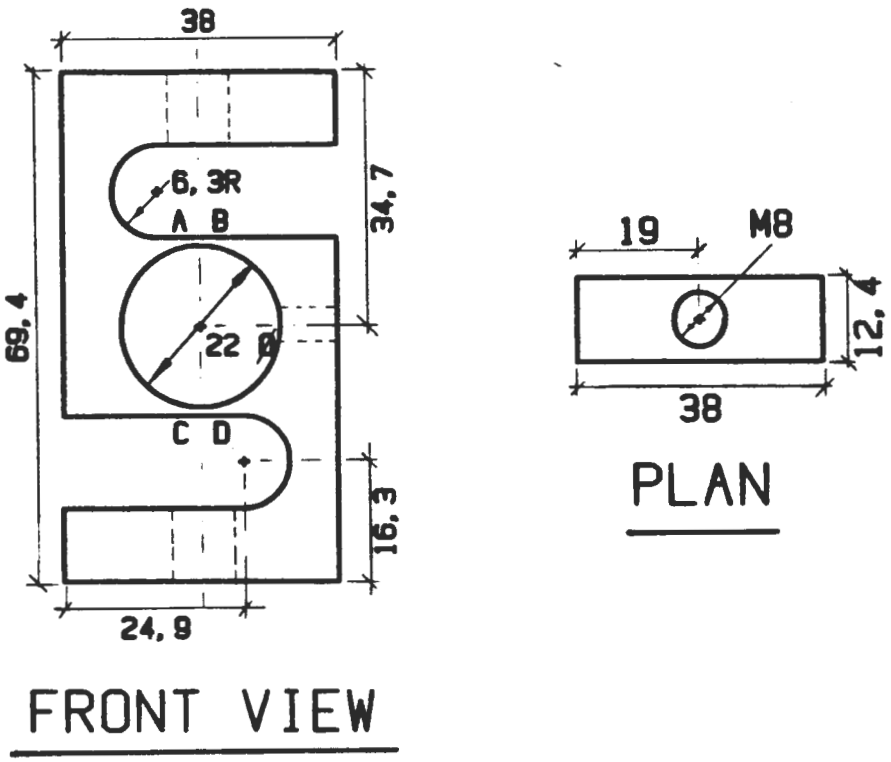

Fig. 3.4 : Load Cell

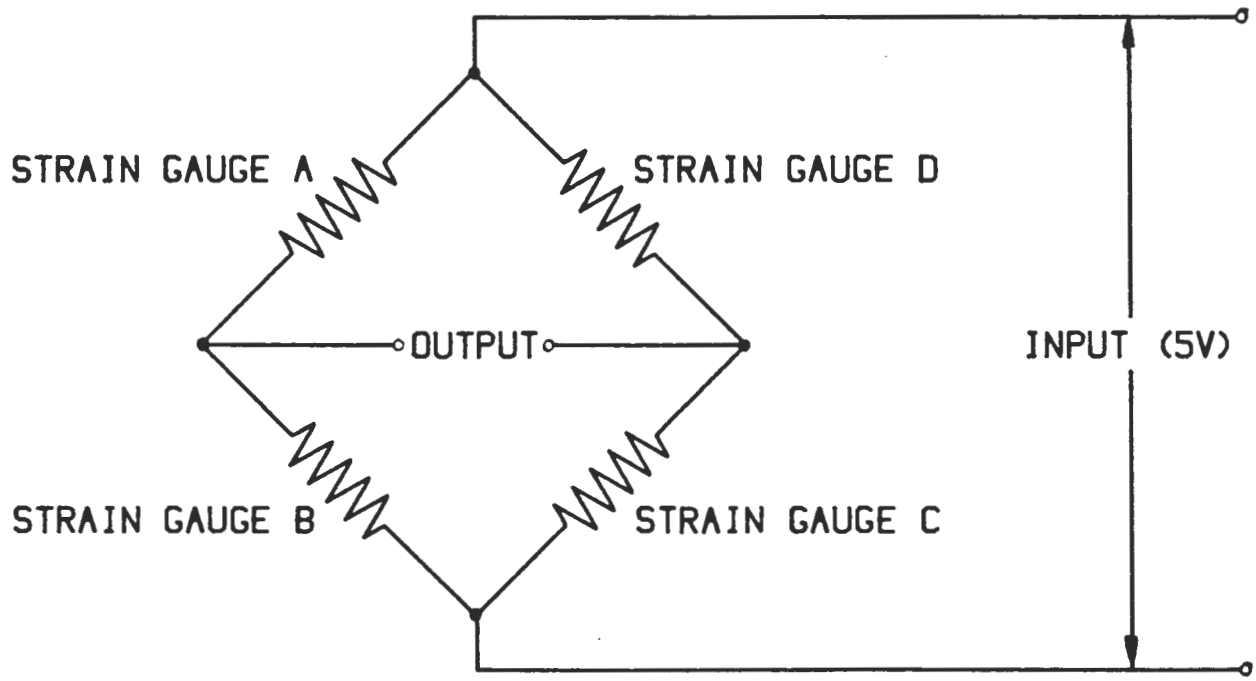

Fig. 3.5 : Wheatstone Bridge Circuit

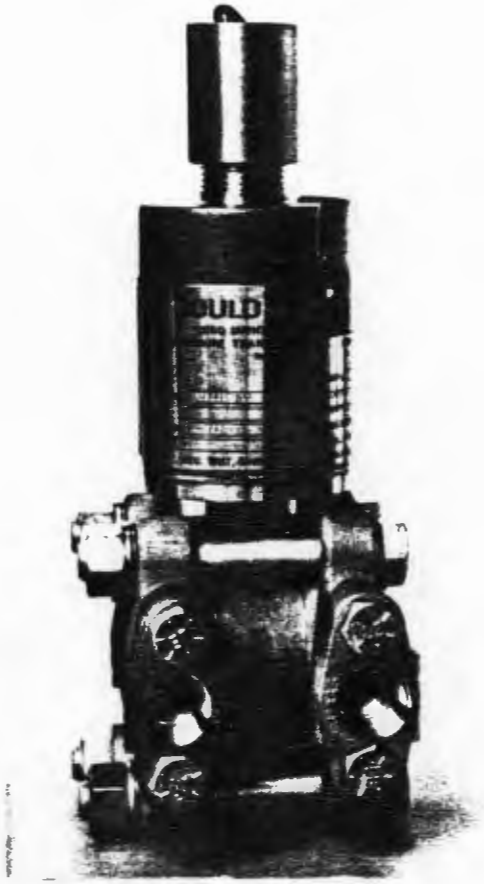

Fig. 3.6 : DP Cell

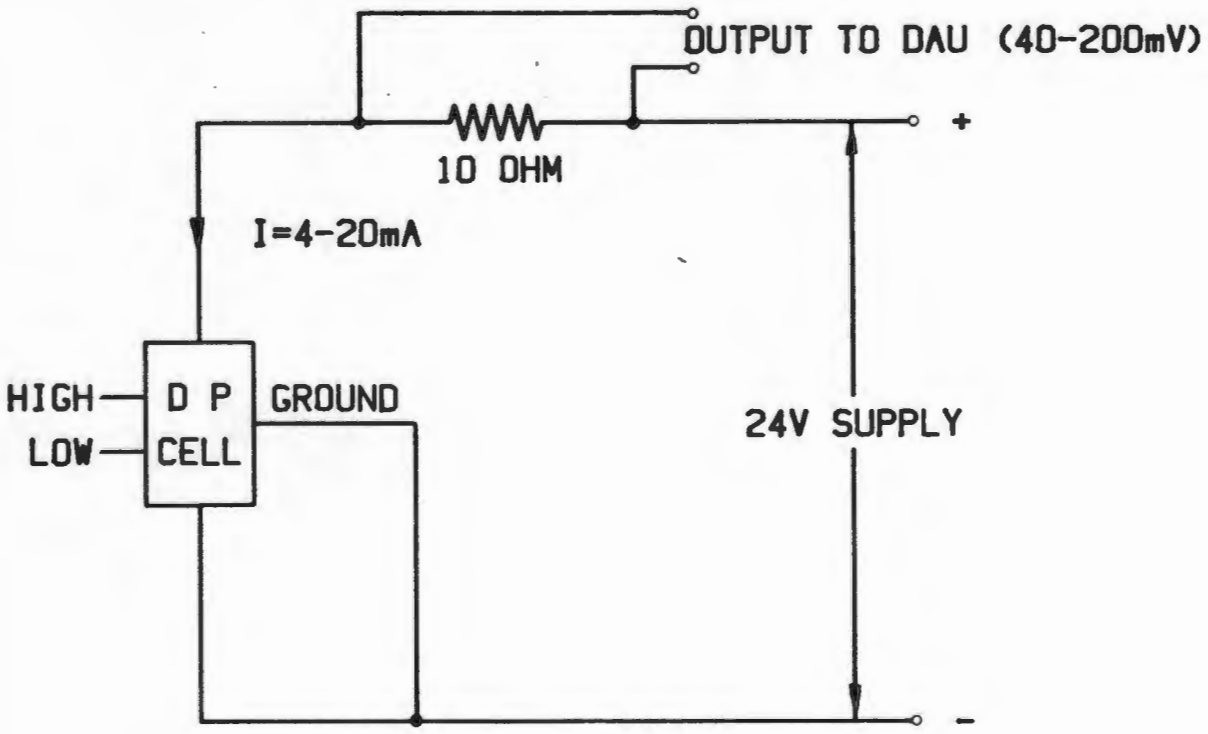

Fig. 3.7 : DP Cell Circuit Diagram

Fig. 3.8 : DAU and HP-75C

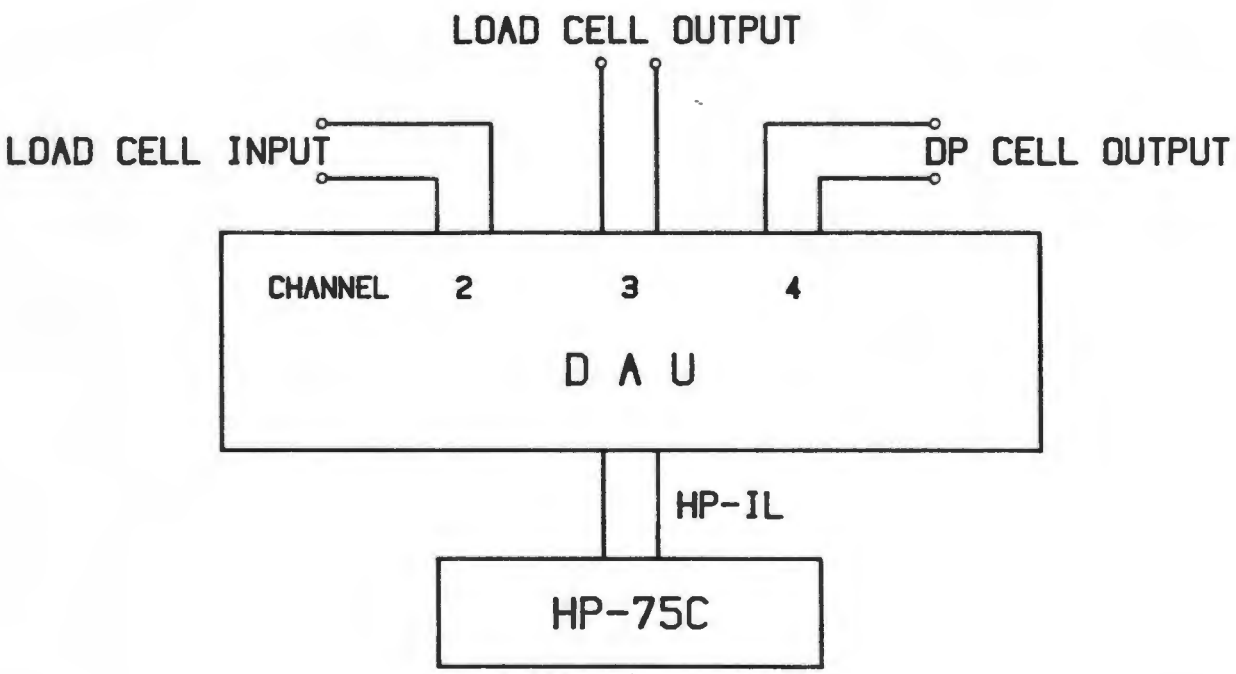

Fig. 3.9 : HP-75C Connection Diagram

```
==========================================================================
HP-75 FILE NAME LDATA6    DATE 85/05/08

TIME 09:56:31

LDATA6       B  281 09:48 05/08/85

1 DATA -483035.925084,923.271333914
2 DATA 0,1.91206999159E-3,2.02484567313E-7
3 DATA 100,1.70571479112E-3,1.2749727666E-7
4 DATA 200,1.4985696247E-3,1.95277580212E-7
5 DATA 300,1.29112014294E-3,1.31275791117E-7
6 DATA 400,1.0832215038E-3,3.21489588565E-7
7 DATA 300,1.28961815298E-3,1.05092551803E-7
8 DATA 200,1.49611646538E-3,1.60312195419E-7
9 DATA 100,1.70304176325E-3,1.78076138523E-7
10 DATA 0,1.91067870361E-3,1.77857620959E-7
```

The first line contains the Calibration Constants m, c

Each consecutive line contains the Applied Load (N), "Output" (V/V), Standard Deviation

NOTE: Each "output" is the average of ten consecutive readings.
The standard deviation is also calculated from these ten consecutive readings.

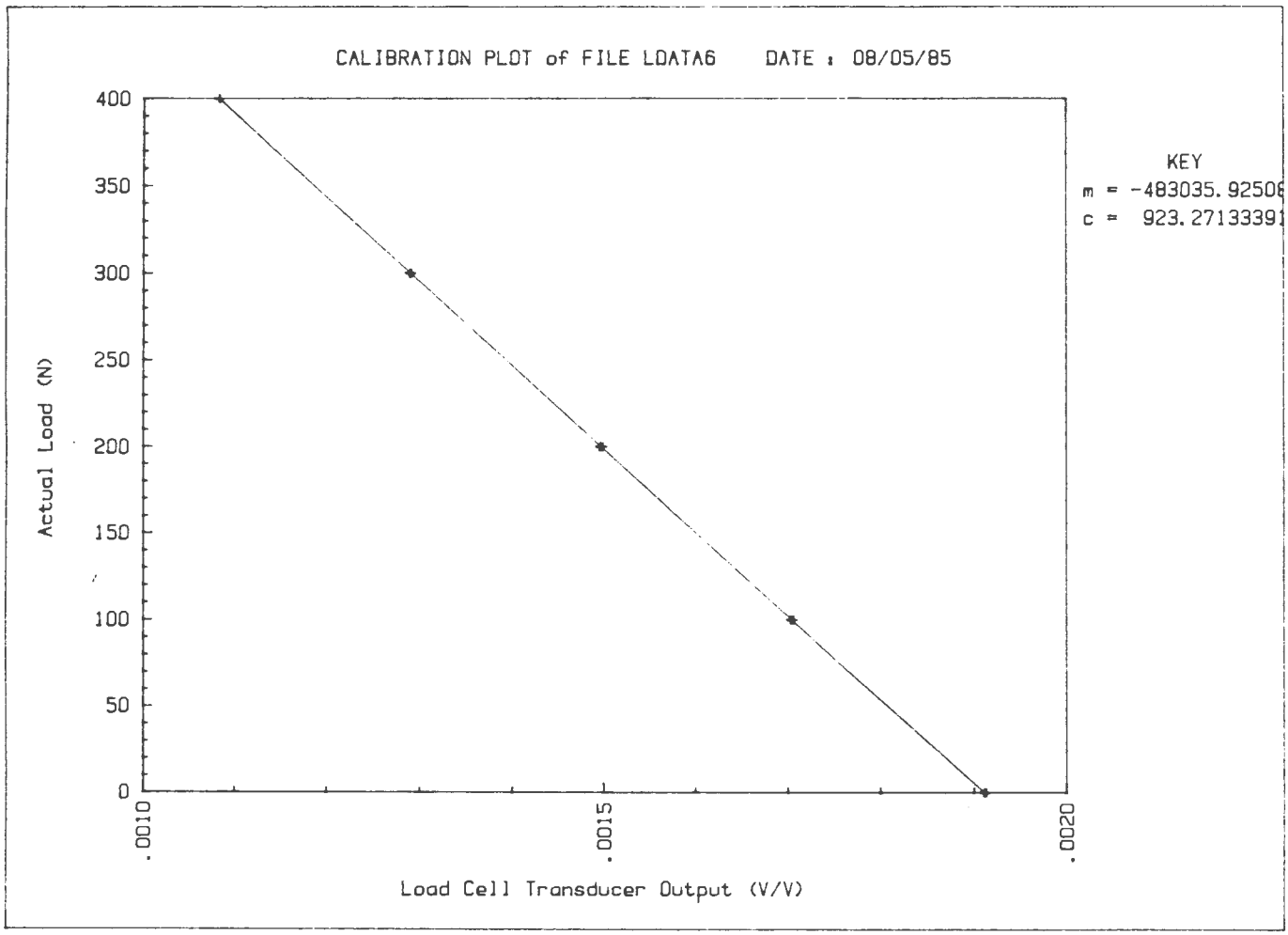

Fig. 3.10 : Load Cell Calibration Output

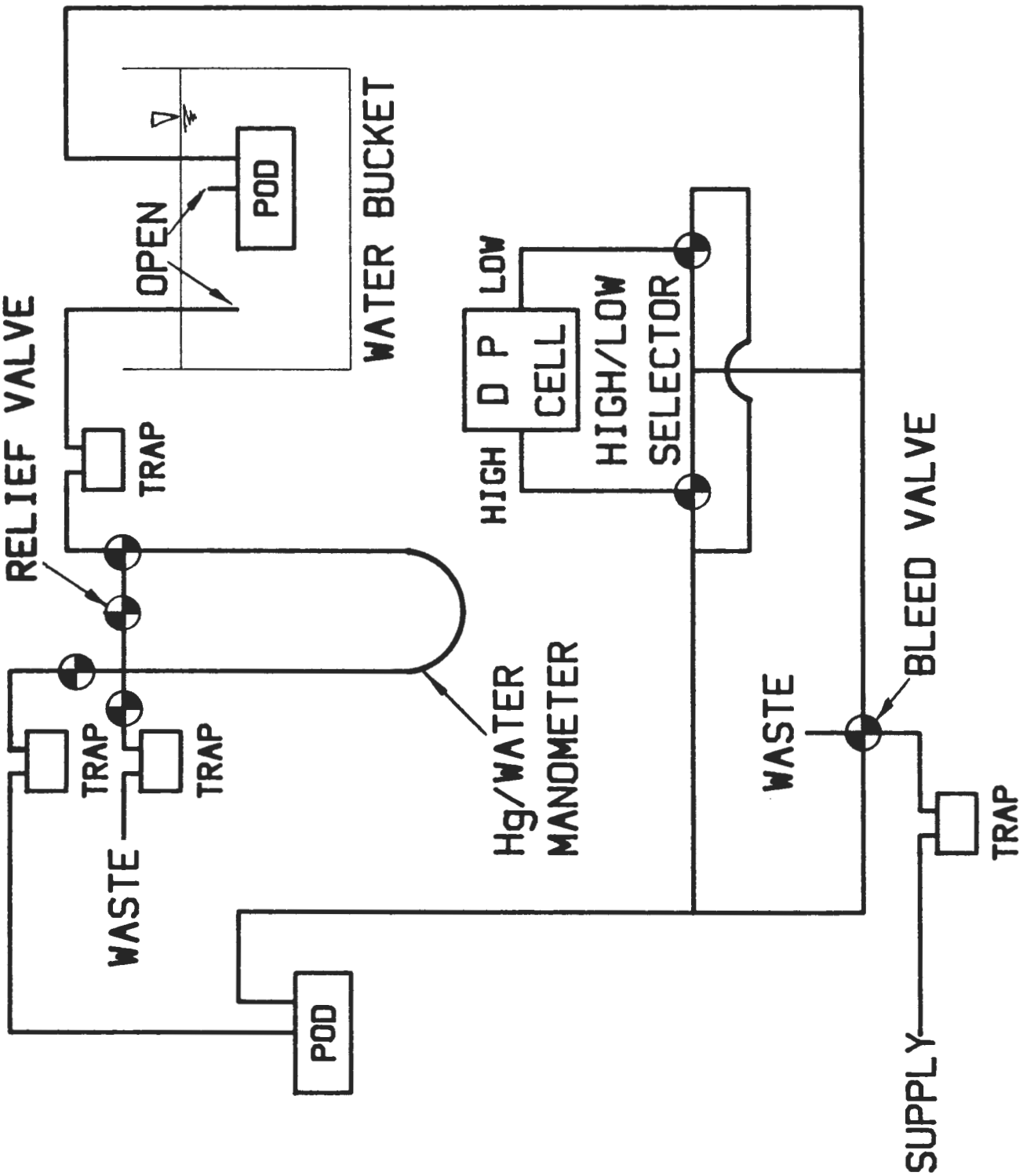

Fig. 3.11 : DP Cell Calibration Connections

```
==========================================================================
HP-75 FILE NAME PCALCH7C   DATE 85/05/17

TIME 10:01:57

PCALCH7C   B  454 09:48 05/17/85

1 DATA -173267.27667,-6909.97752923
2 DATA 176.22684,-.0409554,4.08792259113E-6
3 DATA 2019.952,-.0513582,1.93218356616E-6
4 DATA 4369.244,-.0649039,1.44913767462E-6
5 DATA 6630.712,-.0780495,7.07106781187E-7
6 DATA 8903.158,-.0911888,1.22927259431E-6
7 DATA 11175.604,-.1043237,2.66666666667E-6
8 DATA 13316.314,-.1167708,2.74873708375E-6
9 DATA 11131.692,-.1041796,3.36650164612E-6
10 DATA 8936.092,-.0915566,5.75808610179E-6
11 DATA 6685.602,-.0785465,5.54276304944E-6
12 DATA 4303.376,-.0648057,8.61587681744E-6
13 DATA 2206.578,-.0527283,9.27421754711E-6
14 DATA 16.467,-.0400489,7.50481327031E-6
```

The first line contains the Calibration Constants m, c

Each consecutive line contains the Applied Pressure (Pa), Output (V), Standard Deviation

NOTE: Each output is the average of ten consecutive readings.
The standard deviation is also calculated from these ten consecutive readings.

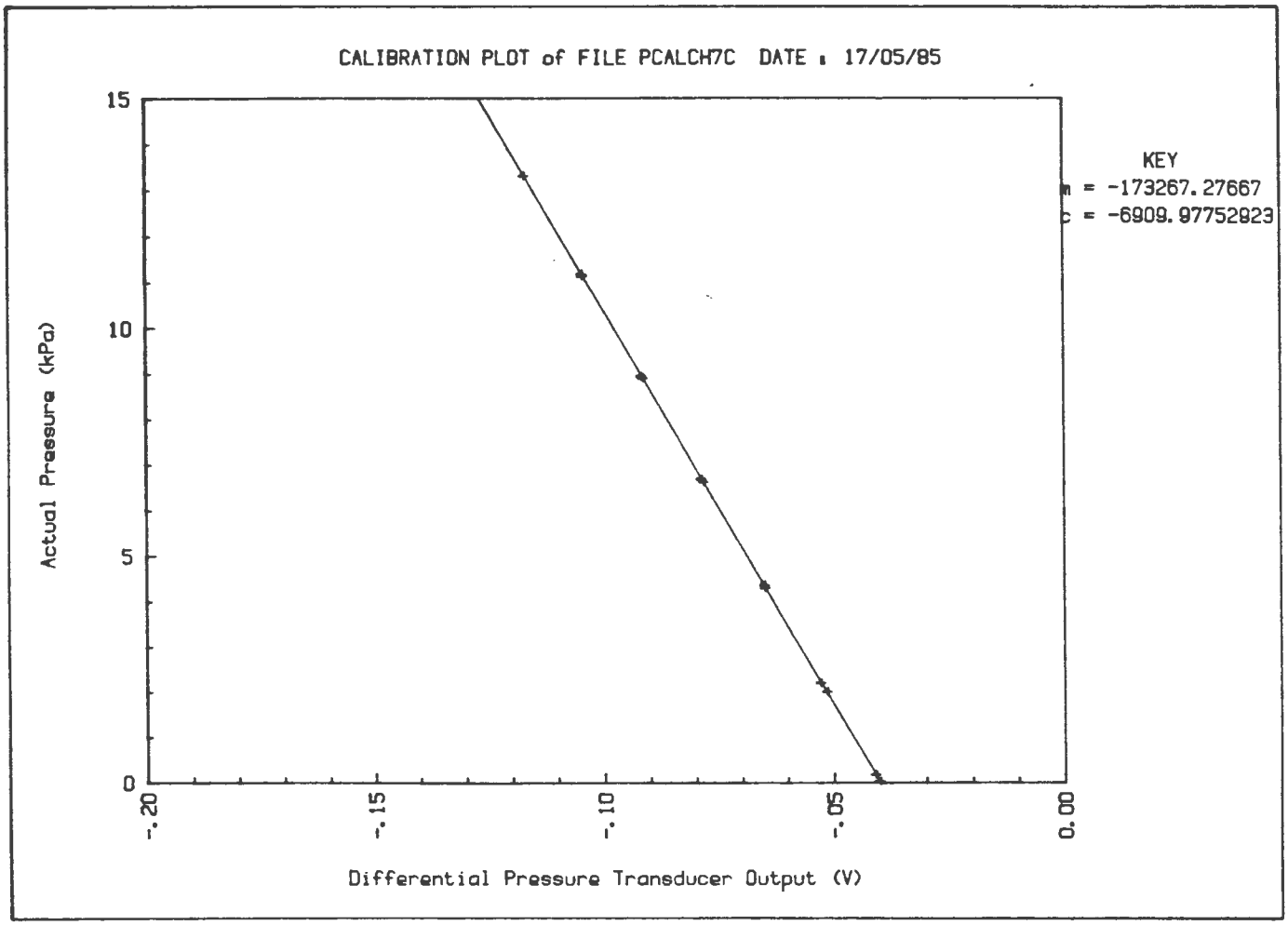

Fig. 3.12 : DP Cell Calibration Output

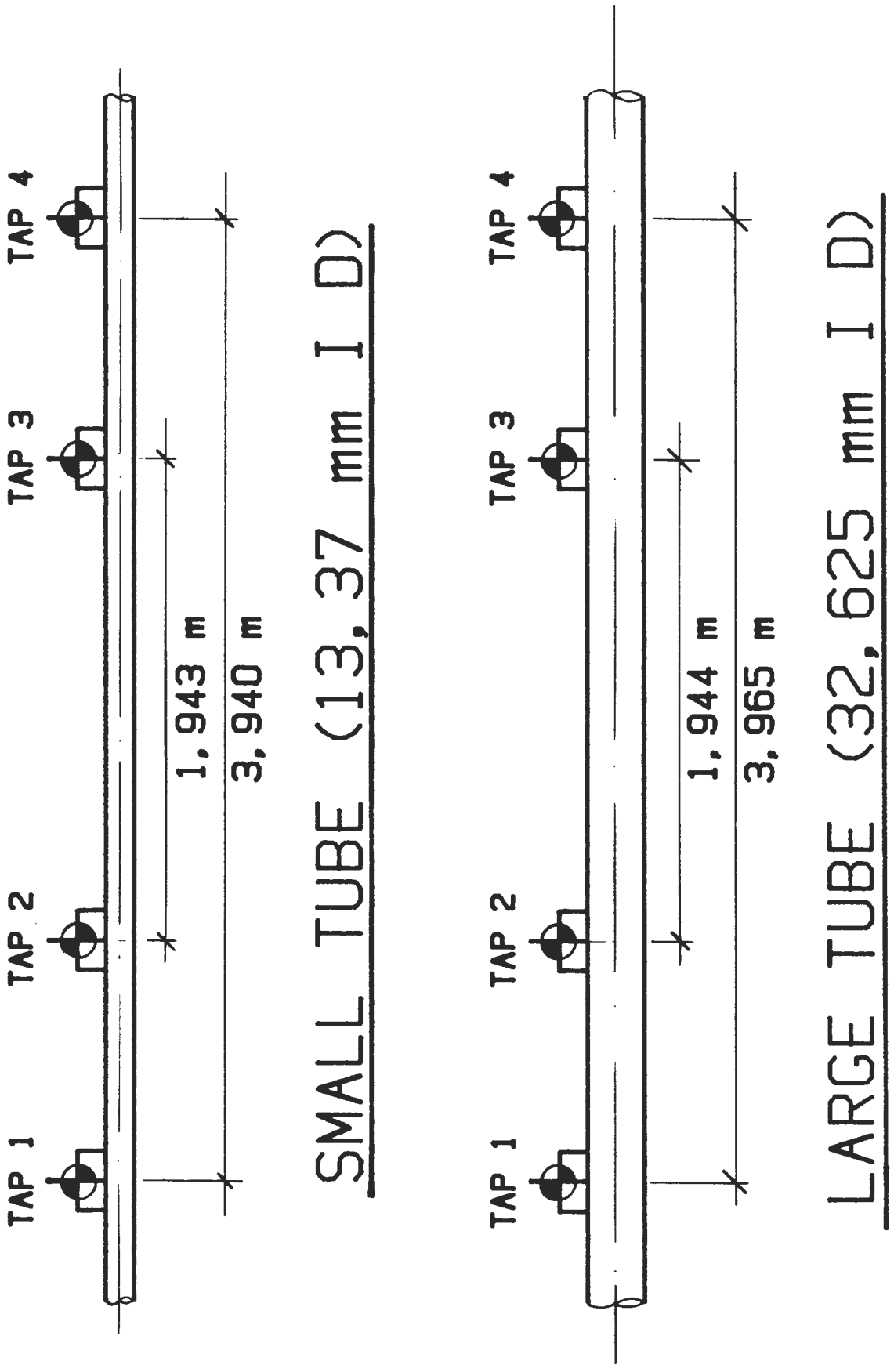

Fig. 3.13 : Tapping Lengths

HP-75C VISCOMETER RUN DATA FILE FORMAT

LINE 1 : Diameter (m), Temperature (°C), S_s , S_m , C_v , L(m)

LINE 2 : Power Supply Voltage (V)

LINE 3 : Load Cell Reading (V/V), DP Cell Output (V), Time(s)

to

LINE 12 : Load Cell Reading (V/V), DP Cell Output (V), Time(s)

Repeated for each Reading

Fig. 3.14 : Data File Format

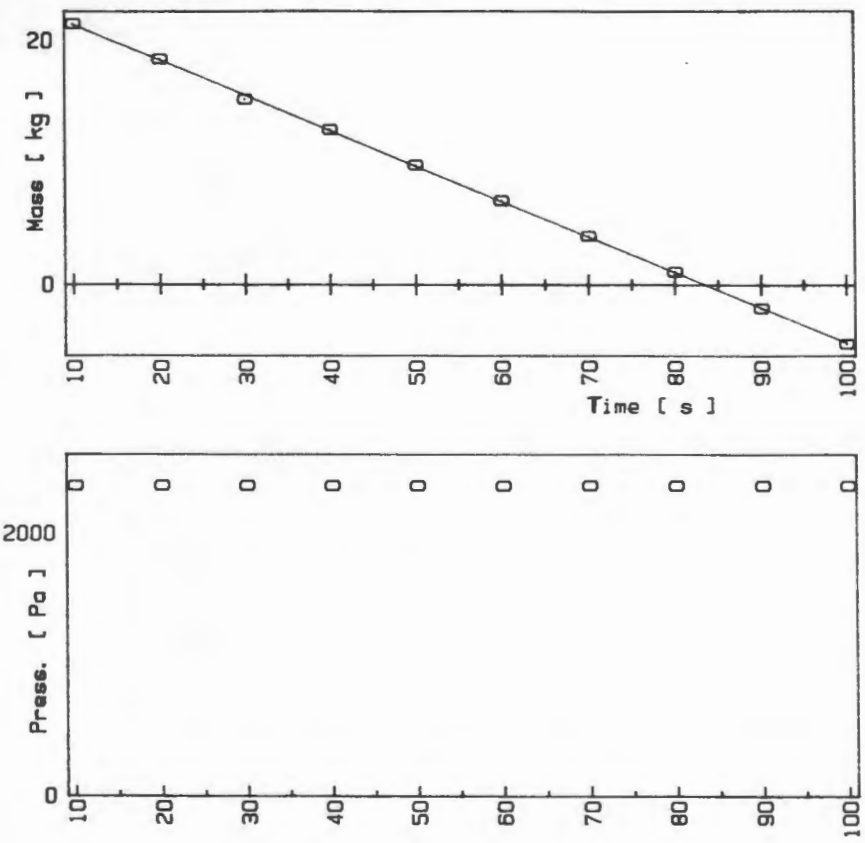

Fig. 3.15 : A READING in Graphical Form

VISCOPX RUN 11.40 24/24/85

RAW FILES TO BE PROCESSED IN THIS RUN :
NAME 1 AL242409
RESULTS FROM DATA FILE AL242409
DIAM .03163
TEMP 17
Ss 2.6500
Sm 1.3933
Cv .2384
LOAD CELL CALIBRATION SLOPE -481572.50141800 CONST 931.26642395
D P CELL CALIBRATION SLOPE -1479336.39488000 CONST -60551.50625940
pH 2.20
Length Between Taps 3.965 m

No	Mass (kg)	Q (M^3/S)	V (m/s)	p (Pa)	P S V
1	-2.883	4.113E-003	5.239	68639	5.405
2	-.655	3.889E-003	4.952	59733	5.405
3	1.898	3.721E-003	4.737	46434	5.405
4	1.046	3.295E-003	4.194	40354	5.405
5	1.766	3.580E-003	4.557	31197	5.405
6	.831	3.513E-003	4.472	45184	5.405
7	6.236	3.311E-003	4.215	27380	5.404
8	-5.949	2.733E-003	3.479	24377	5.404
9	4.666	2.589E-003	3.296	23460	5.404
10	-11.458	1.847E-003	2.352	19481	5.404
11	10.488	1.357E-003	1.728	16359	5.404
12	-10.401	1.149E-003	1.463	15309	5.403
13	16.627	6.288E-004	.801	12898	5.403
14	-.058	2.879E-004	.366	10679	5.403
15	-9.578	1.784E-004	.227	9998	5.403
16	-16.671	1.270E-004	.162	9643	5.404

STORED IN FILE PAL242409

PSV = POWER SUPPLY VOLTAGE

Fig. 3.16 : Print Out from a "VISCOPX" Run

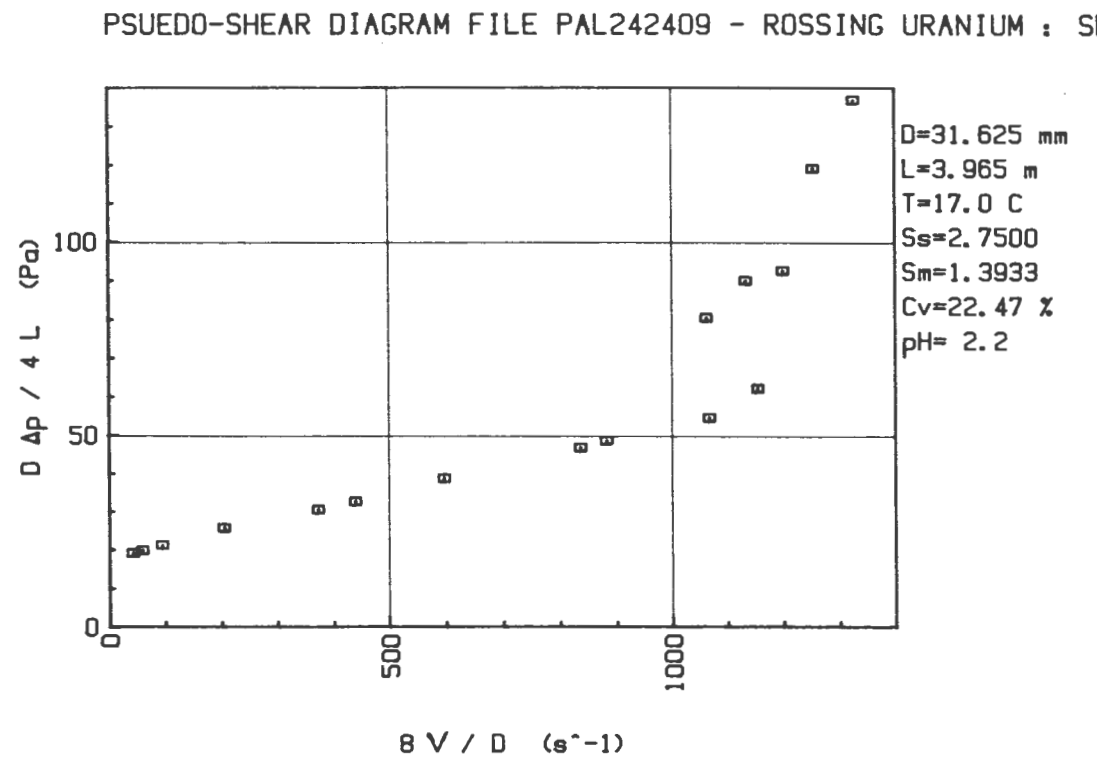

Fig. 3.17 : Processed Data Output as a Pseudo Shear Diagram

CHAPTER 4

END EFFECTS IN THE BBTV

4.1 INTRODUCTION

The output of the BBTV is the pressure drop across the tube, Δp, and the mean slurry velocity, V.

The term Δp, when measured between the two pressure vessels, represents the total energy loss across the tube. This total energy loss may be divided into four components as follows (Fig. 4.1):

1. Losses due to viscous friction
2. Losses due to developing flow (acceleration of the fluid)
3. Entrance and exit losses.
4. Fitting losses (valves, bends, etc.)

For rheological characterisation purposes, we are interested only in the first, viz. losses due to viscous friction. It is essential therefore to either eliminate or account for the other three kinds of energy loss.

From classical Newtonian theory, viscous friction losses are caused by work done against the shear stresses which develop between adjacent fluid laminae. These losses are therefore modelled using shear stresses and the following can be shown from a simple force balance across a tube:

$$\tau_o = \frac{D\Delta p}{4L} \qquad (4.1)$$

In order to account for the other losses, the length L in equation (4.1) is the "hydraulic effective" length, and not the physical tube length (see Fig. 4.1).

Another standard approach used to account for the other losses is by use of a velocity energy head correction factor.

$$H_{tot} = H_f + F_1 \frac{V^2}{2g}$$

where

H_{tot} = total head (energy) loss
H_f = head loss due to viscous friction
F_1 = velocity energy head correction factor

Thus, before rheological characterisation can proceed, it is necessary to determine accurately the hydraulic effective length, or the value of F_1, of the viscometer tubes.

4.2 PREVIOUS WORK

The hydraulic effective length was determined by Lazarus and Sive (Ref. 20) using turbulent flow of clear water, Δp being determined by measuring the difference in air pressure between the two vessels. It was then assumed that this hydraulic effective length would be valid for the rheological characterisation of non-Newtonian slurries.

It should be noted that the overriding concept in the development of the BBTV was simplicity. The above assumption may be open to debate, but it is in line with the concept of simplicity.

4.3 GRAVITY HEAD LAMINAR FLOW OF CLEAR WATER

An experiment was devised to determine the hydraulic effective length of the BBTV tubes using laminar flow of water, using the liquid surface height difference as the driving force.

4.3.1 Theory

With reference to Fig. 4.2

$$\Delta p = \rho g \Delta H$$

$$M = \frac{\Delta H}{2} \times A_{vess} \times \rho$$

$$\therefore \quad \Delta H \equiv \frac{2M}{A_{vess}\rho}$$

$$\therefore \quad \Delta p = \frac{2\,Mg}{A_{vess}}$$

where M = excess mass in L.H. vessel

A_{vess} = cross sectional area of a vessel

From Poiseuille (Ref. 3) $Q = \frac{\pi \Delta p R^4}{8\mu L} = \frac{\pi\, Mg\, R^4}{4 A_{vess} \mu L}$ (4.2)

By definition $M = \rho v$

$\therefore$ For the L.H. vessel $\frac{dM}{dt} = -\rho \frac{dv}{dt} = -\rho Q$

$$\therefore \quad \frac{dM}{dt} = -\frac{\pi\, Mg\, R^4\, \rho}{4\, A_{vess} \mu L} = k\, M$$

where $k = -\frac{\pi\, g\, R^4\, \rho}{4\, A_{vess} \mu L}$

$$\therefore \quad \frac{dM}{M} = k\, dt$$

$$\therefore \quad \int \frac{1}{M}\, dM = k \int 1\, dt$$

$$\therefore \quad \ell n\, M = k\, t + \text{const} \qquad (4.3)$$

at $t = 0$ const $= \ell n\, Me$

where Me = initial excess mass.

Note that equation (4.3) is linear with gradient = k, allowing L to be determined by determining k.

4.3.2 Experimental Procedure

1. The BBTV was approximately half filled with water and the surface levels were allowed to reach equilibrium position.

2. The load cell was calibrated in this position.

3. An excess head was created in the L.H. vessel by pumping water from right to left.

4. The water was then allowed to flow back under gravity head only. Regular readings of mass and time were taken.

This procedure was repeated several times.

4.3.3 Analysis

The data points were plotted as ℓn M against t and typical results are shown in Fig. 4.3. Since the data has a definite curve to it, it would appear that equation 4.3 does not fit the data.

The data was plotted, using the actual physical length, on the conventional Fanning friction factor-Reynolds number diagram, also shown in Fig. 4.3

4.3.4 Discussion

The deviation at high Reynolds number can be explained by a developing flow energy loss (Ref. 21) but no reference could be found for the much larger low Reynolds number deviation, except for the remark by Stokes (see section 2.2.2.2).

4.4 STEADY STATE LAMINAR FLOW OF CLEAR WATER

Using the syphon arrangement shown in Fig. 4.4, a steady state experiment was set up to determine L directly from Poiseuille's Law (equation (4.2)) and to verify the previous results.

4.4.1 Experimental Procedure

1. All components were charged with water.
2. The valve was closed and the load cell was calibrated.
3. The valve was then opened a suitable amount and the aperture held constant.
4. The flow rate Q was measured regularly using the measuring cylinder and a stop watch.
5 When the flow rate had reached steady state, the values of Q and M were noted.
6. Steps 3 to 5 were repeated for several different flow rates.

4.4.2 Results

The results are shown graphically in Fig. 4.5 as a conventional friction factor-Reynolds number diagram. (Actual physical length used for calculations).

4.4.3 Discussion

There is no significant difference between the pseudo-steady state and the steady state experimental results. Since similar results were obtained from two different experiments, the results were assumed to be valid. Referring to Fig. 4.5, low values of Reynolds number were not obtained because of the long time required to reach steady state.

4.5 CORRELATION OF CLEAR WATER LAMINAR FLOW RESULTS

4.5.1 Estimation of Energy Losses in the Developing Flow Region

With reference to Fig. 4.6 (and reference 21), there is a pressure drop due to the fact that the liquid is accelerated in the entrance region of the BBTV tube, from a uniform radial velocity distribution to a parabolic one.

Using the recommended values and equations from reference 21, it can be shown that (referring to Fig. 4.6)

$$\Delta p = P - p_1 = k \rho V^2$$

where P = static pressure in the L.H. vessel

p_1 = pressure where fully developed flow starts

and k = constant in the range 1,92 to 2,1.

The value k = 1,9775, recommended by Schiller (in Ref. 21) was used in the following correlation.

The data collected in section 4.3 was correlated using an effective length factor F and the Reynolds number where F is defined by

$$F = \frac{L}{L_{act}}$$

where L and L_{act} are defined in Fig. 4.1.

Since the entrances and exits of the BBTV tubes are well fared with bell-mouths, the exit and entrance losses were assumed to be negligible.

The results are shown in Fig. 4.7.

4.5.2 Correlation Using a Velocity Energy Head Correction Factor

The data collected in 4.3 was plotted on a pseudo-shear diagram (τ_o vs. 8V/D) together with the theoretical prediction (Poiseuille) in Fig. 4.8 (first graph). The actual tube length was used and the error due to non-viscous friction losses is evident. The total head (energy) loss was modelled using the standard velocity energy head correction factor:

$$H_{tot} = \left(\frac{4\ f\ L_{act}}{D} + F_1\right)\ \frac{V^2}{2g}$$

F_1 was correlated as a linear function of V:

$$F_1 = 17{,}59\ V$$

as shown in Fig. 4.8.

Low velocity data points were ignored for this correlation.

4.6 KAOLIN CLAY SLURRY BBTV TESTS

In order to evaluate the velocity energy head correction factor for non-Newtonian flow, tests were performed on a kaolin clay slurry (C_v = 18%).

4.6.1 Experimental Procedure

Tube pressure tappings were introduced into the BBTV tubes as shown in Fig. 3.13, so that the viscous friction pressure drop could be measured directly. The air pressure difference between the vessels, as well as the tube tapping pressure drop, was measured at each READING.

The basic procedure was as described in Chapter 3.

Several tests were performed using different combinations of the pressure tappings to ensure that fully developed flow existed between the tappings.

4.6.2 Results

Typical results are shown in Fig. 4.9. The difference caused by end effects is significant and can be clearly seen. The laminar/ turbulent transition is indicated at a pseudo-shear rate of 1500 (V = 6 m/s).

4.6.3 Correlation Using a Velocity Energy Head Correction Factor

The velocity energy head correction factor, F_1, was plotted against velocity on logarithmic axes in Fig. 4.10 and linear axes in Fig. 4.11.

$$F_1 = (H_{tot} - H_f) \times \frac{2g}{V^2}$$

In the range $2 < V < 6$ m/s which, in this case, is the range of interest for rheological purposes, F_1 was found to be nearly constant at

$$F_1 = 0{,}32 \quad \text{(Fig. 4.11)}$$

In turbulent flow F_1 decreases ($V > 6$ m/s).

For velocities less than 2 m/s, F_1, increases rapidly with decreasing velocity (Fig. 4.10).

4.7 DISCUSSION

The velocity energy head correction factors are quite different for clear water and kaolin clay slurry (F_1 = 17,59 V and 0,32 respectively).

From theoretical considerations, it might be suspected that they would differ, since the velocity distributions are different.

What this investigation has brought to light is the fact that the end effects for each are significant (Figs. 4.8 (top) and 4.9) and that they are fundamentally different from each other.

Since the kaolin is different from clear water, it can be expected that the value of F_1 = 0,32 will change for other non-Newtonian slurries.

From Fig. 4.9 it can be seen that end effects lead to a pseudo-shear diagram of significantly different shape. There is also no clear indication of laminar/turbulent transition, as is the case using tube pressure tappings. These two factors are of vital importance for rheological characterisation.

4.8 CONCLUSIONS

1. The correlation using the theory of Goldstein (Ref. 21) shown in Fig. 4.7, although showing a similar trend, does not accurately predict the end effects shown by the BBTV with clear water in laminar flow.

2. The BBTV end effects in laminar flow can be correlated using a velocity energy head correction factor of

   $F = 17,59\ V$ for clear water
   and $F_1 = 0,32$ for kaolin (C_v = 18%)

3. The BBTV end effects of non-Newtonian flow are significant and fundamentally different from clear water, and unpredictable.

4. For the BBTV to yield meaningful results, Δp must be determined using tube pressure tappings. Air pressure differences between vessels cannot be used.

5. For each new slurry tested, tests should be done using different combinations of the pressure tappings in order to ensure that fully developed flow exists between the pressure tappings.

6. A low Reynolds number deviation has been reported which may be peculiar to the BBTV.

   For clear water, the probable cause is complex non-linear surface tension effects (Ref. 22). If this is not so, then the effect reported by Stokes in Chapter 2 may have been observed.

   For kaolin, the probable cause is yield stress effects on the walls of the vessels.

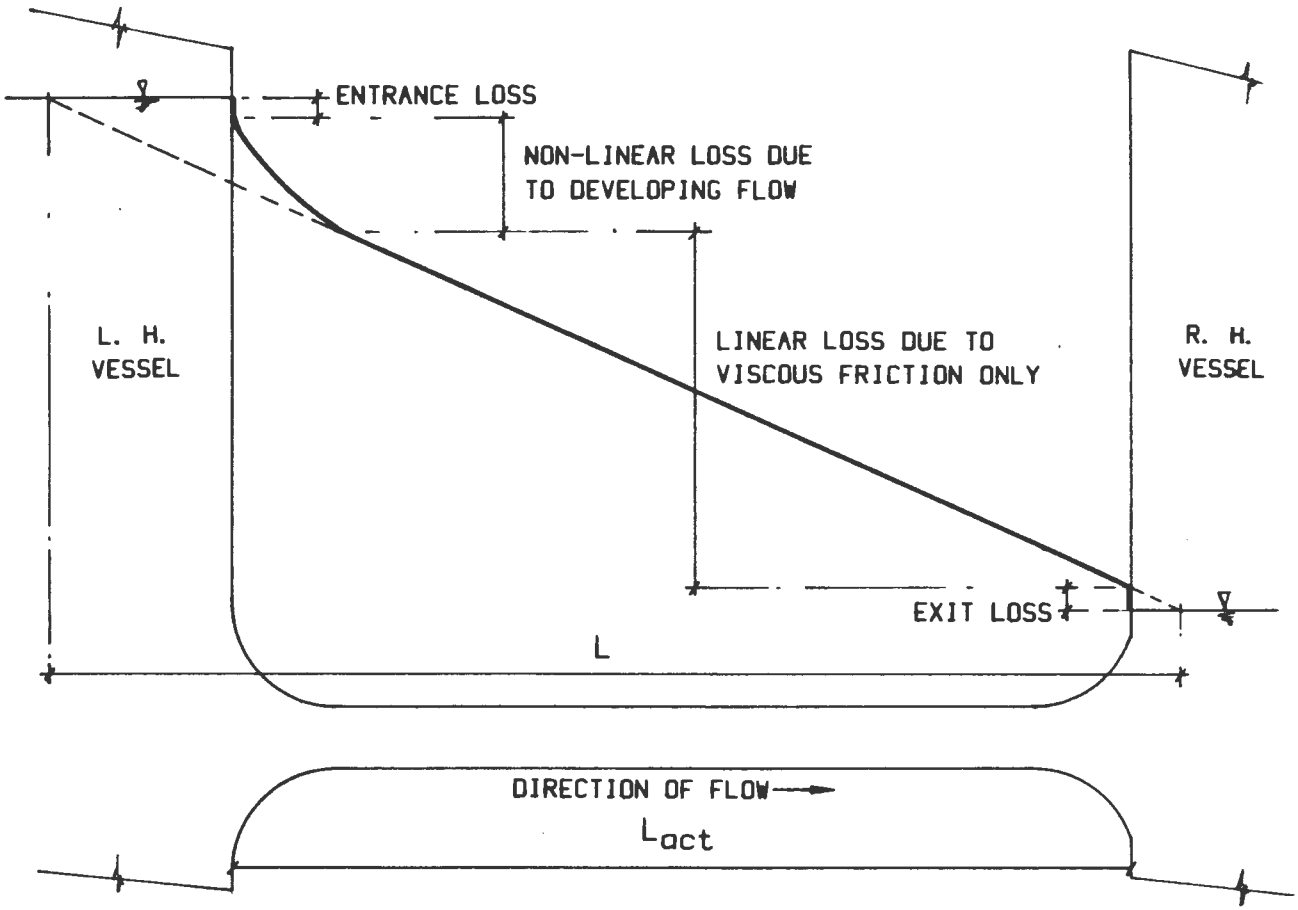

Fig. 4.1 : The hydraulic gradient in a BBTV tube

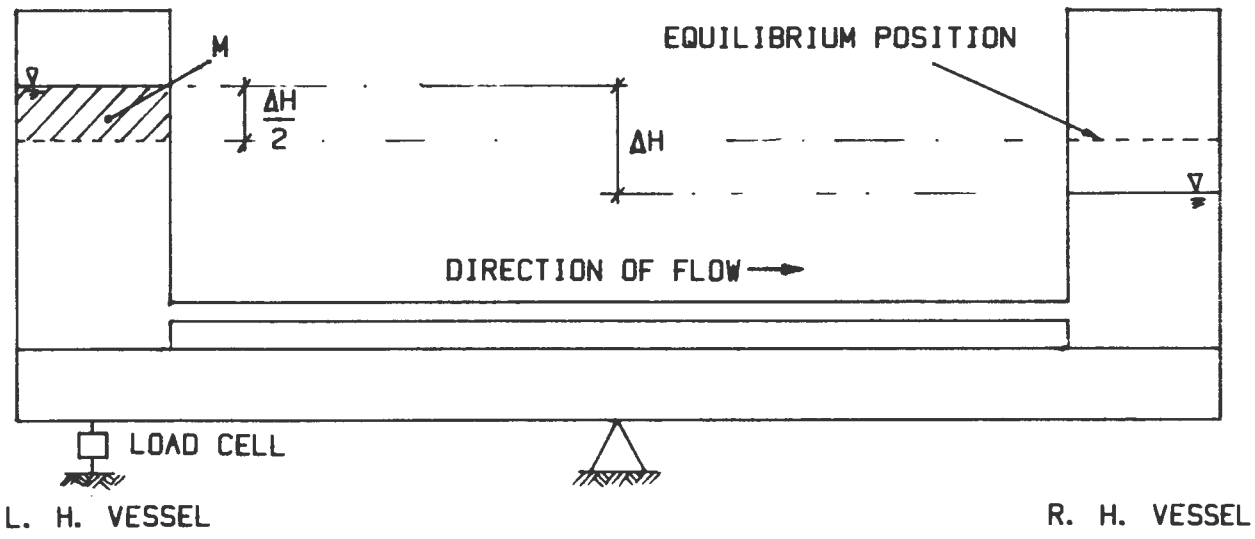

Fig. 4.2 : Apparatus for gravity head laminar flow of clear water

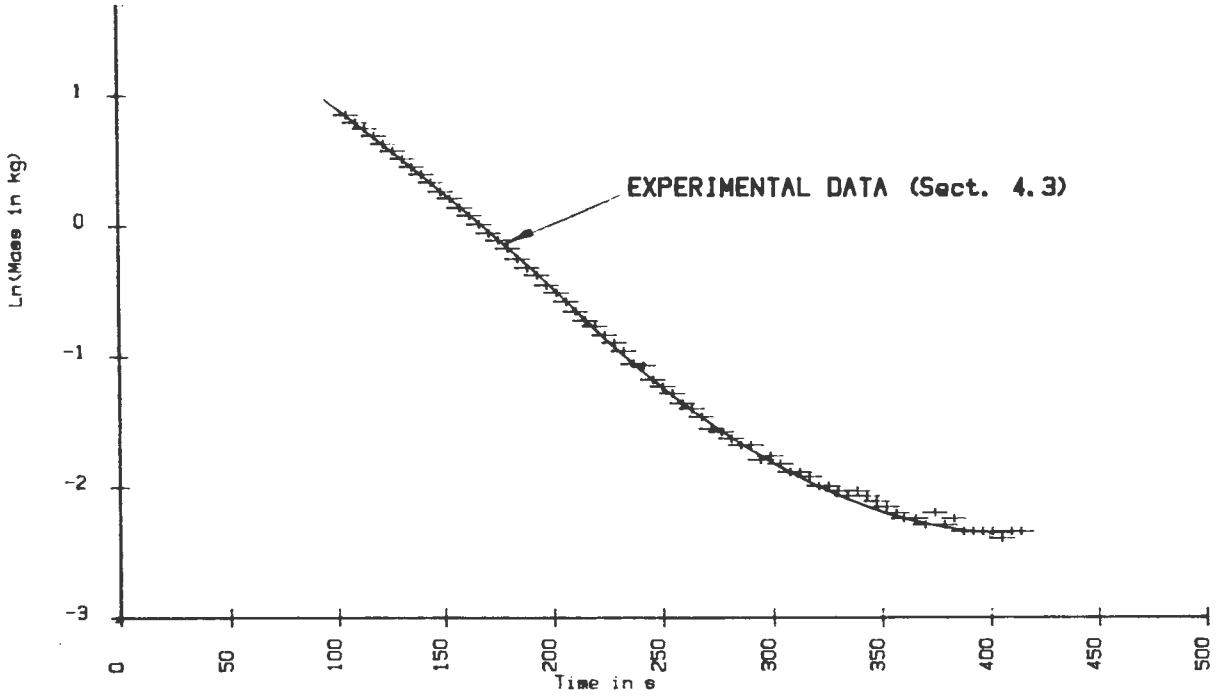

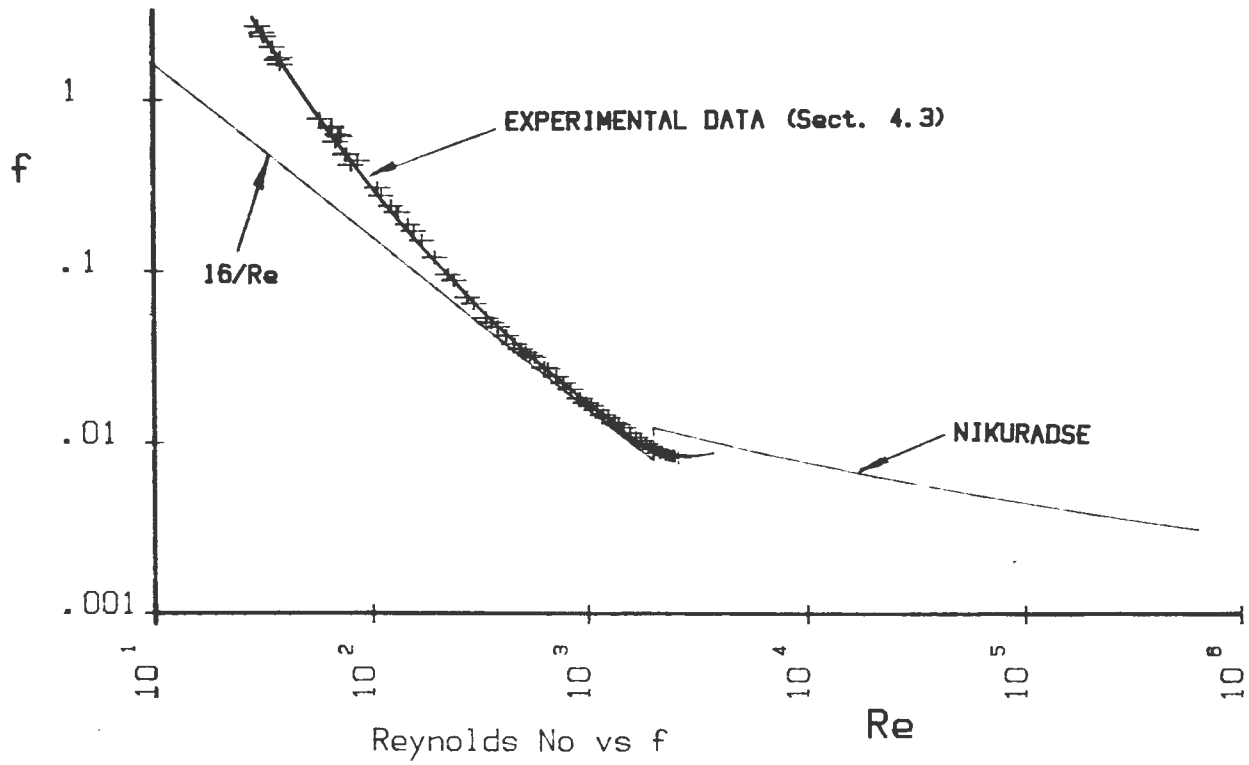

Fig. 4.3 : Experimental results for gravity head laminar flow of clear water

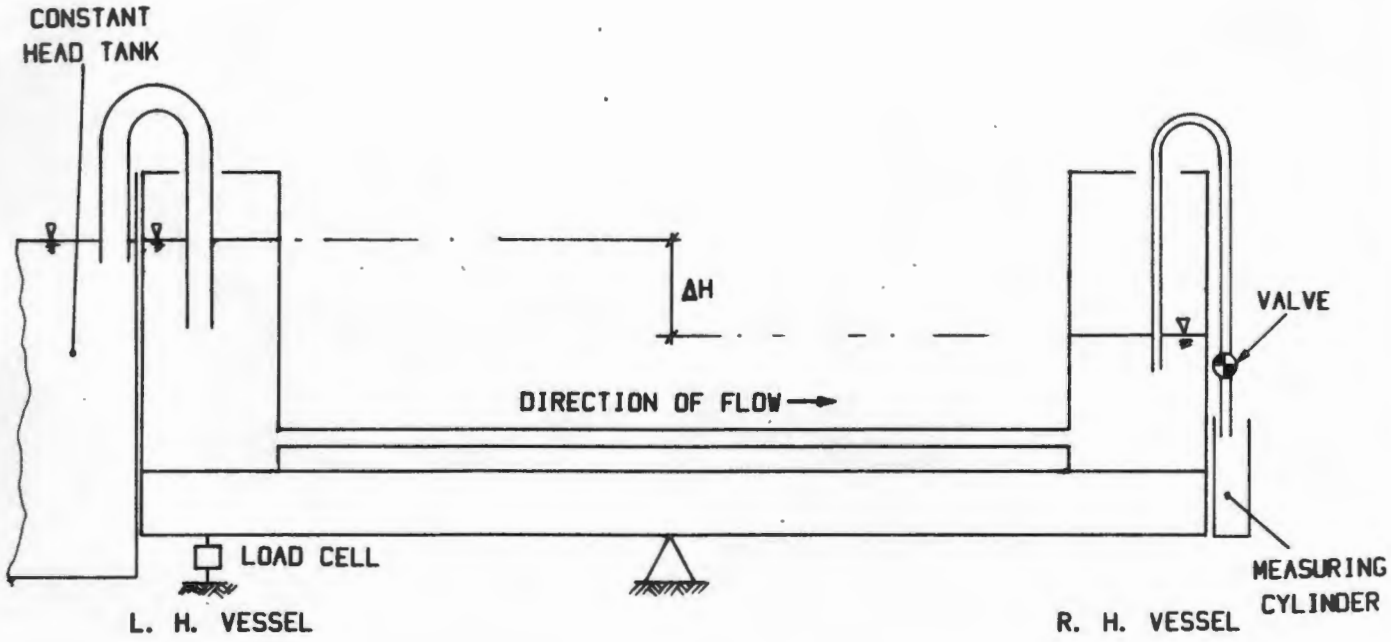

Fig. 4.4 : Apparatus for steady state laminar flow of clear water

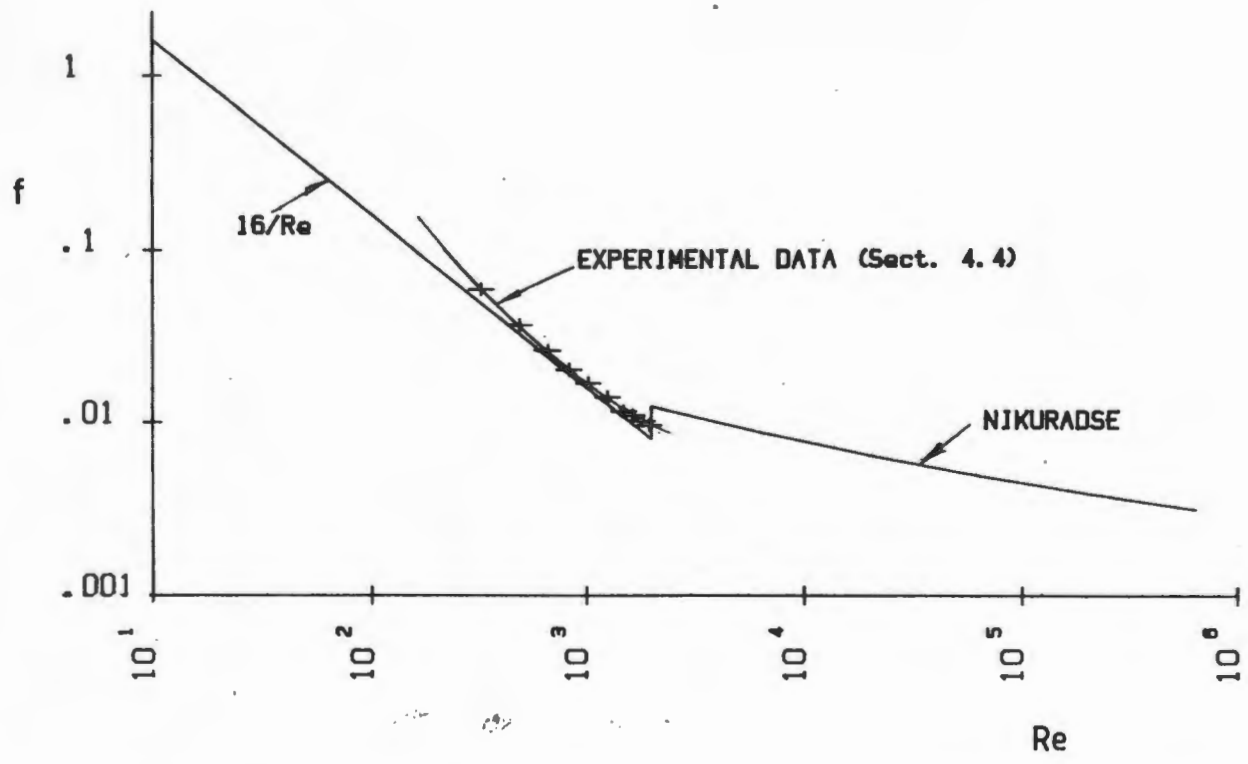

Fig. 4.5 : Experimental results for steady state laminar flow of clear water

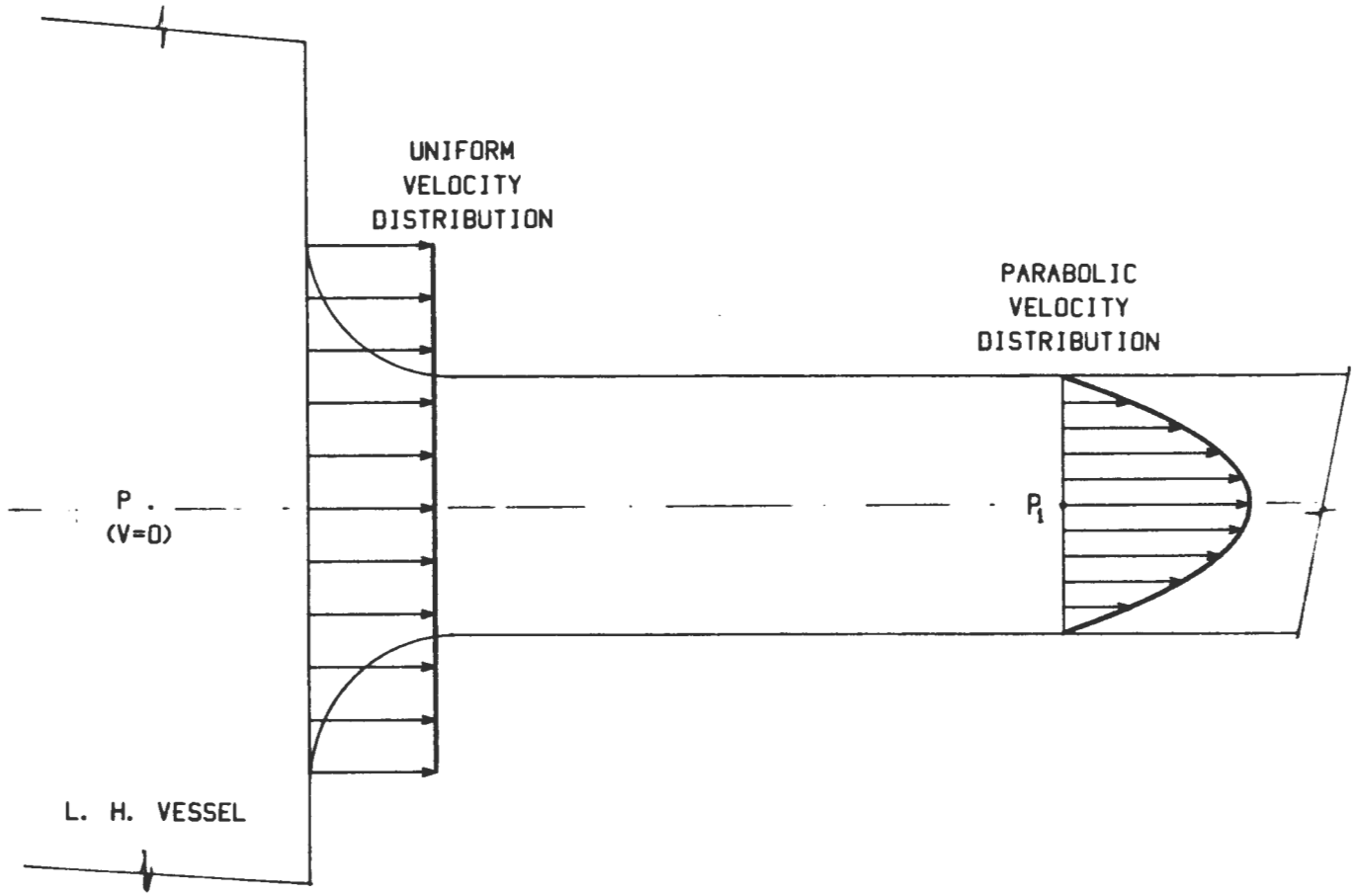

Fig. 4.6 : The velo city distributions in the inlet of a BBTV tube

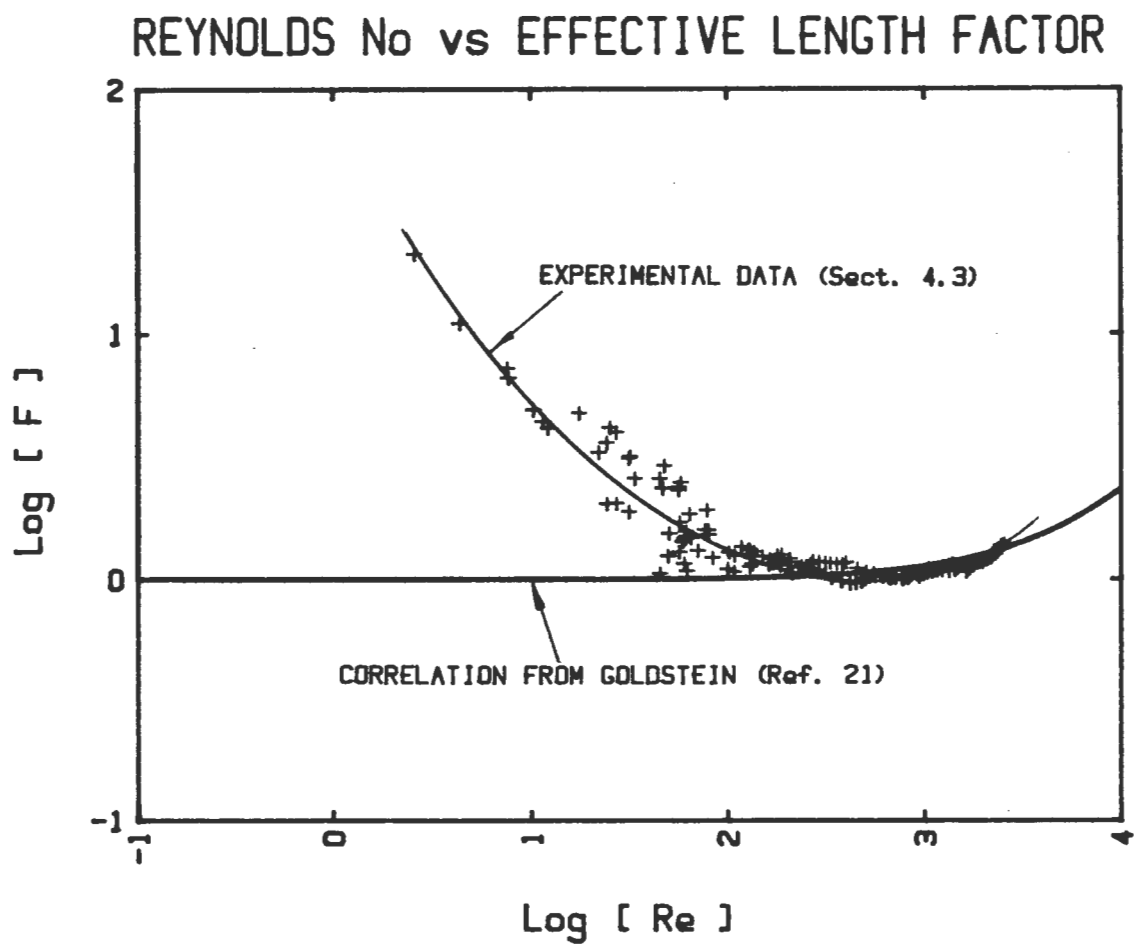

Fig. 4.7 : Correlation using the theory from Goldstein (Ref. 17)

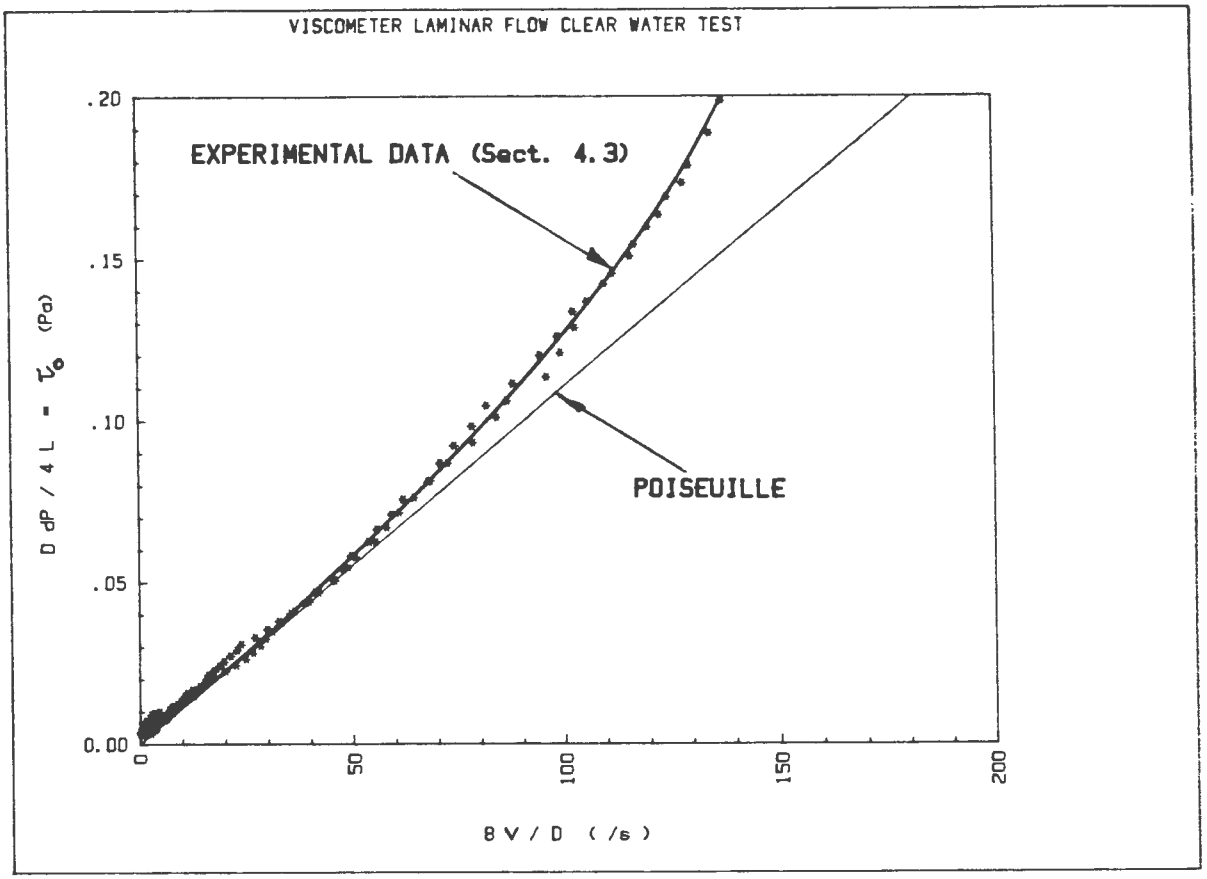

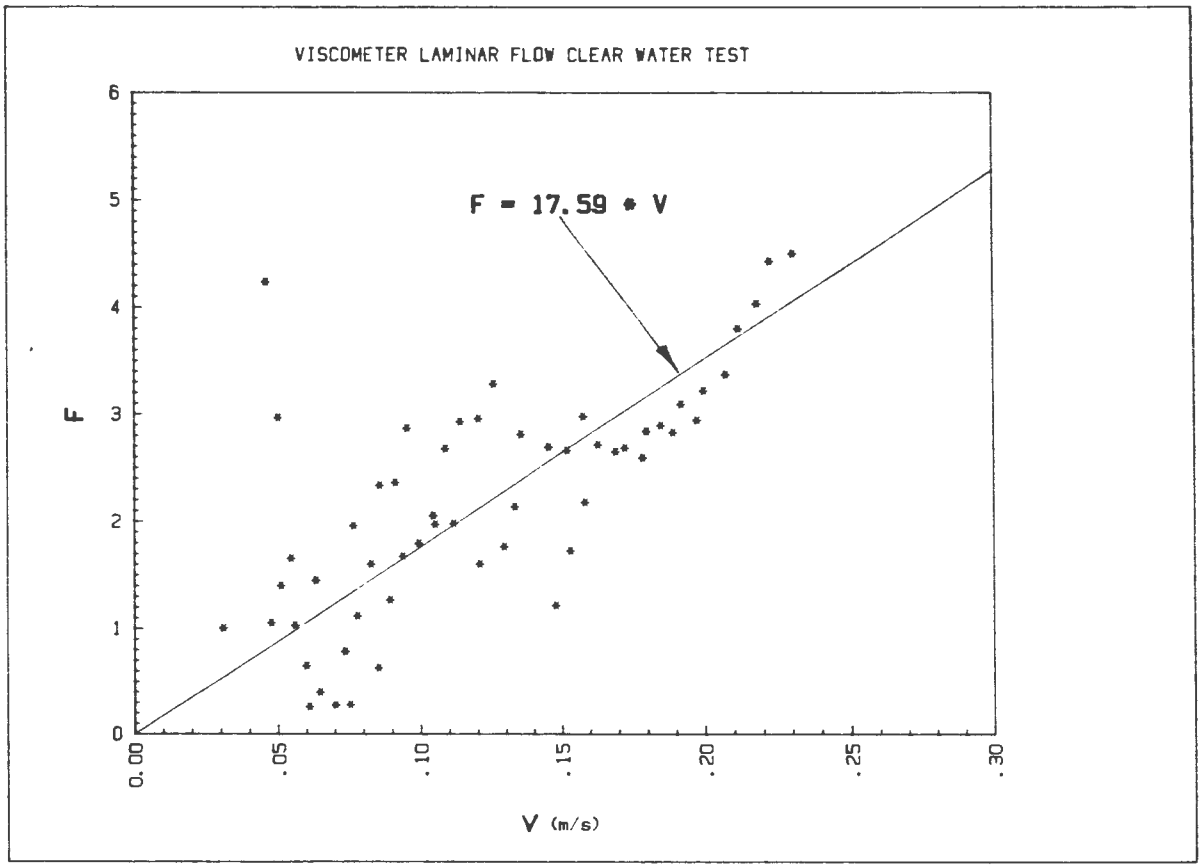

Fig. 4.8 : Experimental results and correlation for clear water

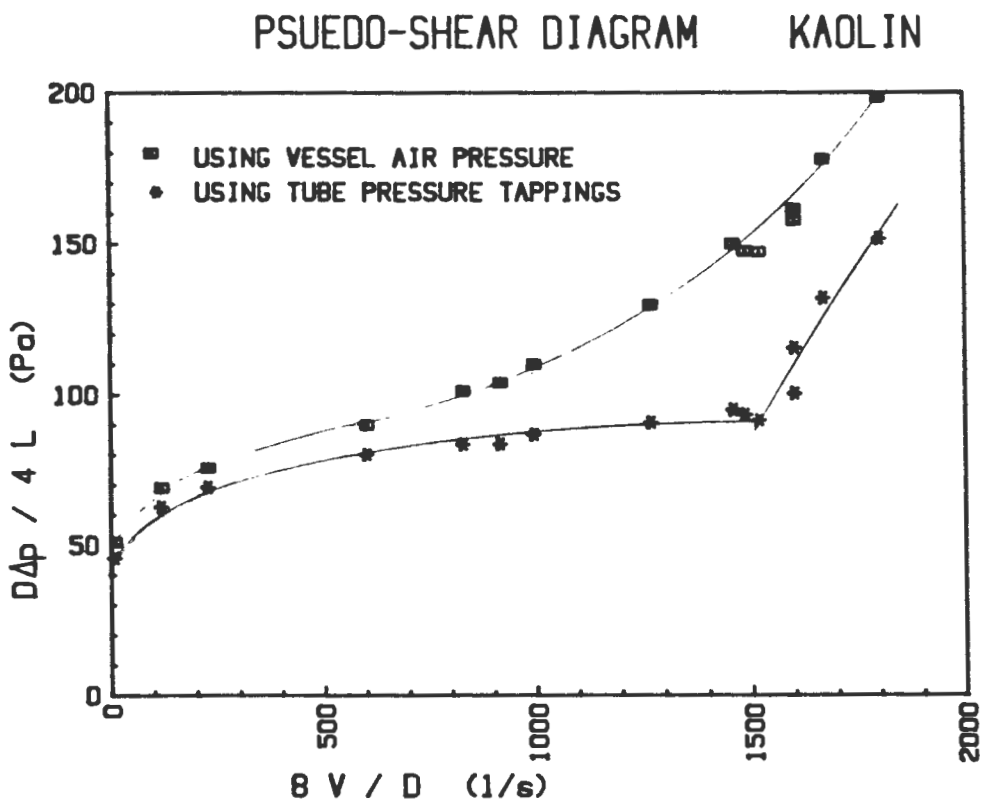

Fig. 4.9 : Experimental results for kaolin

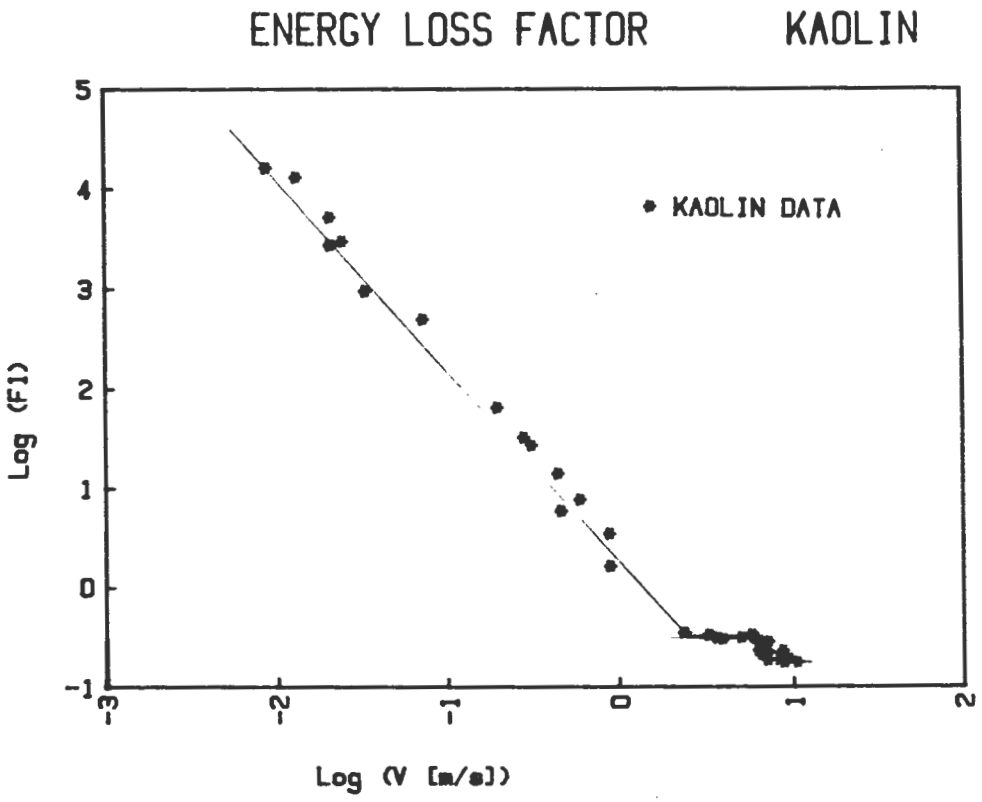

Fig. 4.10 : Velocity energy head correction factor for kaolin plotted o
logarithmic axes

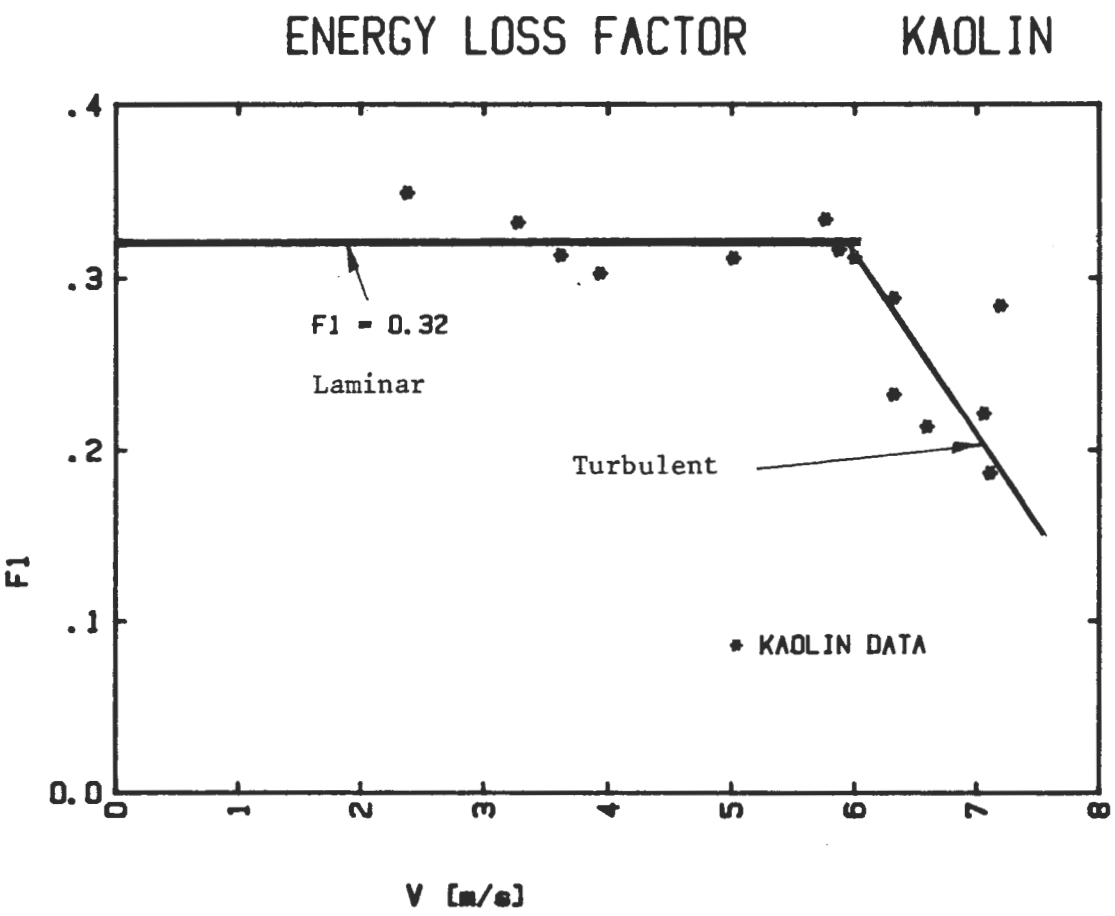

Fig. 4.11 : Velocity energy head correction factor for kaolin plotted on linear axes

CHAPTER 5

RHEOLOGICAL CHARACTERISATION PROCEDURE

5.1 INTRODUCTION

A tube viscometer yields a series of co-ordinates of velocity and pressure drop ($V, \Delta p$). These results must be processed in order to give the required rheology.

The technique recommended in the literature (for example Ref. 4, 5, 6 and 7) is to make use of the Rabinowitsch-Mooney relation (see Appendix A) and reduce the pseudo-shear diagram to a rheogram.

The main argument for the use of the apparent flow behaviour index, n', is that it "has been found to be very nearly a constant over wide ranges of shear stress for a great variety of non-Newtonian fluids" (Ref. 8).

The data accumulated for this thesis indicated either a Bingham Plastic or Yield Pseudo-Plastic rheology, for which n' is clearly not a constant. Figs. 5.1 and 5.2 show the relationship between Ln $[\tau_o]$ and Ln [8V/D] for a Bingham Plastic and a Yield Pseudo-Plastic. The asymptotes to the flow curves are also shown. (n' is defined as the slope of the flow curves.) For a Bingham Plastic (Fig. 5.1) n' lies in the range $0 \leq n' \leq 1$. For a Yield Pseudo-Plastic (Fig. 5.2), n' lies in the range $0 \leq n' \leq n$.

The literature cited acknowledges this possibility, stating that in such a case, n' should be evaluated from the tangent to the curves. For theoretical work, where the derivative can be evaluated satisfactorily, such a solution is perfectly acceptable. For the reduction of experimental data, however, this solution poses major problems.

5.2 SYNTHETIC DATA

In order to evaluate the usefulness and accuracy of the technique using the Rabinowitsch-Mooney relation, a theoretically perfect synthetic set of BBTV data points was generated.

For simplicity (in order to use a linear regression and show degree of accuracy), the Bingham Plastic model was used. The Buckingham equation (Equation 5.1) was used to generate the data points, and these were then set up in a data file compatible with a normal BBTV data file.

$$\frac{8V}{D} = \frac{\tau_o}{\eta_p}\left[1 - \frac{4\tau_y}{3\tau_o} + \frac{\tau_y^4}{3\tau_o^4}\right] \qquad (5.1)$$

Rheological constants used were

$$\tau_y = 120 \text{ Pa}$$
$$\eta_p = 0{,}01 \text{ Pa s}$$

These values are similar to those expected for the "thick" slurries tested in this thesis.

The synthetic data thus generated is presented in Fig. 5.3.

5.3 REDUCTION TECHNIQUE AND RESULTS

The reduction technique used was as follows:-

1. The data points were plotted on a log-log diagram.

2. Using least squares polynominal regression, a curve was fitted to the data.

3. The first derivative of this curve (n') was evaluated at each data point.

4. The true rate of shear was then calculated at each data point using the Rabinowitsch-Mooney relation, thus generating true rheogram points.

5. A least squares linear regression was then performed on the rheogram points, in order to extract the Bingham Plastic rheology constants (τ_y and η_p).

For this technique to be valid, the initial values of τ_y = 120 Pa and η_p = 0,01 Pa s should be obtained in step 5.

This procedure was followed five times, each time using a higher order of polynomial fit. The results are shown in Figs. 5.4, 5.5, 5.6, 5.7, 5.8.

The error inherent in this technique is summarised graphically in Fig. 5.9.

5.4 DISCUSSION OF REDUCTION TECHNIQUE

The reduction technique used above contains significant inherent errors. The yield stress error may be acceptable, but the residual error of some 6% in plastic viscosity would put a lower limit on the accuracy of work in this field. The trend shown in Fig. 5.9 indicates that higher order regression would not resolve this error.

The above results were obtained using a perfect set of data points. Real data will contain experimental error. This would lead to higher inherent error, since the higher order fits would be less stable. The error of 6% was obtained for particular values of τ_y amd η_p. This error could increase or decrease depending on these values, and the range of velocities considered.

On these grounds, this technique has been rejected.

5.5 NEW TECHNIQUE

A new technique for tube viscometer data reduction was developed.

In the absence of a suitable link between the pseudo-shear rate (8V/D) and the true shear rate $(-du/dr)_o$, the principle of extracting rheological constants (i.e. yield stress (τ_y), fluid consistency index (K) and flow behaviour index (n)) from a rheogram was abandoned and these parameters were extracted directly from the pseudo-shear diagram.

Assuming a Yield Pseudo-Plastic rheology, i.e.

$$\frac{8V}{D} = \frac{4n}{K^{1/n}\tau_o^3} (\tau_o - \tau_y)^{\frac{1+n}{n}} \left[\frac{(\tau_o - \tau_y)^2}{1 + 3n} + \frac{2\,\tau_y(\tau_o - \tau_y)}{1 + 2n} + \frac{\tau_y^2}{1+n} \right] \qquad (5.2)$$

The following technique was used:

1. A pseudo-shear diagram was plotted using the pseudo-shear rate (8V/D) as abscissa and wall shear stress (DΔp/4L) as ordinate. Data points in laminar flow only from both tubes are used.

2. The best curve is fitted to the data by eye.

3. τ_y is read off as the ordinate intercept.

4. Three other co-ordinates are then read from the curve. These points are selected to cover the data range as extensive as possible.

5. Using the value of τ_y from step 3 above, these co-ordinates are used successively three times in pairs to solve equation 5.2 for K and n.

6. These values (τ_y, K and n) are then inserted in equation 5.2 to plot three curves through the data.

7. This process is repeated until a satisfactory fit of equation 5.2 to the data points is obtained.

5.6 ILLUSTRATION OF THE NEW TECHNIQUE

In order to illustrate the new technique, the rheological characterisation procedure for the C_v = 17,71% Kaolin slurry is documented below:

1. The pseudo-shear diagram was plotted in Fig. 5.10 using laminar flow data only from both tubes.

2. The best curve through the data was drawn (by hand)(Fig. 5.10).

3. τ_y was read off as the ordinate intercept (Fig. 5.10):
   τ_y = 80 Pa

4. The three points marked 1, 2 and 3 were selected and their co-ordinates were scaled from the graph:

   X1 = 1000 s^{-1} Y1 = 145 Pa
   X2 = 2000 s^{-1} Y2 = 167 Pa
   X3 = 4000 s^{-1} Y3 = 189 Pa

5. Using the value τ_y = 80 Pa and the above three co-ordinates three times in pairs, three sets of values for K and n were obtained by solving equation (5.2) (i.e. given two data points, set up equation (5.2) as two simultaneous equations and solve for the two unknowns).

   Set A: Using 1 and 2 gives K = 1,2953 and n = 0,50225
   Set B: Using 1 and 3 gives K = 2,2942 and n = 0,43245
   Set C: Using 2 and 3 gives K = 4,0027 and n = 0,36625

6. Using these three sets (A, B and C above) of rheological constants, three curves were plotted on the experimental data (Fig. 5.11).

7. This process was repeated using slightly different values for τ_y and points 1, 2 and 3, scaling these each time from the graph.

8. By observation it was decided that set B above gave the best fit. (see Fig. 7.1).

5.7 CONCLUSION

For fluids with a yield stress, the Rabinowitsch-Mooney relation cannot be used for data reduction since n' is not a constant and its value at any particular pseudo-shear rate cannot be accurately determined.

A technique has been developed whereby rheological constants can be extracted directly from the pseudo-shear diagram.

Although this technique relies heavily on an assumed initial rheological model, this was not found to be a problem and the technique worked satisfactorily for data reduction in this thesis.

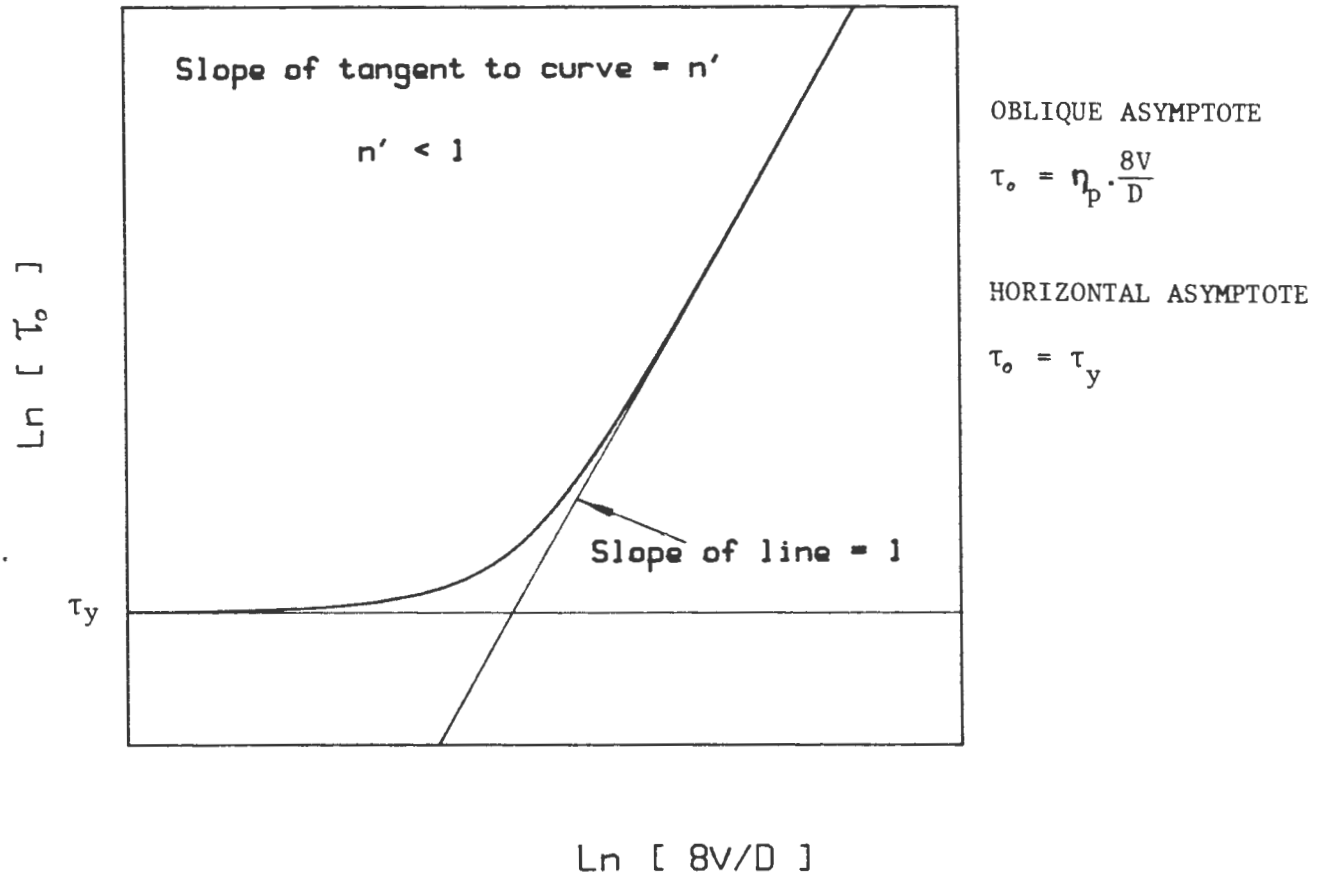

Fig. 5.1 : Tube Flow for a Bingham Plastic - Eq. 5.1
(Logarithmic Axes)

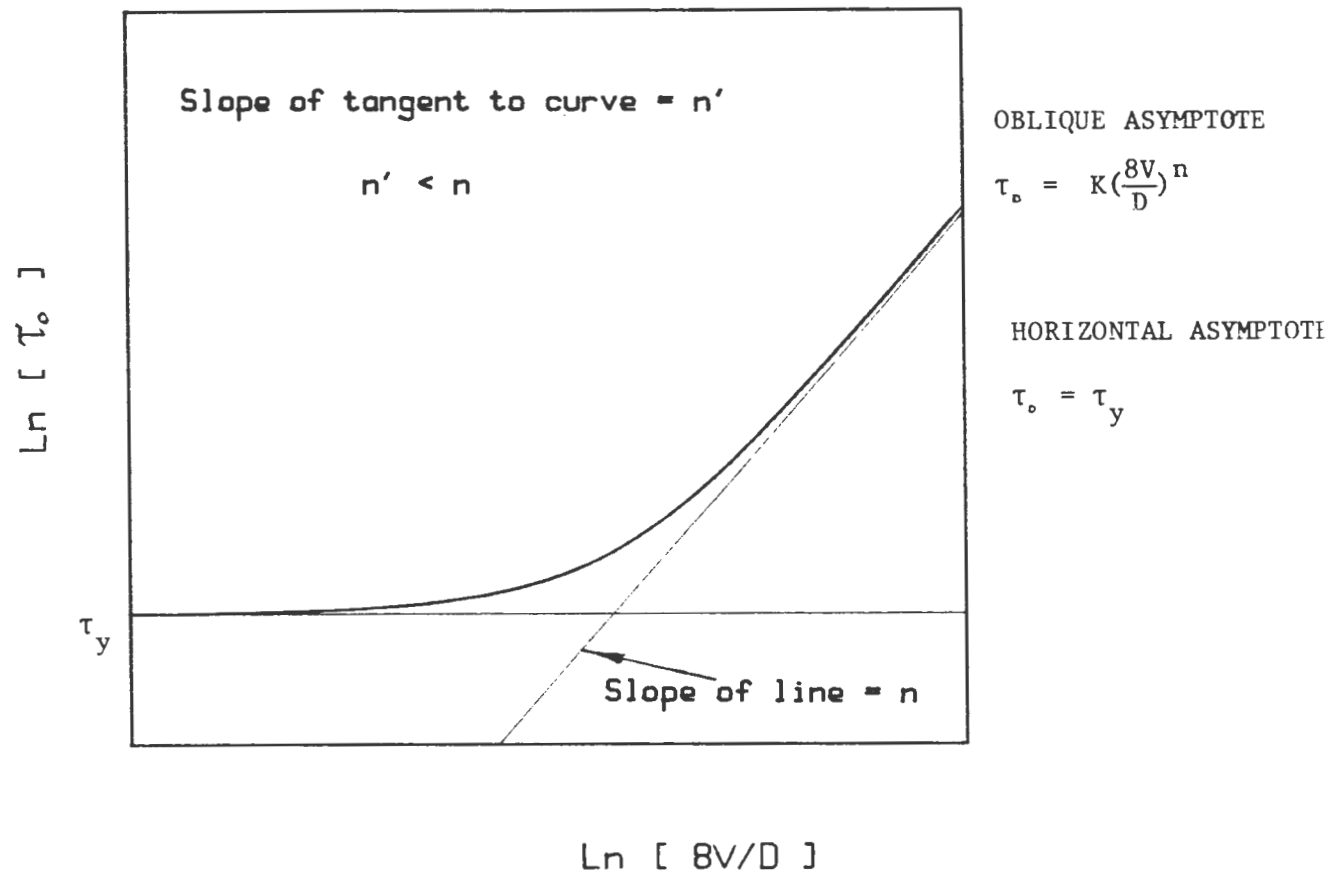

Fig. 5.2 : Tube Flow for a Yield Pseudo-Plastic - Eq. 5.2
(Logarithmic Axes)

BBTV VISCOMETER TEST RESULTS : SYNTH_DAT
A

FILE NAME : PBL18TEST

PARTICLE SIZE RANGE	: SYNTH_DATA
TUBE DIAMETER	: 31.625 mm
TUBE LENGTH	: 3.965 m
SLURRY TEMPERATURE	: 16 C
SOLID RELATIVE DENSITY	: 2.75
MIXTURE RELATIVE DENSITY	: 1.2559
VOLUMETRIC CONCENTRATION	: 14.62 %
pH	: 7

No	v [m/s]	Δp [Pa]	8 V / D Psuedo-Shear Rate [1/s]	D Δp / 4 L Wall Shear Stress [Pa]
1	.006	60607	1	120.85
2	.022	61058	6	121.75
3	.049	61509	12	122.65
4	.086	61961	22	123.55
5	.134	62412	34	124.45
6	.190	62863	48	125.35
7	.256	63315	65	126.25
8	.330	63766	83	127.15
9	.413	64217	104	128.05
10	.504	64669	127	128.95
11	.603	65120	153	129.85
12	.710	65571	180	130.75
13	.824	66023	208	131.65
14	.945	66474	239	132.55
15	1.073	66925	271	133.45
16	1.208	67377	305	134.35
17	1.349	67828	341	135.25
18	1.496	68279	378	136.15
19	1.649	68731	417	137.05
20	1.809	69182	458	137.95
21	1.974	69634	499	138.85
22	2.144	70085	542	139.75
23	2.319	70536	587	140.65
24	2.500	70988	632	141.55
25	2.686	71439	679	142.45
26	2.876	71890	728	143.35
27	3.072	72342	777	144.25
28	3.271	72793	828	145.15
29	3.475	73244	879	146.05
30	3.684	73696	932	146.95

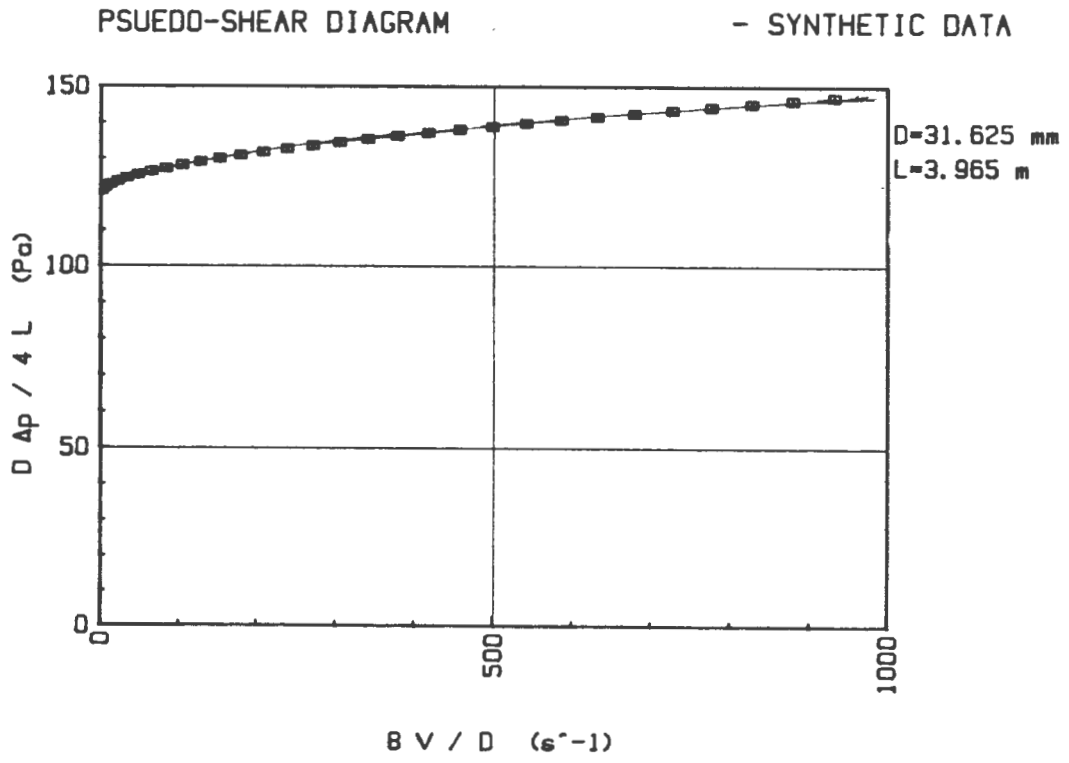

Fig. 5.3 : Synthetic Data

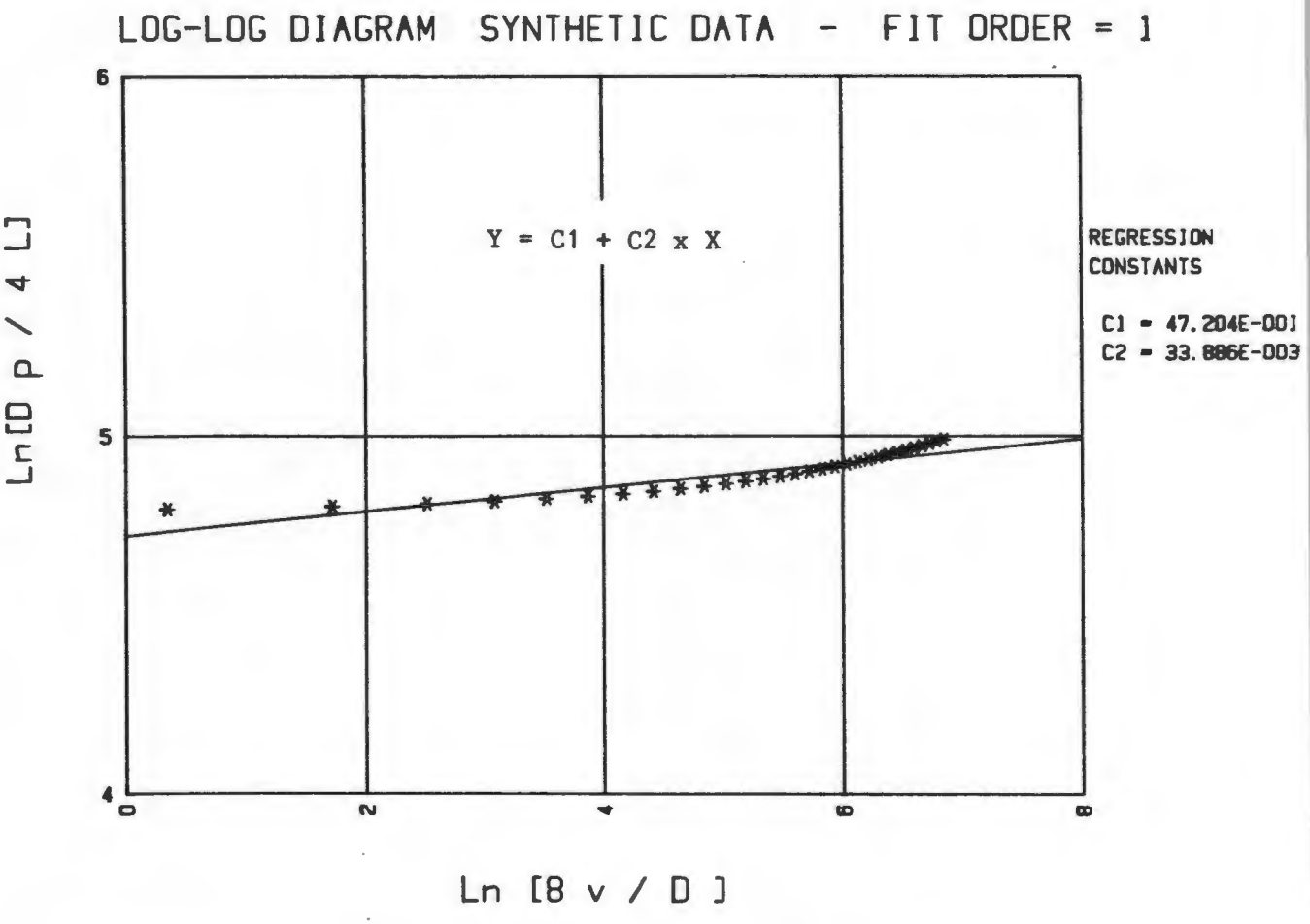

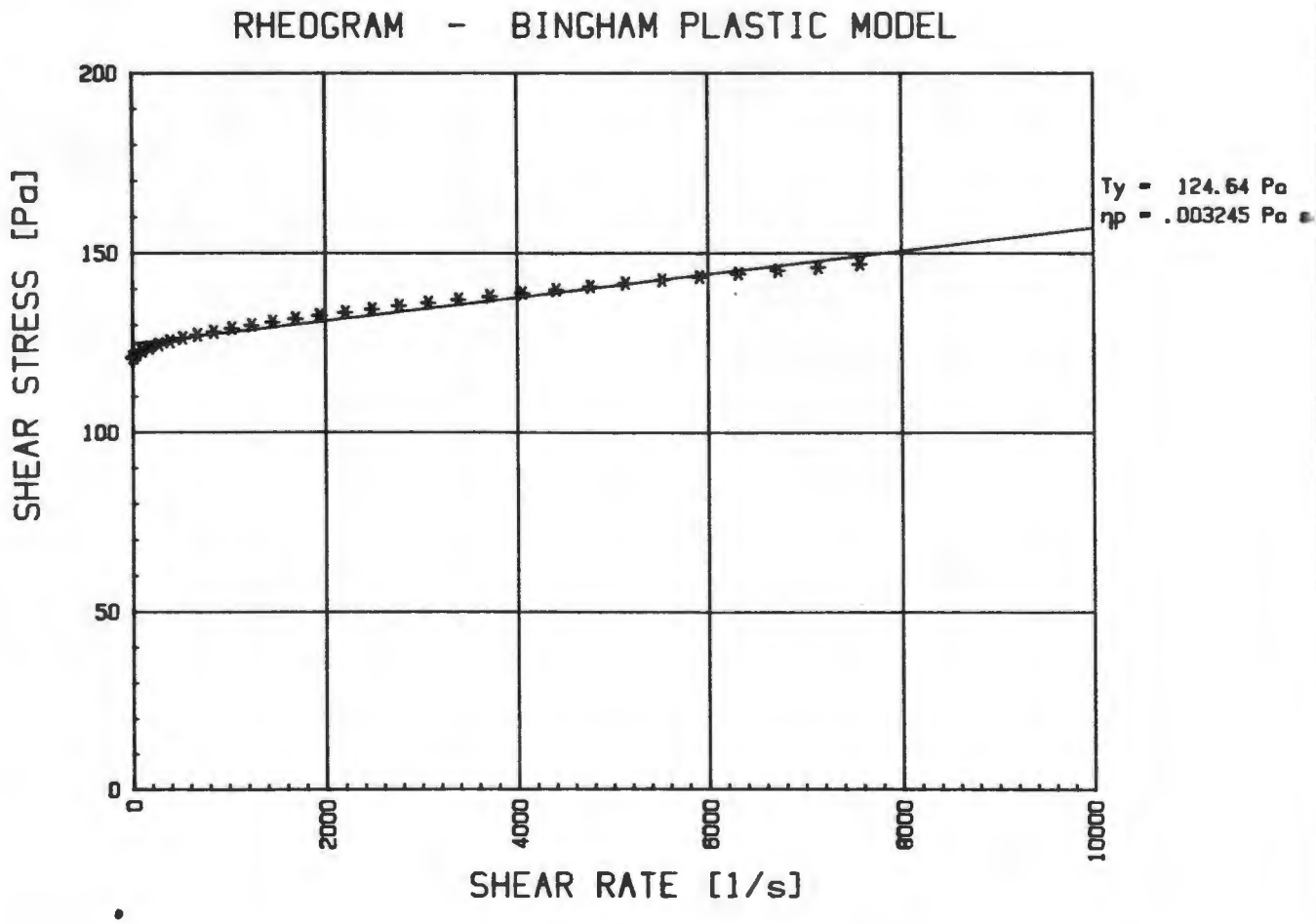

Fig. 5.4 : Data Reduction using a First Order Fit

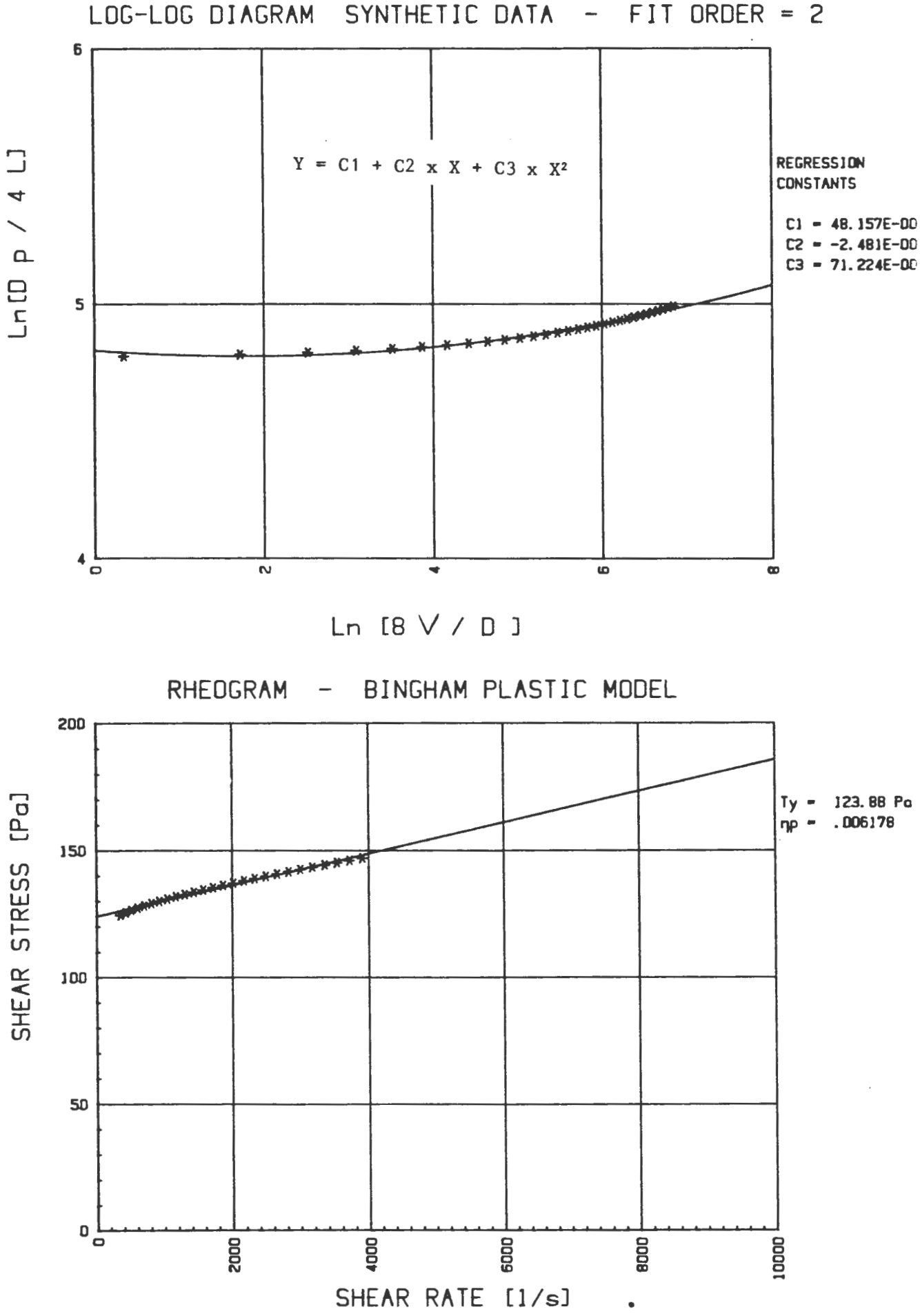

Fig. 5.5 : Data Reduction using a Second Order Fit

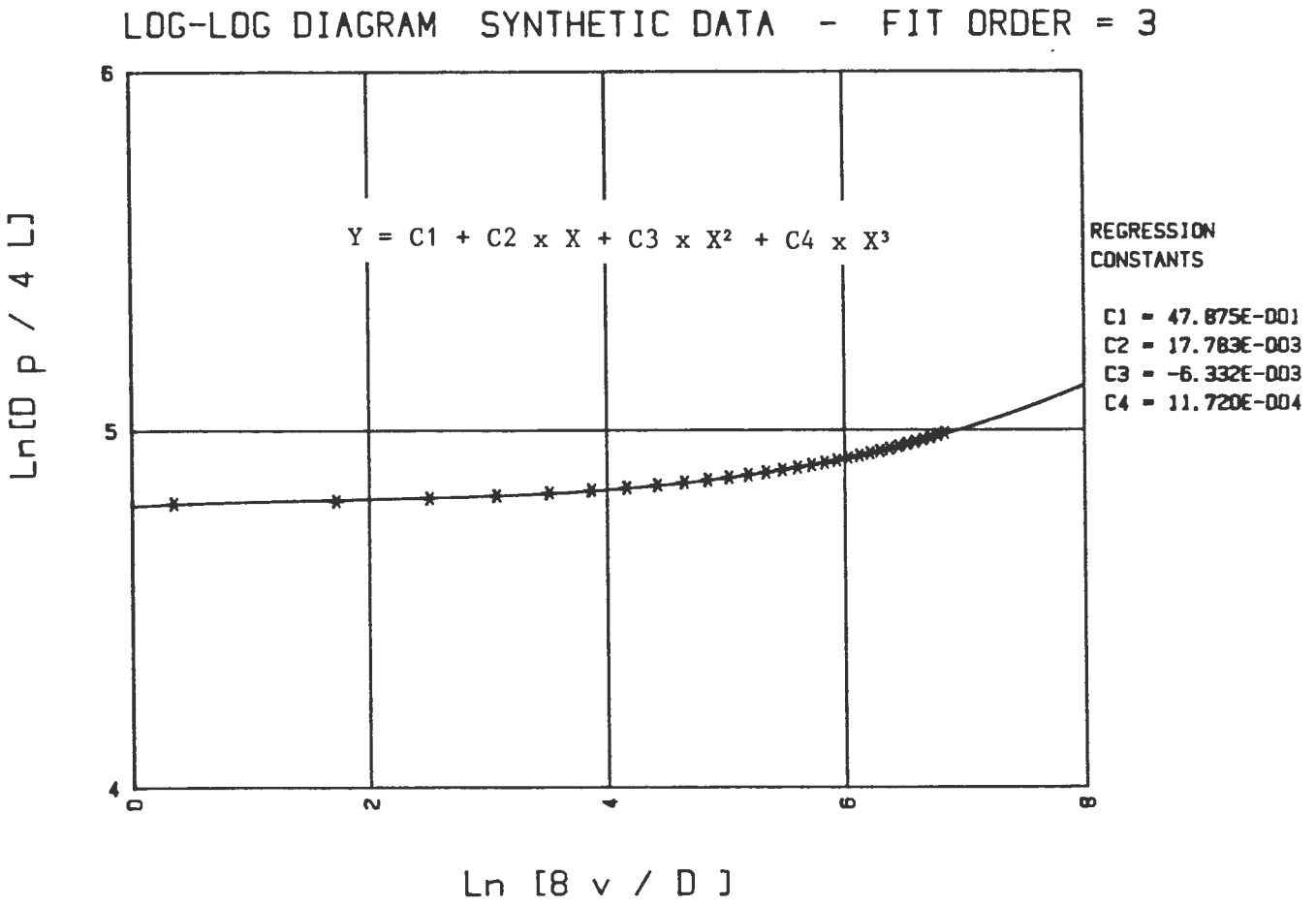

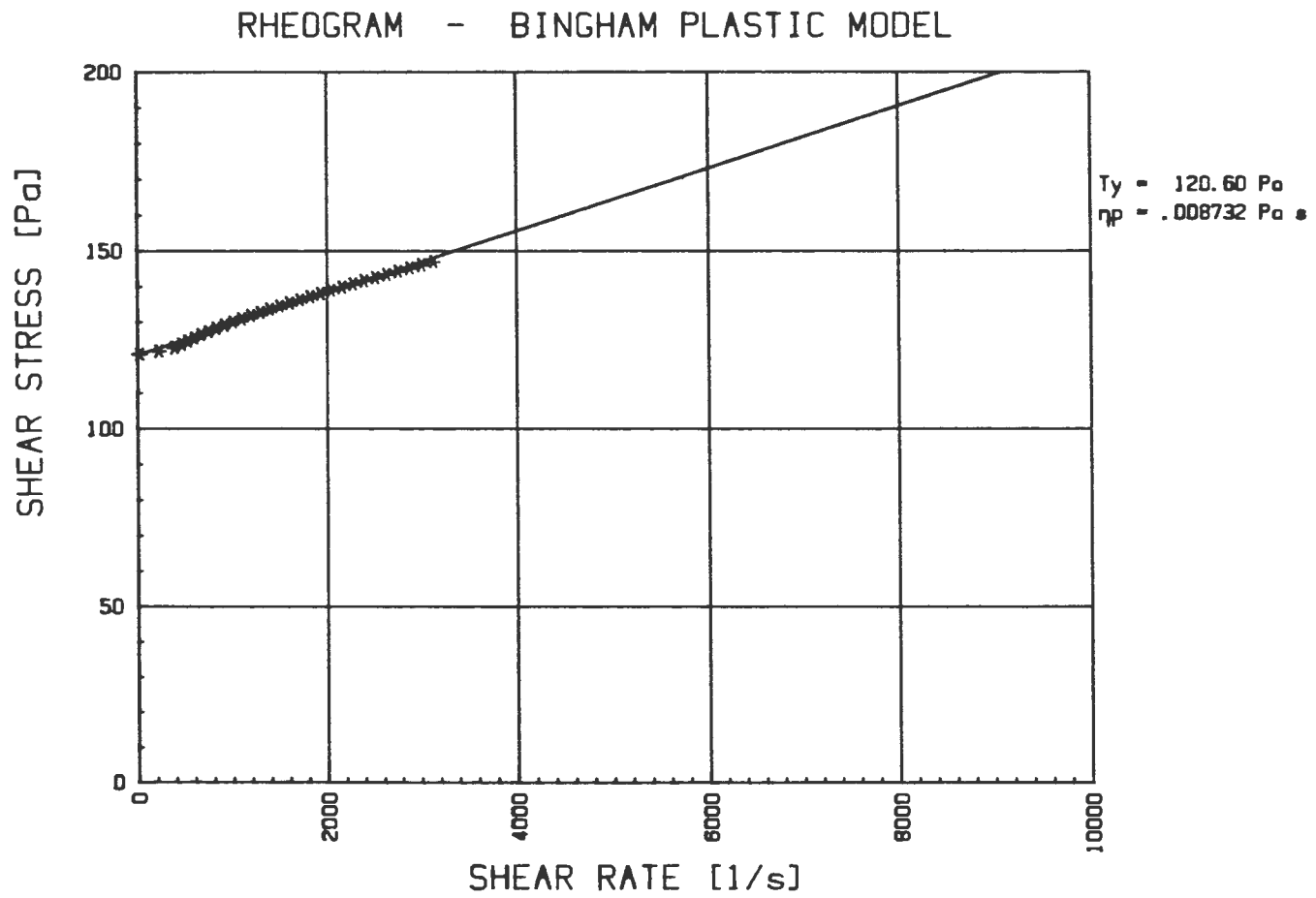

Fig. 5.6 : Data Reduction using a Third Order Fit

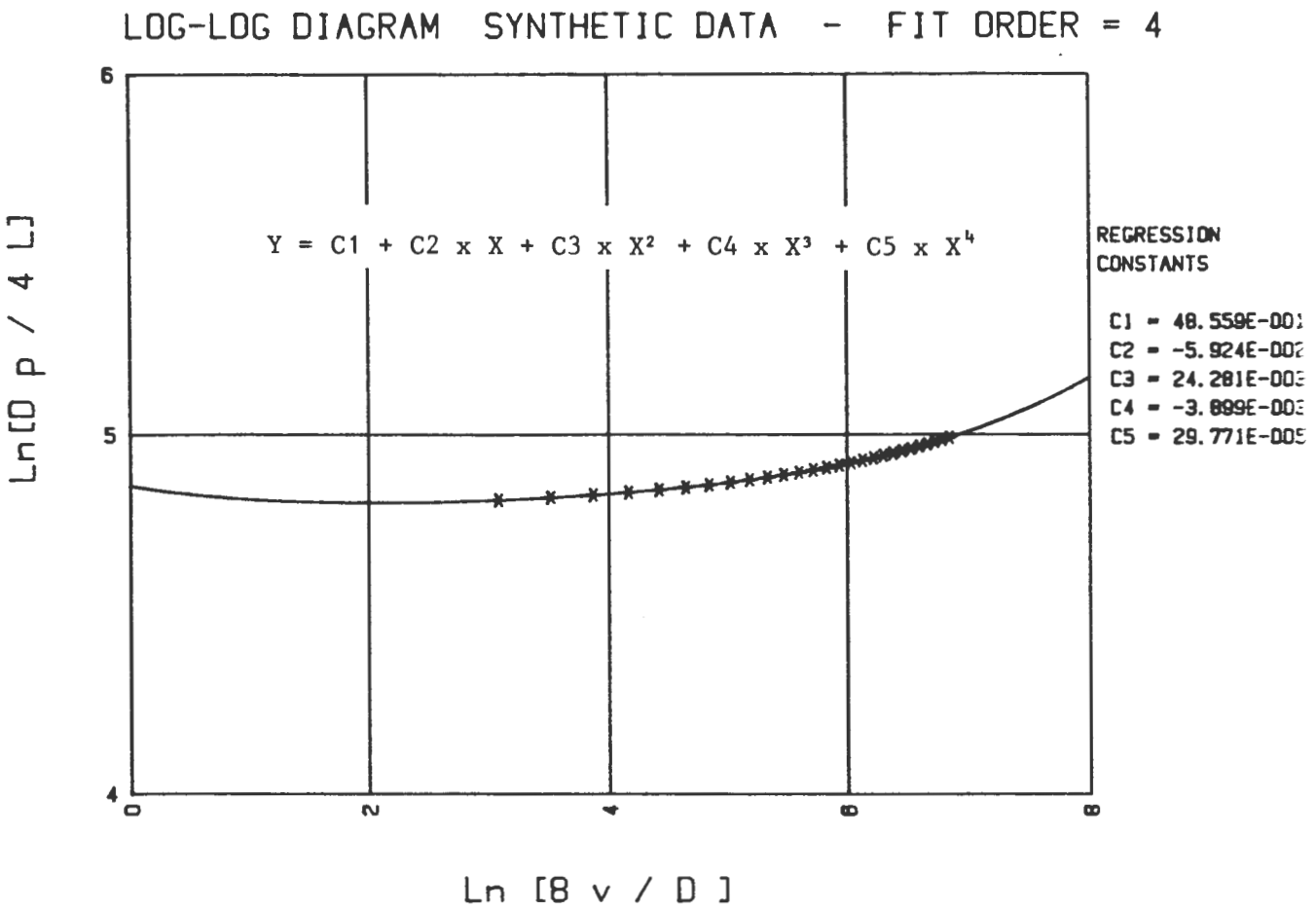

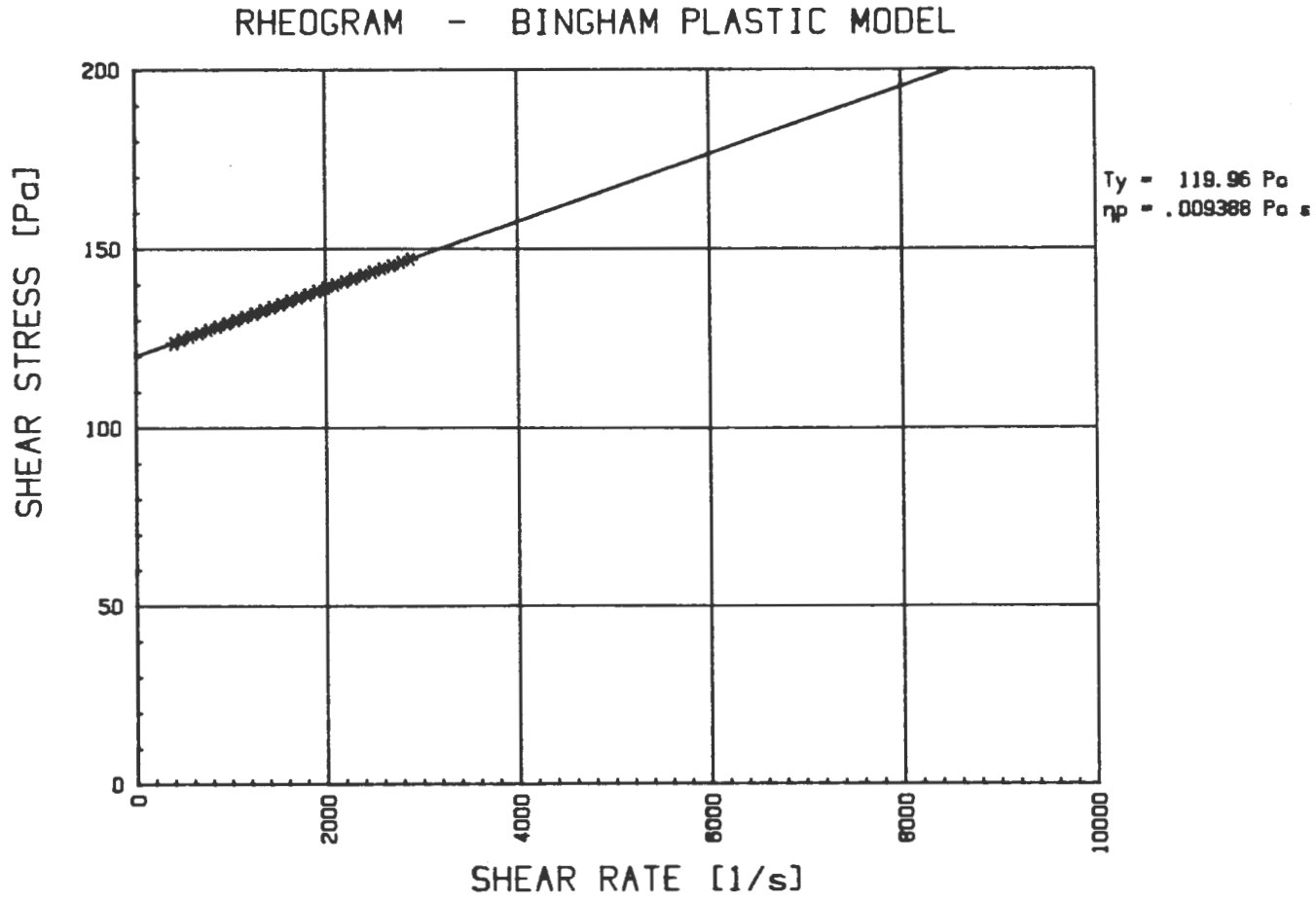

Fig. 5.7 : Data Reduction using a Fourth Order Fit

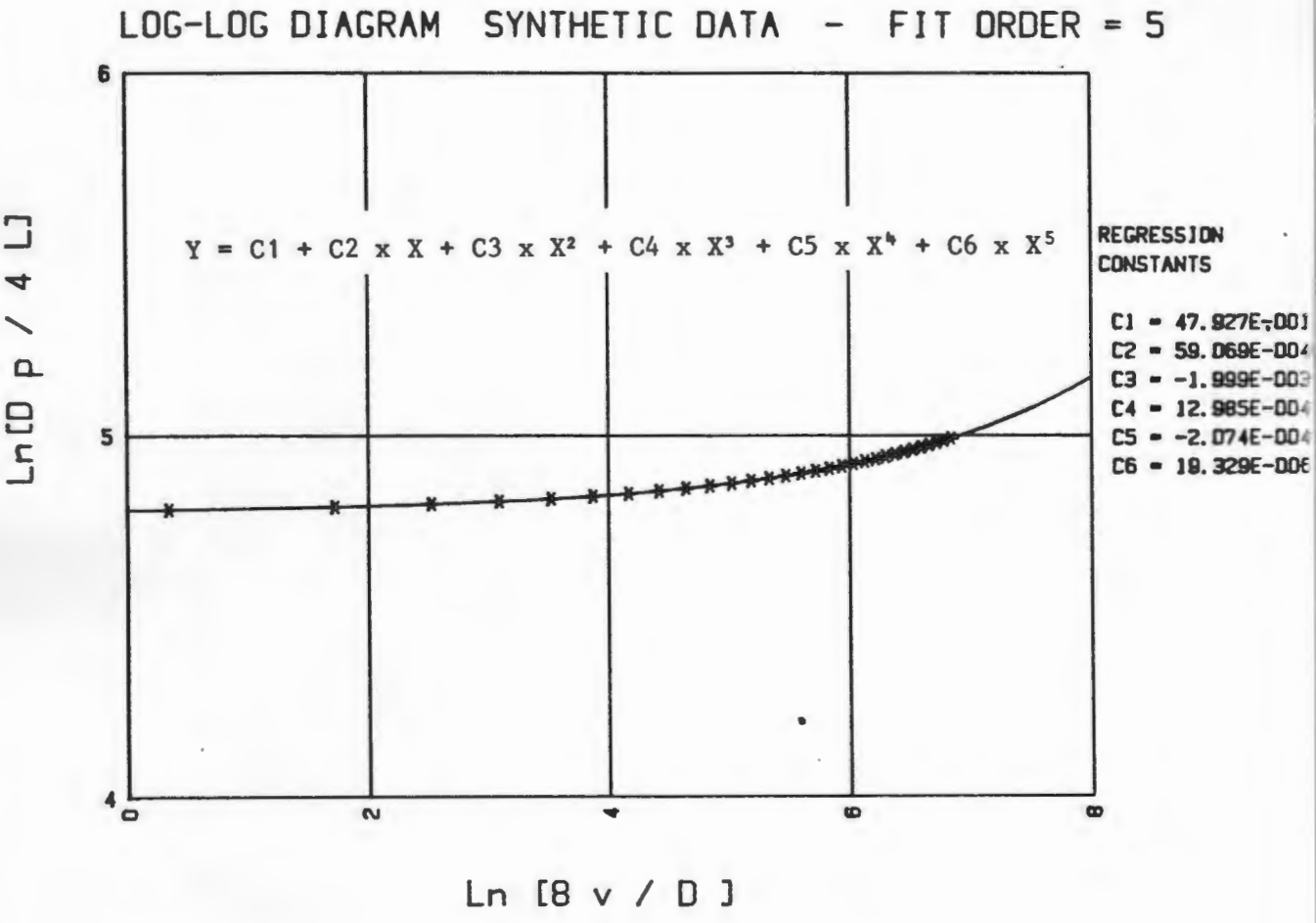

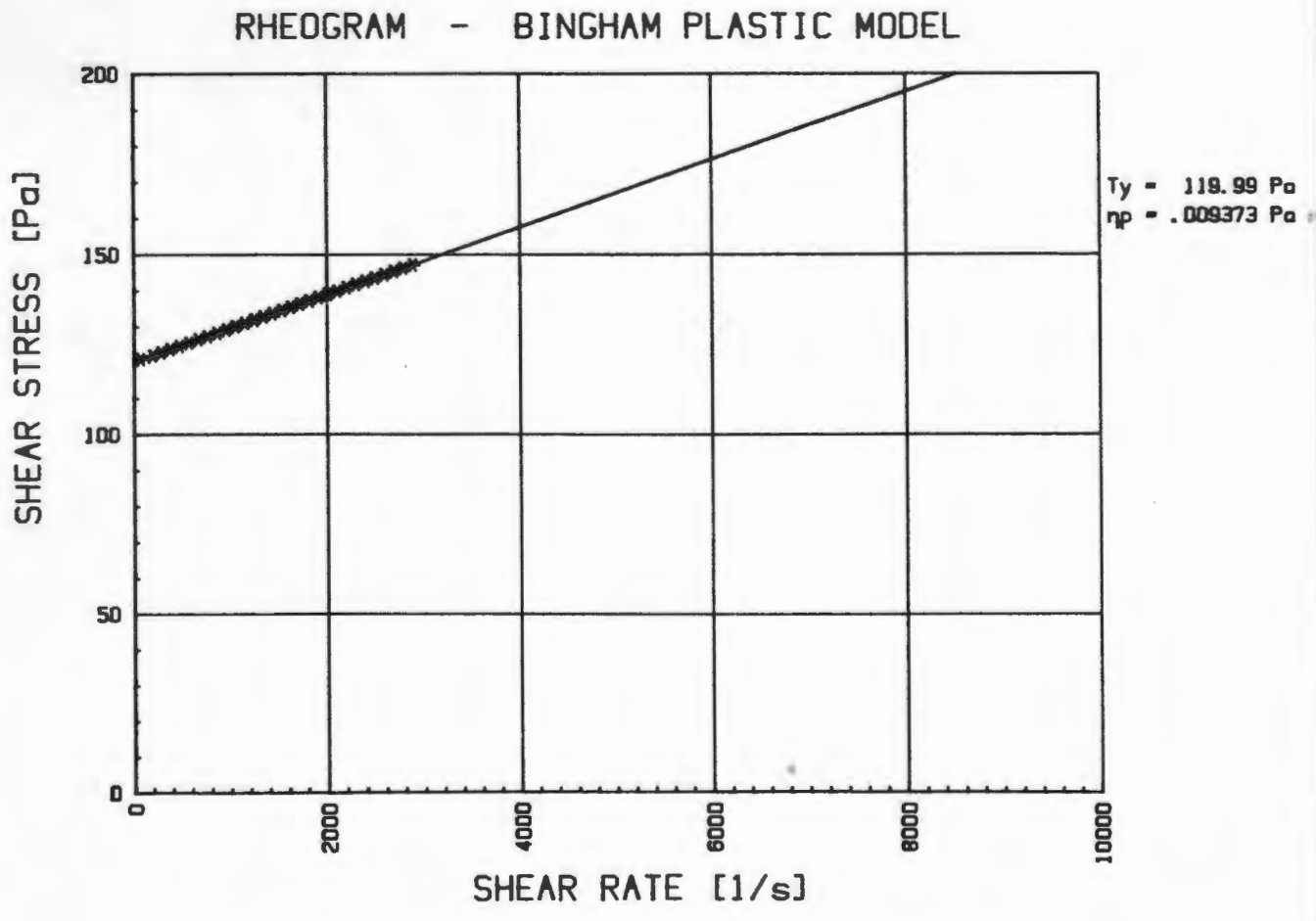

Fig. 5.8 : Data Reduction using a Fifth Order Fit

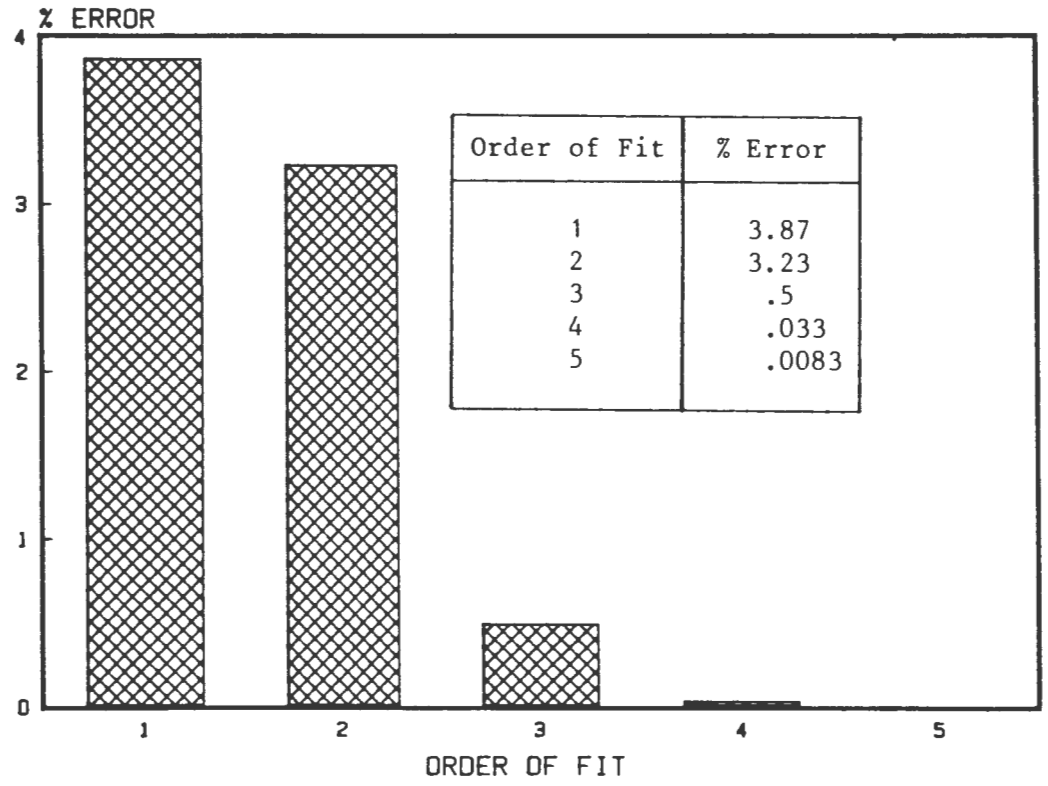

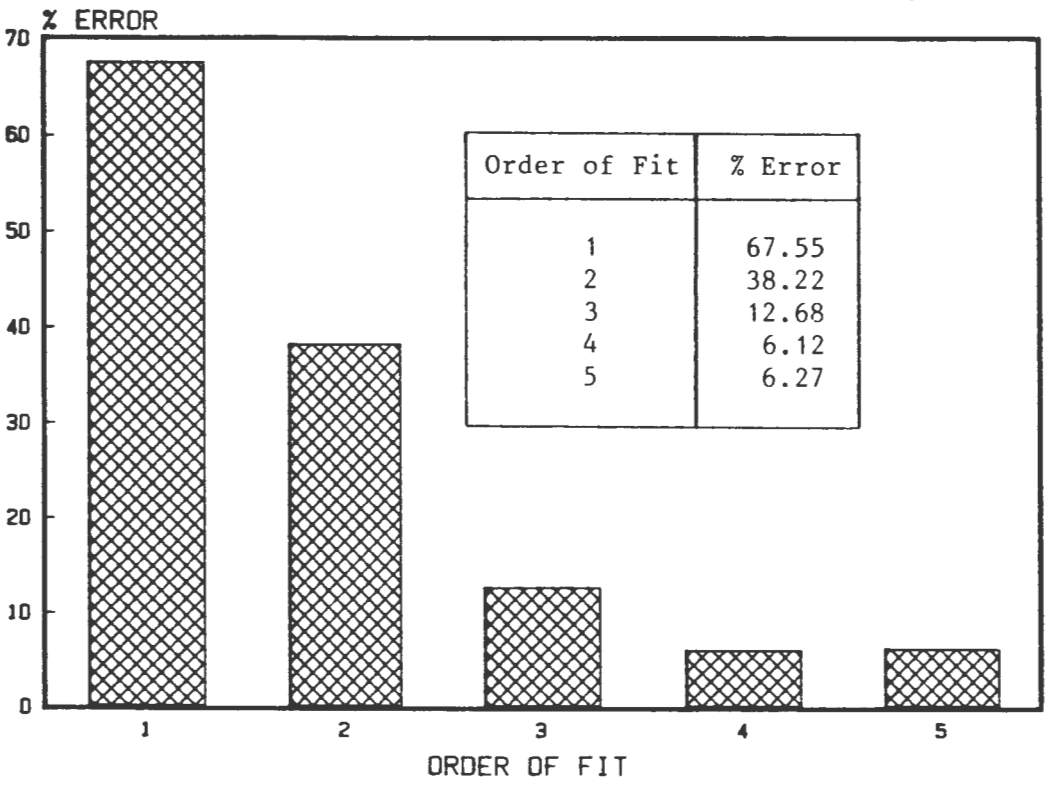

Fig. 5.9 : Summary of Errors

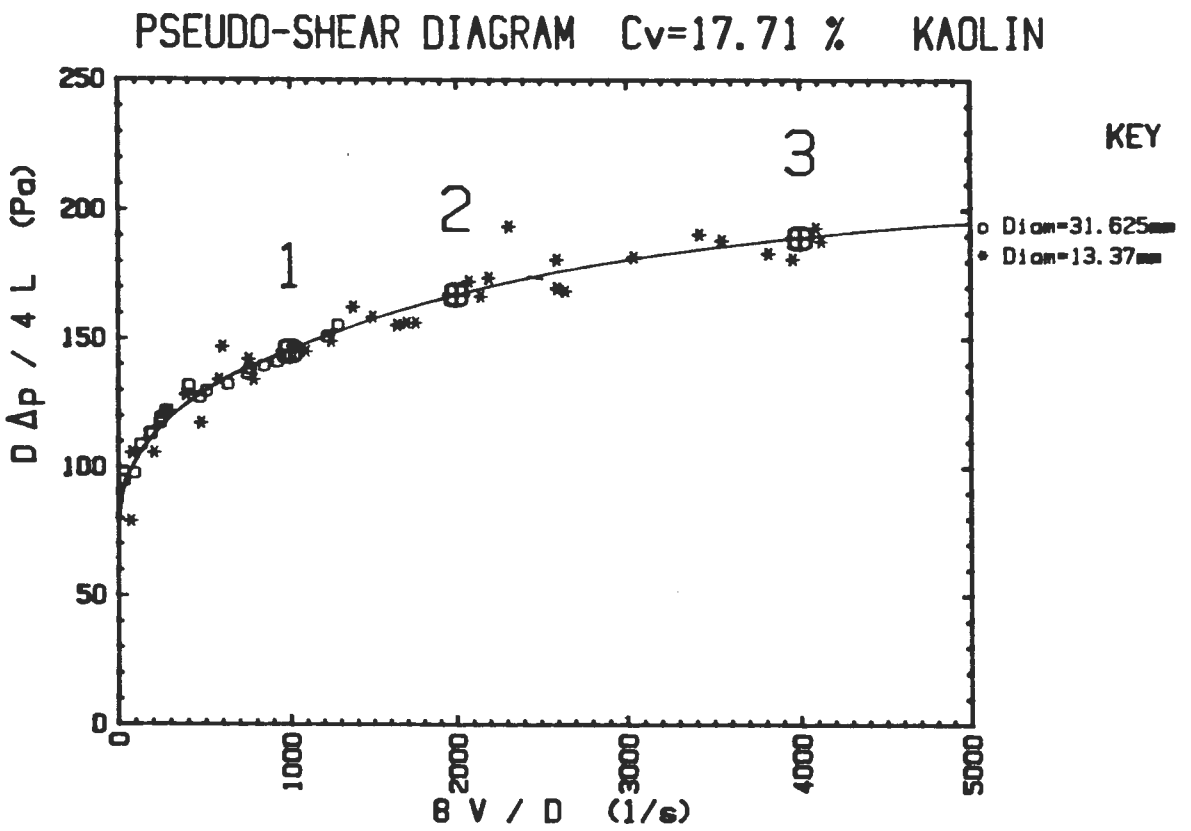

Fig. 5.10 : Best line drawn by hand

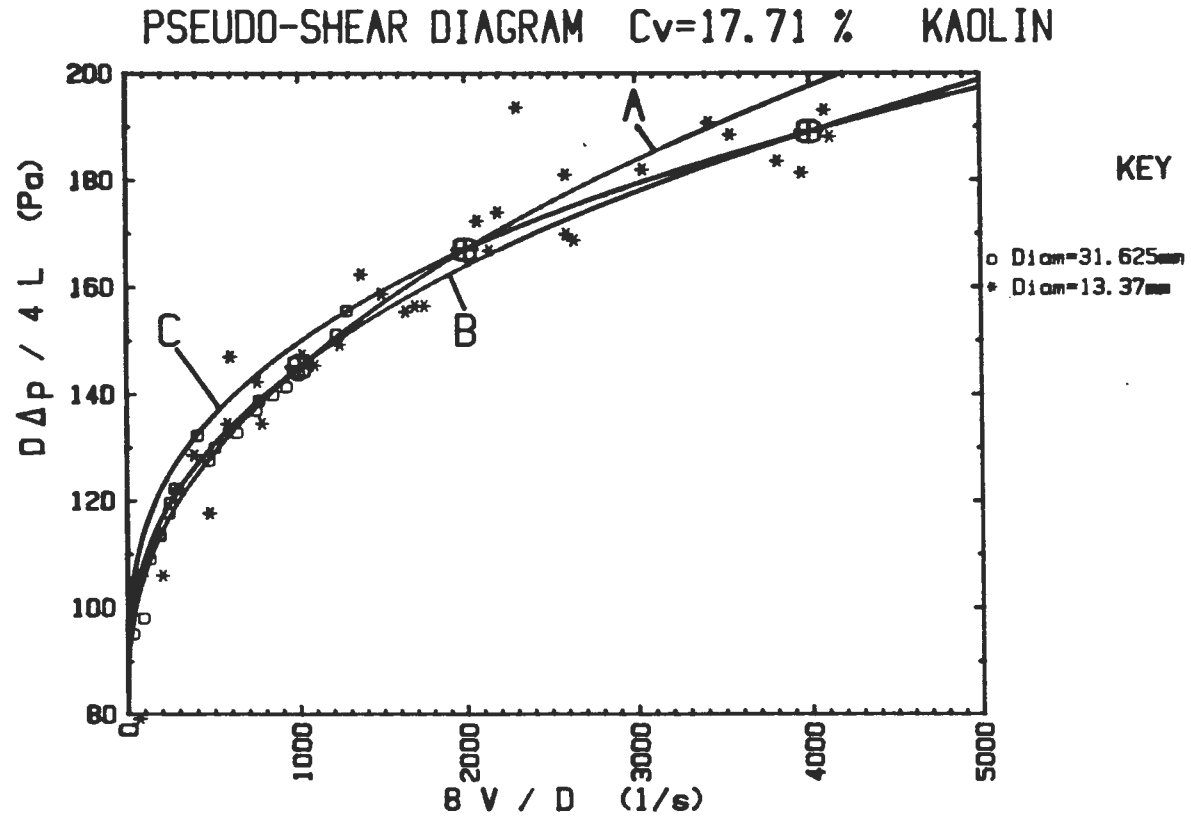

Fig. 5.11 : Results of procedure in graphical form

CHAPTER 6

DESCRIPTION OF MATERIAL TESTED

6.1 TEST PROCEDURE

The required slurries were prepared and tested in the BBTV as well as the rotary viscometer. Volumetric concentration (C_v) was controlled by adding or subtracting supernatant liquor as required. pH was controlled by adding sulphuric acid when necessary.

The particle size distributions were determined using a Malvern 2600/3600 Particle Sizer VF.6.

Solids and mixture relative density and pH determinations were performed on all slurries (see Appendix B).

6.2 KAOLIN

Kaolin from the Serina mine near Cape Town was obtained as a dry powder and mixed with water to the required concentration. The resulting pH was 6,8 and this was maintained throughout the tests. The particle size distribution is shown in Fig. 6.1, showing the following characteristics:

d_{10} = 3 μm $\qquad$ d_{50} = 9 μm $\qquad$ d_{90} = 33 μm

The micrograph of the kaolin (Fig. 6.2) shows that it consisted of irregularly shaped particles with a layered structure.

The kaolin slurry was tested as four concentrations,
viz. C_v = 7,83%; 12,08%; 14,88% and 17,71%.

The Solids Relative Density, S_s, was found to be 2,44.

6.3 URANIUM MINING TAILINGS SLIMES

Slimes were received wet from the Rössing mine and the pH was very low (pH = 2,09) due to the acid leaching process used at the mine. Return Dam Solution (RDS) from the mine was used to dilute the slurries so as to maintain the pH and dissolved salt content.

During the tests, the pH of the slurries rose from 2,09 to 3,43. In order to determine whether this change in pH could affect the rheology, tests were performed at pH = 1,94 and pH = 3,47. Sulphuric acid was used to reduce the pH. No change in rheology was detected.

6.3.1 Particle Size Separation (Uranium Tailings)

A SWECO Vibro-Separator was used for separating the slimes into four particle size ranges.

The mesh sizes used were: 40 mesh (400 µm)
60 mesh (250 µm)
150 mesh (100 µm)

The four particle size ranges were:

$d > 400$ µm
400 µm $> d > 250$ µm
250 µm $> d > 100$ µm
100 µm $> d$

The $d < 100$ µm fraction was left to settle for one week. The supernatant was siphoned off, and the remaining slurry was considered to be of maximum concentration (C_v = 23%). The other three fractions were well dried by the Sweco separation process, and no supernatant was present after standing for one week.

Samples of each fraction were taken for S_s determinations.

6.3.2 Material tested in the BBTV (Uranium Tailings)

Four slurries of different particle size range and concentration were tested.

The approach used was to start with the $d < 100$ µm fraction, and then reconstitute the total slimes in two further steps.

The volumetric concentration and the pH was varied where possible. Each of the slurries was prepared in the following way:

Slurry 1 ($d < 100\ \mu m$ $C_v = 22,3\%$)
The finest fraction was tested at the maximum concentration as explained in 6.3.1.

Slurry 2 ($d < 250\ \mu m$ $C_v = 28,6\%$)
The $250\ \mu m > d > 100\ \mu m$ fraction was added so as to reconstitute the slimes up to the 250 µm size. No RDS was added, resulting in a much higher volumetric concentration, since the fraction added had a very low moisture content. The mixed slurry was tested at this higher concentration.

Slurry 3 ($d < 250\ \mu m$ $C_v = 23,4\%$)
The mixture in the viscometer (Slurry 2) was diluted with RDS to the same concentration as Slurry 1. The diluted mixture was then tested.

Slurry 4 (Total slimes $d < 2000\ \mu m$ $C_v = 23,91\%$)
The remaining coarse fractions were added thus reconstituting the total original slimes. This total slimes slurry was then tested.

6.3.3 Results of Solids Relative Density (S_s) Tests

The results of the S_s determinations for the various particle sizes are set out below.

Particle size d (µm)	Solids relative density S_s
< 100	2,736
100 < d < 250	2,784
250 < d < 400	2,624
> 400	2,628

Due to the larger proportion of smaller particles present, the Solids Relative Density for all four slurries was taken as 2,75.

The particle size distributions are shown in Figs. 6.3, 6.4 and 6.5. The particle size distribution characteristics are set out below.

Slurry	d_{10}(μm)	d_{50} (μm)	d_{90}(μm)
Slurry 1	6	18	64
Slurries 2 & 3	6	29	160
Slurry 4	6	31	200

6.3.4 Micrographs

Fig. 6.6 shows that the uranium slurry consisted of long thin particles and irregularly shaped particles, all sharp edged.

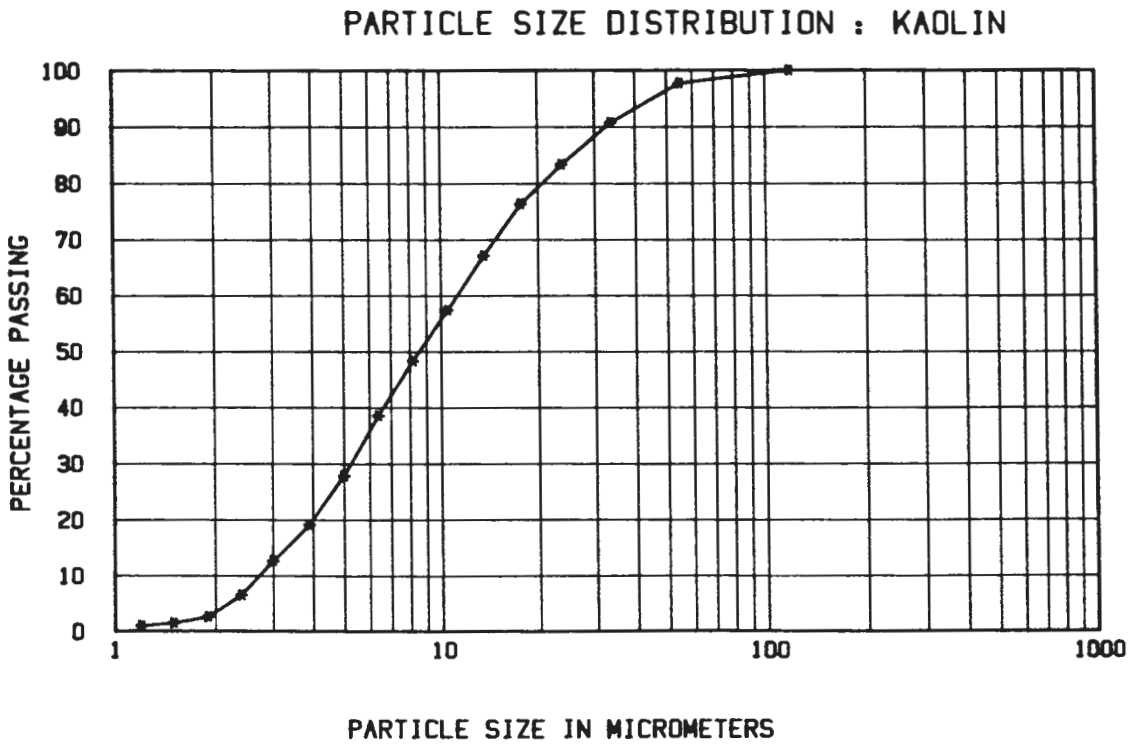

Fig. 6.1 : Particle size distribution of the kaolin slurries

Fig. 6.2 : Micrograph of kaolin particles

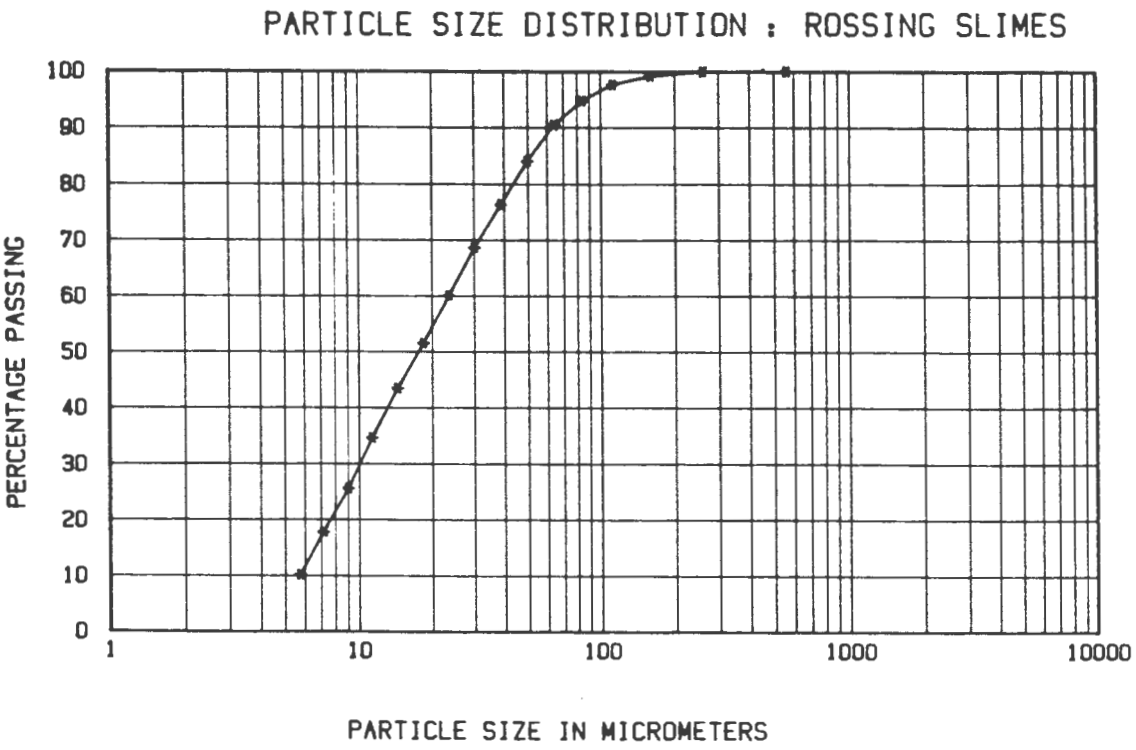

Fig. 6.3 : Particle size distribution of uranium slurries : Slurry 1

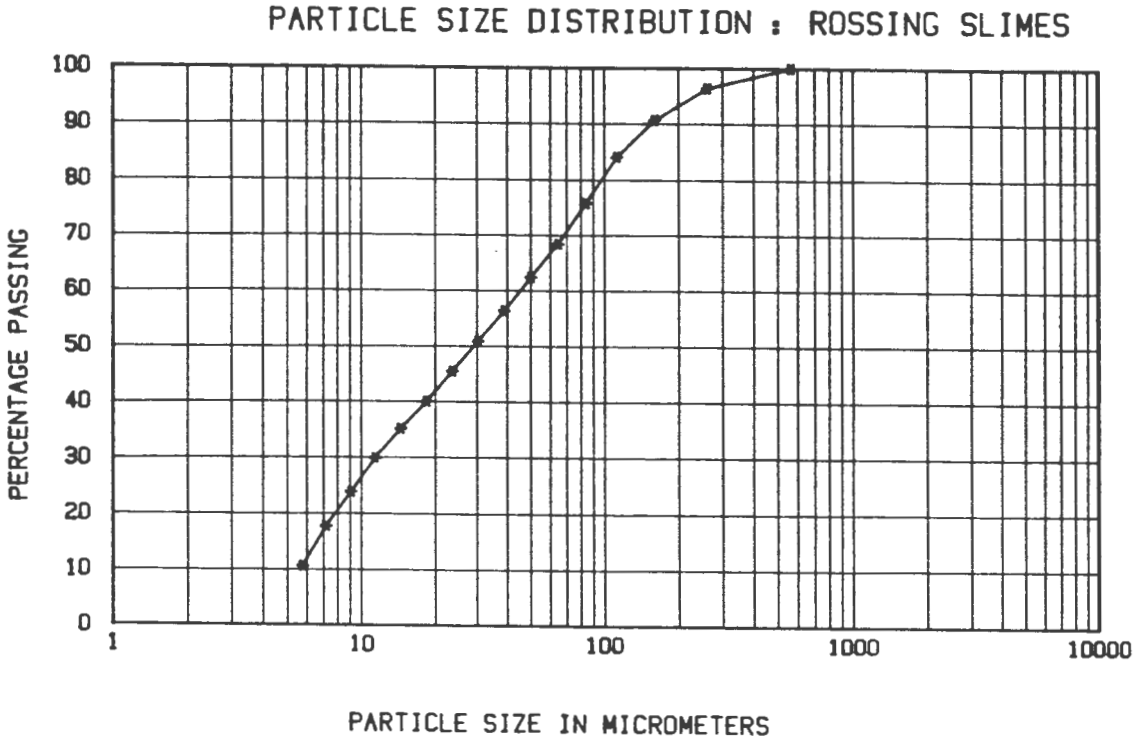

Fig.6.4 : Particle size distribution of uranium slurries : Slurries 2 & 3

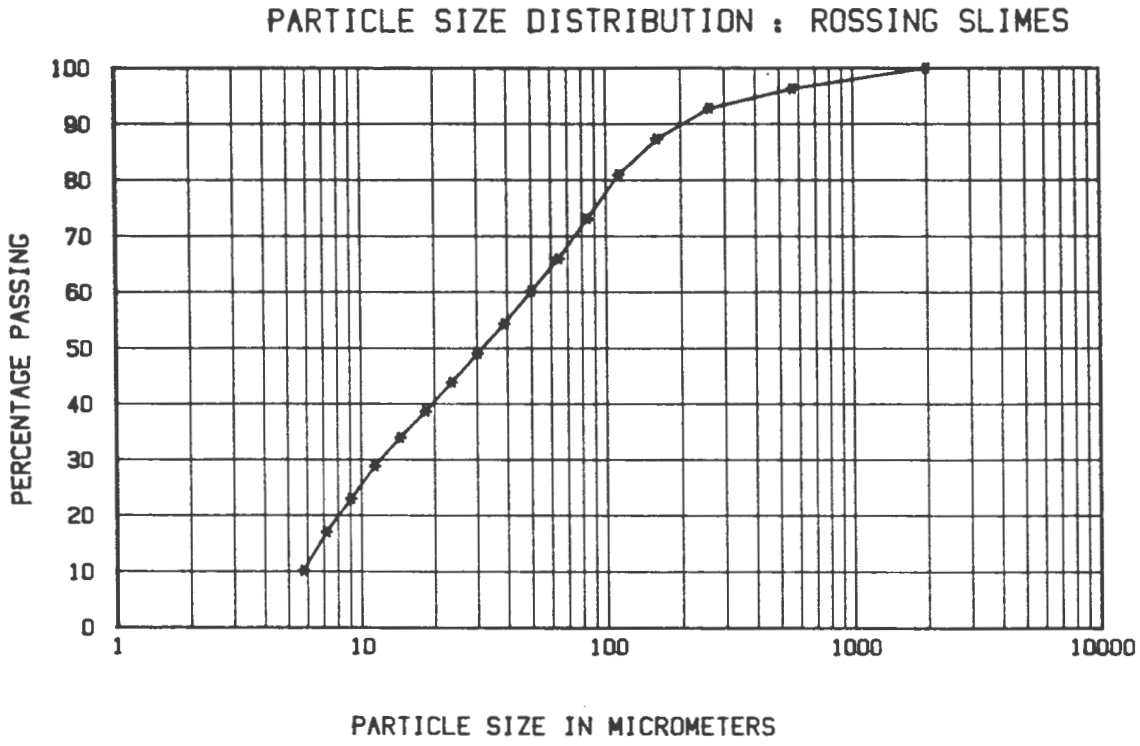

Fig. 6.5 : Particle size distribution of uranium slurries : Slurry 4

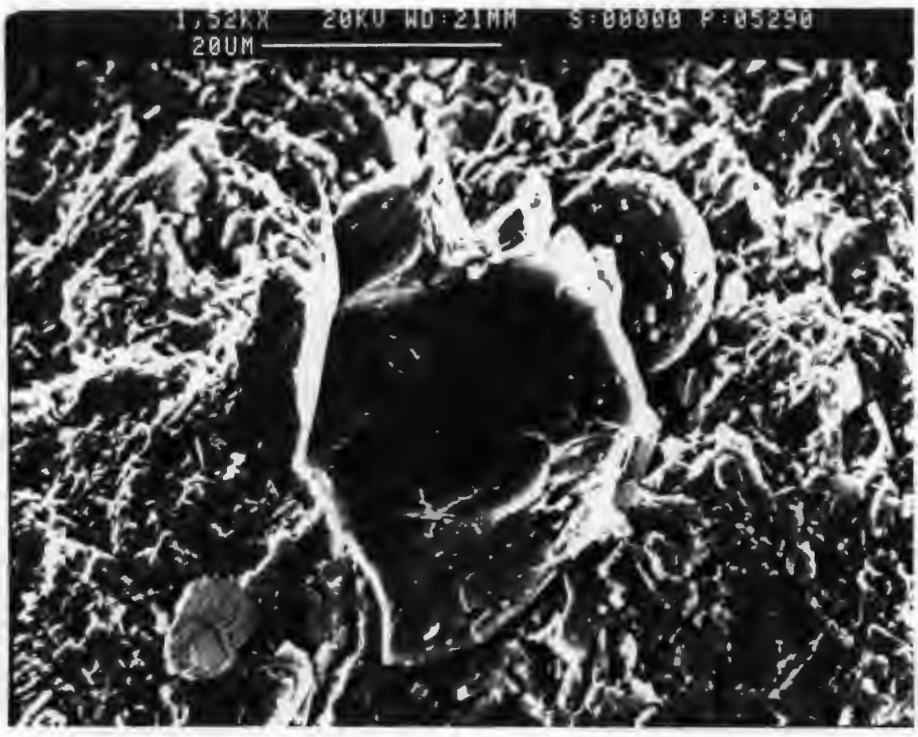

Fig. 6.6 : Micrographs of uranium particles

CHAPTER 7

EXPERIMENTAL RESULTS AND ANALYSIS

7.1 DETAILED EXPERIMENTAL RESULTS

The detailed BBTV experimental results are presented in Appendix C.

7.2 RHEOLOGICAL CHARACTERISATION

The procedure laid out in Chapter 5 was applied to all the BBTV results. The resultant rheologies are presented in Table 7.1 and Figs 7.1 and 7.2. For kaolin, the rheological constants are presented as a function of concentration in Fig. 7.3. The uranium rheological constants are presented as a function of concentration in Fig. 7.4 and maximum particle size in Fig. 7.5.

7.3 TURBULENT FLOW DATA AND PREDICTIONS

As stated earlier, the BBTV is, by its very nature, a miniature pipeline, capable of producing valid turbulent flow data.

Figs. 7.6 and 7.7 show the BBTV data presented as pipe flow diagrams (i.e. hydraulic gradient vs. mean slurry velocity) together with the theoretical predictions for laminar flow and turbulent flow, as laid out in Chapter 2.

7.4 CRITICAL REYNOLDS NUMBERS

Critical Reynolds numbers (Re_{nn} as per equation 2.34) are tabulated in Table 7.2 together with the critical velocities, which were obtained from Figs. 7.6 and 7.7.

Slurry	Volumetric Concentration	BBTV			
	C_v%	τ_y(Pa)	K	n	μ(Pa s)
Kaolin	7,83	6	0,027	0,82	0,0089
"	12,08	23	0,50	0,50	0,010
"	14,88	44	1,17	0,49	0,030
"	17,71	80	2,29	0,43	0,019
Uranium Tailings Slurry 1	22,47	17	0,18	0,74	0,025
Uranium Tailings Slurry 2	28,59	10	0,12	0,81	0,027
Uranium Tailing Slurry 3	21,99	0,67	0,106	0,672	0,0094
Uranium Tailings Slurry 4	23,91	3	0,0497	0,764	0,0085
Solids Relative Density:	Kaolin 2,44		Uranium Tailings 2,75		

Table 7.1 : Summary of Results

SLURRY	Cv [%]	Diam [mm]	Vcrit [m/s]	Re_{cr}crit	Ty [Pa]	K	n	Ss
KAOLIN	7.83	13.370	2.20	4449	6	.027	.8207	2.4449
KAOLIN	7.83	31.625	1.80	7117	6	.027	.8207	2.4449
KAOLIN	12.08	13.370	4.40	7091	23	.500	.5000	2.4449
KAOLIN	12.08	31.625	4.00	9453	23	.500	.5000	2.4449
KAOLIN	14.88	31.625	6.20	8679	44	1.170	.4900	2.4449
KAOLIN	17.71	13.370	7.00	5956	80	2.290	.4300	2.4449
KAOLIN	17.71	31.625	6.00	6770	80	2.290	.4300	2.4449
SLURRY 1	22.47	13.370	5.40	4568	17	.180	.7400	2.7500
SLURRY 1	22.47	31.625	3.90	5732	17	.180	.7400	2.7500
SLURRY 2	28.59	13.370	4.60	3463	10	.120	.8100	2.7500
SLURRY 2	28.59	31.625	3.10	4348	10	.120	.8100	2.7500
SLURRY 3	21.99	13.370	2.00	3571	1	.106	.6720	2.7500
SLURRY 3	21.99	31.625	1.60	4736	1	.106	.6720	2.7500
SLURRY 4	23.91	13.370	1.60	3085	3	.050	.7640	2.7500

Table 7.2 : Critical Flow Values

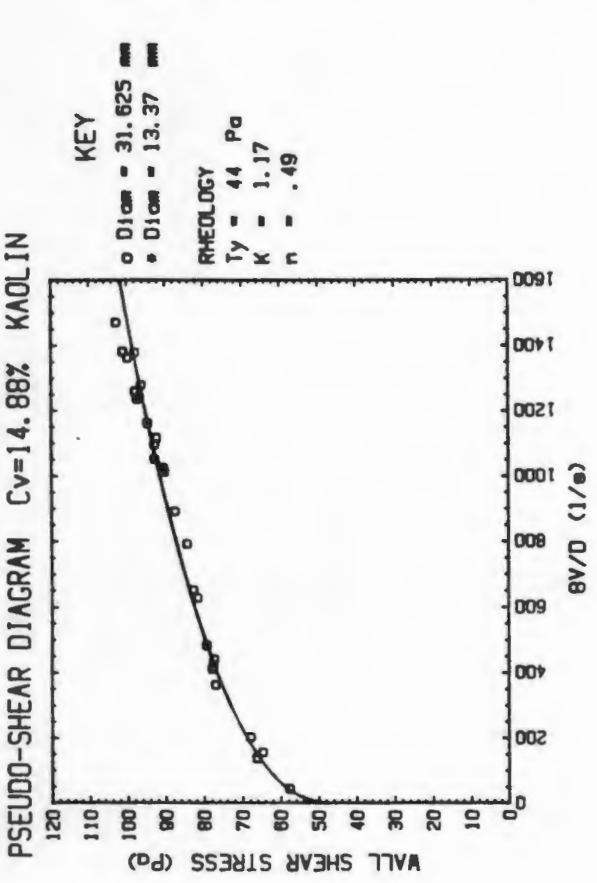

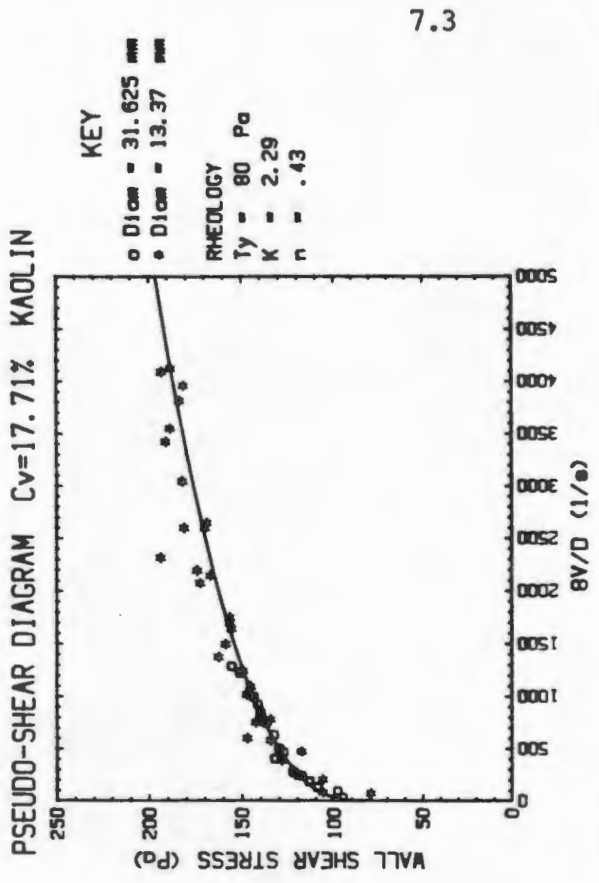

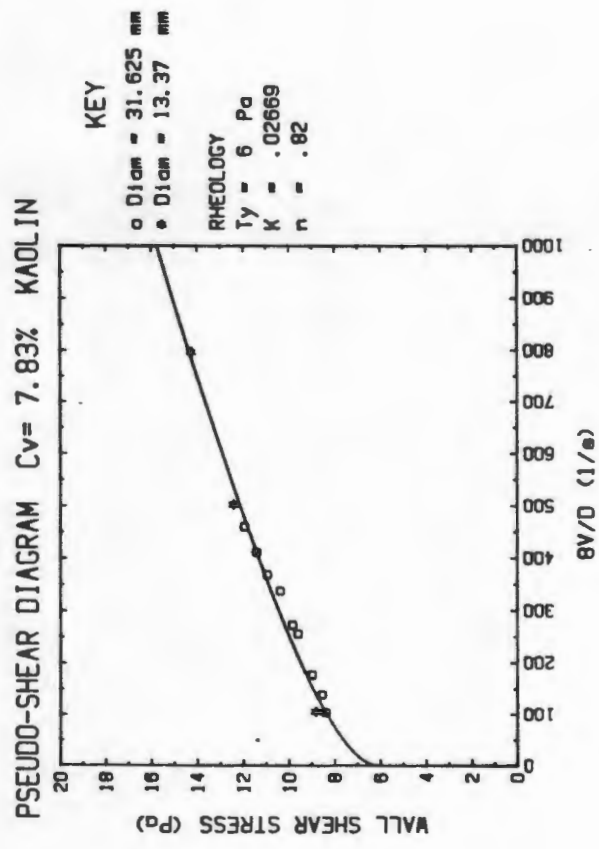

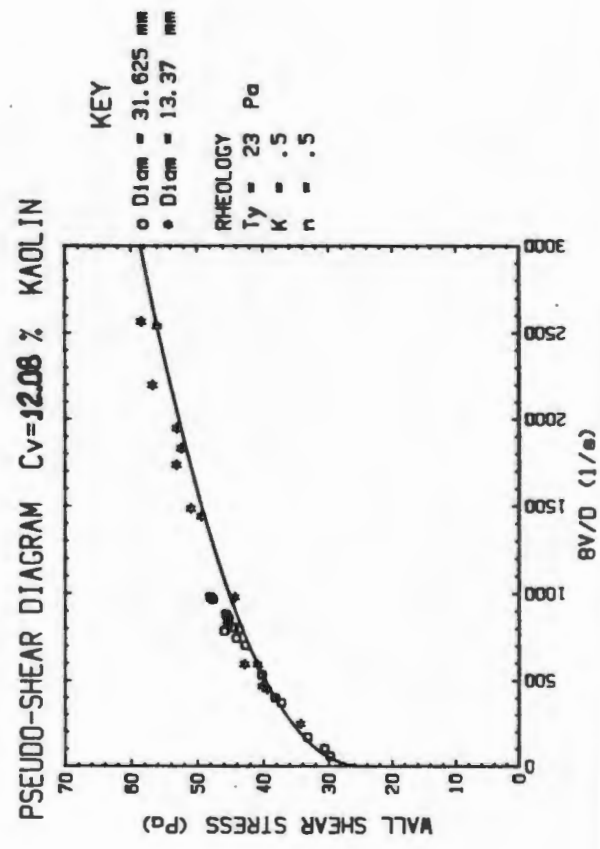

Fig. 7.1 : Rheological Characterisation of Kaolin

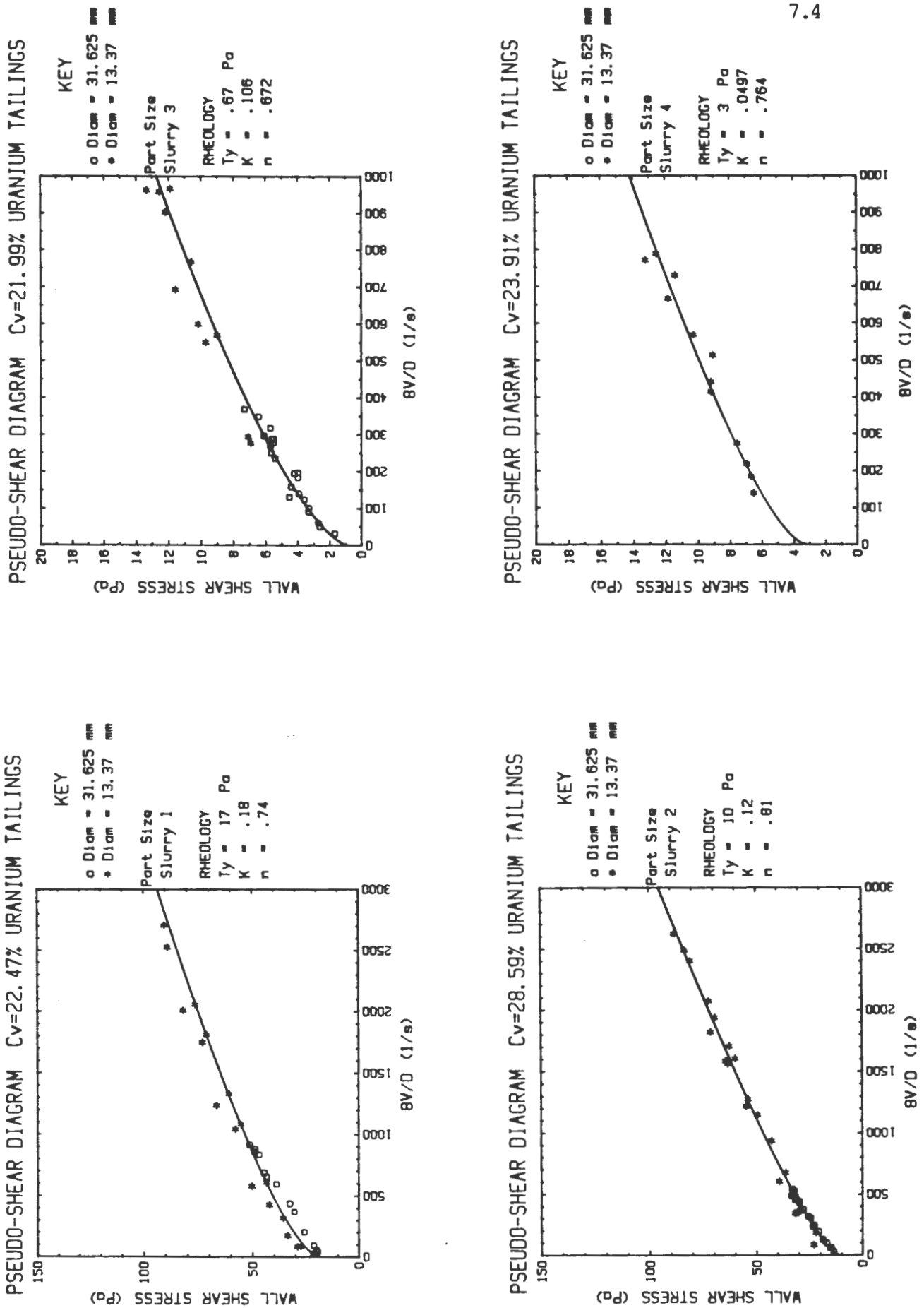

Fig. 7.2 : Rheological Characterisation of Uranium Tailings

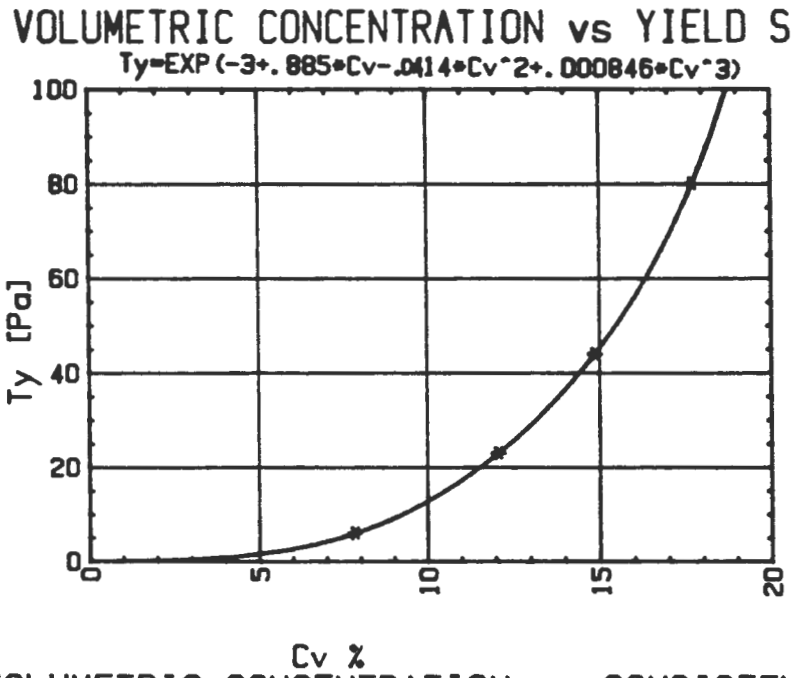

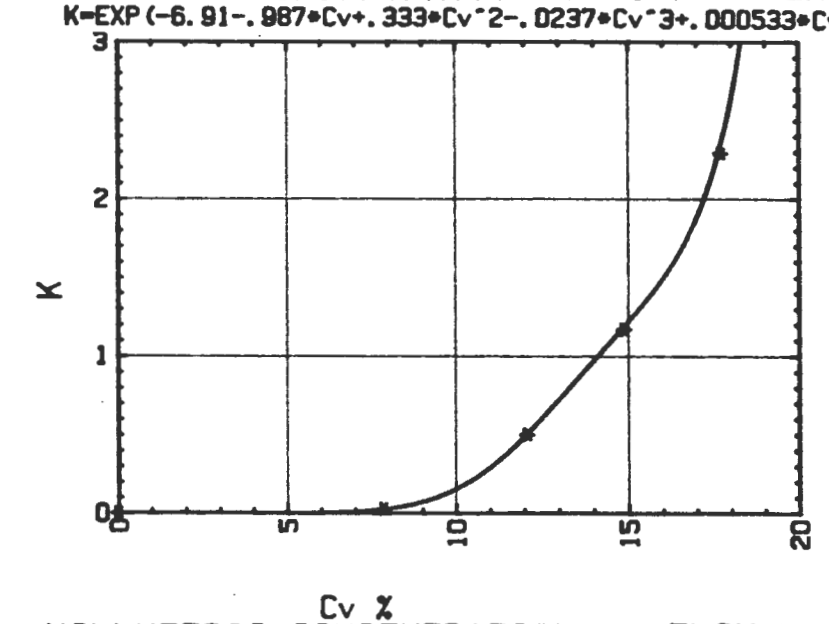

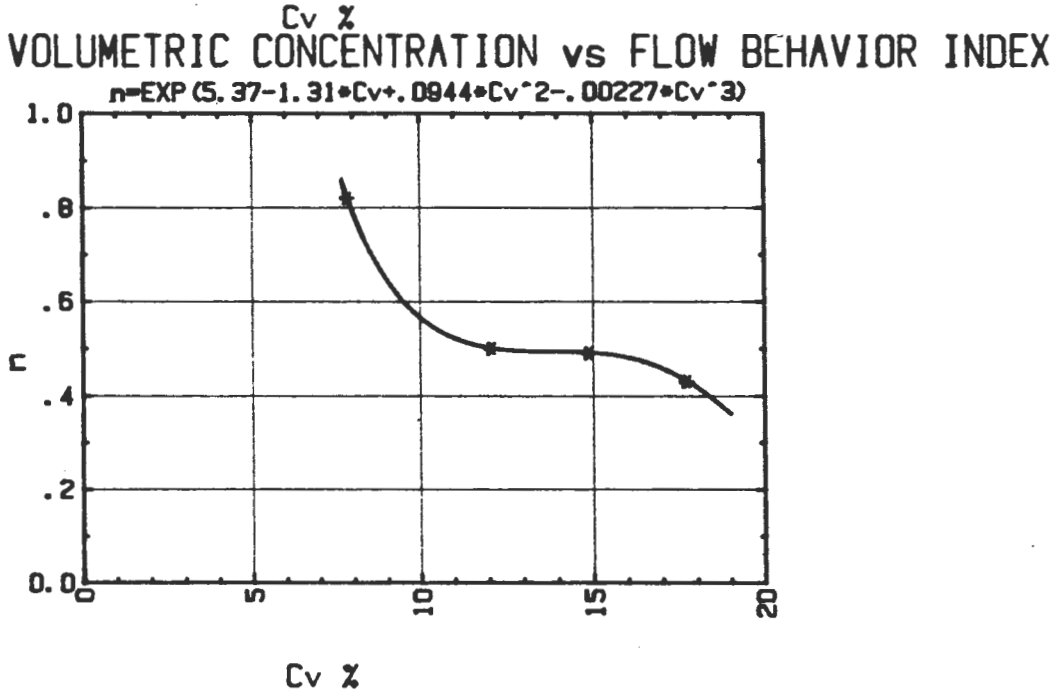

Fig. 7.3 : The rheological constants for kaolin as a function of volumetric concentration

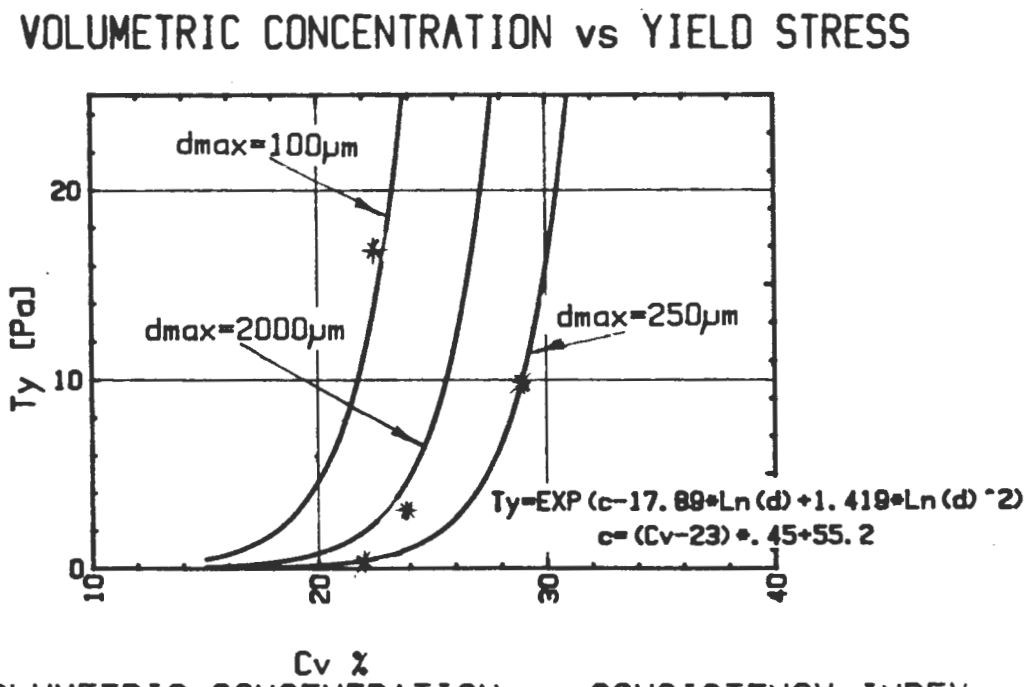

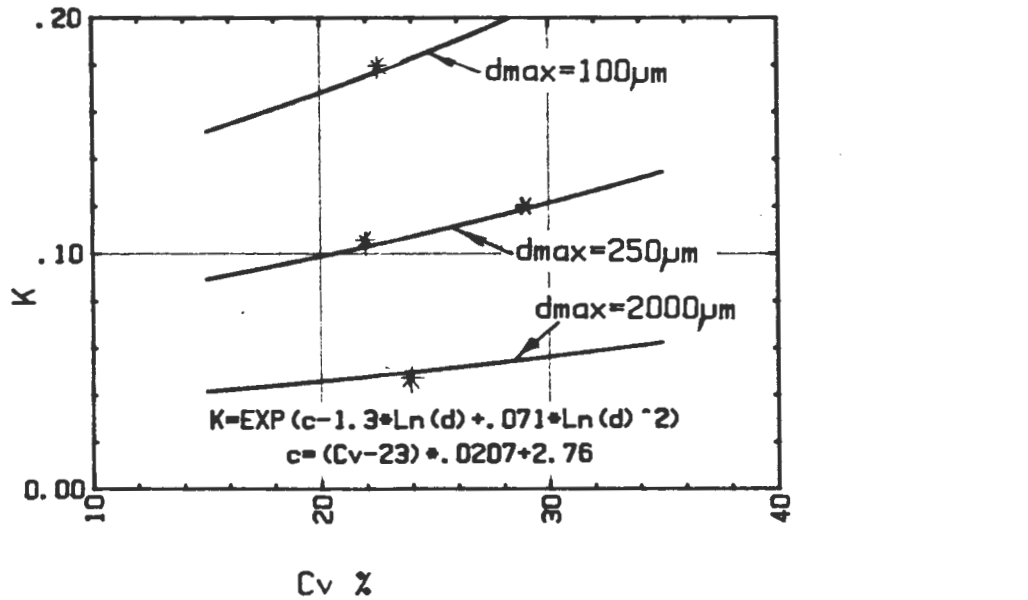

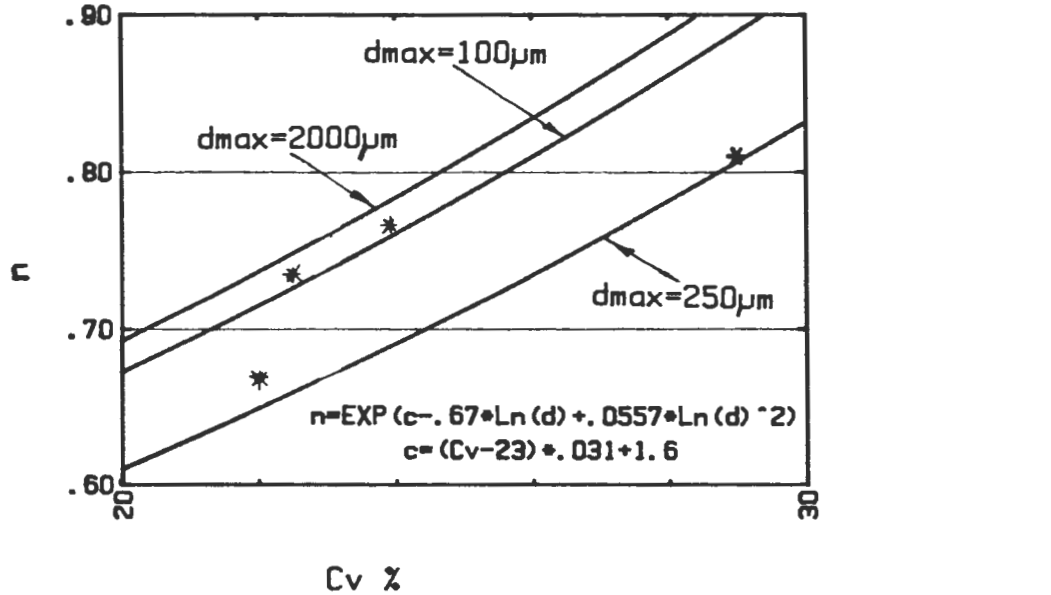

Fig. 7.4 : The rheological constants for uranium tailings as a function of C_v with maximum particle size as parameter

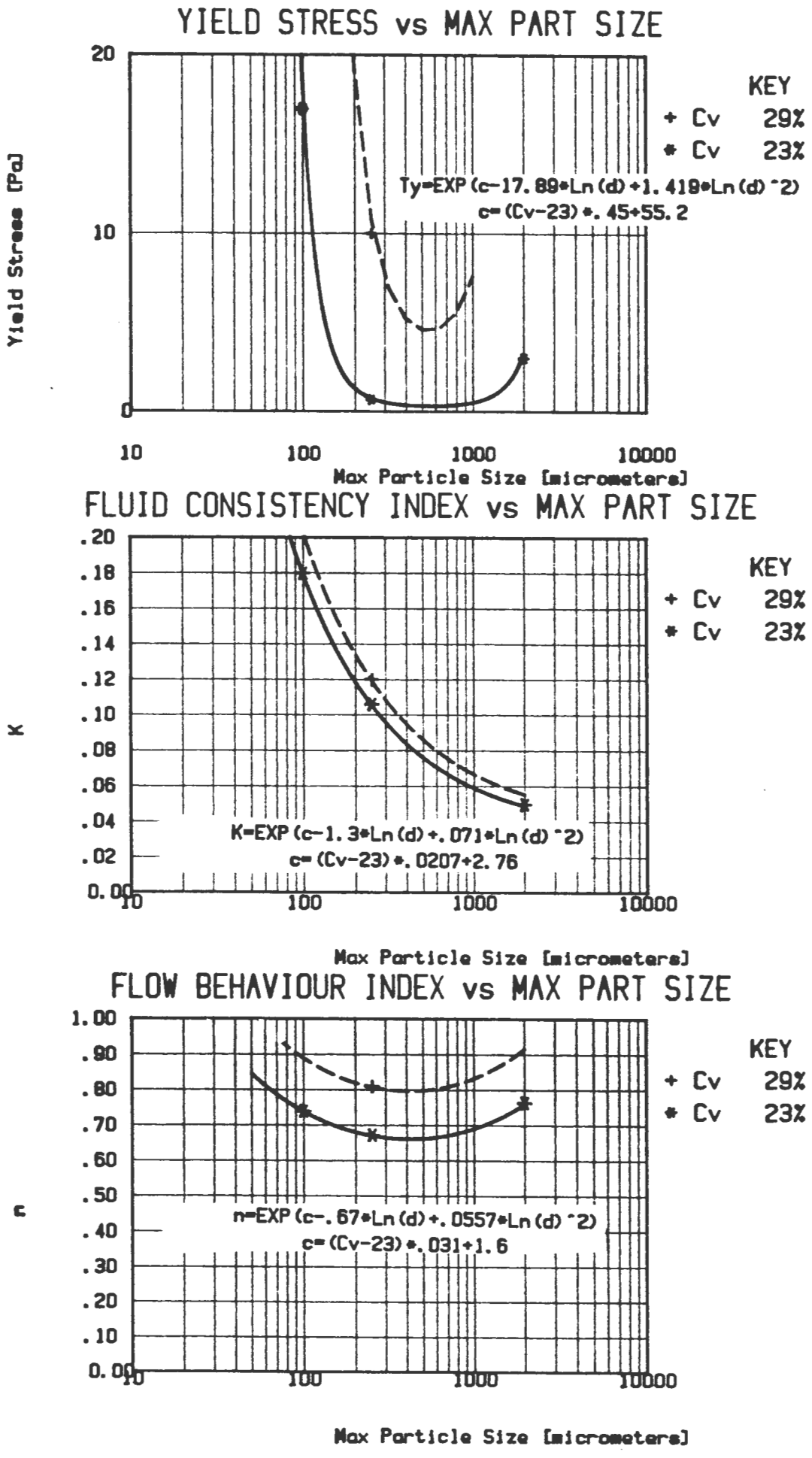

Fig. 7.5 : The rheological constants for uranium tailings as a function of maximum particle size with C_v as parameter

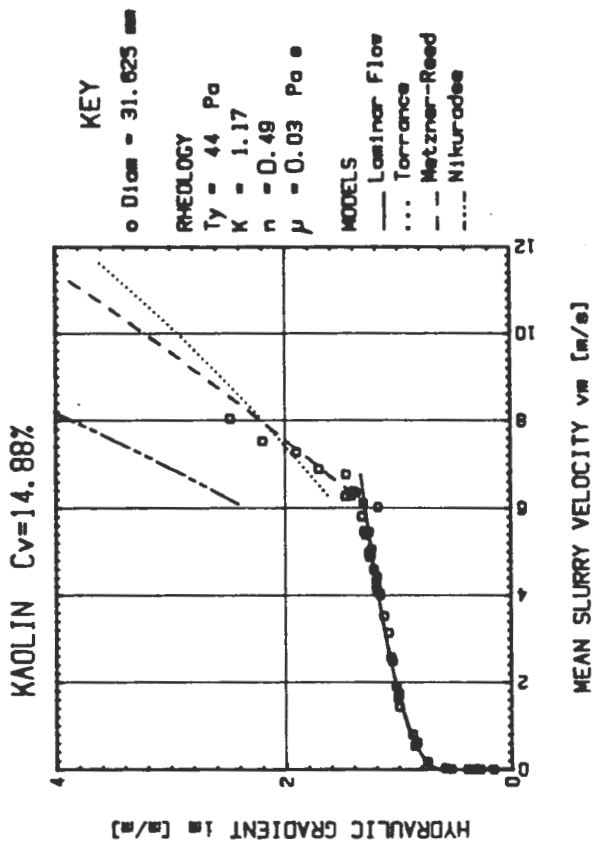

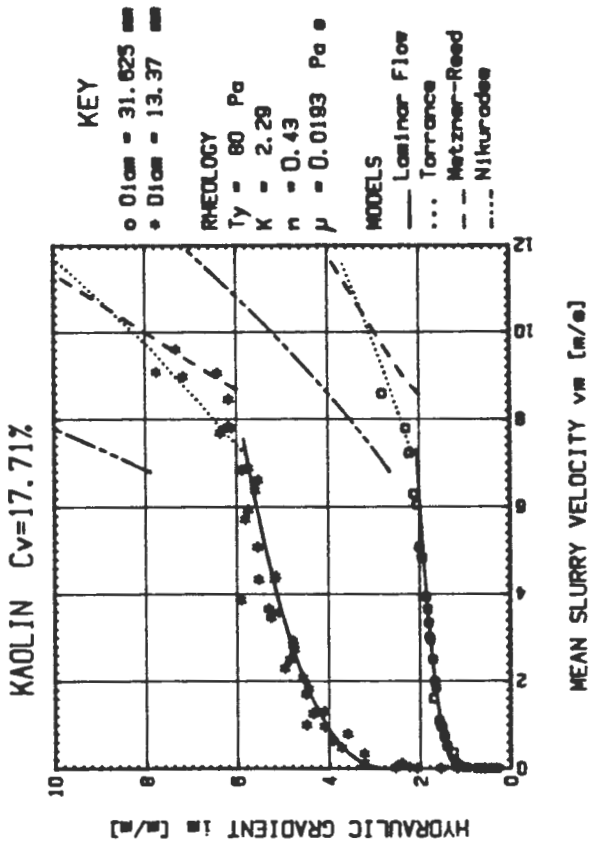

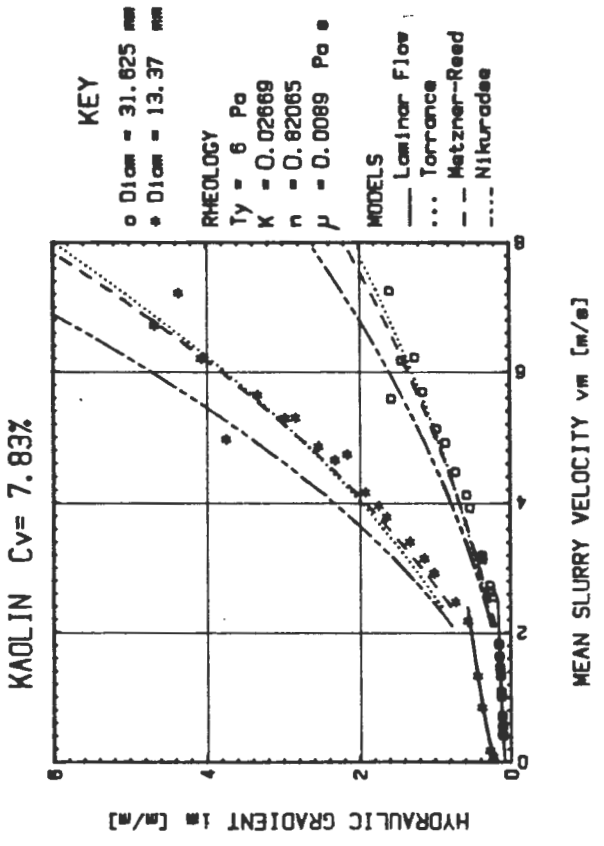

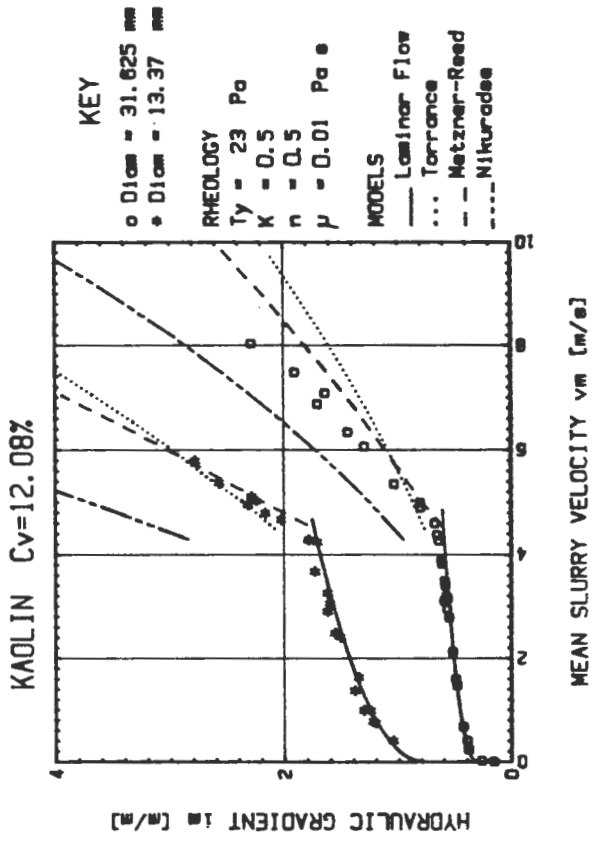

Fig. 7.6 : Flow Predictions : Kaolin

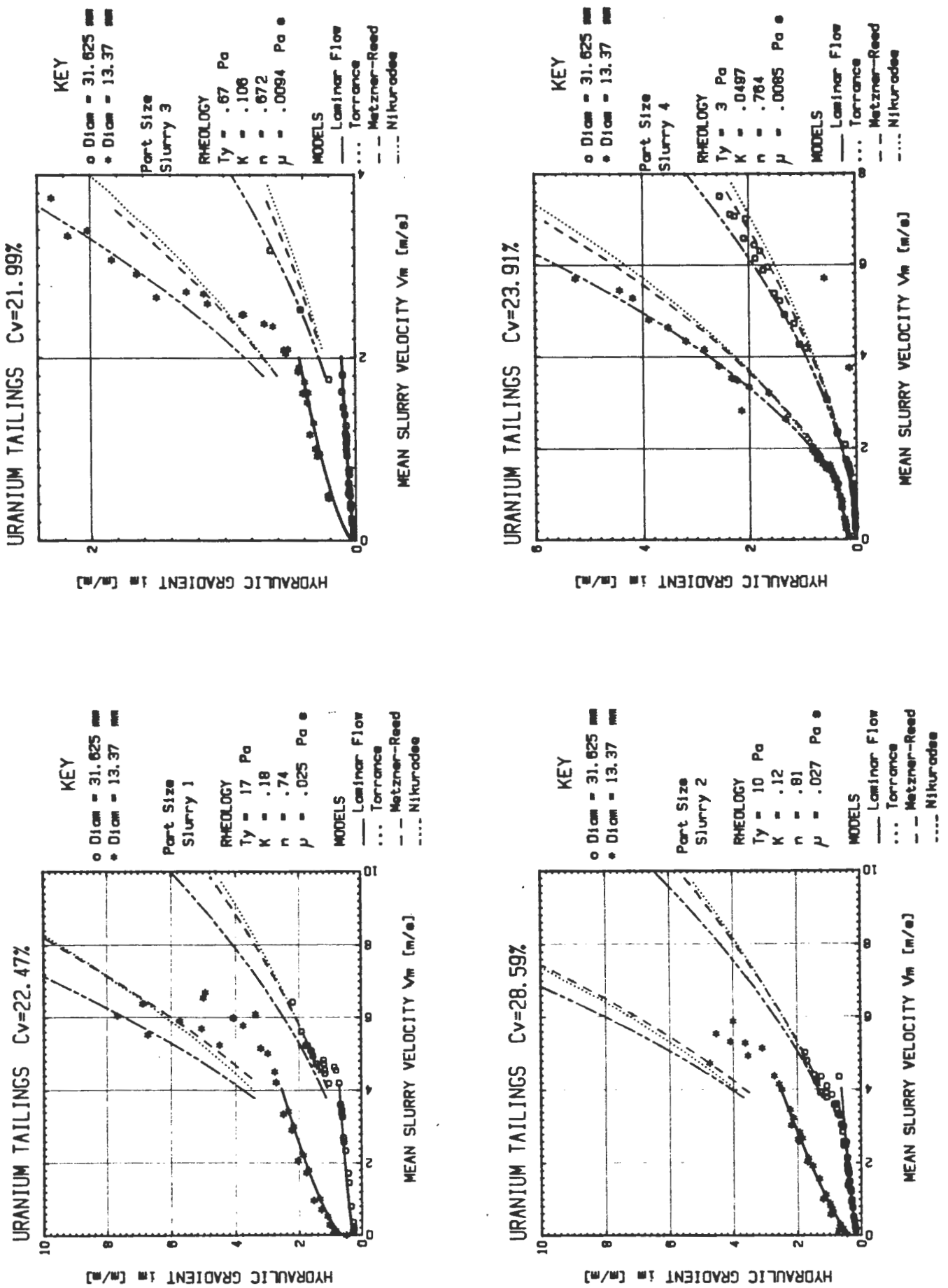

Fig. 7.7 : Flow Predictions : Uranium Tailings

CHAPTER 8

ROTARY VISCOMETER

8.1 INTRODUCTION

Rotary type viscometers are available commercially and the apparent advantages over the BBTV are as follows:

1. The fundamental fluid mechanics principles upon which its operation is based are simple.
2. The technology has been developed to a high degree of sophistication (mechanical bearings, torque measurement, etc.)
3. They are widely accepted industrial instruments.
4. They are accurate (1 to 2% - Ref. 6).
5. They have a very wide range.
6. They are easily calibrated.
7. Their operation is simple.
8. A test can be performed in a short time.
9. A rheogram can be obtained directly (using a chart recorder.)
10. Small samples are required.
11. They are compact in size.
12. They are clean.
13. They are reasonably priced.

The question as to why the BBTV has been developed must therefore be addressed.

For comparison, tests were performed (on the slurries tested in the BBTV) using a Haake Rotovisco rotary viscometer. The uranium tailings slurries 3 and 4 were not tested.

The resultant rheologies were then compared with the rheologies obtained in the BBTV and were also used to predict pipe flow curves for the slurries.

8.2 THE HAAKE ROTOVISCO VISCOMETER

This is a rotating viscometer in which the slurry to be tested is introduced into a gap between a rotating rotor or bob and a fixed cup or beaker, known as the Searle system. The gap is annular, between two coaxial, concentric cylinders, one of which is stationary, while the other rotates. The viscosity of the sample is determined from the resistance to rotation caused by the sample material. The quantities measured are torque and rotational speed. The rotor can be rotated at different fixed speeds.

8.2.1 Physical Description

This instrument is an industry standard, and a detailed description is not included here.

The measuring head was the dual measuring head with a 50/500 scale. The rotor system used was the MV1P system. This comprises a profiled rotor and a profiled cup representing the rotating and stationary measuring parts respectively.

Shear rate is varied by selecting a gear ratio, called a "U" value.

Torque measurements are measured on a graduated scale, called "S'" values.

8.2.2 Operating Procedure

The procedure adopted is as follows:

The cup is approximately half-filled with the slurry to be tested. The cup is then positioned in the meassuring head with the rotor already in position. A shear rate is selected by pushing the gear lever into the appropriate numbered slot (U). A torque reading (S') is then taken.

A number of U and S' readings are thus collected for each slurry.

8.2.3 Determination of Rheograms for Non-Newtonian Slurries using a Haake Rotovisco Viscometer

The rheogram is a graph of shear stress (τ) vs shear rate $\left(\frac{dv}{dr}\right)$.

These quantities are determined from the U and S readings as follows (ref. 5,23)

$$\tau_b = \frac{2\,k}{\pi\, D_b^2\, h} \cdot S' = A' \times S' \qquad (8.1)$$

$$\left(\frac{du}{dr}\right)_b = \frac{4\,\pi\,N}{1-s^{-2}} = \frac{B}{U} \qquad (8.2)$$

where $s = D_c/D_b$ and $U = \frac{9,72}{N}$

and A' and B are given constants as shown below.

Measuring Scale	A' (Pa/div)
500	2,78
50	0,301

B = 972 1/s for the MV1P system (geometric property).

The value of A' was determined by the absolute method described in the manual (Ref. 23). This involves applying a known torque to the rotating head, using standard weights (Fig. 8.1).

In order to account for non-Newtonian behaviour in the measuring gap, the literature (Ref. 1,5,7,10 and others) recommends multiplying the shear rate by the Krieger-Maron correction factor:

$$F_{KM} = 1 + \frac{s^2 - 1}{2s^2}\left(1 + \frac{2}{3}\ell n\, s\right)\left(\frac{1}{n''} - 1\right)$$

$$+ \frac{s^2 - 1}{6s^2}\ell n\, s\left(\left(\frac{1}{n''} - 1\right)^2 + \frac{d\left(\frac{1}{n''} - 1\right)}{d\,\log T}\right) \qquad (8.3)$$

$n'' = d\,\ell n\, T/d\,\ell n\, N$ is the slope of a logarithmic plot of T versus N. The use of equation 8.3 is discussed below.

8.3 EXPERIMENTAL RESULTS

Detailed results are presented in Appendix E.

The rotary viscometer was extremely difficult to read because the torque readings were not repeatable and decayed with time in an exponential fashion. The "correct" reading is thus ambiguous.

The results for each data point presented above are the average of the highest and lowest readings obtained at each speed setting, cycling through the speed range several times.

Fig. 8.2 shows the extent of the changes described above. Fig. 8.3 shows the same information plotted as ℓn T versus ℓn N, the slope of which is n".

Referring to Chapter 5, the data in Fig. 8.3 shows the same trends as Figs. 5.1 or 5.2.

From the arguments outlined in Chapter 5 and the fact that the spread of data in Figs. 8.2 and 8.3 is not due to any random error but a systematic degradation of the sample, it is clear that n" cannot be accurately determined. Also, the last term in equation 8.3 requires the slope of a graph of $\left(\frac{1}{n''} - 1\right)$ vs. logT to be determined, which compounds the problem. For these reasons, no shear rate correction was applied.

8.4 RHEOGRAMS

The rheograms indicated a yield pseudo-plastic rheology. This model was then fitted to the data points for each slurry.

These rheograms are presented in Figs. 8.4 (kaolin) and 8.5 (uranium tailings).

The rheologies are summarised and compared to the BBTV rheologies in Table 8.1.

8.5 COMPARATIVE RHEOGRAMS

For comparison purposes, the BBTV rheologies are also presented in Table 8.1. The respective rheologies are compared graphically in Figs. 8.6 (kaolin) and 8.7 (uranium tailings).

(Note that the rotary viscometer values above shear rates of $1000s^{-1}$ have been extrapolated using the yield pseudo-plastic model).

8.6 PIPE FLOW PREDICTIONS

Pipe flow predictions using the rotary viscometer rheology were plotted against actual flow data points from the BBTV. These are presented in Figs. 8.8 and 8.9.

8.7 DISCUSSION

8.7.1 Rheological comparisons

Comparing rheologies from Table 8.1:

For kaolin, the yield stresses (τ_y) are slightly higher for the BBTV whilst the fluid consistency index (K) is higher by a factor of about 20 for the rotary viscometer and the flow behaviour index (n) is about twice as high for the BBTV.

A similar pattern emerges for the uranium tailings. Yield stresses are similar for both viscometers, the K value is about five times as high for the rotary viscometer and the n value is about 40% higher for the BBTV.

8.7.2 Comparative Rheograms

8.7.2.1 Kaolin (Fig. 8.6)

Generally, the rotary viscometer line lies above the BBTV line. This is probably due to end effects because the kaolin slurries exhibited comparatively large deviations from Newtonian behaviour, viz. high yield stress (τ_y) and low flow behaviour index (n).

The arguments concerning effective bob height h (used to calculate shear stress in equation (8.1)) are analogous to the arguments presented in Chapter 4 concerning the

effective length of a tube which has end effects included - they are not determinable since they are a function of the rheology. The instrument constant A', hence h also, is evaluated using Newtonian fluids, therefore the large deviations shown in Fig. 8.6 are to be expected.

8.7.2.2 Uranium tailings (Fig. 8.7)

For shear rates < 1000 s^{-1}, the two viscometers are in better agreement than for the kaolin slurries. Non-Newtonian deviation is not as severe for the Uranium Tailings slurries (comparatively low τ_y and n values closer to unity) and consequently better accuracy is to be expected from the rotary viscometer.

At high shear rates, however, agreement is not good.

8.7.3 Pipe Flow Predictions

Figs. 8.8 and 8.9 show the pipe flow predictions using the rotary viscometer which compare with Figs. 7.6 and 7.7.

In order to make an objective comparison, energy gradients were predicted using equations 2.21 (for laminar flow) and 2.33 (for turbulent flow) and then compared with the BBTV experimental data using the Log Standard Error criterion (Appendix F).

Log standard errors are summarised in Table 8.2, and are shown graphically in Figs. 8.10 to 8.13. With the exception of Slurry 2, all the log standard errors using the BBTV rheology were less than those using the rotary viscometer rheology. Examination of Figs. 8.12 and 8.13 reveals that, for Slurry 2, the BBTV is in fact better than the rotary viscometer.

8.7.4 Thixotropy

The difficulty in reading the rotary viscometer due to the exponential decay phenomenon described above is well documented in the literature and is known as Thixotropic behaviour.

This author doubts the veracity of thixotropic behaviour as revealed by the rotary viscometer for two reasons:

1. The BBTV has two different diameter tubes, and two different test lengths on each tube. It was desigend thus specifically to detect such deviant behaviour as thixotropy. No such behaviour was detected since the laminar flow curves were coincident.

2. Centrifugal forces are neglected in the analysis of the rotary viscometer. With a solid/liquid mixture, centrifuge action is more likely to be the cause of this deviant behaviour.

In order to determine whether centrifuge action was occurring, samples were taken from the inner and outer surfaces of the rotary viscometer after a test on a kaolin slurry. A particle size distribution analysis was performed on the two samples thus collected, and the results are presented graphically in Fig. 8.14.

These results show that there is a significant particle size distribution gradient across the measuring gap, the coarser material having migrated across the measuring gap under centrifugal force.

This evidence supports the fact that centrifuge action is indeed occurring.

Other effects caused by centrifuge action, but which would be much more difficult to measure, are:

1. Concentration gradient across the measuring gap.
2. Build-up of "settled" solids on the outer surface, reducing the size of the measuring gap.

The behaviour of a solid/liquid mixture in the measuring gap is therefore complex, yielding results which are virtually impossible to interpret.

8.8 CONCLUSION

The rotary type viscometer in its standard form is less suitable for the rheological characterisation of the slurries tested in this thesis than the BBTV.

Slurry	Volumetric Concentration	ROTARY VISCOMETER				BBTV			
	C_v%	τ_y(Pa)	K	n	μ(Pa s)	τ_y(Pa)	K	n	μ(Pa s)
Kaolin	7,83	8	0,97	0,36	0,010	6	0,027	0,82	0,0089
"	12,08	24	5,62	0,24	0,026	23	0,50	0,50	0,010
"	14,88	40	19,8	0,15	0,030	44	1,17	0,49	0,030
"	17,71	60	49	0,14	0,044	80	2,29	0,43	0,019
Uranium Tailings Slurry 1	22,47	8	1,06	0,50	0,028	17	0,18	0,74	0,025
Uranium Tailings Slurry 2	28,59	12	0,45	0,61	0,03	10	0,12	0,81	0,027

Table 8.1 : Summary and comparison of viscometer results.

SLURRY	LOG STANDARD ERROR	
	BBTV	ROTARY VISCOMETER
Kaolin C_v = 7,83%	0,071	0,24
Kaolin C_v = 12,08%	0,043	0, 15
Kaolin C_v = 14,88%	0,030	0,13
Kaolin C_v = 17,71%	0,027	0,17
Uranium Slurry 1	0,098	0,11
Uranium Slurry 2	0,086	0,073
AVERAGE	0,059	0,15

Table 8.2 : Log Standard Error Comparison - BBTV vs. Rotary Viscometer

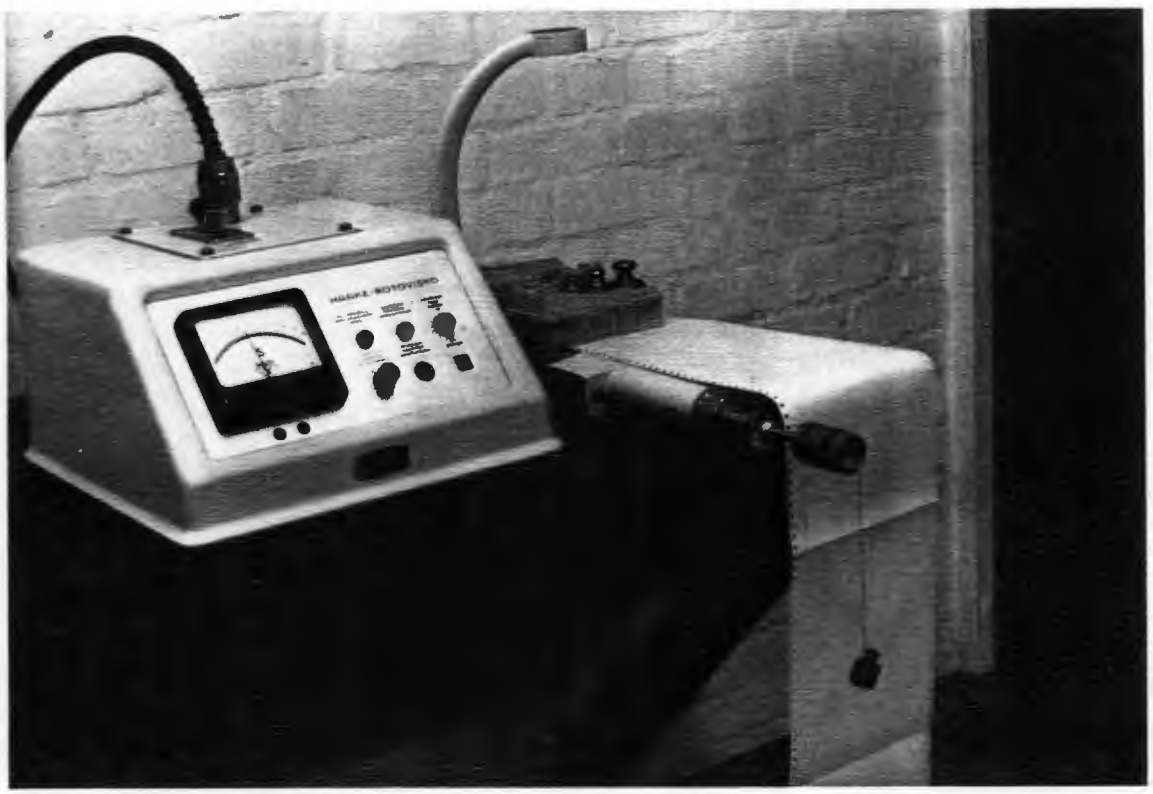

Fig. 8.1 : Absolute calibration of the measuring head

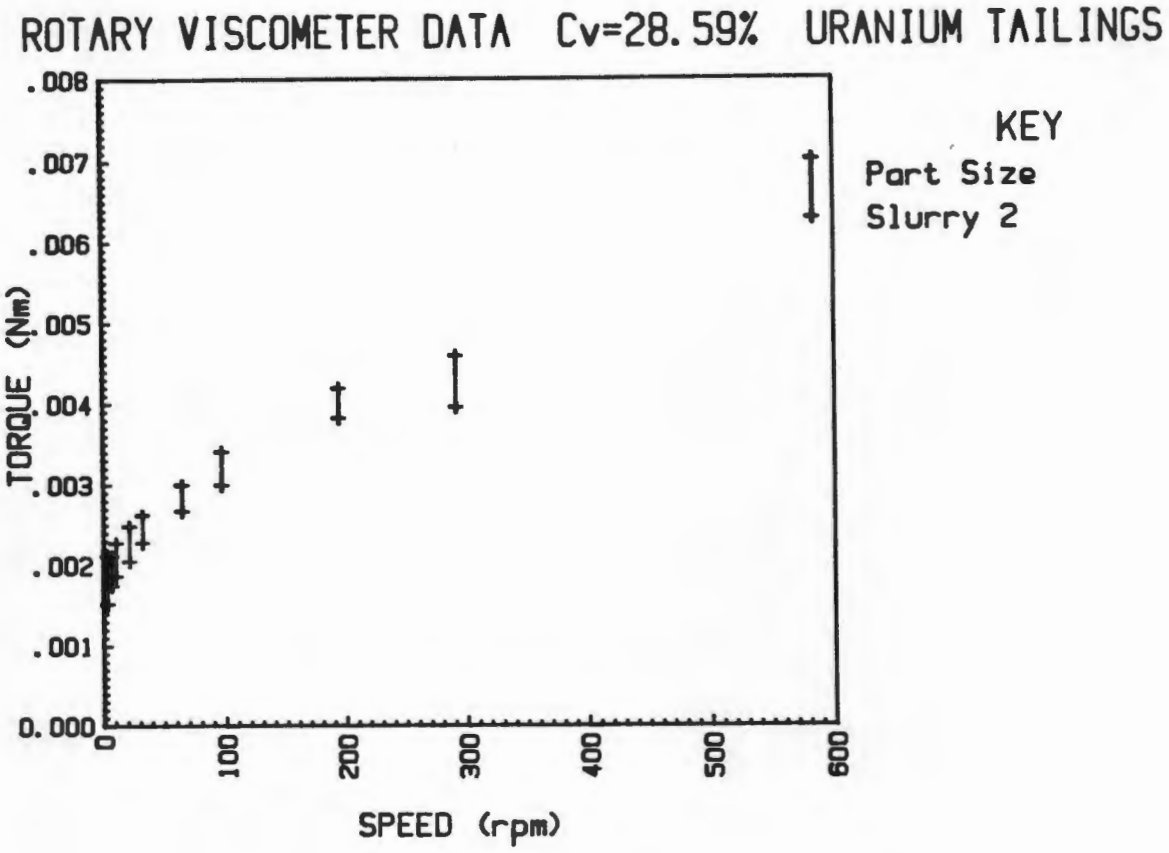

Fig. 8.2 : Spread of rotary viscometer readings on linear axes

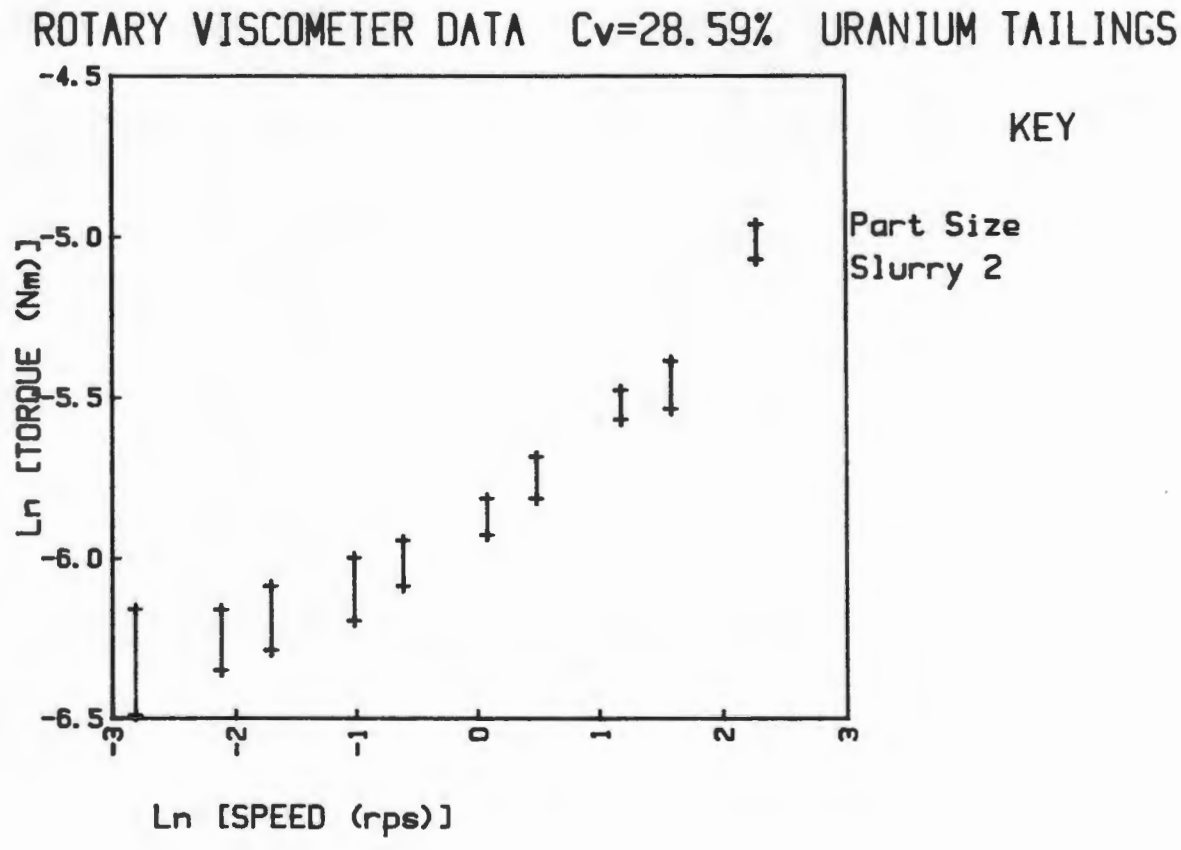

Fig. 8.3 : Spread of rotary viscometer readings on logarithmic axes

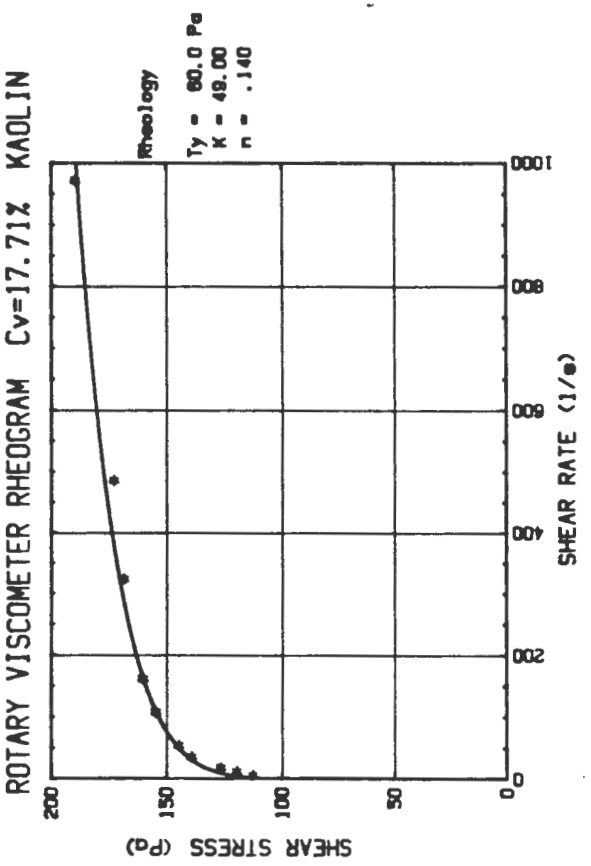

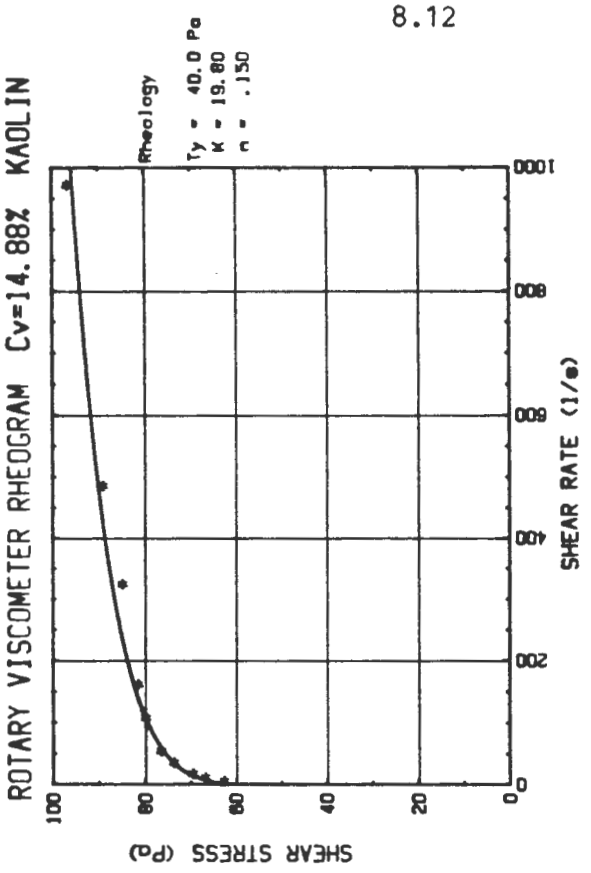

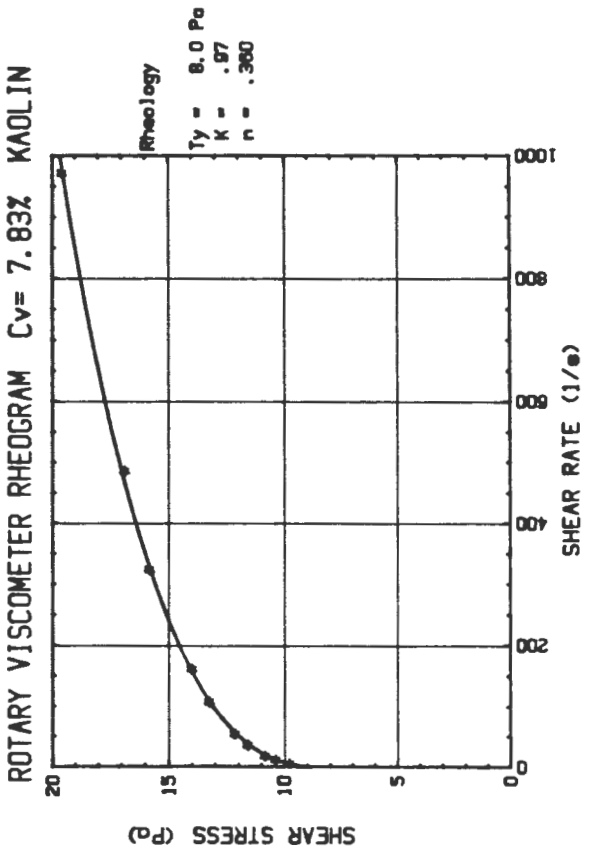

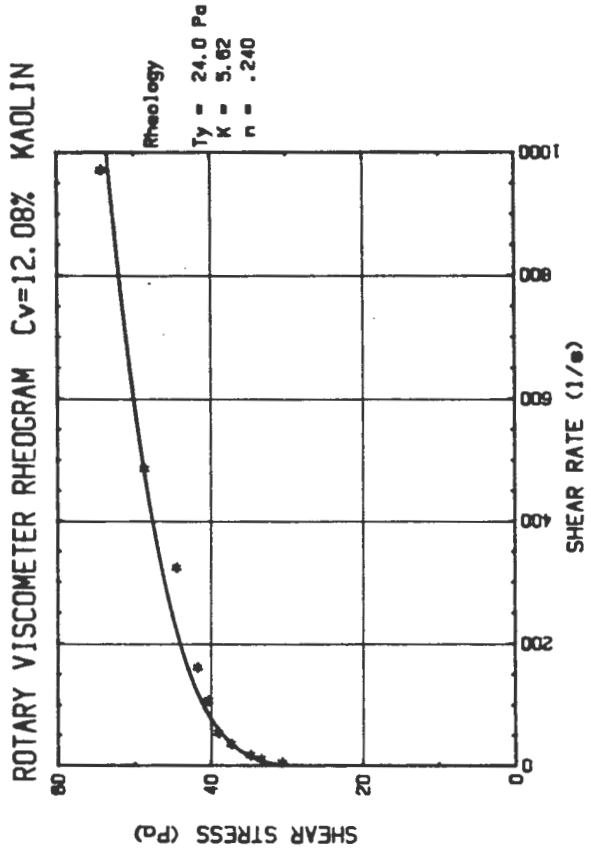

Fig. 8.4 : Rotary viscometer rheograms : kaolin

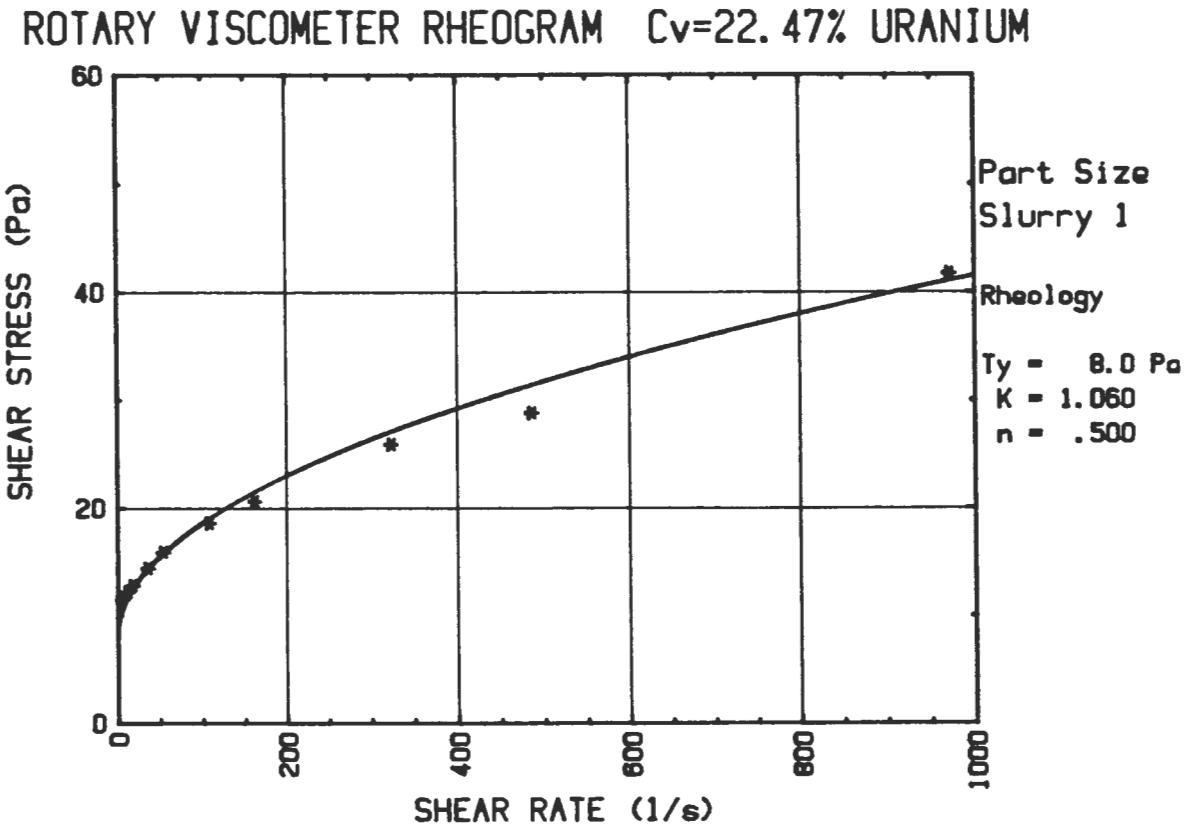

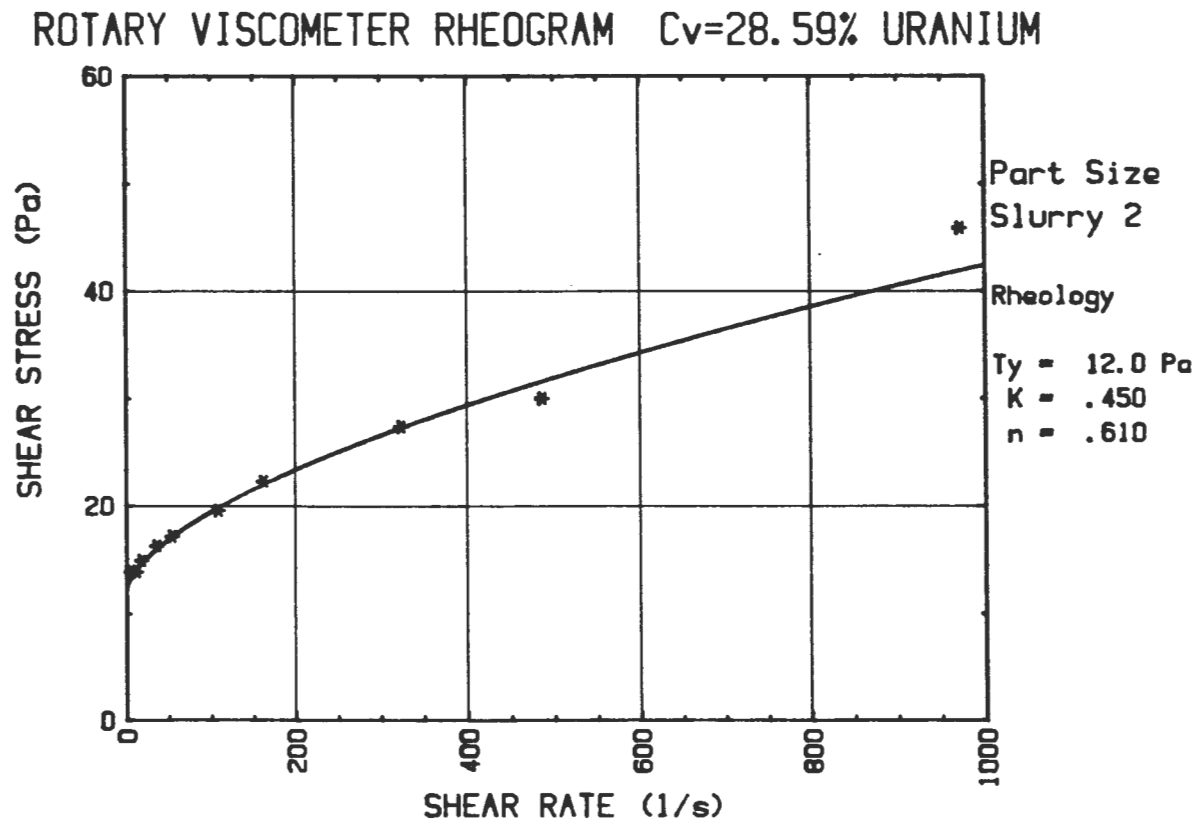

Fig. 8.5 : Rotary viscometer rheograms : uranium tailings

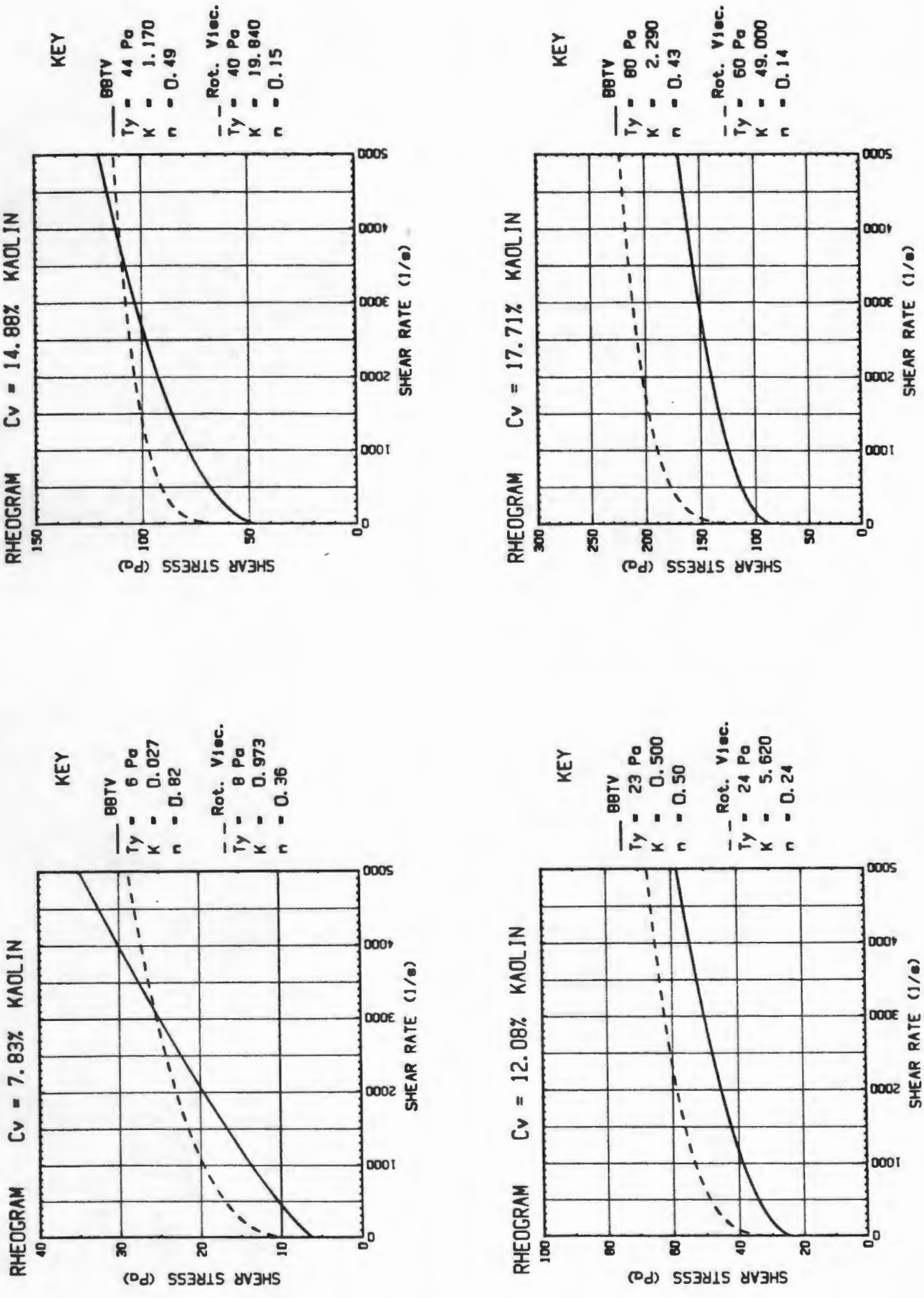

Fig. 8.6 : Comparative rheograms for kaolin

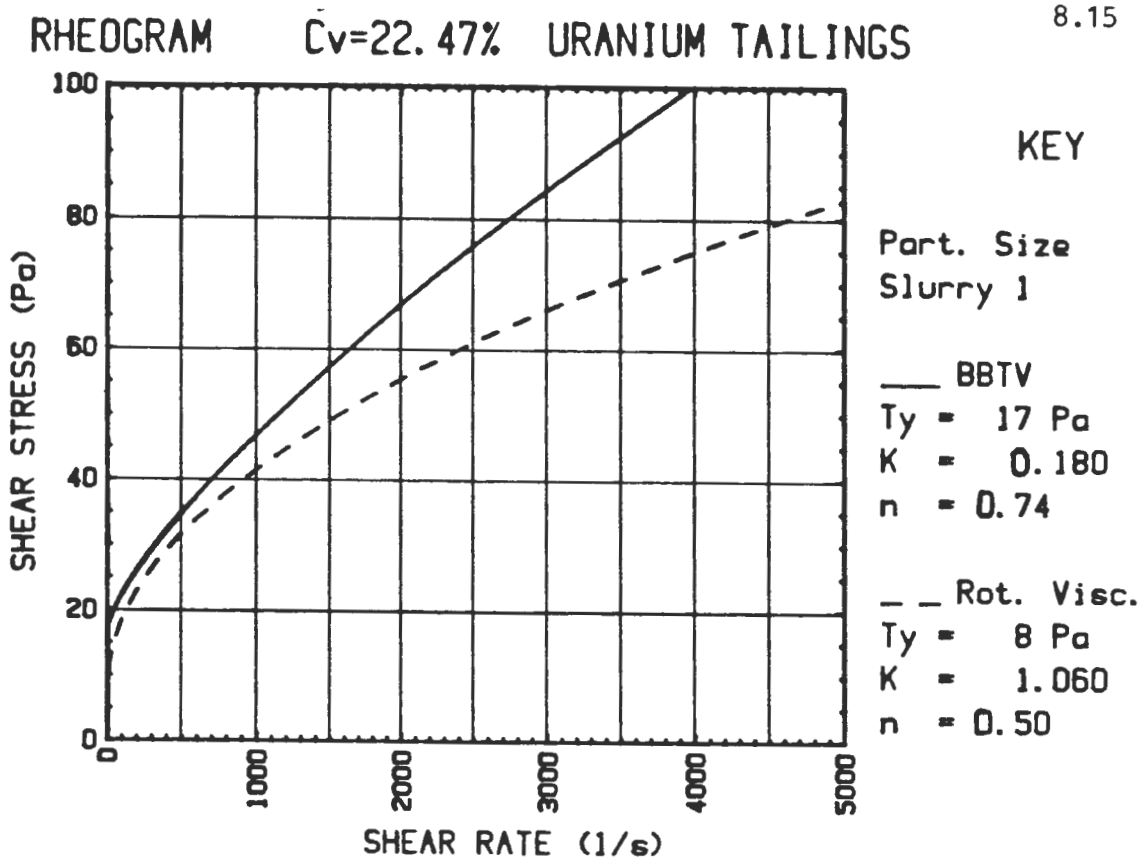

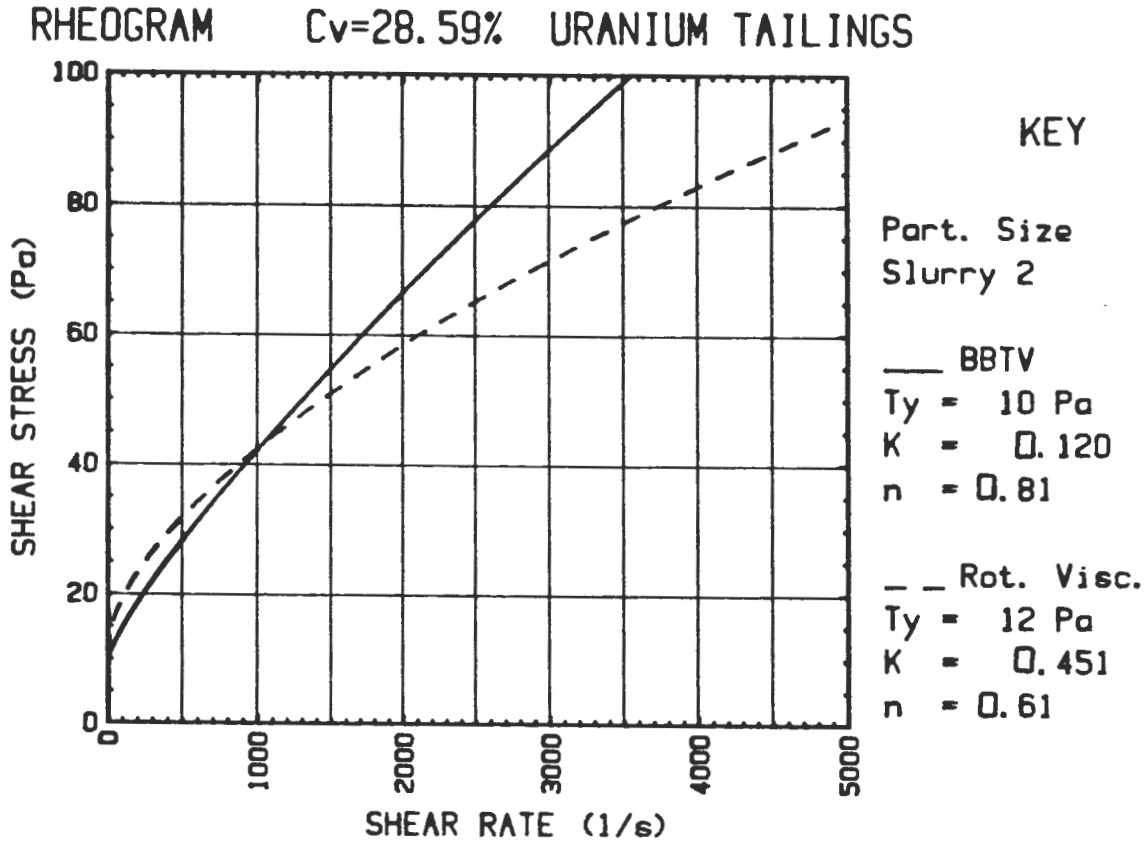

Fig. 8.7 : Comparative rheograms for uranium tailings

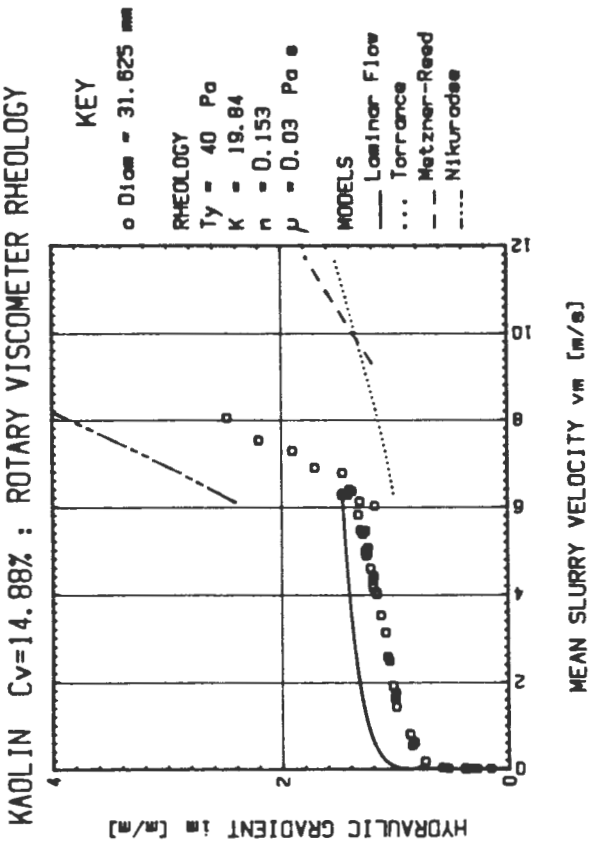

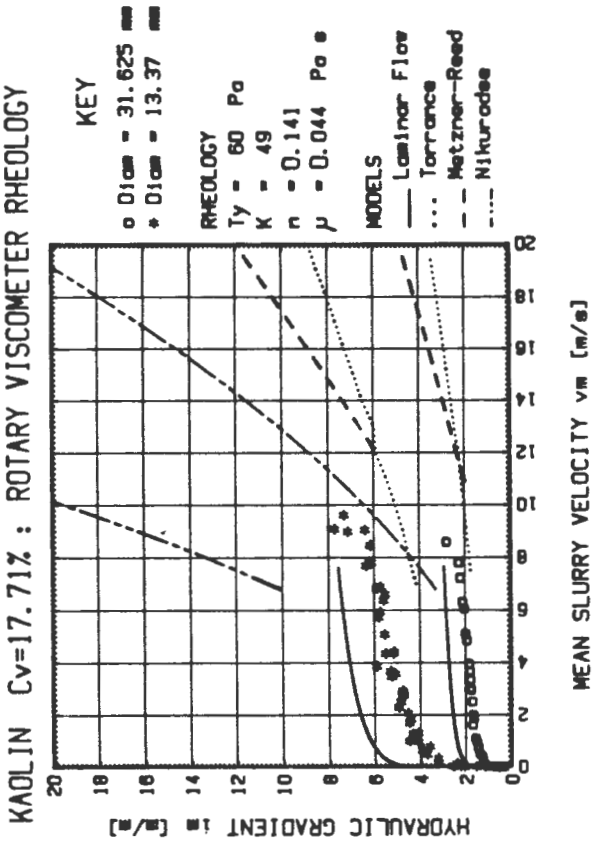

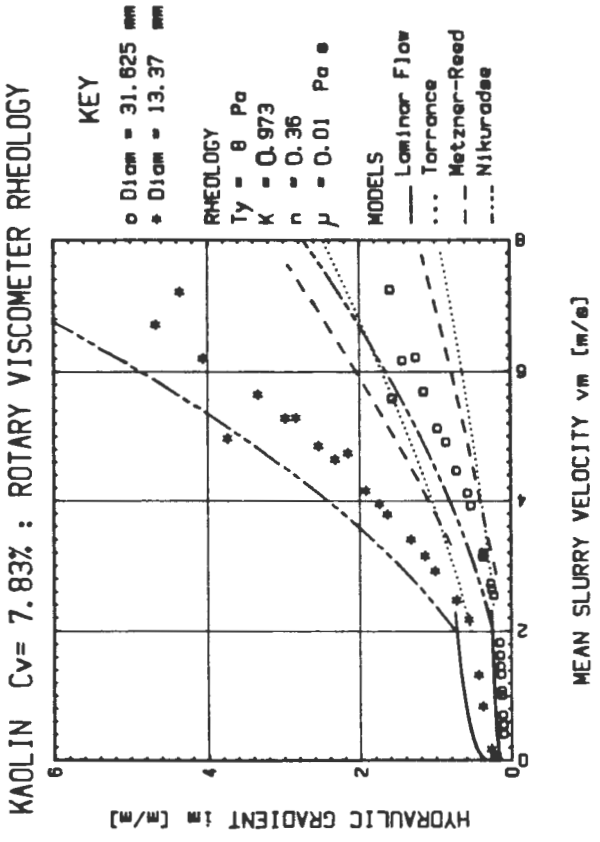

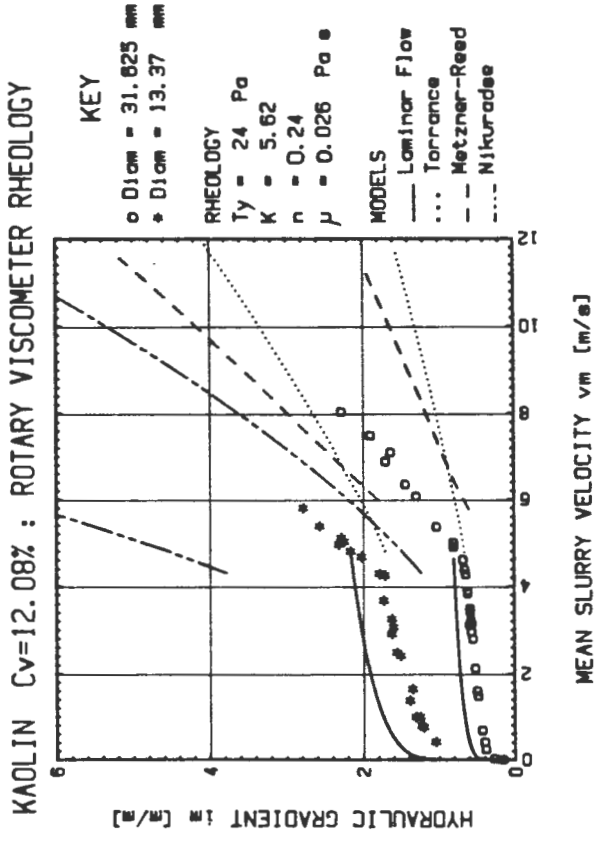

Fig. 8.6 : Pipe flow predictions for kaolin

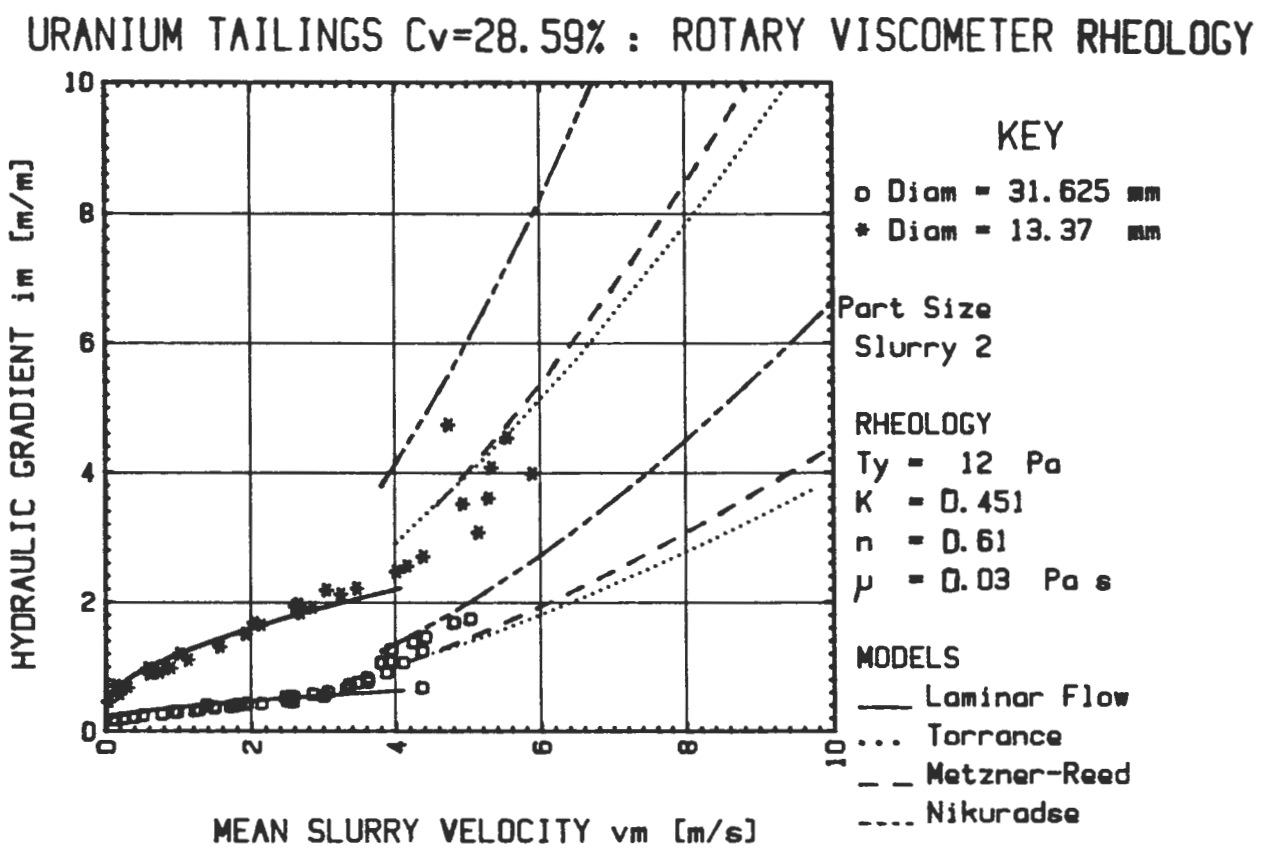

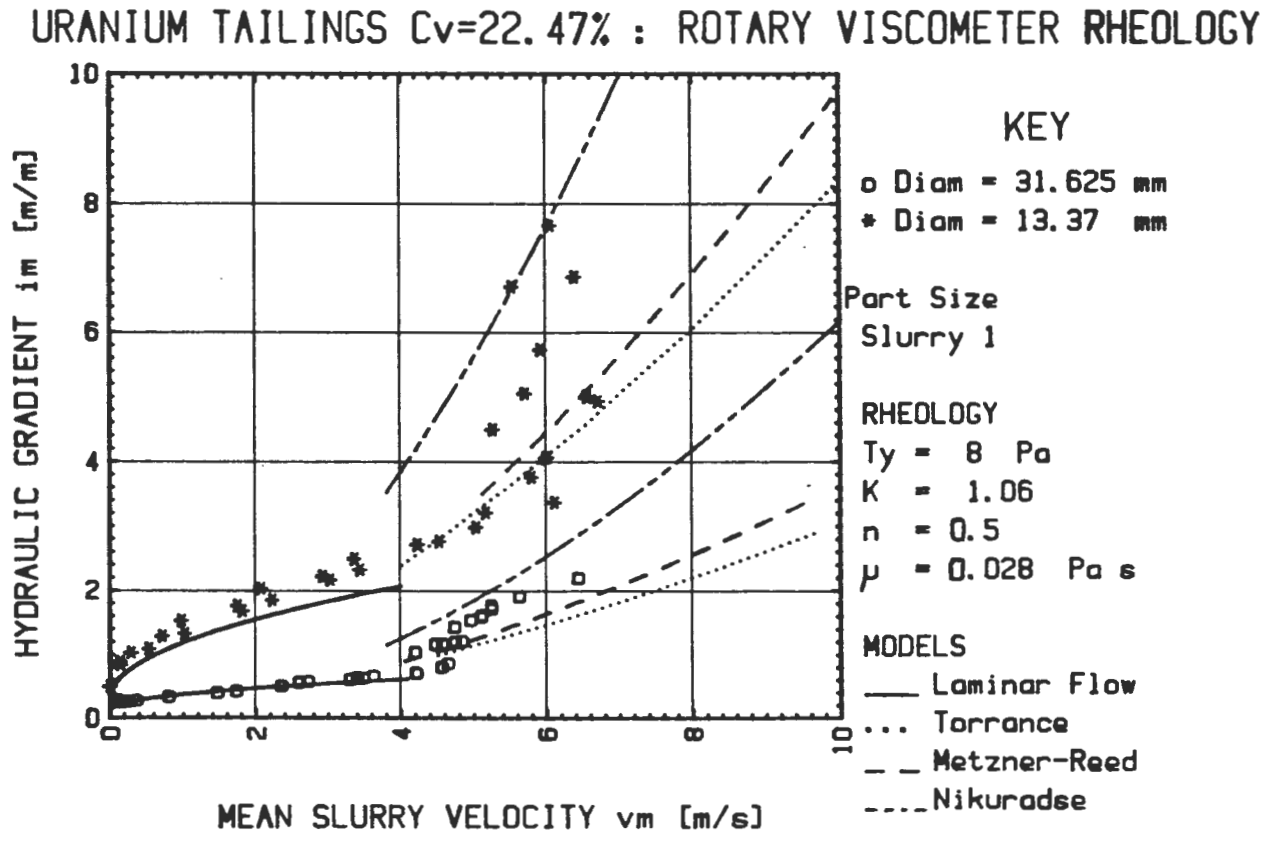

Fig. 8.9 : Pipe flow predictions for uranium tailings

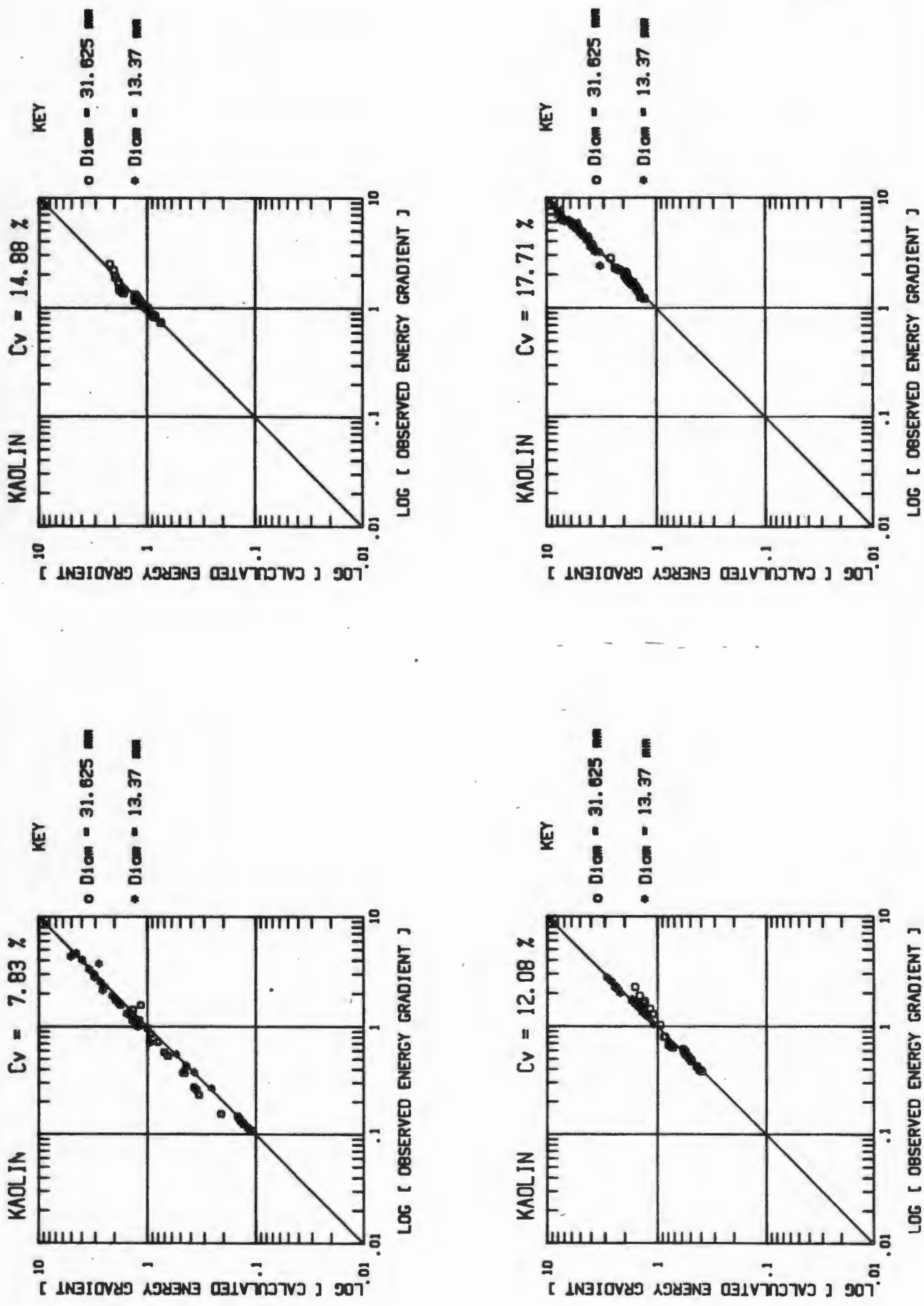

Fig. 8.10 : Kaolin BBTV Log Standard Error Plots

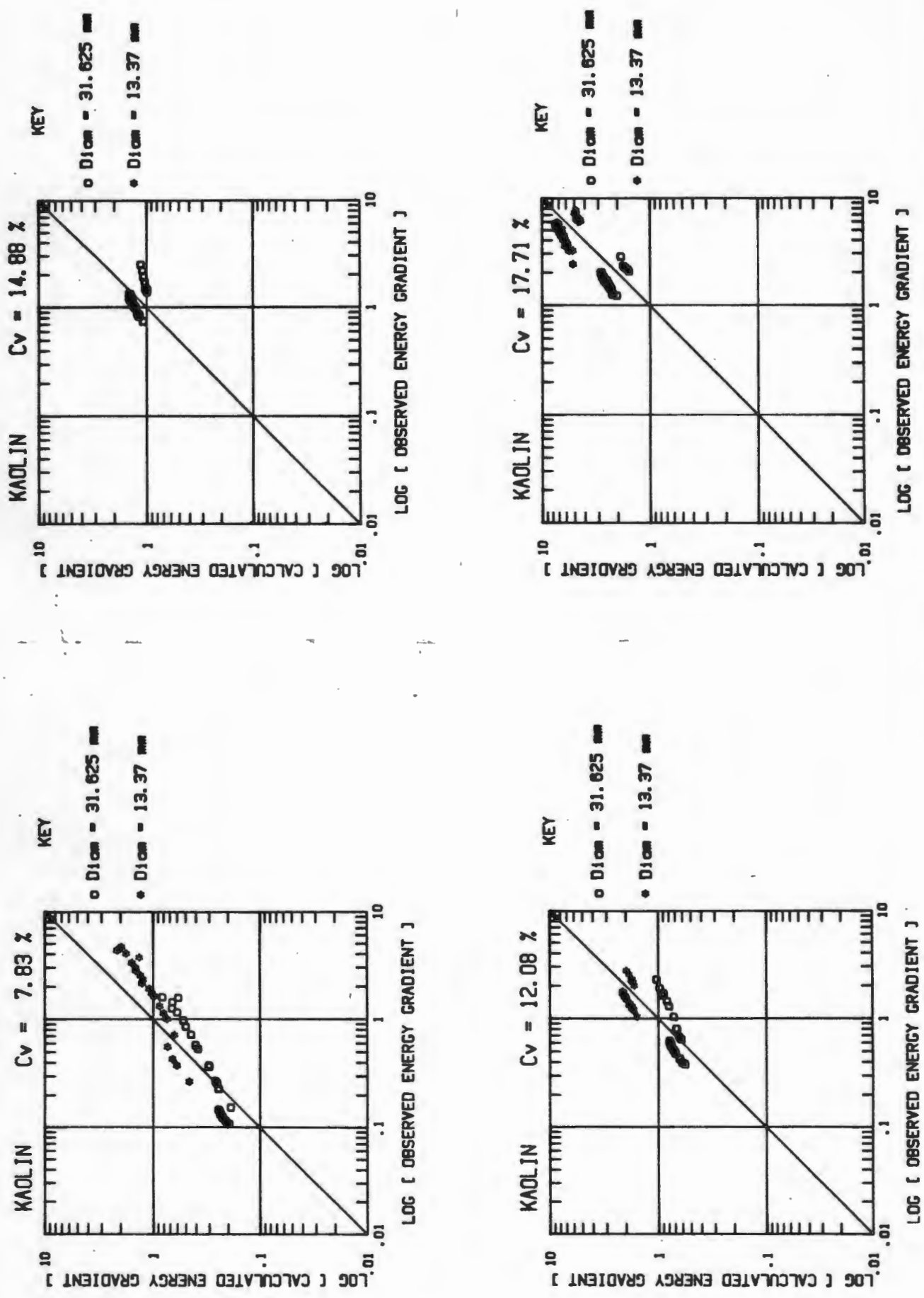

Fig. 8.11 : Kaolin Rotary Viscometer Log Standard Error Plots

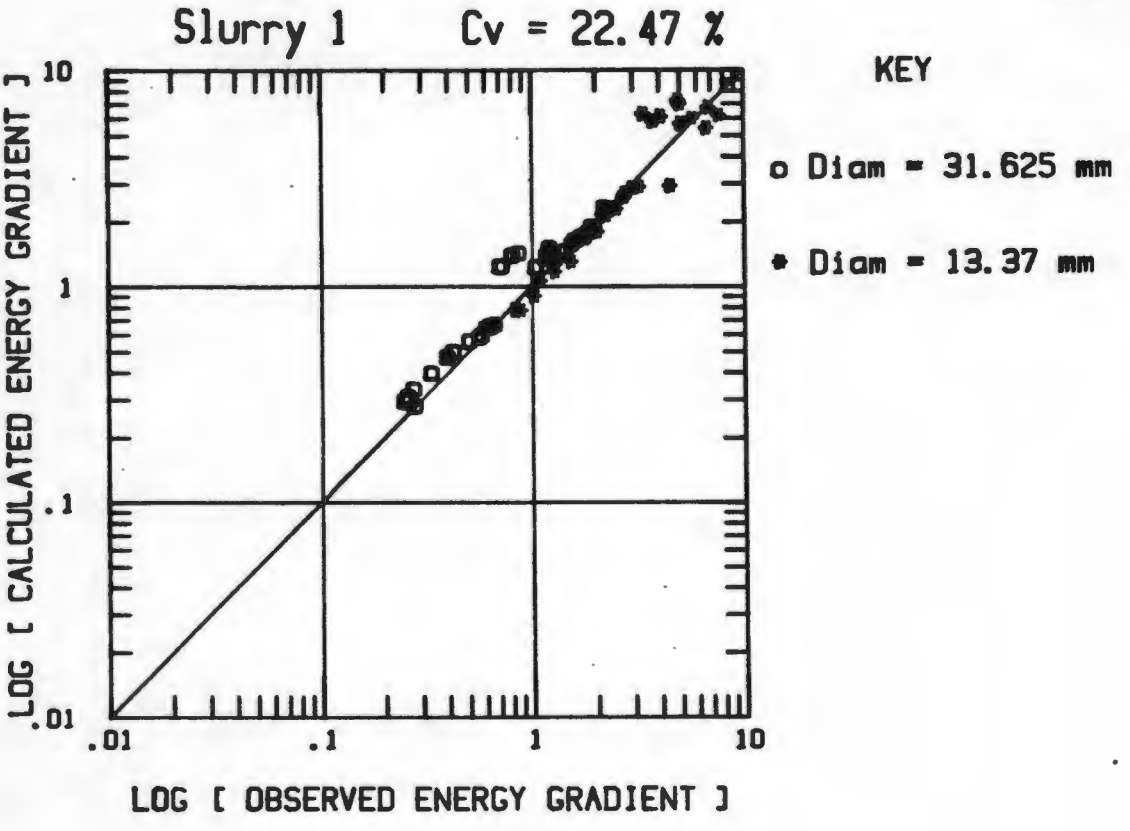

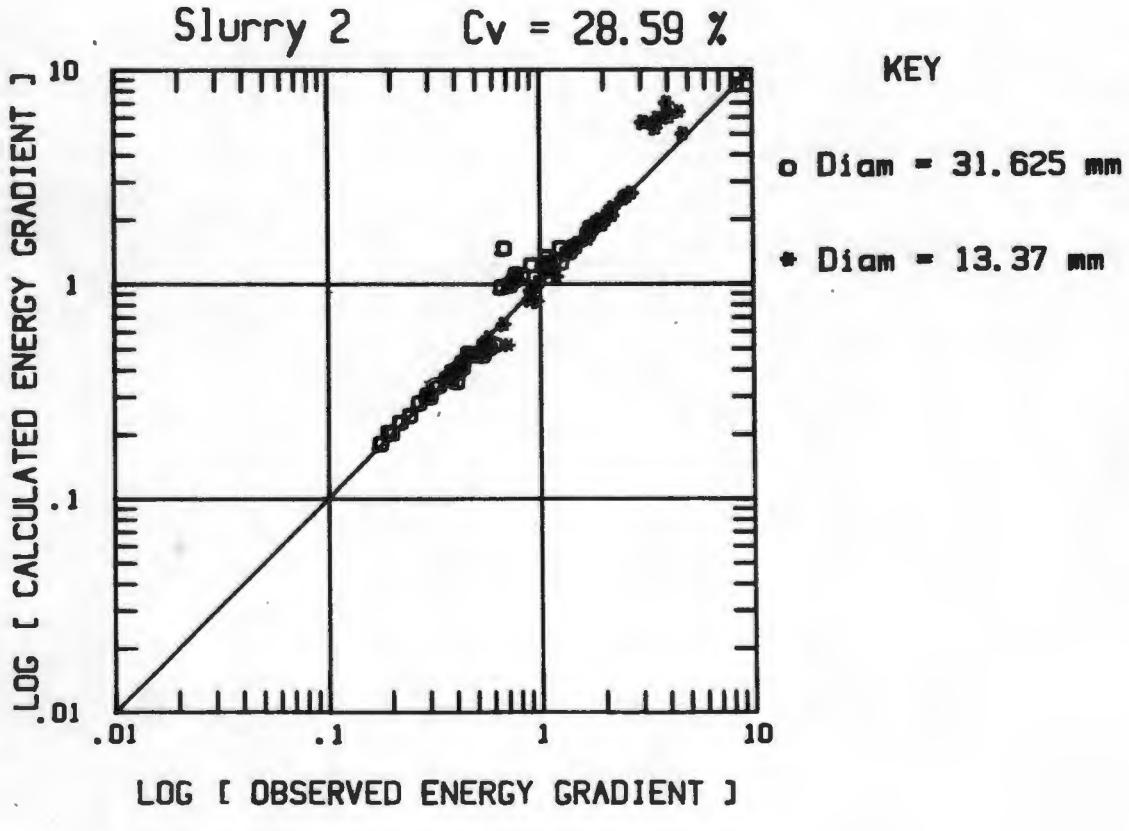

Fig. 8.12 : Uranium BBTV Log Standard Error Plots

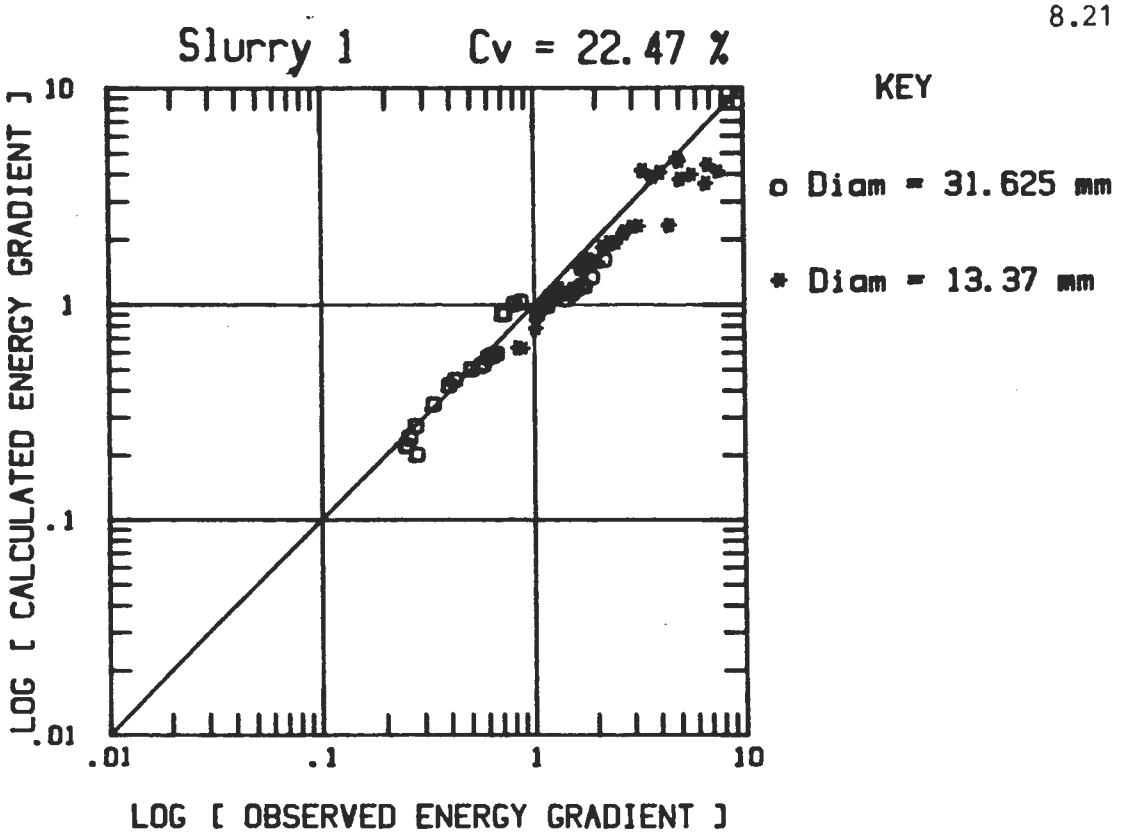

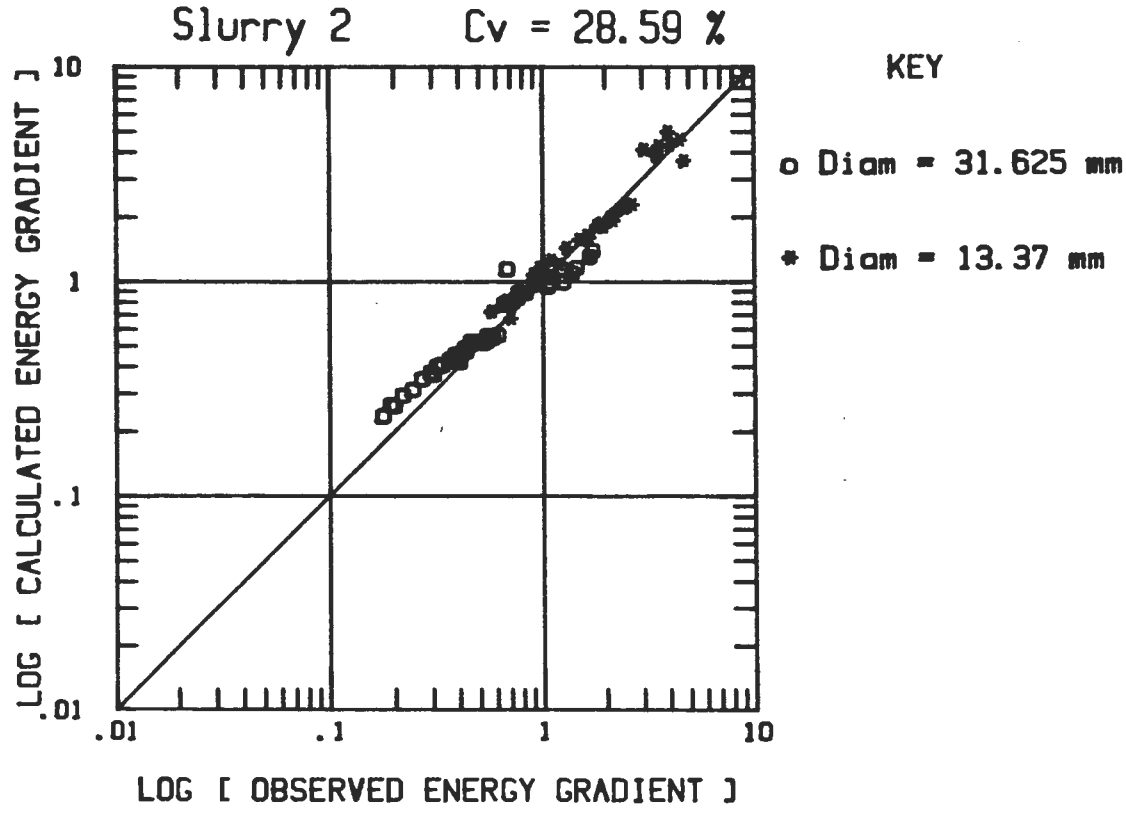

Fig. 8.13 : Uranium Rotary Viscometer Log Standard Error Plots

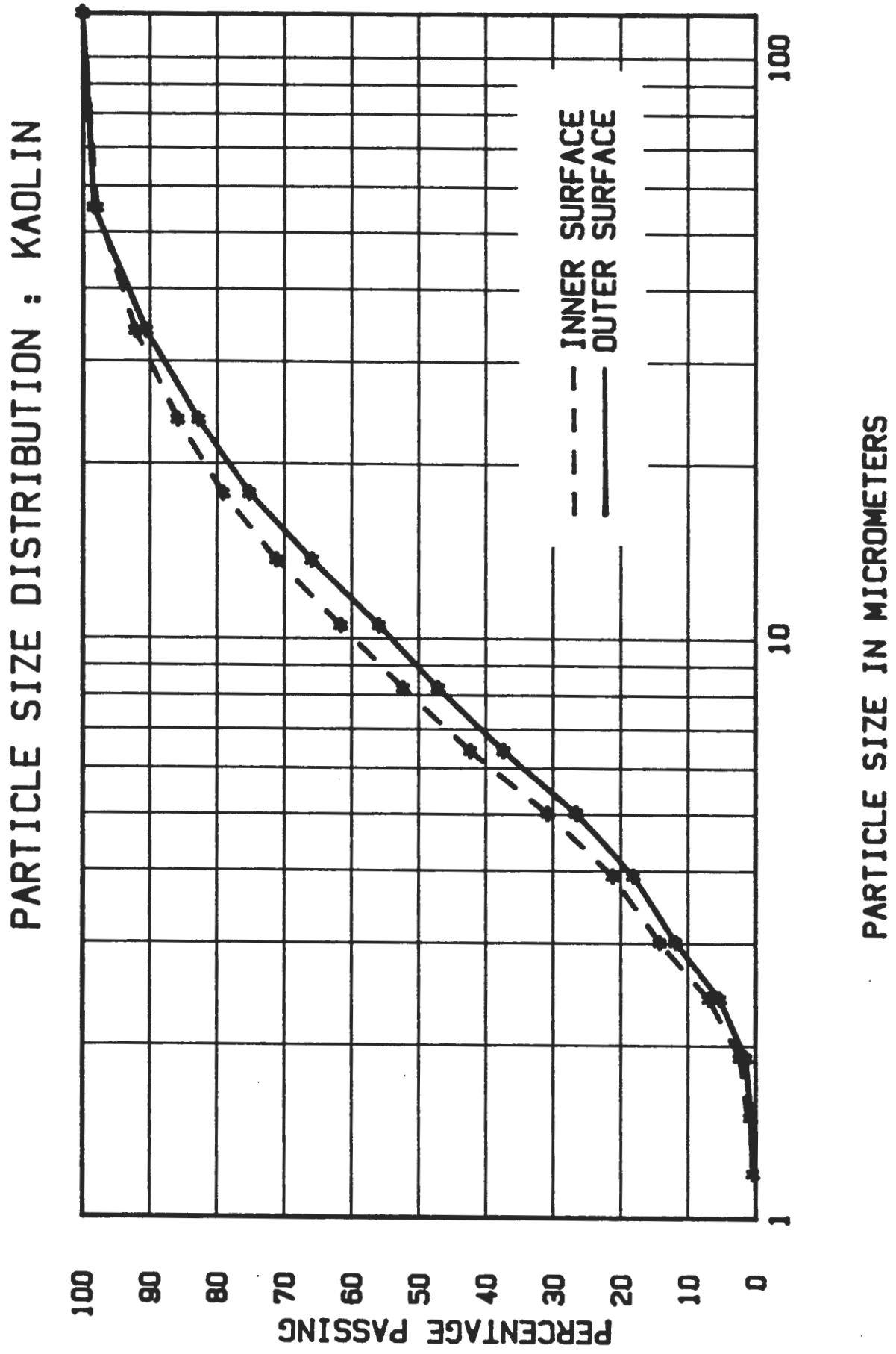

Fig. 8.14 : Particle size distribution at the inner and outer surfaces

CHAPTER 9

DISCUSSION OF BBTV EXPERIMENTAL RESULTS AND ANALYSIS

9.1 OBSERVATIONS DURING TESTS - FLOW VISUALISATION

The BBTV has transparent tubes, allowing flow visualisation by the operator. Although the slurries were opaque, the velocity of particles in the fluid layers nearest the tube wall was observable.

At low velocities the higher concentration kaolin slurries exhibited plug flow, i.e. almost constant velocity across the tube diameter. The other slurries showed a definite velocity gradient near the tube wall, which increased with increasing velocity.

In all cases, the onset of turbulence was characterised by a pulsating unstable flow, appearing to oscillate at a frequency of approximately 2 Hz. This phenomenon was apparent in the transducer readings, as well as by observation of the flow in the tubes and was greater for the uranium tailings slurries than for the kaolin slurries.

This phenomenon is reported in Reference 3 (page 43) where it is stated that the first production of eddies occurs in "flashes" which become more numerous at higher velocities.

9.2 OBSERVATIONS FROM THE PSEUDO-SHEAR DIAGRAMS

(Figs 7.1 and 7.2 and Appendix C)

Each set of data results in clearly defined laminar flow curves, characterised by a yield-pseudoplastic rheology. The results from each tube indicate a laminar flow region, transition region and subsequent turbulent flow region.

It should be noted that the procedure laid out in Chapter 5 allows for a Bingham Plastic model as well, since in such a case, n would be unity.

The maximum velocity attainable in the BBTV is approximately 9 m/s.

The principal differences between the kaolin and the uranium tailings slurries were as follows:

(i) The yield stresses for the kaolin were much higher than uranium;

(ii) The n values for kaolin (flow behaviour indices) were lower than uranium, producing a more curved rheogram.

9.3 LAMINAR FLOW PREDICTIONS

Figs. 7.1, 7.2, 7.3 and 7.4 show that the experimental points are in excellent agreement with the theoretical predictions, validating the procedure in Chapter 5.

9.4 TURBULENT FLOW PREDICTIONS

Fig. 7.6 shows that the predictions of Torrance and Metzner and Reed were in good agreement with the experimental points for the kaolin slurries. The simple approach using Nikuradse was too high, but was closest for the C_v = 7,83% slurry which had the highest n value.

For the uranium tailings (Fig. 7.7), the predictions of Torrance and Metzner and Reed were not as good, but were better for the large tube than the small tube. The simple approach using Nikuradse was much closer than for kaolin, especially for the small tube.

9.5 LAMINAR/TURBULENT TRANSITION

As noted in Chapter 2, the onset of turbulent flow depends greatly upon the amount of mechanical disturbance present. Maximum disturbance will produce a lower bound critical Reynolds number of 2320 for Newtonian fluids.

The BBTV has very little mechanical disturbance, and therefore critical Reynolds numbers higher than 2320 are to be expected.

Table 7.2 indicates critical Reynolds numbers greater than 3000. The work of Hanks *et al* (in Ref. 5) shows that for a Bingham plastic, the critical Reynolds number is dependent on both τ_y and diameter and can occur at Reynolds numbers in excess of 100 000. Although a similar theory of the yield-pseudoplastic model does not yet exist, this would explain both the high critical Reynolds numbers and the fact that the critical Reynolds number is not the same for both tubes.

The onset of turbulence occurred in "flashes", especially for the uranium slurries, causing unstable flow and the scatter shown by the smaller tube with uranium tailings (e.g. Fig. 7.7, Slurry 1, C_v = 22,47%). Examination of the larger tube results, on the same diagram, show that at higher Reynolds numbers (higher velocity), the flow "settles down" and is in good agreement with Torrance and Metzner and Reed.

CHAPTER 10

CONCLUSIONS

1. The BBTV must be used with line pressure tappings as in a conventional pipeline rig. The air pressure difference between the two vessels cannot be used to accurately predict the friction head loss across a tube, since the end corrections are not determinable.

2. The data reduction technique recommended in the literature using the Rabinowitsch-Mooney relation cannot be used for fluids with a yield stress since n' (the apparent flow behaviour index) is not constant and cannot be accurately determined.

3. A technique involving the extraction of rheological constants directly from the pseudo-shear diagram has been developed and has been validated.

4. The rotary type viscometer, in its standard form, is less suitable than the BBTV for the rheological characterisation of the slurries tested.

5. The BBTV is an instrument which is capable of correctly characterising the slurries tested. These rheologies are presented in Table 7.1.

6. The BBTV is in fact a miniature pipeline and is capable of collecting turbulent flow data and indicating the laminar-turbulent transition.

7. The turbulent flow predictions of Torrance and Metzner-Reed show good agreement for the slurries tested in the BBTV.

8. The turbulent flow prediction using Nikuradse can be used for fluids with a low yield stress and negligible rheogram curvature (n value close to unity).

REFERENCES

1. LAZARUS, J.H.; Hydraulic Transportation of Solids - Postgraduate Course Notes; UCT, 1983.

2. LAZARUS, J.H.; Rössing Tailings System Phase 1 : Preliminary Calculations Mechanistic Approach - Research Report for Rössing Uranium - HTRU; UCT, 1985.

3. BARR, G.; A Monograph of Viscometry; Oxford University Press; 1931.

4. WASP, E.J., KENNY, J.P. and GHANDI, R.L.; Solid-Liquid Flow Slurry Pipeline Transportation; Gulf Publishing Co.; 1979.

5. GOVIER, G.W. and AZIZ, K.; The Flow of Complex Mixtures in Pipes; van Nostrand Reinhold Co.; 1972.

6. VAN WAZER, J.R., LYONS, J.W., KIM, K.Y. and COLWELL, R.E.; Viscosity and Flow Measurement; Interscience Publishers; 1963.

7. SKELLAND, A.H.P.; Non-Newtonian Flow and Heat Transfer; John Wiley and Sons; 1967.

8. METZNER, A.B. and REED, J.C.; Flow of Non-Newtonian Fluids - Correlation of the Laminar, Transition, and Turbulent-flow Regions; A.I.Ch.E. Journal; Dec. 1955.

9. TORRANCE, B. McK; Friction Factors for Turbulent Non-Newtonian Fluid Flow in Circular Pipes; S.A. Mechanical Engineer; Nov 1963.

10. KRIEGER, I.M. and MARON, S.H.; Direct Determination of the Flow Curves of Non-Newtonian Fluids. III Standardized Treatment of Viscometric Data; Journal of Applied Physics; Jan, 1954.

11. IWANAMI, S. and TACHIBANA, M.S.; Viscosity and Pipeloss of Fly Ash Slurry; Hydrotransport 1, 1970.

12. FADDICK, R.R.; Flow Properties of Coal-Water Slurries; Hydrotransport 3; 1974.

13. SHOOK, C.A., HAAS, D.B., HUSBAND, W.H.W., RICHARDSON, A.D. and SMITH L.G.; A Vertical Tube Viscometer for Suspensions Containing Coarse Particles; Hydrotransport 4; 1976.

14. YAMAGATA, Y., KOKUBO, T., SUZUKI, S. and MORO, T.; Rheological Study of Viscosities and Pipeline Flow of Coal-Oil Mixtures; Hydrotransport 7; 1980.

15. LAZARUS, J.H.; Rheological Characterisation for Optimising Specific Power Consumption of a Phosphate Ore Pipeline; Hydrotransport 7; 1980.

16. DUCKWORTH, R.A., PULLUM L. and LOCKYEAR, C.F.; The Hydraulic Transport of Coarse Coal at High Concentration; CSIRO, Division of Mineral Engineering, Australia, 1982.

17. HANKS, R.W. and HANKS, K.W.; A New Viscometer for Determining the Effect of Particle Size Distributions and Concentration on Slurry Rheology; Seventh International Technical Conference on Slurry Transportation; 1982.

18. HORSLEY, R.R.; Viscometer and Pipe Loop Tests on Gold Slime Slurry at Very High Concentrations by Weight, With and Without Additives; Hydrotransport 8; 1982.

19. WANT, F.M., COLOMBERA, P.M., NGUYEN, Q.D. and BOGER, D.V.; Pipeline Design for the Transport of High Density Bauxite Residue Slurries; Hydrotransport 8; 1982.

20. LAZARUS, J.H. and SIVE, A.W.; A Novel Balanced Beam Tube Viscometer and the Rheological Characterisation of High Concentration Fly Ash Slurries; Hydrotransport 9; 1984.

21. GOLDSTEIN, S.; Modern Developments in Fluid Dynamics; Oxford University Press; 1938, Section 139.

22. DINSDALE, A. and MOORE, F.; Viscosity and its Measurement; Monographs for Students; Chapman and Hall Limited; 1962.

23. HAAKE; Rotovisco Instruction Manual.

APPENDICES

CONTENTS OF APPENDICES

Appendix A	The Rabinowitsch-Mooney Relation Derivation
Appendix B	Ancilliary Tests
Appendix C	Detailed BBTV Results
Appendix D	Verification of Viscometer Programme Suite by Hand Calculation
Appendix E	Rotary Viscometer Detailed Results
Appendix F	Log Standard Error Determinations

APPENDIX A

THE RABINOWITSCH-MOONEY RELATION DERIVATION

A.1. INTRODUCTION

The Rabinowitsch-Mooney relation (as applied to tube flow) relates the pseudo-shear rate to the true shear rate at the tube wall. This is useful in tube viscometry in reducing bulk flow parameters to a rheogram.

$$\text{i.e.} \quad \left[-\frac{du}{dr}\right]_o = \frac{8V}{D}\left[\frac{3n' + 1}{4n'}\right] \tag{A1}$$

$$\text{where} \quad n' = \frac{d\,(\ell n\, \tau_o)}{d\,(\ell n\, \frac{8V}{D})} \tag{A2}$$

A.2. DERIVATION

We start with the completely general constitutive equation for circular tube flow:-

$$-\frac{du}{dr} = f(\tau) \tag{A3}$$

A force balance on a cylindrical element of radius r and length dL yields

$$\pi r^2\, dp = 2\pi r \tau\, dL$$

$$\therefore \quad \frac{dp}{dL} = \frac{2\tau}{r}$$

$$\text{and} \quad \frac{dp}{dL} = \frac{2\tau_o}{R}$$

$$\therefore \quad r = \frac{R\tau}{\tau_o}, \quad r^2 = \frac{R^2\tau^2}{\tau_o^2} \text{ and } dr = \frac{R}{\tau_o}\, d\tau \tag{A4}$$

also $\tau_o = \frac{D\Delta p}{4L}$.

The flow rate can be obtained by integrating the velocity profile:

$$Q = 2\pi \int_o^R u.r.dr \qquad (A5)$$

Integrating by parts:

$$Q = \pi \left[u\, r^2 - \int r^2 \frac{du}{dr}\, dr \right]_o^R \qquad (A6)$$

Assuming that $u_o = 0$ (no slip at the tube wall)

$$Q = -\pi \int_o^R r^2 \frac{du}{dr}\, dr$$

$$= \pi \int_o^{\tau_o} \frac{R^2\tau^2}{\tau_o^2} \cdot \left(-\frac{du}{dr}\right) \cdot \frac{R}{\tau_o} \cdot d\tau \qquad \text{(substituting A4)}$$

$$= \frac{\pi R^3}{\tau_o^3} \int_o^{\tau_o} \tau^2 \cdot f(\tau) \cdot d\tau \qquad (A7)$$

Substituting $R = D/2$

$$\frac{8Q}{\pi D^3} = \frac{2V}{D} = \frac{1}{\tau_o^3} \int_o^{\tau_o} \tau^2 \cdot f(\tau) \cdot d\tau$$

$$\therefore \frac{8V}{D} = \frac{4}{\tau_o^3} \int_o^{\tau_o} \tau^2 \cdot f(\tau) \cdot d\tau \qquad (A8)$$

Now, differentiating with respect to τ_o (product rule)

$$\frac{d\left(\frac{8V}{D}\right)}{d\,\tau_o} = \frac{-12}{\tau_o^4} \int_o^{\tau_o} \tau^2 \cdot f(\tau) \cdot d\tau + \frac{4}{\tau_o^3} \cdot \frac{d}{d\tau_o} \left[\int_o^{\tau_o} \tau^2 \cdot f(\tau) \cdot d\tau \right] \qquad (A9)$$

The first term on the R.H.S

$$\frac{-12}{\tau_o^4}\int_o^{\tau_o}\tau^2\,.\,f(\tau)\,.\,d\tau = \frac{-3}{\tau_o}\left[\frac{4}{\tau_o^3}\int_o^{\tau_o}\tau^2\,.\,f(\tau)\,.\,d\tau\right]$$

$$= \frac{-3}{\tau_o}\,.\,\frac{8V}{D} \qquad \text{(substituting A8)}$$

The second term on the RHS is treated with the Liebniz formula

---

[The Liebniz formula states:-

$$\frac{d}{d\alpha}\int_{u_o(\alpha)}^{u_1(\alpha)} F(x,\alpha)\,dx = f(u_1,\alpha)\frac{d\,u_1}{d\,\alpha} - F(u_o,\alpha)\frac{du_o}{d\,\alpha} + \int_{u_o(\alpha)}^{u_1(\alpha)}\frac{\partial F(x,\alpha)}{\partial\alpha}\,.\,dx$$

Now, let $\alpha = \tau_o$; $u_o(\alpha) = 0$; $u_1(\alpha) = \tau_o$; $x = \tau$;
and $F(x,\alpha) = F(\tau,\tau_o) = \tau^2 f(\tau)$ (i.e. $F(\tau)$ only)]

Then $\dfrac{d}{d\tau_o}\left[\int_o^{\tau_o}\tau^2\,.\,f(\tau)\,.\,d\tau\right] = \tau_o^2\,.\,f(\tau_o)\,.\,1 - 0 + \int_o^{\tau_o} 0\,.\,d\tau$

$$= \tau_o^2\,.\,f(\tau_o)$$

$$\therefore \quad \frac{d\left(\frac{8V}{D}\right)}{d\,\tau_o} = \frac{-3}{\tau_o}\cdot\left(\frac{8V}{D}\right) + \frac{4}{\tau_o^3}\,.\,\tau_o^2\,.\,f(\tau_o)$$

$$\therefore \quad f(\tau_o) = \left(-\frac{du}{dr}\right)_o = \frac{1}{4}\left[3\left(\frac{8V}{D}\right) + \tau_o\frac{d\left(\frac{8V}{D}\right)}{d\tau_o}\right]$$

$$= \frac{\left(\frac{8V}{D}\right)}{4}\left[3 + \frac{\tau_o}{\left(\frac{8V}{D}\right)}\cdot\frac{d\left(\frac{8V}{D}\right)}{d\tau_o}\right] \qquad \text{(A10)}$$

Examining the last term:-

$$\left[\text{Consider } \frac{x}{y} \cdot \frac{dy}{dx} = \frac{x}{1} \cdot \frac{1}{y} \cdot \frac{dy}{dx}\right.$$

Now $\quad \frac{d(\ell n\ x)}{dx} = \frac{1}{x}$ and $\frac{d(\ell n\ y)}{dy} = \frac{1}{y}$

$$\therefore \quad \frac{x}{y} \cdot \frac{dy}{dx} = \frac{dx}{d(\ell n\ x)} \cdot \frac{d(\ell n\ y)}{dy} \cdot \frac{dy}{dx}$$

$$= \frac{d(\ell n\ y)}{d(\ell n\ x)} \qquad \left.\right]$$

Similarly

$$\left(-\frac{du}{dr}\right)_o = \frac{\left(\frac{8V}{D}\right)}{4}\left[3 + \frac{d\left(\ell n\ \left(\frac{8V}{D}\right)\right)}{d\ (\ell n\ (\tau_o))}\right] \qquad \text{(A11)}$$

$$\text{Let } n' = \frac{d\ (\ell n\ (\tau_o))}{d\ \left(\ell n\ \left(\frac{8V}{D}\right)\right)} \qquad \text{(A2)}$$

$$\text{Then } \left[-\frac{du}{dr}\right]_o = \frac{8V}{D}\left[\frac{3n' + 1}{4n'}\right] \qquad \text{(A1) q.e.d.}$$

A.3 CONCLUSION

Since no assumptions are made concerning the nature of the fluid, the result is perfectly general, and can be applied to any fluid, provided that there is no slip at the tube wall.

APPENDIX B

ANCILLIARY TESTS

		Page
B.1	Relative Density Determinations	B.1
B.2	pH Determinations	B.2
B.3	Particle Size Distribution Determinations	B.3

APPENDIX B

ANCILLIARY TESTS

B.1 RELATIVE DENSITY DETERMINATIONS

The following method was used for determining S_s and S_m values (adapted from Practical Physics, Part II by J.J. Lategan).

Aim: To determine the relative density of a slurry mixture using a density bottle or measuring cylinder.

Method: Find the mass of a clean dry density bottle (or measuring cylinder). Pour in the mixture using a funnel or syringe until the bottle is about half-full. Weigh. Fill the remaining space in the bottle with water. (With a measuring cylinder, fill to a convenient mark). Shake gently to remove air bubbles (use a vacuum pump if necessary), insert the stopper, wipe away excess water and weigh again. Empty the bottle, rinse with water, fill completely with water, insert stopper, wipe off excess water and weigh again.

Readings:

Mass of bottle = M1 g

Mass of bottle + solid = M2 g

Mass of bottle + solid + H_2O = M3 g

Mass of bottle full of water = M4 g (g=gram)

Calculations:

Mass of solid = M2 - M1 g

Mass of water filling the bottle = M4 - M1 g

Mass of water filling the space left by the solid = M3 - M1 g

therefore:

Mass of water having a volume equal to that of the solid = (M4-M1) - (M3-M2) g

$$\text{therefore R.D.} = \frac{M2-M1}{(M4-M1) - (M3-M2)}$$

Mass determinations were made using an August Sauter Chemical balance accurate to ± 0,1 mg.

B.2 pH DETERMINATIONS

pH Determinations were made using a Radiometer model pHM 80 pH meter and a GK 2401C glass electrode calibrated using Radiometer buffer (Disodium hydrogen phosphate/potassium dihydrogen phosphate) of pH = 7,02 (± 0,001) at 20°C, calibrated at the measuring temperature.

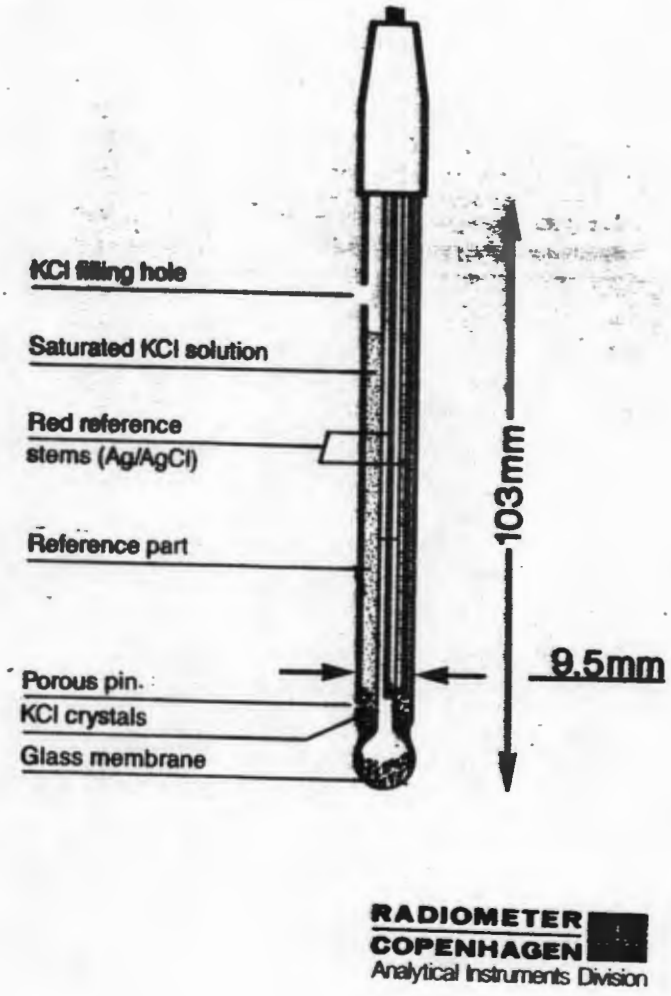

GK2401C Combined Electrode

B.3 PARTICLE SIZE DISTRIBUTION DETERMINATIONS

The particle size distributions were determined using a Malvern 2600/3600 Particle Sizer VF.6.

As a reference guide, Coulter Calibration Standard particles were analysed using the Malvern instrument (pages B.8 - B.11).

MALVERN INSTRUMENTS LTD,SPRING LANE,MALVERN,ENGLAND.

RESULTS FROM BLOCK 1

RUN NUMBER= 3 TIME=00-30-50 LOG DIFFERENCE= 2.93

SAMPLE % VOLUME CONCENTRATION= 0.0217 BEAM OBSCURATION= 0.19

SIZE MICRONS	WEIGHT % UNDER	WEIGHT IN BAND MICRONS		%	LIGHT ENERGY CALCULATED	LIGHT ENERGY MEASURED
118.4	100.0					
54.9	97.7	118.4-	54.9	2.3	82	82
33.7	90.7	54.9-	33.7	7.0	126	126
23.7	83.2	33.7-	23.7	7.4	176	177
17.7	76.2	23.7-	17.7	7.0	237	236
13.6	67.1	17.7-	13.6	9.2	327	329
10.5	57.4	13.6-	10.5	9.7	449	449
8.2	48.3	10.5-	8.2	9.1	614	615
6.4	38.6	8.2-	6.4	9.8	805	802
5.0	27.8	6.4-	5.0	10.7	1018	1026
3.9	19.1	5.0-	3.9	8.7	1256	1255
3.0	12.6	3.9-	3.0	6.5	1472	1472
2.4	6.5	3.0-	2.4	6.1	1667	1659
1.9	2.6	2.4-	1.9	3.9	1831	1853
1.5	1.5	1.9-	1.5	1.1	1981	1964
1.2	1.0	1.5-	1.2	0.5	2047	2047

D(50%) (UM)= 8.63	V M D (UM)= 14.37	S M D (UM)= 5.94
D(10%) (UM)= 2.77	D(90%)(UM)= 32.79	SPAN = 3.48

Kaolin - 63 mm Lens

100 MICRON
MALVERN 2600/3600 PARTICLE SIZER VF.6

MALVERN INSTRUMENTS LTD,SPRING LANE,MALVERN,ENGLAND.

RESULTS FROM BLOCK 1

RUN NUMBER= 9 TIME=01-39-50 LOG DIFFERENCE= 3.16

SAMPLE % VOLUME CONCENTRATION= 0.0062 BEAM OBSCURATION= 0.23

SIZE MICRONS	WEIGHT % UNDER	WEIGHT IN BAND MICRONS		%	LIGHT ENERGY CALCULATED	LIGHT ENERGY MEASURED
188.0	100.0					
87.2	97.0	188.0-	87.2	3.0	159	152
53.5	87.2	87.2-	53.5	9.8	239	240
37.6	77.5	53.5-	37.6	9.7	318	320
28.1	68.9	37.6-	28.1	8.5	405	404
21.5	60.3	28.1-	21.5	8.6	531	534
16.7	51.7	21.5-	16.7	8.6	694	695
13.0	43.0	16.7-	13.0	8.7	910	913
10.1	33.7	13.0-	10.1	9.3	1147	1145
7.9	24.2	10.1-	7.9	9.5	1386	1396
6.2	16.5	7.9-	6.2	7.7	1606	1606
4.8	11.0	6.2-	4.8	5.5	1746	1747
3.8	6.9	4.8-	3.8	4.1	1832	1826
3.0	4.0	3.8-	3.0	2.9	1889	1924
2.4	2.5	3.0-	2.4	1.5	1966	1960
1.9	1.5	2.4-	1.9	1.0	2047	2047

D(50%) (UM)= 15.99 | V M D (UM)= 26.47 | S M D (UM)= 9.78

D(10%) (UM)= 4.57 | D(90%)(UM)= 63.07 | SPAN = 3.66

Slurry 1 - 100 mm Lens

100 MICRON 300MM LENS

MALVERN 2600/3600 PARTICLE SIZER VF.6

MALVERN INSTRUMENTS LTD,SPRING LANE,MALVERN,ENGLAND.

RESULTS FROM BLOCK 1

RUN NUMBER= 15 TIME=02-12-30 LOG DIFFERENCE= 2.91

SAMPLE % VOLUME CONCENTRATION= 0.0058 BEAM OBSCURATION= 0.19

SIZE MICRONS	WEIGHT % UNDER	WEIGHT IN BAND MICRONS		%	LIGHT ENERGY CALCULATED	LIGHT ENERGY MEASURED
564.0	100.0					
261.6	99.9	564.0-	261.6	0.1	31	26
160.4	99.2	261.6-	160.4	0.7	54	54
112.8	97.7	160.4-	112.8	1.5	86	85
84.3	94.8	112.8-	84.3	2.9	130	130
64.6	90.5	84.3-	64.6	4.3	197	198
50.2	84.1	64.6-	50.2	6.4	293	292
39.0	76.4	50.2-	39.0	7.7	430	435
30.3	68.7	39.0-	30.3	7.7	598	594
23.7	60.1	30.3-	23.7	8.6	798	802
18.5	51.6	23.7-	18.5	8.5	1029	1032
14.5	43.5	18.5-	14.5	8.1	1272	1275
11.4	34.6	14.5-	11.4	8.8	1526	1516
9.1	25.5	11.4-	9.1	9.1	1753	1778
7.2	17.7	9.1-	7.2	7.8	1945	1938
5.8	10.2	7.2-	5.8	7.6	2047	2047

D(50%) (UM)= 17.69 | V M D (UM)= 28.78 | S M D (UM)= 11.51

D(10%) (UM)= 5.74 | D(90%)(UM)= 63.54 | SPAN = 3.27

Slurry 1 - 300mm Lens

250 MICRON
MALVERN 2600/3600 PARTICLE SIZER VF.6

MALVERN INSTRUMENTS LTD,SPRING LANE,MALVERN,ENGLAND.

RESULTS FROM BLOCK 1

RUN NUMBER= 13 TIME=01-56-50 LOG DIFFERENCE= 3.06

SAMPLE % VOLUME CONCENTRATION= 0.0061 BEAM OBSCURATION= 0.20

SIZE MICRONS	WEIGHT % UNDER	WEIGHT IN BAND MICRONS		%	LIGHT ENERGY CALCULATED	LIGHT ENERGY MEASURED
188.0	100.0					
87.2	84.2	188.0-	87.2	15.8	260	259
53.5	69.8	87.2-	53.5	14.4	300	302
37.6	62.3	53.5-	37.6	7.5	348	347
28.1	55.2	37.6-	28.1	7.1	414	415
21.5	48.4	28.1-	21.5	6.8	531	535
16.7	41.9	21.5-	16.7	6.5	691	689
13.0	34.9	16.7-	13.0	7.0	901	905
10.1	27.4	13.0-	10.1	7.6	1132	1134
7.9	19.9	10.1-	7.9	7.5	1371	1379
6.2	13.9	7.9-	6.2	5.9	1587	1587
4.8	9.9	6.2-	4.8	4.0	1726	1734
3.8	6.0	4.8-	3.8	3.9	1824	1820
3.0	3.1	3.8-	3.0	2.9	1896	1925
2.4	2.0	3.0-	2.4	1.2	1977	1966
1.9	1.2	2.4-	1.9	0.8	2047	2047

D(50%) (UM)= 23.09 | V M D (UM)= 44.08 | S M D (UM)= 11.73

D(10%) (UM)= 4.86 | D(90%)(UM)= 124.03 | SPAN = 5.16

Slurries 2 and 3 - 100mm Lens

250 MICRON 300MM LENS
MALVERN 2600/3600 PARTICLE SIZER VF.6

MALVERN INSTRUMENTS LTD,SPRING LANE,MALVERN,ENGLAND.

RESULTS FROM BLOCK 1

RUN NUMBER= 18 TIME=02-23-40 LOG DIFFERENCE= 2.71

SAMPLE % VOLUME CONCENTRATION= 0.0091 BEAM OBSCURATION= 0.25

SIZE MICRONS	WEIGHT % UNDER	WEIGHT IN BAND MICRONS		%	LIGHT ENERGY CALCULATED	LIGHT ENERGY MEASURED
564.0	100.0					
261.6	96.4	564.0-	261.6	3.6	64	64
160.4	90.8	261.6-	160.4	5.7	95	96
112.8	84.2	160.4-	112.8	6.6	130	130
84.3	76.0	112.8-	84.3	8.2	172	172
64.6	68.6	84.3-	64.6	7.4	230	233
50.2	62.6	64.6-	50.2	6.0	303	300
39.0	56.6	50.2-	39.0	6.0	400	402
30.3	51.0	39.0-	30.3	5.5	521	523
23.7	45.6	30.3-	23.7	5.4	676	676
18.5	40.2	23.7-	18.5	5.4	867	870
14.5	35.3	18.5-	14.5	4.9	1079	1083
11.4	30.0	14.5-	11.4	5.3	1327	1317
9.1	23.9	11.4-	9.1	6.1	1586	1605
7.2	17.7	9.1-	7.2	6.2	1842	1837
5.8	10.6	7.2-	5.8	7.1	2047	2047

D(50%) (UM)= 29.08	V M D (UM)= 63.38	S M D (UM)= 13.20
D(10%) (UM)= 5.56	D(90%)(UM)= 154.77	SPAN = 5.13

Slurries 2 and 3 - 300mm Lens

Coulter Calibration Standard Data Sheet

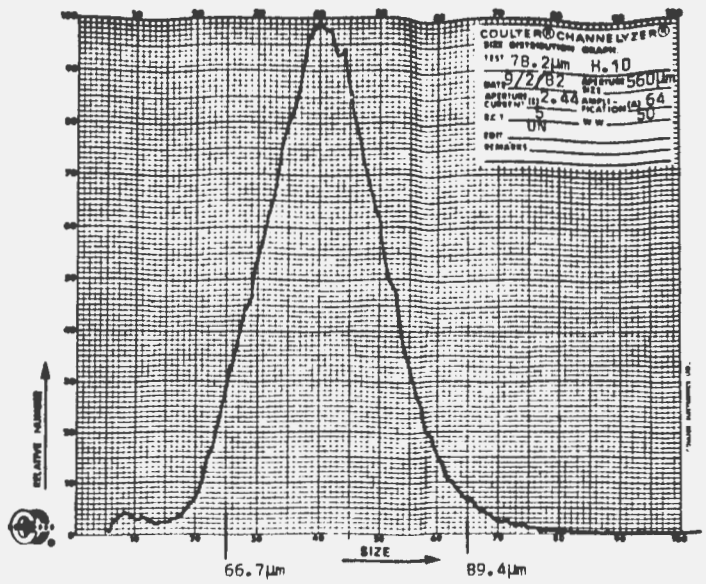

With a COULTER COUNTER® TAII/PCA system it may be easier to calibrate using the peak splitting method whereby the calibration point is the junction of two consecutive channels containing equal number (population) data, the 'number peak split', (figure E).

CHOICE OF CALIBRATION STANDARD Generally the latex dispersions, because they are the most stable, will be chosen. The COULTER COUNTER® needs to be calibrated at only one size level for each aperture, preferably between 5 and 20% of the aperture diameter, as it has an essentially linear response to particle volume over its working range

The instrument should usually be calibrated with the electrolyte to be used for the subsequent analyses, although the later models (TAII, TA, T, ZM & ZBI are independent of electrolyte composition over quite a wide range of conductivities and temperature

REDISPERSION OF CALIBRATION STANDARDS COULTER® calibration suspensions contain both a preservative and a surface active agent specifically chosen to reduce any tendency of the particles to agglomerate or cake upon storage

Before use, shake the vial vigorously for several seconds, and ensure that no sediment is left in the vial. Add one drop to each 100ml (approx) of electrolyte. Further dispersion by ultrasonic agitation should not be necessary, but will do no harm. The half count calibration procedure as described by Coulter Electronics Ltd was originally chosen because of its independence of minor changes in dispersion quality; doublets, triplets etc are excluded from the calibration.

Dispersions of dry calibration material must be made by spatulating into a surfactant such as COULTER® Dispersant. Further dispersion with ultrasonic energy is desirable

FREQUENCY OF CALIBRATION It is expected that the COULTER COUNTER® and aperture combination in use will not require calibration at intervals of less than one week as long as the aperture is kept clean. It is recommended that recalibration is performed weekly, and immediately after any servicing, and data recorded to monitor any long term drift in the electronic components.

INDICATIONS OF INSTABILITY OR DETERIORATION. Inability to obtain expected values may indicate product instability or deterioration. Particle suspensions should not be allowed to dry out, calibration powders must be kept dry until use. Discard diluted calibration standard suspensions after use.

If three or more consecutive calibrations fall outside your expected range, it may mean that the instrument is not operating properly or that the calibration standard is changing in one or more ways. The calibration of the COULTER COUNTER® SHOULD NOT BE CHANGED unless one or more of the following steps make it necessary.

a. Check that the aperture wafer and the aperture tube are clean and free from bubbles.

b. Check background count of electrolyte diluent.

c. Check the performance of your COULTER COUNTER® by using another batch of calibration standard suitable for that aperture tube

d. Consult your COULTER® Service Representative

REFERENCES

1. Harfield J.G. and Wood W.M., Standard Calibration Materials for the COULTER COUNTER®. Proc. Particle Size Analysis Conference, Bradford 1970, Society for Analytical Chemistry, 1971, 293-300.
2. Theory of the COULTER COUNTER® – Bulletin T-1; Coulter Electronics Inc. 1957 (Reprinted in most Coulter Electronics Ltd instruction manuals).
3. Matthews B.A. and Rhodes C.T., J. Coll. Interf. Sci., 32, 339-348, 1970.
4. Varney G., PhD Thesis, Bristol University, 1966.

Coulter Electronics Limited, Northwell Drive, Luton, Beds., England
Telephone (0582) 582442 Telex: 825074

COULTER® CALIBRATION STANDARD

Assay Sheet

BATCH	H.10
MATERIAL	P.D.V.B. LATEX
DO NOT USE AFTER	FEBRUARY 1987

FOR USE WITH THE COULTER COUNTER® MODELS TAII/PCA, TA, ZM, ZB, ZBI, ZF, FN C.1000, P.64/P.128, D INDUSTRIAL, T, B & A.

SINGLET NUMBER MEDIAN DIAMETER (figure A)	78.2 µm

Other parameters:

NUMBER MODE (C.1000) (figure B)	76.8 µm DIAMETER 2.37×10^5 fl VOLUME
WEIGHT PEAK SPLIT (TAII & TA) (figure C)	79.5 µm DIAMETER
1 : 2 WEIGHT PEAK SPLIT (TAII/TA) (figure D)	77.0 µm DIAMETER
NUMBER PEAK SPLIT (TAII/PCA) (figure E)	78.2 µm DIAMETER
SIZE DISTRIBUTION (C.1000)	– see overleaf

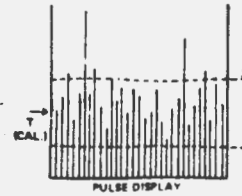

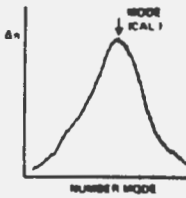

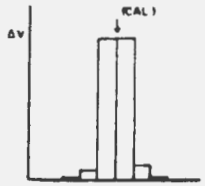

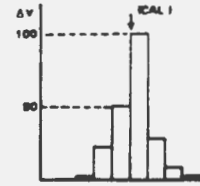

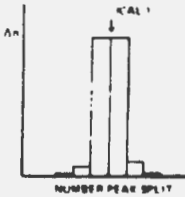

ASSAY VALUES have been determined using COULTER COUNTER® Models TAII/PCA, ZM and CHANNELYZER® C.1000 which are calibrated and checked with primary reference particles (1). The electrolyte used is ISOTON® II, a buffered saline diluent prepared by Coulter Electronics Ltd.

All particles have a coefficient of variation from their mean size of less than 13% by diameter

FOR IN VITRO DIAGNOSTIC USE ONLY

CALIBRATION PARTICLE SUSPENSIONS: Particles are suspended at a concentration in distilled water, containing preservative, such that one drop per 100ml of electrolyte will give approximately the correct concentration (approx 5% coincidence) for calibration of an aperture of 10x their nominal diameter. Each vial of suspension will be sufficient for over 100 calibrations. Polystyrene (Dinyl benzene (polystyrene D.V.B.) latices are the most durable, and will not change size upon immersion in alcohols, ketones or any aqueous electrolyte. They appear to remain stable, as packed, for an indefinite period, however it is recommended that they are discarded after 5 years.

Polystyrene or polyvinyl toluene latices may swell or dissolve in some organic electrolytes.

SIZE CALIBRATION: The COULTER COUNTER® can be self-calibrated by measuring a suspension of a narrow size range of the material under investigation at a known concentration. From the immersed relative density (g/ml) of the material and from the total volume measured, the calibration factor can be calculated for the COULTER COUNTER® and sensing aperture in use (2). This procedure will remove any doubt concerning the accurate calibration with very irregular or conducting materials.

In practice it is more convenient to calibrate using narrow range particles which have already been sized by a variety of other techniques

Extensive electron microscopy showed that an original reference latex produced by the Dow Chemical Co. (Midland, Michigan, U.S.A.) with a stated mean size of 3.49µm was in fact 3.40µm diameter (3,4). Harfield and Wood (1) confirmed this size with a COULTER COUNTER® MODEL S self-calibrated by the integration of data from a sample of stamins, and verified by reference to N.B.S. Standard Reference Material 1033 glass beads, and also by reference to a packed volume of latex particles.

Using a series of aperture tubes and COULTER COUNTER® models (TAII/PCA, ZM, C.1000) correctly calibrated as above, each calibration material is sized by the 'T' count technique, establishing the quoted size as the number median of the singlet particle population using standard COULTER COUNTER® apertures. The limits of the singlet size are defined as one-half and three-halves of the mean particle volume. In order to calibrate any other COULTER COUNTER® an identical 'half-count' calibration procedure must be used (see Coulter Electronics Ltd instruction manuals). This 'singlet number median diameter' (figure A) is given on the calibration material vial, and above.

When using a COULTER® CHANNELYZER® it may be more convenient to calibrate on the modal size of the particles, – the 'number mode (C.1000)'; (figure B).

When calibrating a COULTER COUNTER® model TAII or TA it may be easier to use the peak splitting method whereby the calibration point is the junction of two consecutive channels containing equal weight, (volume) data, – the 'weight peak split'; (figure C).

Earlier calibration methods for the TAII or TA used the '1:2 weight peak split' whereby the calibration point is the junction of two consecutive channels containing twice the weight in the right hand channel as in the left; (figure D).

MALVERN INSTRUMENTS LTD,SPRING LANE,MALVERN,ENGLAND.

RESULTS FROM BLOCK 1

RUN NUMBER= 6 TIME=00-45-20 LOG DIFFERENCE= 5.04

SAMPLE % VOLUME CONCENTRATION= 0.0206 BEAM OBSCURATION= 0.18

SIZE MICRONS	WEIGHT % UNDER	WEIGHT IN BAND MICRONS		%	LIGHT ENERGY CALCULATED	LIGHT ENERGY MEASURED
118.4	100.0					
54.9	5.6	118.4-	54.9	94.4	2047	2047
33.7	5.6	54.9-	33.7	0.0	871	700
23.7	2.0	33.7-	23.7	3.5	350	181
17.7	1.0	23.7-	17.7	1.1	285	336
13.6	1.0	17.7-	13.6	0.0	277	134
10.5	0.9	13.6-	10.5	0.0	186	178
8.2	0.8	10.5-	8.2	0.2	165	153
6.4	0.7	8.2-	6.4	0.0	158	140
5.0	0.7	6.4-	5.0	0.0	171	155
3.9	0.7	5.0-	3.9	0.0	201	177
3.0	0.7	3.9-	3.0	0.0	253	225
2.4	0.7	3.0-	2.4	0.0	360	306
1.9	0.7	2.4-	1.9	0.0	517	447
1.5	0.7	1.9-	1.5	0.0	746	662
1.2	0.7	1.5-	1.2	0.1	1085	977

D(50%) (UM)= 84.81 | V M D (UM)= 83.12 | S M D (UM)= 42.11

D(10%) (UM)= 57.90 | D(90%)(UM)= 111.71 | SPAN = 0.63

Calibration Standard - 63mm Lens

BRATION STANDARD 100MM LENS

VERN 2600/3600 PARTICLE SIZER VF.6

MALVERN INSTRUMENTS LTD,SPRING LANE,MALVERN,ENGLAND.

RESULTS FROM BLOCK 1

RUN NUMBER= 8 TIME=00-55-50 LOG DIFFERENCE= 5.14

SAMPLE % VOLUME CONCENTRATION= 0.0374 BEAM OBSCURATION= 0.20

SIZE MICRONS	WEIGHT % UNDER	WEIGHT IN BAND MICRONS		%	LIGHT ENERGY CALCULATED	LIGHT ENERGY MEASURED
188.0	100.0					
87.2	94.6	188.0-	87.2	5.4	1827	1725
53.5	0.0	87.2-	53.5	94.6	2047	2047
37.6	0.0	53.5-	37.6	0.0	1538	1390
28.1	0.0	37.6-	28.1	0.0	667	409
21.5	0.0	28.1-	21.5	0.0	234	207
16.7	0.0	21.5-	16.7	0.0	319	433
13.0	0.0	16.7-	13.0	0.0	307	169
10.1	0.0	13.0-	10.1	0.0	244	227
7.9	0.0	10.1-	7.9	0.0	246	180
6.2	0.0	7.9-	6.2	0.0	180	160
4.8	0.0	6.2-	4.8	0.0	180	167
3.8	0.0	4.8-	3.8	0.0	205	182
3.0	0.0	3.8-	3.0	0.0	245	231
2.4	0.0	3.0-	2.4	0.0	325	307
1.9	0.0	2.4-	1.9	0.0	431	444

D(50%) (UM)= 71.28 | V M D (UM)= 73.94 | S M D (UM)= 70.86

D(10%) (UM)= 57.01 | D(90%)(UM)= 85.55 | SPAN = 0.40

Calibration Standard - 100mm Lens

IBRATION STANDARDS 300MM LENS

.VERN 2600/3600 PARTICLE SIZER VF.6

MALVERN INSTRUMENTS LTD,SPRING LANE,MALVERN,ENGLAND.

RESULTS FROM BLOCK 1

RUN NUMBER= 10 TIME=01-08-20 LOG DIFFERENCE= 4.76

SAMPLE % VOLUME CONCENTRATION= 0.0389 BEAM OBSCURATION= 0.19

SIZE MICRONS	WEIGHT % UNDER	WEIGHT IN BAND MICRONS		%	LIGHT ENERGY CALCULATED	LIGHT ENERGY MEASURED
564.0	100.0					
261.6	100.0	564.0-	261.6	0.0	375	366
160.4	100.0	261.6-	160.4	0.0	654	636
112.8	100.0	160.4-	112.8	0.0	996	977
84.3	85.8	112.8-	84.3	14.2	1398	1390
64.6	0.0	84.3-	64.6	85.8	1830	1815
50.2	0.0	64.6-	50.2	0.0	2047	2047
39.0	0.0	50.2-	39.0	0.0	1747	1730
30.3	0.0	39.0-	30.3	0.0	836	740
23.7	0.0	30.3-	23.7	0.0	236	235
18.5	0.0	23.7-	18.5	0.0	535	696
14.5	0.0	18.5-	14.5	0.0	429	350
11.4	0.0	14.5-	11.4	0.0	341	383
9.1	0.0	11.4-	9.1	0.0	330	275
7.2	0.0	9.1-	7.2	0.0	222	280
5.8	0.0	7.2-	5.8	0.0	200	282

D(50%) (UM)= 76.09 | V M D (UM)= 77.89 | S M D (UM)= 76.71

D(10%) (UM)= 66.93 | D(90%)(UM)= 92.70 | SPAN = 0.34

Calibration Standard - 300mm Lens

APPENDIX C

DETAILED BBTV TEST RESULTS

	Page
Kaolin C_v = 7,83%	C.1
Kaolin C_v = 12,08%	C.6
Kaolin C_v = 14,88	C.11
Kaolin C_v = 17,71%	C.16
Uranium Tailings : Slurry 1	C.22
" " : 2	C.26
" " : 3	C.32
" " : 4	C.39

APPENDIX C.1

Kaolin C_v = 7,83%

BBTV VISCOMETER TEST RESULTS : KAOLIN

FILE NAME : PKL8

PARTICLE SIZE RANGE	:	KAOLIN
TUBE DIAMETER	:	31.625 mm
TUBE LENGTH	:	3.965 m
SLURRY TEMPERATURE	:	17 C
SOLID RELATIVE DENSITY	:	2.4449
MIXTURE RELATIVE DENSITY	:	1.1132
VOLUMETRIC CONCENTRATION	:	7.83 %
pH	:	7

No	V [m/s]	p [Pa]	8 V / D Pseudo-Shear Rate [1/s]	d p / 4 L Wall Shear Stress [Pa]
1	.411	4206	104	8.39
2	1.079	4939	273	9.85
3	2.544	8977	643	17.90
4	3.191	14392	807	28.70
5	3.920	20812	992	41.50
6	4.117	22513	1042	44.89
7	4.467	28120	1130	56.07
8	4.908	33298	1242	66.40
9	5.122	37795	1296	75.36
10	5.688	44836	1439	89.40
11	6.212	48845	1572	97.40
12	6.167	55754	1560	111.17
13	5.582	61080	1412	121.79
14	7.244	61908	1833	123.45
15	1.336	5205	338	10.38
16	3.138	14673	794	29.26
17	2.724	10531	689	21.00
18	1.821	5989	461	11.94
19	1.013	4820	256	9.61
20	1.629	5723	412	11.41
21	.702	4510	178	8.99

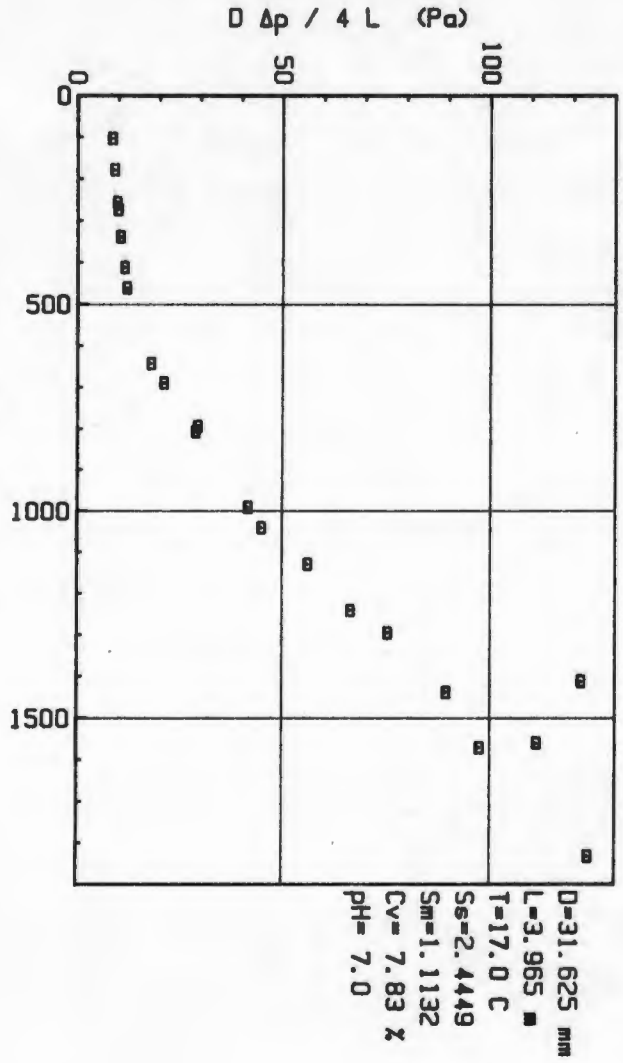

PSUEDO-SHEAR DIAGRAM FILE PKL8 - KAOLIN

BBTV TEST RESULTS : KAOLIN Cv=7.83%

BBTV VISCOMETER TEST RESULTS : KAOLIN

FILE NAME : PAL8

PARTICLE SIZE RANGE	: KAOLIN
TUBE DIAMETER	: 31.625 mm
TUBE LENGTH	: 3.965 m
SLURRY TEMPERATURE	: 17 C
SOLID RELATIVE DENSITY	: 2.4449
MIXTURE RELATIVE DENSITY	: 1.1132
VOLUMETRIC CONCENTRATION	: 7.83 %
pH	: 7

No	V [m/s]	p [Pa]	8 V / D Pseudo-Shear Rate [1/s]	d p / 4 L Wall Shear Stress [Pa]
1	3.131	14366	792	28.65
2	2.635	10068	667	20.08
3	1.821	5989	461	11.94
4	1.013	4820	256	9.61
5	1.461	5490	369	10.95
6	.549	4288	139	8.55

PSUEDO-SHEAR DIAGRAM FILE PAL8 - KAOLIN

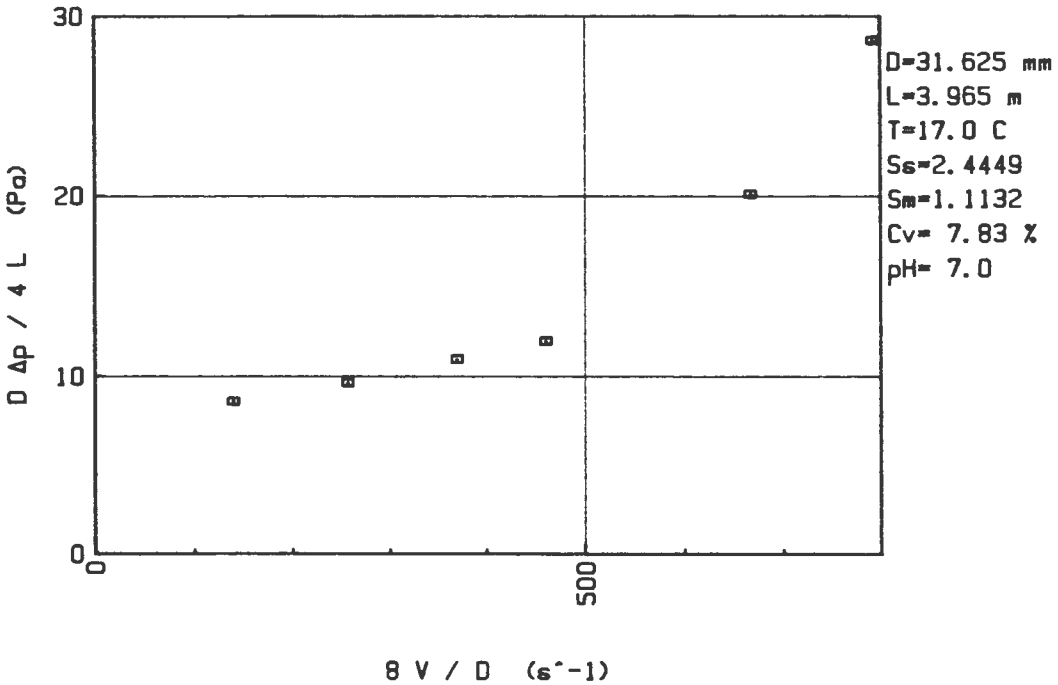

BBTV TEST RESULTS : KAOLIN Cv=7.83%

BBTV VISCOMETER TEST RESULTS : KAOLIN

FILE NAME : PAS8

PARTICLE SIZE RANGE	: KAOLIN
TUBE DIAMETER	: 13.37 mm
TUBE LENGTH	: 3.94 m
SLURRY TEMPERATURE	: 17 C
SOLID RELATIVE DENSITY	: 2.4449
MIXTURE RELATIVE DENSITY	: 1.1132
VOLUMETRIC CONCENTRATION	: 7.83 %
pH	: 7

No	V [m/s]	p [Pa]	8 V / D Pseudo-Shear Rate [1/s]	d p / 4 L Wall Shear Stress [Pa]
1	2.918	38919	1746	33.02
2	2.469	27868	1477	23.64
3	2.177	21670	1302	18.38
4	1.333	16788	797	14.24
5	.841	14643	503	12.42
6	.176	10412	106	8.83
7	.078	8992	47	7.63

PSUEDO-SHEAR DIAGRAM FILE PAS8 - KAOLIN

BBTV TEST RESULTS : KAOLIN Cv=7.83%

BBTV VISCOMETER TEST RESULTS : KAOLIN

FILE NAME : PKS8

PARTICLE SIZE RANGE : KAOLIN
TUBE DIAMETER : 13.37 mm
TUBE LENGTH : 3.94 m
SLURRY TEMPERATURE : 17 C
SOLID RELATIVE DENSITY : 2.4449
MIXTURE RELATIVE DENSITY : 1.1132
VOLUMETRIC CONCENTRATION : 7.83 %
pH : 7

No	V [m/s]	p [Pa]	8 V / D Pseudo-Shear Rate [1/s]	d p / 4 L Wall Shear Stress [Pa]
1	3.147	43890	1883	37.23
2	3.402	51138	2036	43.38
3	3.784	63077	2264	53.51
4	3.953	67145	2366	56.96
5	4.155	74039	2486	62.81
6	4.737	83240	2834	70.62
7	4.645	89749	2779	76.14
8	4.855	98166	2905	83.28
9	5.290	109572	3165	92.96
10	5.282	115090	3161	97.64
11	5.644	128715	3377	109.20
12	4.970	144366	2974	122.47
13	6.202	156867	3711	133.08
14	7.215	168183	4317	142.68
15	6.713	180358	4017	153.01

PSUEDO-SHEAR DIAGRAM FILE PKS8 - KAOLIN

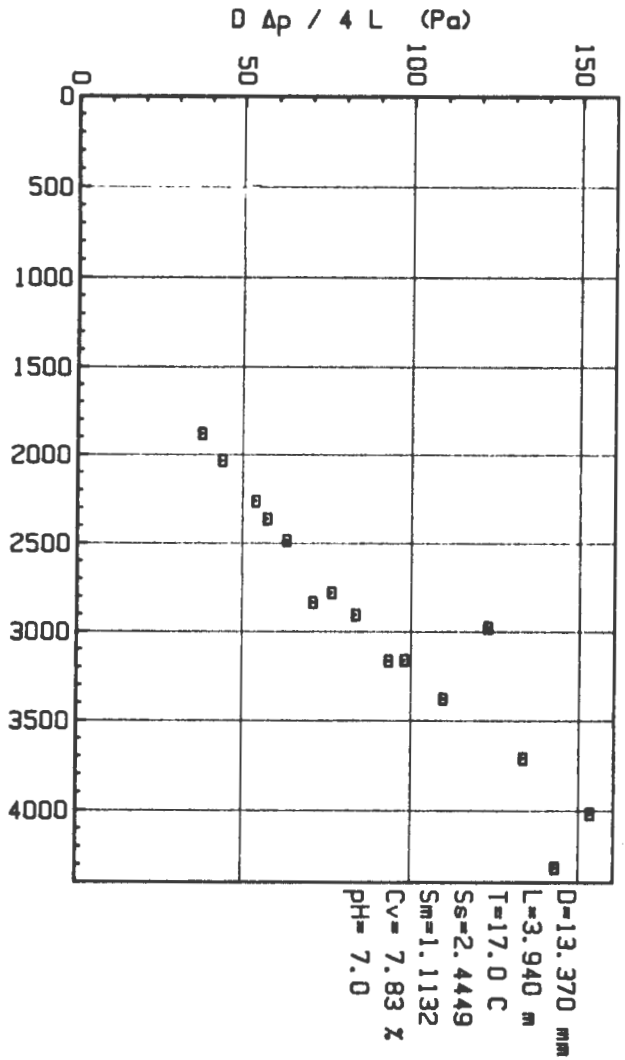

BBTV TEST RESULTS : KAOLIN Cv=7.83%

APPENDIX C.2

Kaolin C_v = 12,08%

BBTV VISCOMETER TEST RESULTS : KAOLIN

FILE NAME : PKL121308

PARTICLE SIZE RANGE	: KAOLIN	
TUBE DIAMETER	: 31.625	mm
TUBE LENGTH	: 3.965	m
SLURRY TEMPERATURE	: 17	C
SOLID RELATIVE DENSITY	: 2.4449	
MIXTURE RELATIVE DENSITY	: 1.1745	
VOLUMETRIC CONCENTRATION	: 12.08	%
pH	: 7	

No	V [m/s]	p [Pa]	8 V / D Pseudo-Shear Rate [1/s]	d p / 4 L Wall Shear Stress [Pa]
1	.005	6122	1	12.21
2	.024	10501	6	20.94
3	.409	15368	103	30.64
4	2.118	20161	536	40.20
5	4.601	26360	1164	52.56
6	4.903	31271	1240	62.35
7	5.354	40191	1354	80.14
8	6.067	50458	1535	100.61
9	6.341	56124	1604	111.91
10	6.877	66183	1740	131.97
11	7.087	63654	1793	126.93
12	7.483	73876	1893	147.31
13	8.036	88664	2033	176.80

PSUEDO-SHEAR DIAGRAM FILE PKL121308 - KAOLIN

BBTV TEST RESULTS : KAOLIN Cv=12.08%

BBTV VISCOMETER TEST RESULTS : KAOLIN

FILE NAME : PAL121308

PARTICLE SIZE RANGE : KAOLIN
TUBE DIAMETER : 31.625 mm
TUBE LENGTH : 3.965 m
SLURRY TEMPERATURE : 17 C
SOLID RELATIVE DENSITY : 2.4449
MIXTURE RELATIVE DENSITY : 1.1745
VOLUMETRIC CONCENTRATION : 12.08 %
pH : 7

No	V [m/s]	p [Pa]	8 V / D Pseudo-Shear Rate [1/s]	d p / 4 L Wall Shear Stress [Pa]
1	4.997	31315	1264	62.44
2	4.271	24984	1080	49.82
3	3.882	24067	982	47.99
4	3.155	21862	798	43.59
5	2.788	21419	705	42.71
6	1.595	19155	403	38.20
7	.241	14924	61	29.76
8	.678	16685	171	33.27
9	1.477	18697	374	37.28
10	2.952	22094	747	44.06
11	3.403	22691	861	45.25
12	3.831	23859	969	47.58
13	3.491	22868	883	45.60
14	4.379	25575	1108	51.00
15	3.110	23001	787	45.87
16	3.190	22291	807	44.45

PSUEDO-SHEAR DIAGRAM FILE PAL121308 - KAOLIN

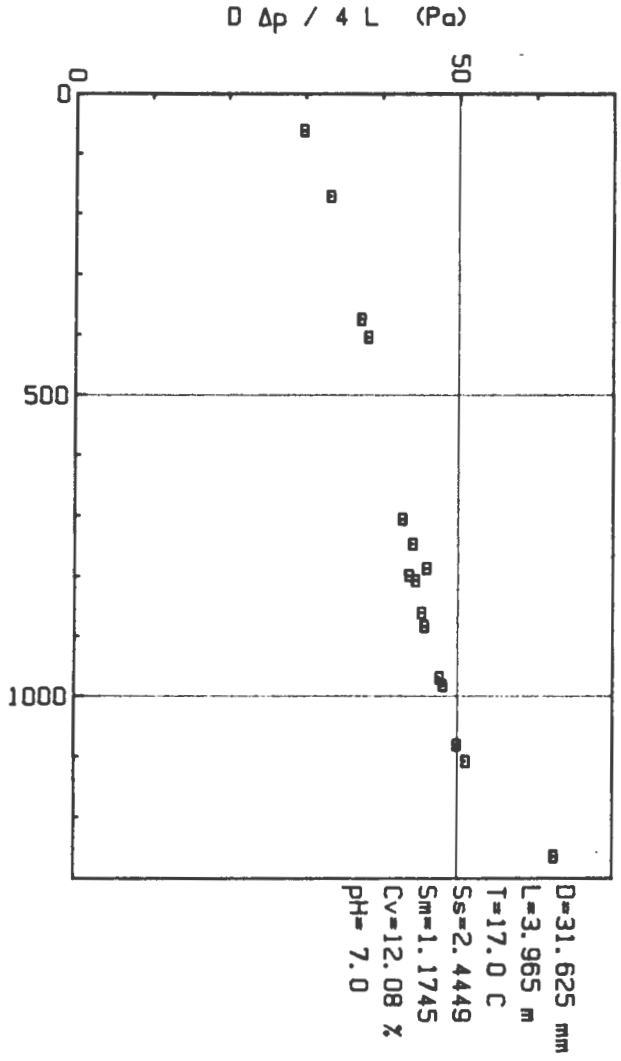

BBTV TEST RESULTS : KAOLIN Cv=12.08%

BBTV VISCOMETER TEST RESULTS : KAOLIN

FILE NAME : PKS121308

PARTICLE SIZE RANGE	: KAOLIN	
TUBE DIAMETER	: 13.37	mm
TUBE LENGTH	: 3.94	m
SLURRY TEMPERATURE	: 17	C
SOLID RELATIVE DENSITY	: 2.4449	
MIXTURE RELATIVE DENSITY	: 1.1745	
VOLUMETRIC CONCENTRATION	: 12.08	%
pH	: 7	

No	V (m/s)	p (Pa)	8 V / D Pseudo-Shear Rate (1/s)	d p / 4 L Wall Shear Stress (Pa)
1	.788	47277	471	40.11
2	1.378	53491	825	45.38
3	2.906	62633	1739	53.13
4	4.249	65947	2542	55.95
5	5.028	86568	3008	73.44
6	4.960	89355	2968	75.80
7	5.381	99158	3220	84.12

PSUEDO-SHEAR DIAGRAM FILE PKS121308 - KAOLIN

BBTV TEST RESULTS : KAOLIN Cv=12.08%

BBTV VISCOMETER TEST RESULTS : KAOLIN

FILE NAME : PAS121308

PARTICLE SIZE RANGE	:	KAOLIN
TUBE DIAMETER	:	13.37 mm
TUBE LENGTH	:	3.94 m
SLURRY TEMPERATURE	:	17 C
SOLID RELATIVE DENSITY	:	2.4449
MIXTURE RELATIVE DENSITY	:	1.1745
VOLUMETRIC CONCENTRATION	:	12.08 %
pH	:	7

No	V [m/s]	p [Pa]	8 V / D Pseudo-Shear Rate [1/s]	d p / 4 L Wall Shear Stress [Pa]
1	3.259	62559	1950	53.07
2	2.487	60029	1488	50.93
3	.997	50458	596	42.81
4	.996	48135	596	40.84
5	.416	40428	249	34.30
6	.754	46478	451	39.43
7	1.641	52174	982	44.26
8	2.414	58165	1445	49.34
9	3.065	61745	1834	52.38
10	3.679	66819	2201	56.69
11	4.291	68816	2568	58.38
12	4.676	78048	2798	66.21
13	4.803	83506	2874	70.84
14	5.114	88214	3060	74.84
15	5.801	107279	3471	91.01

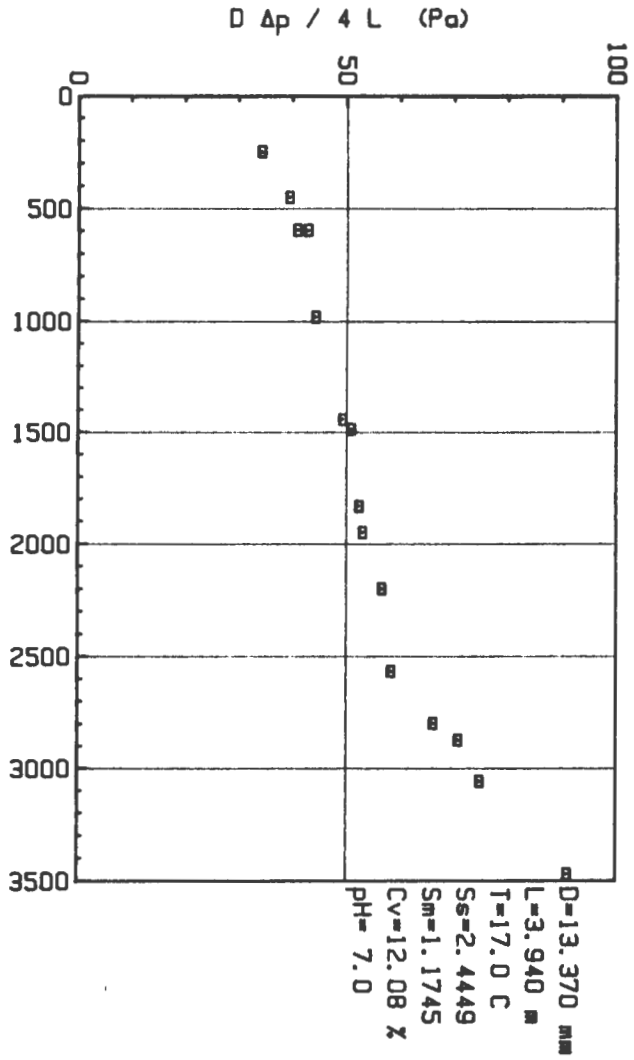

PSUEDO-SHEAR DIAGRAM FILE PAS121308 - KAOLIN

BBTV TEST RESULTS : KAOLIN Cv=12.08%

APPENDIX C.3

Kaolin C_v = 14,88%

BBTV VISCOMETER TEST RESULTS : KAOLIN

FILE NAME : PKL153107

PARTICLE SIZE RANGE	: KAOLIN	
TUBE DIAMETER	: 31.625	mm
TUBE LENGTH	: 3.965	m
SLURRY TEMPERATURE	: 17	C
SOLID RELATIVE DENSITY	: 2.4449	
MIXTURE RELATIVE DENSITY	: 1.212	
VOLUMETRIC CONCENTRATION	: 14.67	%
pH	: 7	

No	V [m/s]	p [Pa]	8 V / D Pseudo-Shear Rate [1/s]	d p / 4 L Wall Shear Stress [Pa]
1	.008	15087	2	30.08
2	.016	20812	4	41.50
3	.176	28874	44	57.58
4	.620	32395	157	64.60
5	1.670	38816	422	77.40
6	1.746	38742	442	77.25
7	3.525	43816	892	87.37
8	4.006	45177	1013	90.08
9	4.337	46468	1097	92.66
10	5.061	48195	1280	96.10
11	5.456	49030	1380	97.77
12	4.598	47366	1163	94.45
13	6.388	54393	1616	108.46

PSUEDO-SHEAR DIAGRAM FILE PKL153107 - KAOLIN

BBTV TEST RESULTS : KAOLIN Cv=14.88%

BBTV VISCOMETER TEST RESULTS : KAOLIN

FILE NAME : PAL153107

PARTICLE SIZE RANGE	: KAOLIN	
TUBE DIAMETER	: 31.625	mm
TUBE LENGTH	: 3.965	m
SLURRY TEMPERATURE	: 17	C
SOLID RELATIVE DENSITY	: 2.4449	
MIXTURE RELATIVE DENSITY	: 1.215	
VOLUMETRIC CONCENTRATION	: 14.88	%
pH	: 7	

No	V [m/s]	p [Pa]	8 V / D Pseudo-Shear Rate [1/s]	d p / 4 L Wall Shear Stress [Pa]
1	1.436	38579	363	76.93
2	2.485	40901	629	81.56
3	4.164	46464	1053	92.65
4	4.058	45532	1027	90.79
5	4.981	49023	1260	97.75
6	5.390	50010	1363	99.72
7	6.281	55133	1589	109.93
8	6.772	56937	1713	113.53
9	6.892	66351	1743	132.30
10	7.283	73920	1842	147.40
11	7.526	85341	1904	170.17
12	8.044	96288	2035	192.00

PSUEDO-SHEAR DIAGRAM FILE PAL153107 - KAOLIN

BBTV TEST RESULTS : KAOLIN Cv=14.88%

BBTV VISCOMETER TEST RESULTS : KAOLIN

FILE NAME : PBL153107

PARTICLE SIZE RANGE	: KAOLIN	
TUBE DIAMETER	: 31.625	mm
TUBE LENGTH	: 1.944	m
SLURRY TEMPERATURE	: 17	C
SOLID RELATIVE DENSITY	: 2.4449	
MIXTURE RELATIVE DENSITY	: 1.215	
VOLUMETRIC CONCENTRATION	: 14.88	%
pH	: 7	

No	V [m/s]	p [Pa]	8 V / D Pseudo-Shear Rate [1/s]	d p / 4 L Wall Shear Stress [Pa]
1	6.119	24991	1548	101.64
2	6.022	22484	1523	91.44
3	4.921	23741	1245	96.56
4	4.889	23919	1237	97.28

PSUEDO-SHEAR DIAGRAM FILE PBL153107 - KAOLIN

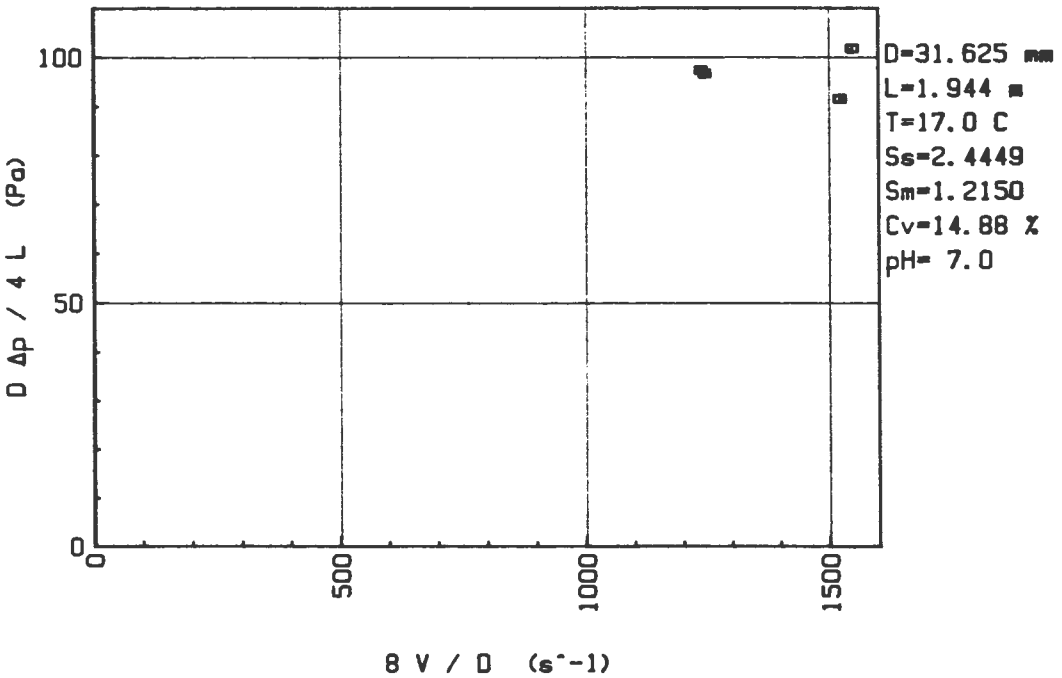

BBTV TEST RESULTS : KAOLIN Cv=14.88%

BBTV VISCOMETER TEST RESULTS : KAOLIN

FILE NAME : PCL153107

PARTICLE SIZE RANGE	: KAOLIN	
TUBE DIAMETER	: 31.625	mm
TUBE LENGTH	: 1.944	m
SLURRY TEMPERATURE	: 17	C
SOLID RELATIVE DENSITY	: 2.4449	
MIXTURE RELATIVE DENSITY	: 1.215	
VOLUMETRIC CONCENTRATION	: 14.88	%
pH	: 7	

No	V [m/s]	p [Pa]	8 V / D Pseudo-Shear Rate [1/s]	d p / 4 L Wall Shear Stress [Pa]
1	3.133	20706	792	84.21
2	2.577	20319	652	82.64
3	.546	16270	138	66.17
4	.804	16670	203	67.80
5	1.628	19111	412	77.72
6	1.912	19466	484	79.17
7	4.050	22203	1025	90.30
8	4.422	22661	1119	92.16
9	5.466	24821	1383	100.95
10	5.817	25250	1471	102.69
11	6.359	26286	1609	106.90
12	6.272	27987	1587	113.82
13	.003	3016	1	12.26
14	.008	5368	2	21.83
15	.006	6403	2	26.04
16	.030	11211	7	45.60

PSUEDO-SHEAR DIAGRAM FILE PCL153107 - KAOLIN

BBTV TEST RESULTS : KAOLIN Cv=14.88%

APPENDIX C.4

Kaolin C_v = 17,71%

BBTV VISCOMETER TEST RESULTS : KAOLIN

FILE NAME : PKL180508

PARTICLE SIZE RANGE	: KAOLIN	
TUBE DIAMETER	: 31.625	mm
TUBE LENGTH	: 3.965	m
SLURRY TEMPERATURE	: 16	C
SOLID RELATIVE DENSITY	: 2.4449	
MIXTURE RELATIVE DENSITY	: 1.2559	
VOLUMETRIC CONCENTRATION	: 17.71	%
pH	: 7	

No	V [m/s]	p [Pa]	8 V / D Pseudo-Shear Rate [1/s]	d p / 4 L Wall Shear Stress [Pa]
1	.005	11818	1	23.56
2	.006	16566	1	33.03
3	.009	24318	2	48.49
4	.012	29244	3	58.31
5	.029	38253	7	76.28
6	.072	44241	18	88.22
7	.134	47603	34	94.92
8	1.996	65143	505	129.90
9	.752	56819	190	113.30
10	.956	58949	242	117.55
11	.982	59926	249	119.49
12	1.855	63935	469	127.49
13	2.505	66553	634	132.71
14	2.950	68654	746	136.90
15	3.343	70089	846	139.76

PSUEDO-SHEAR DIAGRAM FILE PKL180508 - KAOLIN

BBTV TEST RESULTS : KAOLIN Cv=17.71%

BBTV VISCOMETER TEST RESULTS : KAOLIN

FILE NAME : PAL180508

PARTICLE SIZE RANGE : KAOLIN
TUBE DIAMETER : 31.625 mm
TUBE LENGTH : 3.965 m
SLURRY TEMPERATURE : 16 C
SOLID RELATIVE DENSITY : 2.4449
MIXTURE RELATIVE DENSITY : 1.2559
VOLUMETRIC CONCENTRATION : 17.71 %
pH : 7

No	V [m/s]	p [Pa]	8 V / D Pseudo-Shear Rate [1/s]	d p / 4 L Wall Shear Stress [Pa]
1	.372	49082	94	97.87
2	.520	54644	132	108.96
3	.735	56982	186	113.62
4	1.093	61287	277	122.21
5	1.601	66272	405	132.15
6	3.016	69527	763	138.64
7	3.659	70851	926	141.28
8	4.837	75751	1224	151.05
9	5.084	77957	1286	155.45
10	6.048	80059	1530	159.64
11	6.294	82589	1592	164.68
12	7.220	86458	1826	172.40
13	7.791	89256	1971	177.98
14	8.589	109671	2173	218.68
15	3.946	71967	998	143.50

PSUEDO-SHEAR DIAGRAM FILE PAL180508 - KAOLIN

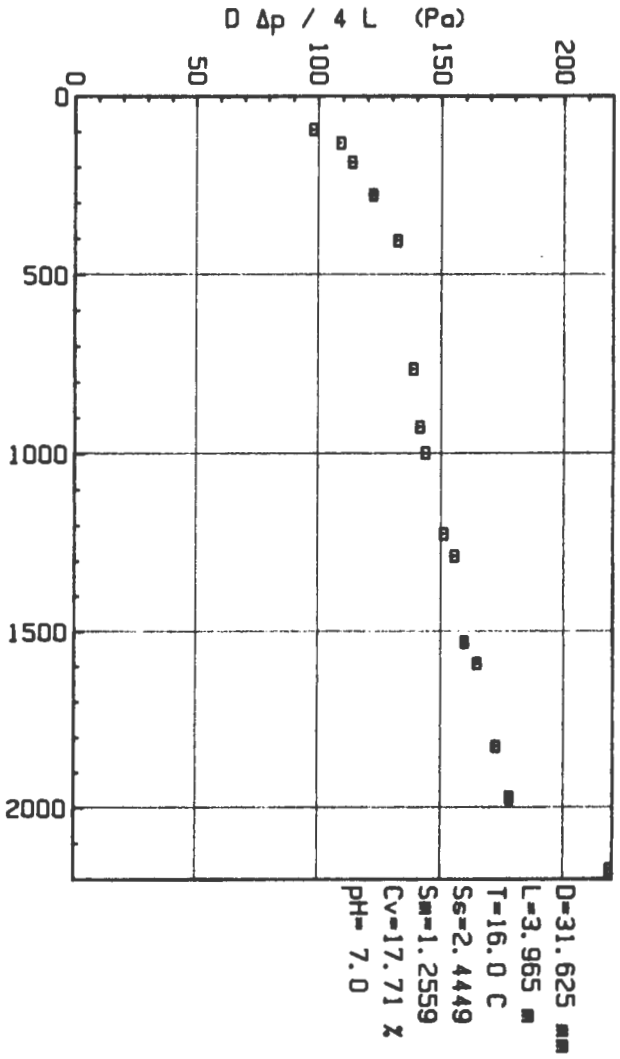

BBTV TEST RESULTS : KAOLIN Cv=17.71%

BBTV VISCOMETER TEST RESULTS : KAOLIN

FILE NAME : PKS180708

PARTICLE SIZE RANGE : KAOLIN
TUBE DIAMETER : 13.37 mm
TUBE LENGTH : 1.943 m
SLURRY TEMPERATURE : 16 C
SOLID RELATIVE DENSITY : 2.4449
MIXTURE RELATIVE DENSITY : 1.2559
VOLUMETRIC CONCENTRATION : 17.71 %
pH : 7

No	V [m/s]	p [Pa]	8 V / D Pseudo-Shear Rate [1/s]	d p / 4 L Wall Shear Stress [Pa]
1	.011	11137	7	19.16
2	.011	22513	7	38.73
3	.017	29599	10	50.92
4	.017	39526	10	68.00
5	.026	48668	15	83.72
6	.139	61523	83	105.84
7	.489	70991	292	122.12
8	.972	78099	581	134.35
9	1.706	85577	1021	147.22
10	1.833	84438	1097	145.26
11	2.502	92205	1497	158.62
12	2.931	90903	1754	156.38
13	3.672	101066	2197	173.86
14	4.347	98699	2601	169.79
15	5.721	110815	3423	190.63
16	6.618	105312	3960	181.17

PSUEDO-SHEAR DIAGRAM FILE PKS180708 - KAOLIN

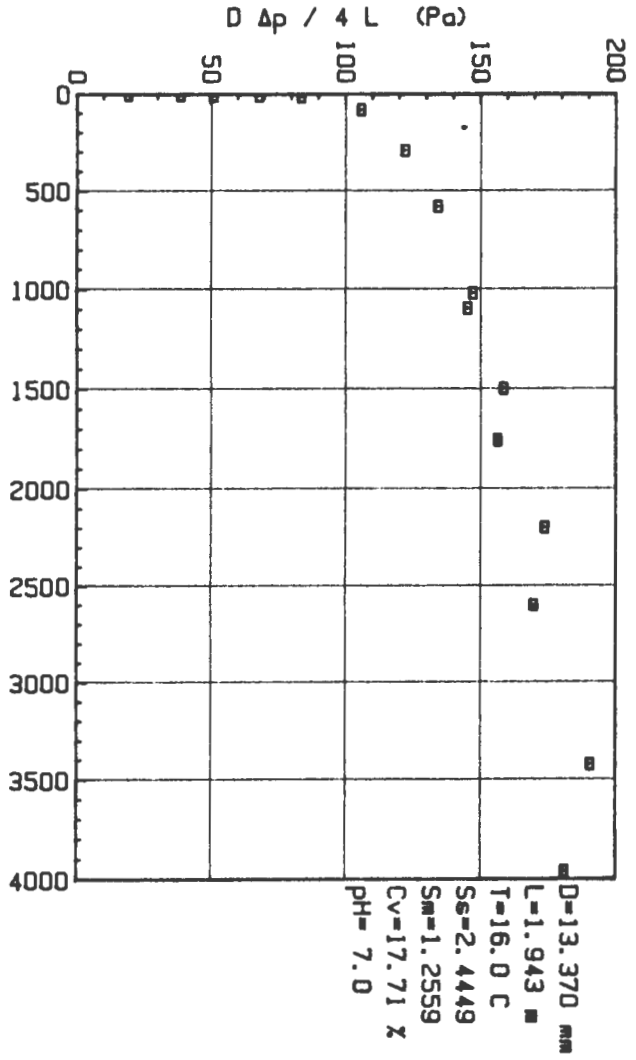

BBTV TEST RESULTS : KAOLIN Cv=17.71%

BBTV VISCOMETER TEST RESULTS : KAOLIN

FILE NAME : PAS180708

PARTICLE SIZE RANGE : KAOLIN
TUBE DIAMETER : 13.37 mm
TUBE LENGTH : 1.943 m
SLURRY TEMPERATURE : 16 C
SOLID RELATIVE DENSITY : 2.4449
MIXTURE RELATIVE DENSITY : 1.2559
VOLUMETRIC CONCENTRATION : 17.71 %
pH : 7

No	V [m/s]	p [Pa]	8 V / D Pseudo-Shear Rate [1/s]	d p / 4 L Wall Shear Stress [Pa]
1	1.262	82678	755	142.23
2	1.311	78136	784	134.42
3	2.083	86702	1246	149.15
4	2.837	90859	1698	156.30
5	3.589	96913	2147	166.72
6	4.423	98048	2647	168.67
7	5.089	105696	3045	181.83
8	6.381	106584	3818	183.35
9	5.934	109483	3551	188.34
10	6.892	109262	4124	187.96
11	7.805	116436	4670	200.30
12	8.461	117531	5062	202.19
13	9.066	122132	5425	210.10
14	9.612	139455	5751	239.90
15	8.988	136481	5378	234.79
16	9.084	147576	5435	253.87

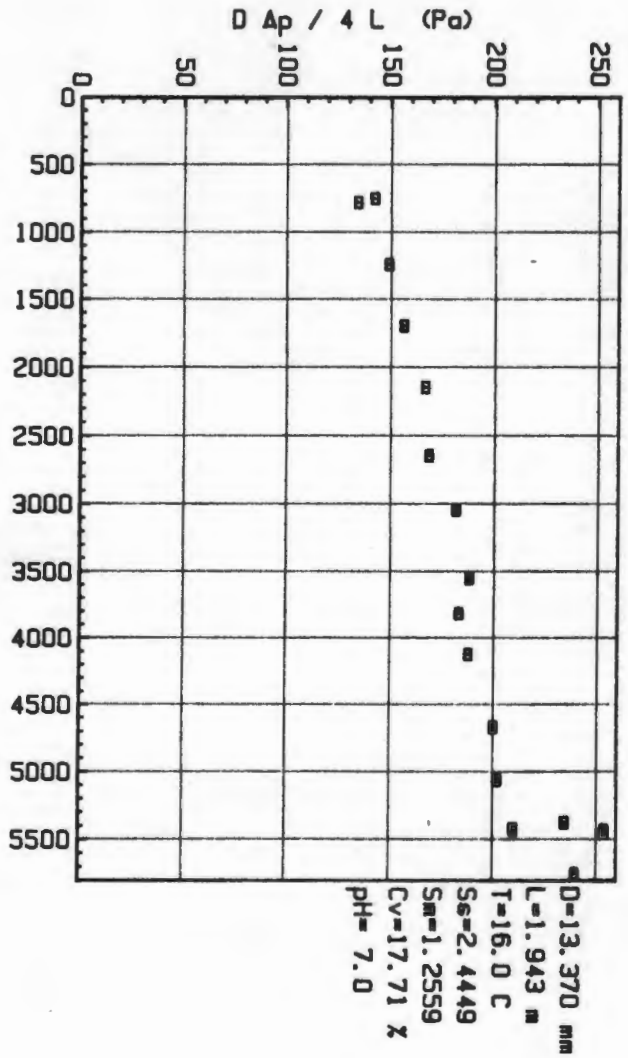

PSUEDO-SHEAR DIAGRAM FILE PAS180708 - KAOLIN

BBTV TEST RESULTS : KAOLIN Cv=17.71%

BBTV VISCOMETER TEST RESULTS : KAOLIN

FILE NAME : PKS180608

PARTICLE SIZE RANGE	:	KAOLIN
TUBE DIAMETER	:	13.37 mm
TUBE LENGTH	:	1.943 m
SLURRY TEMPERATURE	:	16 C
SOLID RELATIVE DENSITY	:	2.4449
MIXTURE RELATIVE DENSITY	:	1.2559
VOLUMETRIC CONCENTRATION	:	17.71 %
pH	:	7

No	V [m/s]	p [Pa]	8 V / D Pseudo-Shear Rate [1/s]	d p / 4 L Wall Shear Stress [Pa]
1	.044	42795	26	73.62
2	.124	45961	74	79.07
3	.347	61583	208	105.94
4	.796	68373	476	117.62
5	.650	74689	389	128.49
6	1.003	85429	600	146.96
7	2.744	90277	1642	155.30
8	2.300	94335	1376	162.28
9	3.471	100134	2077	172.26
10	4.343	105119	2599	180.83
11	3.870	112486	2316	193.51
12	6.841	112161	4093	192.95
13	7.686	121081	4599	208.29
14	7.834	117856	4687	202.75

PSUEDO-SHEAR DIAGRAM FILE PKS180608 - KAOLIN

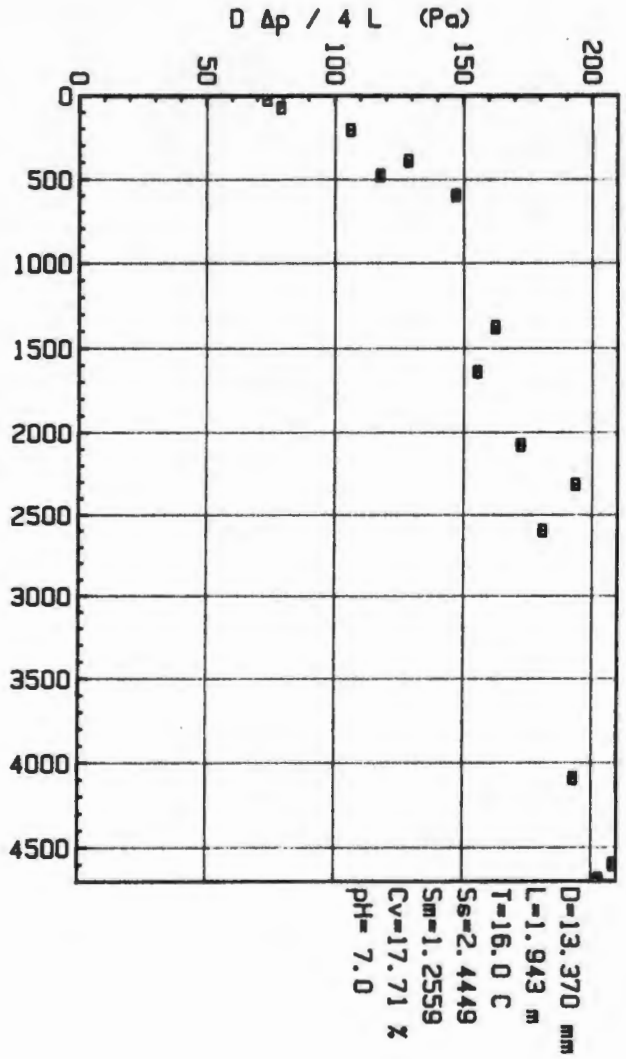

BBTV TEST RESULTS : KAOLIN Cv=17.71%

APPENDIX C.5

URANIUM TAILINGS : SLURRY 1

A1

BBTV VISCOMETER TEST RESULTS : Slurry 1

FILE NAME : PUS242309

PARTICLE SIZE RANGE	: Slurry 1
TUBE DIAMETER	: 13.37 mm
TUBE LENGTH	: 1.943 m
SLURRY TEMPERATURE	: 17 C
SOLID RELATIVE DENSITY	: 2.75
MIXTURE RELATIVE DENSITY	: 1.3933
VOLUMETRIC CONCENTRATION	: 22.47 %
pH	: 2.2

No	v [m/s]	dP [Pa]	8 v / D Psuedo-Shear Rate [1/s]	d p / 4 L Wall Shear Stress [Pa]
1	.007	9362	4	16.11
2	.140	16833	84	28.96
3	.293	19540	175	33.61
4	.720	24436	431	42.04
5	.973	29141	582	50.13
6	1.745	33579	1044	57.76
7	2.072	38668	1240	66.52
8	2.926	42381	1751	72.91
9	3.362	47544	2011	81.79
10	4.227	51686	2529	88.91
11	5.167	61035	3092	105.00
12	6.011	77352	3596	133.07
13	5.991	77175	3585	132.76
14	5.704	96199	3413	165.49
15	6.556	95163	3923	163.71
16	5.526	127724	3307	219.72

PSUEDO-SHEAR DIAGRAM FILE PUS242309 - ROSSING URANIUM : SLIMES

BBTV TEST RESULTS : SLURRY 1

A2

BBTV VISCOMETER TEST RESULTS : Slurry 1

FILE NAME : PAS242309

PARTICLE SIZE RANGE	: Slurry 1
TUBE DIAMETER	: 13.37 mm
TUBE LENGTH	: 3.94 m
SLURRY TEMPERATURE	: 17 C
SOLID RELATIVE DENSITY	: 2.75
MIXTURE RELATIVE DENSITY	: 1.3933
VOLUMETRIC CONCENTRATION	: 22.47 %
pH	: 2.2

No	v [m/s]	dP [Pa]	8 v / D Psuedo-Shear Rate [1/s]	d p / 4 L Wall Shear Stress [Pa]
1	.144	32292	86	27.39
2	.534	42055	320	35.68
3	1.019	51183	610	43.42
4	1.812	65015	1084	55.16
5	2.228	71494	1333	60.65
6	3.028	83669	1812	70.98
7	3.439	89808	2058	76.19
8	4.525	106584	2707	90.42
9	5.030	115208	3010	97.74
10	6.110	130061	3656	110.34
11	5.794	145047	3467	123.05
12	5.257	173450	3145	147.15
13	6.706	190374	4013	161.50
14	5.916	221232	3540	187.68
15	6.388	264991	3822	224.81
16	6.055	295821	3623	250.96

PSUEDO-SHEAR DIAGRAM FILE PAS242309 - ROSSING URANIUM : SLIMES

BBTV TEST RESULTS : SLURRY 1

A3

BBTV VISCOMETER TEST RESULTS : Slurry 1

FILE NAME : PUL242409

PARTICLE SIZE RANGE	:	Slurry 1
TUBE DIAMETER	:	31.625 mm
TUBE LENGTH	:	3.965 m
SLURRY TEMPERATURE	:	17 C
SOLID RELATIVE DENSITY	:	2.75
MIXTURE RELATIVE DENSITY	:	1.3933
VOLUMETRIC CONCENTRATION	:	22.47 %
pH	:	2.2

No	v [m/s]	dP [Pa]	8 v / D Psuedo-Shear Rate [1/s]	d p / 4 L Wall Shear Stress [Pa]
1	.103	10777	26	21.49
2	2.719	22291	688	44.45
3	2.595	21721	656	43.31
4	3.394	24540	859	48.93
5	3.621	25723	916	51.29
6	4.205	27839	1064	55.51
7	4.646	33593	1175	66.99
8	4.568	45310	1155	90.35
9	4.836	46952	1223	93.62
10	4.732	55784	1197	111.23
11	5.095	61745	1289	123.12
12	5.244	66583	1326	132.77
13	5.622	74216	1422	147.99
14	5.110	62662	1293	124.95
15	6.431	85237	1627	169.96

PSUEDO-SHEAR DIAGRAM FILE PUL242409 - ROSSING URANIUM : SLIMES

BBTV TEST RESULTS : SLURRY 1

APPENDIX C.6

URANIUM TAILINGS : SLURRY 2

B1

BBTV VISCOMETER TEST RESULTS : Slurry 2

FILE NAME : PUS302509

PARTICLE SIZE RANGE	: Slurry 2
TUBE DIAMETER	: 13.37 mm
TUBE LENGTH	: 1.943 m
SLURRY TEMPERATURE	: 17 C
SOLID RELATIVE DENSITY	: 2.75
MIXTURE RELATIVE DENSITY	: 1.5004
VOLUMETRIC CONCENTRATION	: 28.59 %
pH	: 2.2

No	v [m/s]	dP [Pa]	8 v / D Psuedo-Shear Rate [1/s]	d p / 4 L Wall Shear Stress [Pa]
1	.145	13401	87	23.05
2	.582	18445	348	31.73
3	1.011	22765	605	39.16
4	2.038	31892	1220	54.86
5	2.612	36863	1563	63.41
6	2.651	37410	1586	64.36
7	3.045	41552	1822	71.48
8	4.013	46996	2401	80.85
9	4.383	51286	2623	88.23
10	5.141	58461	3076	100.57
11	4.930	66885	2950	115.06
12	5.280	68550	3160	117.93
13	5.325	77559	3186	133.42
14	5.882	75814	3520	130.42
15	4.734	90104	2833	155.00
16	5.541	86243	3315	148.36

PSUEDO-SHEAR DIAGRAM FILE PUS302509 - ROSSING URANIUM : SLIMES

BBTV TEST RESULTS : SLURRY 2

B2

BBTV VISCOMETER TEST RESULTS : Slurry 2

FILE NAME : PAS302609

PARTICLE SIZE RANGE	: Slurry 2
TUBE DIAMETER	: 13.37 mm
TUBE LENGTH	: 3.94 m
SLURRY TEMPERATURE	: 17 C
SOLID RELATIVE DENSITY	: 2.75
MIXTURE RELATIVE DENSITY	: 1.5004
VOLUMETRIC CONCENTRATION	: 28.59 %
pH	: 2.2

No	v [m/s]	dP [Pa]	8 v / D Psuedo-Shear Rate [1/s]	d p / 4 L Wall Shear Stress [Pa]
1	4.160	98433	2489	83.51
2	3.466	85267	2074	72.34
3	3.242	81849	1940	69.44
4	2.852	73891	1706	62.69
5	2.684	70695	1606	59.97
6	2.133	63520	1276	53.89
7	1.919	58180	1148	49.36
8	1.564	50458	936	42.81
9	1.129	42662	676	36.19
10	.818	37277	489	31.62
11	.605	34422	362	29.20
12	.309	25975	185	22.04
13	.040	17557	24	14.89
14	.197	22084	118	18.74
15	.736	34925	441	29.63
16	.893	37706	535	31.99

PSUEDO-SHEAR DIAGRAM FILE PAS302609 - ROSSING URANIUM : SLIMES

BBTV TEST RESULTS : SLURRY 2

B3

BBTV VISCOMETER TEST RESULTS : Slurry 2

FILE NAME : PUL302509

PARTICLE SIZE RANGE	: Slurry 2
TUBE DIAMETER	: 31.625 mm
TUBE LENGTH	: 3.965 m
SLURRY TEMPERATURE	: 17 C
SOLID RELATIVE DENSITY	: 2.75
MIXTURE RELATIVE DENSITY	: 1.5004
VOLUMETRIC CONCENTRATION	: 28.59 %
pH	: 2.2

No	v [m/s]	dP [Pa]	8 v / D Psuedo-Shear Rate [1/s]	d p / 4 L Wall Shear Stress [Pa]
1	1.376	15684	348	31.27
2	2.475	20713	626	41.30
3	3.308	25457	837	50.76
4	3.620	29821	916	59.46
5	3.867	35295	978	70.38
6	3.912	42026	990	83.80
7	3.936	48979	996	97.66
8	4.237	53757	1072	107.19
9	4.364	48239	1104	96.19
10	3.601	32118	911	64.04
11	3.465	29244	876	58.31
12	3.059	23678	774	47.21
13	2.854	22277	722	44.42
14	2.497	18487	632	36.86
15	1.793	15945	454	31.79
16	1.835	15807	464	31.52

PSUEDO-SHEAR DIAGRAM FILE PUL302509 - ROSSING URANIUM : SLIMES

BBTV TEST RESULTS : SLURRY 2

BBTV VISCOMETER TEST RESULTS : Slurry 2

FILE NAME : PAL302609

PARTICLE SIZE RANGE	:	Slurry 2
TUBE DIAMETER	:	31.625 mm
TUBE LENGTH	:	3.965 m
SLURRY TEMPERATURE	:	17 C
SOLID RELATIVE DENSITY	:	2.75
MIXTURE RELATIVE DENSITY	:	1.5004
VOLUMETRIC CONCENTRATION	:	28.59 %
pH	:	2.2

No	v [m/s]	dP [Pa]	8 v / D Psuedo-Shear Rate [1/s]	d p / 4 L Wall Shear Stress [Pa]
1	4.798	65370	1214	130.35
2	4.408	56612	1115	112.88
3	4.102	41330	1038	82.41
4	3.352	27854	848	55.54
5	2.556	20013	646	39.91
6	2.572	17720	651	35.33
7	2.577	20904	652	41.68
8	2.556	19555	647	38.99
9	1.928	16759	488	33.42
10	1.912	16300	484	32.50
11	1.478	14717	374	29.35
12	1.702	15028	431	29.97
13	1.722	15102	436	30.11
14	1.486	14044	376	28.00
15	.926	11773	234	23.48
16	.961	11581	243	23.09

PSUEDO-SHEAR DIAGRAM FILE PAL302609 - ROSSING URANIUM : SLIMES

BBTV TEST RESULTS : SLURRY 2

BBTV VISCOMETER TEST RESULTS : Slurry 2

FILE NAME : PBL302609

PARTICLE SIZE RANGE	: Slurry 2
TUBE DIAMETER	: 31.625 mm
TUBE LENGTH	: 3.965 m
SLURRY TEMPERATURE	: 17 C
SOLID RELATIVE DENSITY	: 2.75
MIXTURE RELATIVE DENSITY	: 1.5004
VOLUMETRIC CONCENTRATION	: 28.59 %
pH	: 2.2

No	v [m/s]	dP [Pa]	8 v / D Psuedo-Shear Rate [1/s]	d p / 4 L Wall Shear Stress [Pa]
1	5.025	67603	1271	134.80
2	3.800	41301	961	82.35
3	4.361	26226	1103	52.30
4	3.006	21167	760	42.21
5	2.134	16625	540	33.15
6	1.268	12794	321	25.51
7	1.749	14983	442	29.88
8	1.213	12291	307	24.51
9	.772	10412	195	20.76
10	1.256	12868	318	25.66
11	.505	9436	128	18.82
12	.235	7749	59	15.45
13	.128	6877	32	13.71
14	.974	11448	246	22.83
15	.247	7498	62	14.95
16	.392	8504	99	16.96

PSUEDO-SHEAR DIAGRAM FILE PBL302609 - ROSSING URANIUM : SLIMES

BBTV TEST RESULTS : SLURRY 2

APPENDIX C.7

URANIUM TAILINGS : SLURRY 3

BBTV VISCOMETER TEST RESULTS : Slurry 3

FILE NAME : PUS252709

PARTICLE SIZE RANGE : Slurry 3
TUBE DIAMETER : 13.37 mm
TUBE LENGTH : 3.94 m
SLURRY TEMPERATURE : 17 C
SOLID RELATIVE DENSITY : 2.75
MIXTURE RELATIVE DENSITY : 1.4092
VOLUMETRIC CONCENTRATION : 23.38 %
pH : 2.2

No	v [m/s]	dP [Pa]	8 v / D Psuedo-Shear Rate [1/s]	d p / 4 L Wall Shear Stress [Pa]
1	1.295	16507	775	14.00
2	1.040	14436	622	12.25
3	1.804	20516	1079	17.40
4	2.038	22217	1219	18.85
5	2.105	25501	1259	21.63
6	2.419	26936	1447	22.85
7	2.396	33771	1434	28.65
8	2.597	43106	1554	36.57
9	2.973	47129	1779	39.98
10	2.964	55428	1774	47.02
11	3.159	60070	1890	50.96
12	3.176	75000	1901	63.63
13	3.294	78595	1971	66.68
14	3.430	88107	2052	74.75
15	3.548	91569	2123	77.68
16	3.630	99025	2172	84.01

PSUEDO-SHEAR DIAGRAM FILE PUS252709 - ROSSING URANIUM : SLIMES

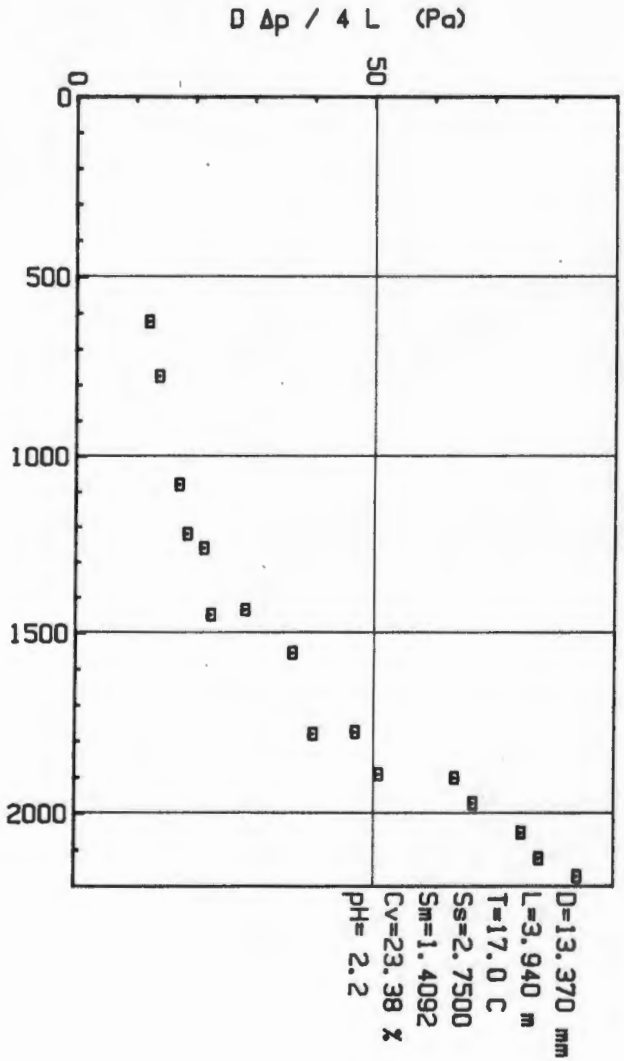

BBTV TEST RESULTS : SLURRY 3

BBTV VISCOMETER TEST RESULTS : Slurry 3

FILE NAME : PAS252709

PARTICLE SIZE RANGE : Slurry 3
TUBE DIAMETER : 13.37 mm
TUBE LENGTH : 3.94 m
SLURRY TEMPERATURE : 17 C
SOLID RELATIVE DENSITY : 2.75
MIXTURE RELATIVE DENSITY : 1.4092
VOLUMETRIC CONCENTRATION : 23.38 %
pH : 2.2

No	v [m/s]	dP [Pa]	8 v / D Psuedo-Shear Rate [1/s]	d p / 4 L Wall Shear Stress [Pa]
1	2.864	31734	1714	26.92
2	2.508	27661	1501	23.47
3	1.609	17883	963	15.17
4	.752	11329	450	9.61
5	.238	6610	142	5.61
6	.729	11241	436	9.54
7	.978	13371	585	11.34
8	1.642	18046	983	15.31
9	1.514	16862	906	14.31
10	1.435	16167	858	13.72
11	2.142	22750	1282	19.30
12	2.296	23623	1374	20.04
13	2.467	25206	1476	21.38
14	2.467	27040	1476	22.94
15	2.365	27484	1415	23.32
16	2.734	28046	1636	23.79

BBTV TEST RESULTS : SLURRY 3

PSUEDO-SHEAR DIAGRAM FILE PAS252709 - ROSSING URANIUM : SLIMES

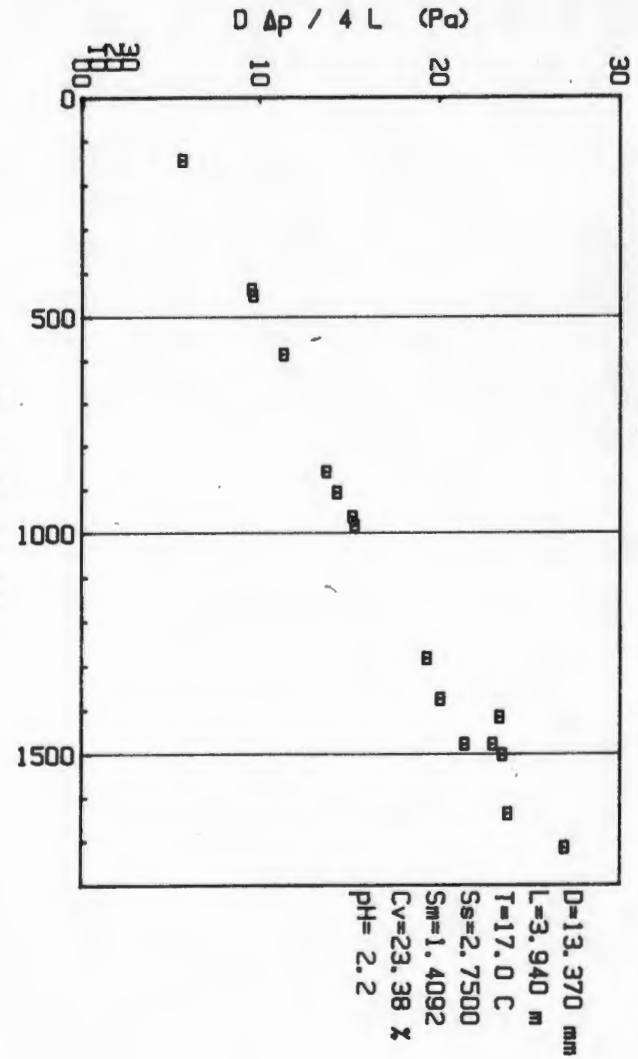

BBTV VISCOMETER TEST RESULTS : Slurry 3

FILE NAME : PBS252709

PARTICLE SIZE RANGE : Slurry 3
TUBE DIAMETER : 13.37 mm
TUBE LENGTH : 3.94 m
SLURRY TEMPERATURE : 17 C
SOLID RELATIVE DENSITY : 2.75
MIXTURE RELATIVE DENSITY : 1.4092
VOLUMETRIC CONCENTRATION : 23.38 %
pH : 2.2

No	v [m/s]	dP [Pa]	8 v / D Psuedo-Shear Rate [1/s]	d p / 4 L Wall Shear Stress [Pa]
1	4.253	122487	2545	103.91
2	3.895	133715	2330	113.44
3	4.612	140638	2760	119.31
4	4.732	149070	2832	126.46
5	4.933	154677	2951	131.22
6	5.019	162355	3003	137.73
7	5.090	162991	3046	138.27
8	5.019	172237	3003	146.12
9	5.326	178509	3187	151.44
10	5.253	187681	3143	159.22
11	5.657	200359	3385	169.97
12	5.868	206942	3511	175.56
13	6.097	217815	3648	184.78
14	6.317	231440	3780	196.34
15	6.244	238985	3736	202.74
16	6.396	243051	3827	206.19

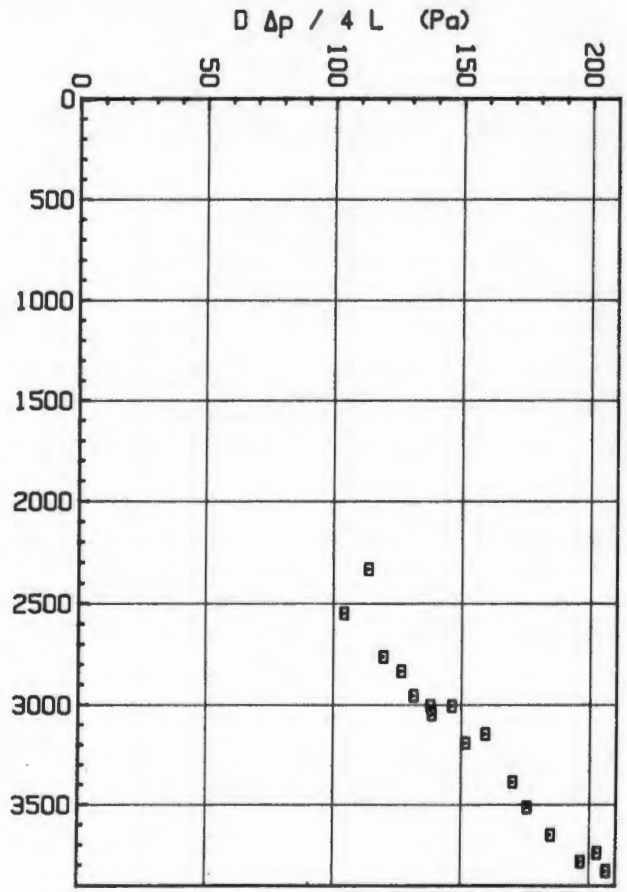

PSUEDO-SHEAR DIAGRAM FILE PBS252709 - ROSSING URANIUM : SLIMES

BBTV TEST RESULTS : SLURRY 3

BBTV VISCOMETER TEST RESULTS : Slurry 3

FILE NAME : PUL252709

PARTICLE SIZE RANGE	: Slurry 3
TUBE DIAMETER	: 31.625 mm
TUBE LENGTH	: 3.965 m
SLURRY TEMPERATURE	: 17 C
SOLID RELATIVE DENSITY	: 2.75
MIXTURE RELATIVE DENSITY	: 1.4092
VOLUMETRIC CONCENTRATION	: 23.38 %
pH	: 2.2

No	v [m/s]	dP [Pa]	8 v / D Psuedo-Shear Rate [1/s]	d p / 4 L Wall Shear Stress [Pa]
1	.124	3035	31	6.05
2	1.998	1729	506	3.45
3	1.872	9002	473	17.95
4	1.047	3405	265	6.79
5	.795	3183	201	6.35
6	1.258	3888	318	7.75
7	1.671	5020	423	10.01
8	2.195	8859	555	17.66
9	2.053	10042	519	20.02
10	2.285	11877	578	23.68
11	2.425	15353	613	30.61
12	2.784	19629	704	39.14
13	2.854	20457	722	40.79
14	2.658	17424	672	34.74
15	2.544	17084	643	34.07
16	2.902	20812	734	41.50

BBTV TEST RESULTS : SLURRY 3

PSUEDO-SHEAR DIAGRAM FILE PUL252709 - ROSSING URANIUM : SLIMES

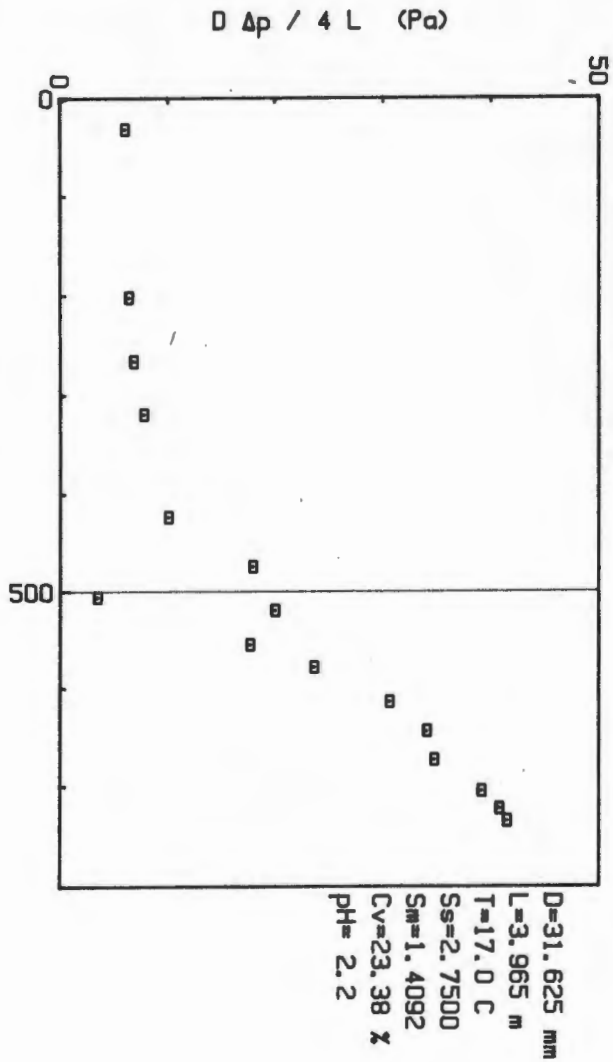

C5

BBTV VISCOMETER TEST RESULTS : Slurry 3

FILE NAME : PAL252709

PARTICLE SIZE RANGE	: Slurry 3
TUBE DIAMETER	: 31.625 mm
TUBE LENGTH	: 3.965 m
SLURRY TEMPERATURE	: 17 C
SOLID RELATIVE DENSITY	: 2.75
MIXTURE RELATIVE DENSITY	: 1.4092
VOLUMETRIC CONCENTRATION	: 23.38 %
pH	: 2.2

No	v [m/s]	dP [Pa]	8 v / D Psuedo-Shear Rate [1/s]	d p / 4 L Wall Shear Stress [Pa]
1	1.630	4791	412	9.55
2	1.849	6093	468	12.15
3	1.546	4539	391	9.05
4	1.942	5230	491	10.43
5	1.158	3844	293	7.66
6	1.545	4484	391	8.94
7	.883	2986	223	5.95
8	.236	1817	60	3.62
9	.990	3622	250	7.22
10	.501	2587	127	5.16
11	.170	1832	43	3.65
12	.561	2592	142	5.17
13	.105	1551	27	3.09
14	.042	1477	11	2.95
15	.243	1788	61	3.56
16	.024	1166	6	2.33

PSUEDO-SHEAR DIAGRAM FILE PAL252709 - ROSSING URANIUM : SLIMES

BBTV TEST RESULTS : SLURRY 3

C6

BBTV VISCOMETER TEST RESULTS : Slurry 3

FILE NAME : PBL252709

PARTICLE SIZE RANGE	: Slurry 3	
TUBE DIAMETER	: 31.625	mm
TUBE LENGTH	: 3.965	m
SLURRY TEMPERATURE	: 17	C
SOLID RELATIVE DENSITY	: 2.75	
MIXTURE RELATIVE DENSITY	: 1.4092	
VOLUMETRIC CONCENTRATION	: 23.38	%
pH	: 2.2	

No	v (m/s)	dP (Pa)	8 v / D Psuedo-Shear Rate (1/s)	d p / 4 L Wall Shear Stress (Pa)
1	3.239	25028	819	49.91
2	2.979	21862	754	43.59
3	3.108	24899	786	49.65
4	4.241	42928	1073	85.60
5	4.390	44762	1110	89.26
6	5.060	52810	1280	105.30
7	5.594	63668	1415	126.96
8	5.663	69793	1432	139.17
9	6.832	79764	1728	159.05
10	6.713	86184	1698	171.85
11	6.720	96665	1700	192.75
12	7.311	101769	1849	202.93
13	8.300	112629	2100	224.58
14	7.487	116821	1894	232.94
15	7.670	125944	1940	251.13
16	8.485	130727	2146	260.67

PSUEDO-SHEAR DIAGRAM FILE PBL252709 - ROSSING URANIUM : SLIMES

BBTV TEST RESULTS : SLURRY 3

APPENDIX C.8

URANIUM TAILINGS : SLURRY 4

D1

BBTV VISCOMETER TEST RESULTS : Slurry 4

FILE NAME : PUS250910

PARTICLE SIZE RANGE	: Slurry 4
TUBE DIAMETER	: 13.37 mm
TUBE LENGTH	: 3.943 m
SLURRY TEMPERATURE	: 17 C
SOLID RELATIVE DENSITY	: 2.75
MIXTURE RELATIVE DENSITY	: 1.4184
VOLUMETRIC CONCENTRATION	: 23.91 %
pH	: 2.2

No	v [m/s]	dP [Pa]	8 v / D Psuedo-Shear Rate [1/s]	d p / 4 L Wall Shear Stress [Pa]
1	3.529	89956	2112	76.26
2	2.823	82737	1689	70.14
3	3.340	77160	1998	65.41
4	3.207	62862	1919	53.29
5	2.640	50813	1579	43.07
6	1.956	31537	1170	26.73
7	2.022	31108	1210	26.37
8	1.753	28105	1049	23.82
9	1.895	29910	1134	25.35
10	1.646	22617	985	19.17
11	1.774	25827	1061	21.89
12	1.548	21729	926	18.42
13	1.527	19318	914	16.38
14	1.318	14791	788	12.54
15	1.405	16862	841	14.29
16	.951	12099	569	10.26

PSUEDO-SHEAR DIAGRAM FILE PUS250910 - ROSSING URANIUM : SLIMES

BBTV TEST RESULTS : SLURRY 4

D2

BBTV VISCOMETER TEST RESULTS : Slurry 4

FILE NAME : PAS250910

PARTICLE SIZE RANGE	: Slurry 4
TUBE DIAMETER	: 13.37 mm
TUBE LENGTH	: 3.943 m
SLURRY TEMPERATURE	: 17 C
SOLID RELATIVE DENSITY	: 2.75
MIXTURE RELATIVE DENSITY	: 1.4184
VOLUMETRIC CONCENTRATION	: 23.91 %
pH	: 2.2

No	v [m/s]	dP [Pa]	8 v / D Psuedo-Shear Rate [1/s]	d p / 4 L Wall Shear Stress [Pa]
1	1.648	24141	986	20.46
2	1.630	19022	975	16.13
3	1.508	17868	902	15.15
4	1.289	15590	771	13.22
5	1.500	17883	898	15.16
6	1.220	13430	730	11.38
7	1.349	15723	807	13.33
8	.859	10703	514	9.07
9	1.115	13948	667	11.82
10	.459	8903	275	7.55
11	.694	10812	415	9.17
12	.234	7695	140	6.52
13	.365	8193	218	6.95
14	.093	5747	56	4.87
15	.740	10826	442	9.18
16	.310	7868	185	6.67

PSUEDO-SHEAR DIAGRAM FILE PAS250910 - ROSSING URANIUM : SLIMES

BBTV TEST RESULTS : SLURRY 4

03

BBTV VISCOMETER TEST RESULTS : Slurry 4

FILE NAME : PBS250910

PARTICLE SIZE RANGE	: Slurry 4
TUBE DIAMETER	: 13.37 mm
TUBE LENGTH	: 3.943 m
SLURRY TEMPERATURE	: 17 C
SOLID RELATIVE DENSITY	: 2.75
MIXTURE RELATIVE DENSITY	: 1.4184
VOLUMETRIC CONCENTRATION	: 23.91 %
pH	: 2.2

No	v [m/s]	dP [Pa]	8 v / D Psuedo-Shear Rate [1/s]	d p / 4 L Wall Shear Stress [Pa]
1	3.484	86110	2085	73.00
2	3.742	4717	2239	4.00
3	3.788	99380	2267	84.24
4	4.152	109927	2484	93.19
5	4.335	123345	2594	104.56
6	4.633	136171	2772	115.43
7	4.797	150150	2870	127.28
8	5.271	161600	3154	136.99
9	5.440	171172	3255	145.10
10	5.704	22424	3413	19.01
11	5.695	202715	3408	171.84
12	6.284	237746	3760	201.54
13	6.649	258309	3978	218.97

PSUEDO-SHEAR DIAGRAM FILE PBS250910 - ROSSING URANIUM : SLIMES

BBTV TEST RESULTS : SLURRY 4

BBTV VISCOMETER TEST RESULTS : Slurry 4

FILE NAME : PUL250910

PARTICLE SIZE RANGE : Slurry 4
TUBE DIAMETER : 31.625 mm
TUBE LENGTH : 3.965 m
SLURRY TEMPERATURE : 17 C
SOLID RELATIVE DENSITY : 2.75
MIXTURE RELATIVE DENSITY : 1.4184
VOLUMETRIC CONCENTRATION : 23.91 %
pH : 2.2

No	v [m/s]	dP [Pa]	8 v / D Psuedo-Shear Rate [1/s]	d p / 4 L Wall Shear Stress [Pa]
1	7.509	98847	1900	197.10
2	7.112	91102	1799	181.66
3	7.069	87826	1788	175.13
4	6.578	81021	1664	161.56
5	7.011	79640	1774	158.80
6	6.132	72663	1551	144.89
7	6.430	73353	1627	146.27
8	6.301	69059	1594	137.71
9	5.871	66938	1485	133.47
10	5.943	63594	1503	126.81
11	5.367	58934	1358	117.52
12	5.206	54970	1317	109.61
13	4.903	51459	1240	102.61
14	4.711	44693	1192	89.12
15	4.257	40827	1077	81.41
16	4.174	36493	1056	72.77

PSUEDO-SHEAR DIAGRAM FILE PUL250910 - ROSSING URANIUM : SLIMES

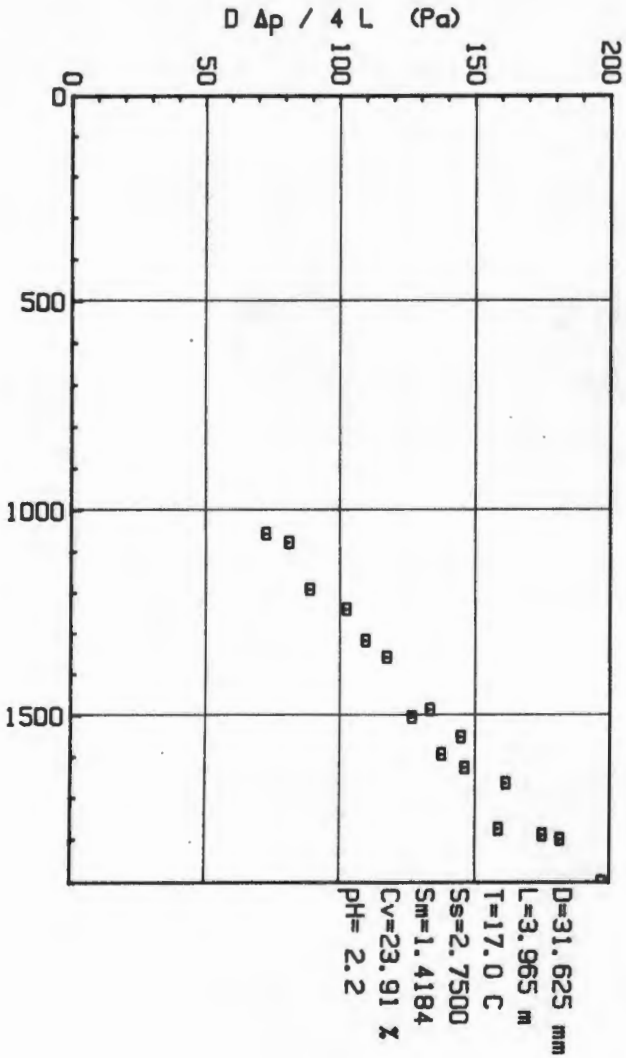

BBTV TEST RESULTS : SLURRY 4

BBTV VISCOMETER TEST RESULTS : Slurry 4

FILE NAME : PAL250910

PARTICLE SIZE RANGE : Slurry 4
TUBE DIAMETER : 31.625 mm
TUBE LENGTH : 3.965 m
SLURRY TEMPERATURE : 17 C
SOLID RELATIVE DENSITY : 2.75
MIXTURE RELATIVE DENSITY : 1.4184
VOLUMETRIC CONCENTRATION : 23.91 %
pH : 2.2

No	v [m/s]	dP [Pa]	8 v / D Psuedo-Shear Rate [1/s]	d p / 4 L Wall Shear Stress [Pa]
1	3.048	21126	771	42.13
2	2.341	13563	592	27.05
3	2.311	13760	584	27.44
4	2.072	8139	524	16.23
5	1.621	6403	410	12.77
6	1.734	7547	439	15.05
7	1.540	5452	390	10.87
8	1.481	4663	375	9.30
9	1.021	2379	258	4.74
10	1.136	2838	287	5.66
11	.763	1729	193	3.45
12	1.436	4539	363	9.05
13	1.046	2320	265	4.63
14	1.212	3193	306	6.37
15	.626	1447	158	2.89
16	.988	2320	250	4.63

PSUEDO-SHEAR DIAGRAM FILE PAL250910 - ROSSING URANIUM : SLIMES

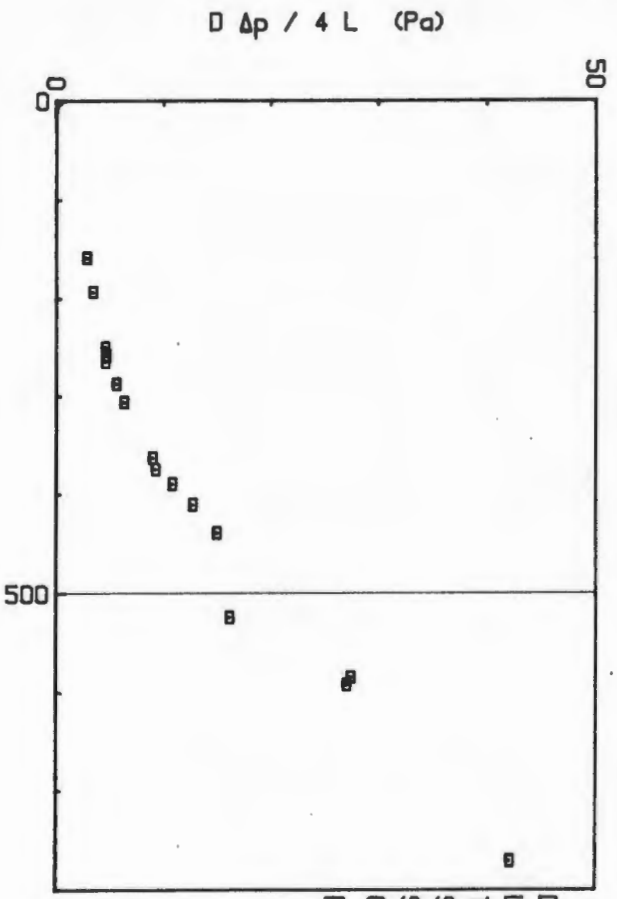

BBTV TEST RESULTS : SLURRY 4

D6

BBTV VISCOMETER TEST RESULTS : Slurry 4

FILE NAME : PBL250910

PARTICLE SIZE RANGE	: Slurry 4
TUBE DIAMETER	: 31.625 mm
TUBE LENGTH	: 3.965 m
SLURRY TEMPERATURE	: 17 C
SOLID RELATIVE DENSITY	: 2.75
MIXTURE RELATIVE DENSITY	: 1.4184
VOLUMETRIC CONCENTRATION	: 23.91 %
pH	: 2.2

No	v [m/s]	dP [Pa]	8 v / D Psuedo-Shear Rate [1/s]	d p / 4 L Wall Shear Stress [Pa]
1	1.136	3090	287	6.16
2	1.631	5723	413	11.41
3	.827	1901	209	3.79
4	.247	1063	62	2.12
5	.800	1926	202	3.84
6	.265	964	67	1.92
7	.804	1975	203	3.94
8	.336	1314	85	2.62
9	.515	1507	130	3.00
10	.473	1211	120	2.41
11	.553	1595	140	3.18
12	.558	1433	141	2.86
13	.608	1640	154	3.27
14	.575	1433	146	2.86
15	.532	1655	135	3.30

PSUEDO-SHEAR DIAGRAM FILE PBL250910 - ROSSING URANIUM : SLIMES

BBTV TEST RESULTS : SLURRY 4

APPENDIX D

Verification of Viscometer Programme Suite by Hand Calculation

APPENDIX D

VERIFICATION OF VISCOMETER PROGRAMME SUITE BY HAND CALCULATION

D.1 INTRODUCTION

In order to ensure that a computer programme contains no arithmetical errors, it is necessary to perform a parallel operation. Using a realistic set of input data, the necessary calculations are performed:

(a) by the computer programmes in the normal way;

(b) by hand.

the output of these two operations should be identical. Any arithmetical (or other) error will then be manifested as a difference between the output of the two operations.

D.2 INPUT DATA SET

In order to ensure the validity of this verification, it is necessary to perform the parallel operation from the earliest possible stage. In this case, the earliest possible stage is the digitisation of analogue voltages from the transducers and power supply. The preparation of the input data was therefore effected as follows:

D.2.1 Load Cell

1. The viscometer vessels were approximately half filled with tap water. All valves were then closed. The dry mass of a measuring cylinder was determined and the transducer was calibrated.

2. The load cell and power supply voltages were noted.

3. Using the drain tap on the L.H. vessel, approximately three litres of water was drained into a container. The mass of this water was determined, and then it was transferred to the R.H. vessel.

4. Steps 2 and 3 above were executed nine times.

5. The final voltages were noted.

D.2.2 Differential Pressure Transducer

1. The transducer was calibrated.

2. In this case, transducer readings yield pressure differentials directly from the calibration equation. Therefore, the input data was generated directly from the calibration equation.

D.2.3 Time

The time between readings was arbitrarily selected, and varied to yield realistic velocities.

D.3 RESULTS

The following are the results of the data preparation and represents the input Data Set to be used for the parallel operation.

D.3.1 Load Cell

D.3.1.1 Load cell calibration

Slope = -482414,245 N/(V/V) Constant = 940,58311 N

D.3.1.2 Mass transfer data

The power supply voltage remained constant at 5,9242V

Reading No.	Load Cell voltage (V)	Mass transferred (g)
1	0,006402	
		2887
2	,007097	
		2886
3	,0079	
		2903,5
4	,008492	
		2869
5	,009186	
		2892
6	,009889	
		2878,5
7	,010587	
		2925
8	,011296	
		2957,5
9	,012015	
		2916
10	,012723	

These ten readings were used successively six times to generate data for three rheogram points for each tube diameter.

D.3.2 Pressure

Differential pressure transducer calibration:

Slope = -1488877,22147 Pa/V Constant = -60170,5907022 Pa

Data selected for the three rheogram points were:

Points No.	Transducer Voltage (V)
1	0,042
2	0,044
3	0,046

D.3.3 Time

The time intervals between load cell readings for the three rheogram points were:

Point No.	Time interval between readings (s)
1	10
2	5
3	1,875

D.3.4 Other constants required

Other data required for calculations:

Tube diameter (large)	31,625	mm
(small)	13,37	mm
S_m (slurry relative density)	1,2559	(realistic value)
ρ_w (density of water)	998,9	kg/m³
L (tube length)	4	m

D.3.5 Input Data File

These results were then inserted into a data file in a form compatible with the computer programmes.

The parallel operations were then performed.

D.4 HAND CALCULATIONS

D.4.1 Mean slurry velocity (V_m)

The mass transfer rate (dM/dt) is determined from a least squares linear regression of [t;M] co-ordinates:- (From D.3.1.2)

Reading No.	Cumulative Mass (kg)	Cumulative time (s) Point 1	Point 2	Point 3
1	0	0	0	0
2	2,887	10	5	1,875
3	5,753	20	10	3,785
4	8,6565	30	15	5,625
5	11,5255	40	20	7,5
6	14,4175	50	25	9,375
7	17,296	60	30	11,25
8	20,221	70	35	13,125
9	23,1785	80	40	15
10	26,0945	90	45	16,875
dM/dt (kg/s)	0,290	0,579		1,545
$Q = \left[\frac{dM}{dt}\right]/\rho_m$ (m³/s)	$2,309 \times 10^{-4}$	$4,619 \times 10^{-4}$		$1,232 \times 10^{-3}$
Large tube V = Q/A (m/s)	0,294	0,588		1,568
Small tube V = Q/A (m/s)	1,645	3,290		8,773

D.4.2 Pressure Differential

From the calibration constants, and the voltage values:

	Point 1	Point 2	Point 3
Δp (Pa)	2362	5340	8318

D.4.3 Pseudo-Shear Diagram Co-ordinates

Large Tube

Point No.	$\frac{D \Delta p}{4 L}$	$\frac{8 V_m}{D}$
1	4,669	74,372
2	10,555	148,996
3	16,441	396,901

Small Tube

Point No.	$\frac{D \Delta p}{4 L}$	$\frac{8 V_m}{D}$
1	1,974	985,490
2	4,462	1970
3	6,951	5253

D.5 COMPUTER OUTPUTS

D.5.1 Mean Slurry Velocity

Figs. 1, 3 and 5 show the Mass vs. Time diagrams from which the velocity is calculated in Fig. 7. Note that these diagrams (Figs. 1, 3 and 5) are the same for both tubes.

D.5.2 Pressure Differential

Pressure differentials are the average of the points in Figs. 2, 4 and 6.

D.5.3 Pseudo-Shear Diagrams

The pseudo-shear diagrams are shown in Figs. 8 and 9.

D.6 CONCLUSIONS

The results differ by amounts which can be ascribed to truncation errors. Essentially the results of the parallel operations are identical. It can therefore be assumed that the Viscometer programme suite contains no errors.

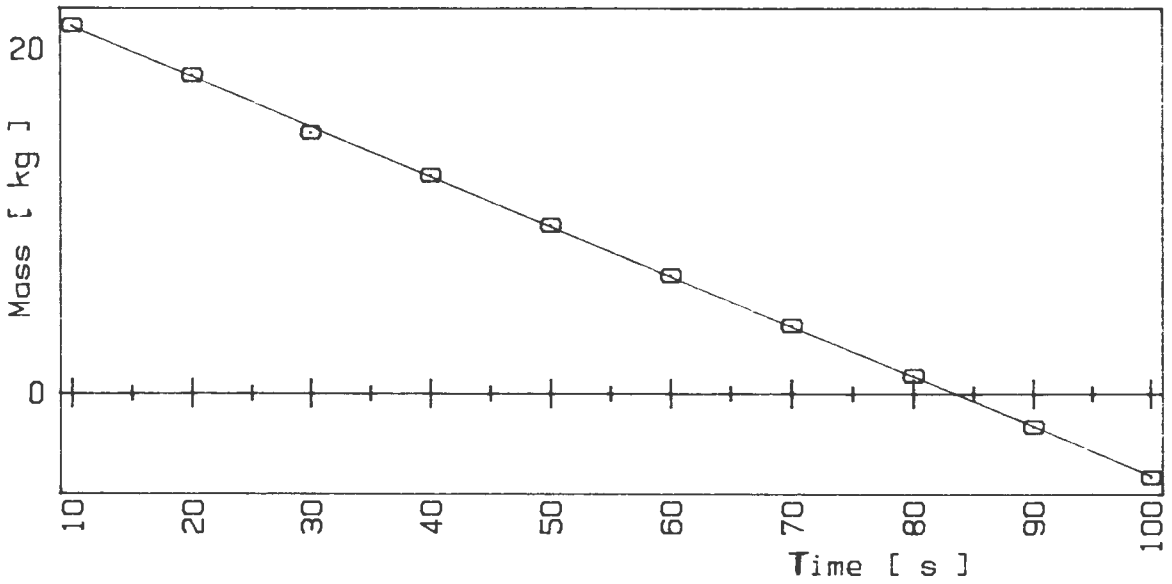

Fig.D.1 : Mass vs. Time Graph for Point 1.

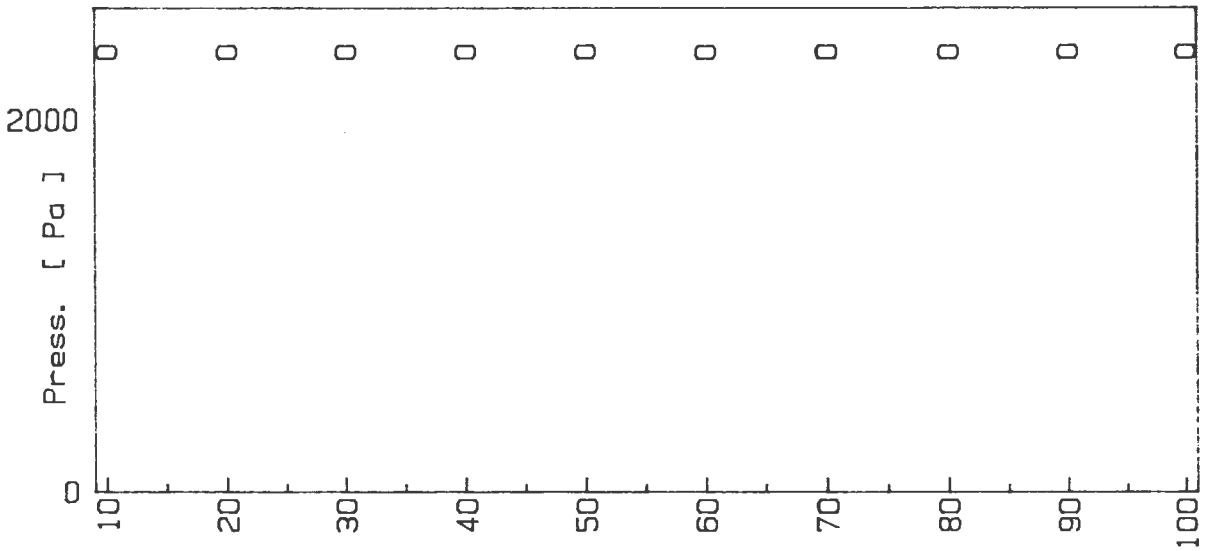

Fig. D.2 : Pressure vs. Time Graph for Point 1.

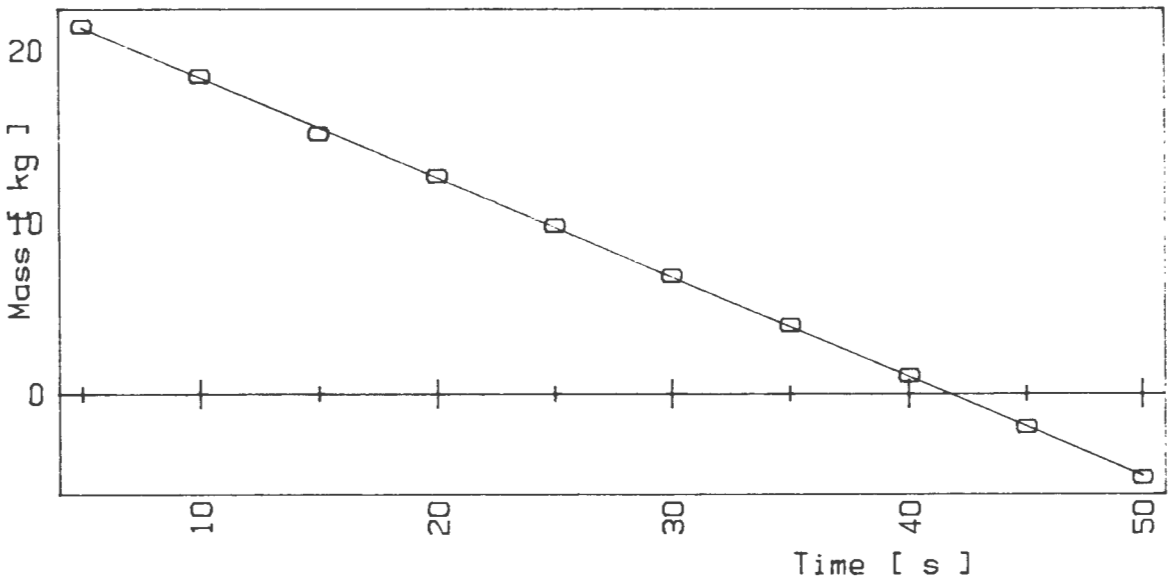

Fig. D.3 : Mass v. Time Graph for Point 2.

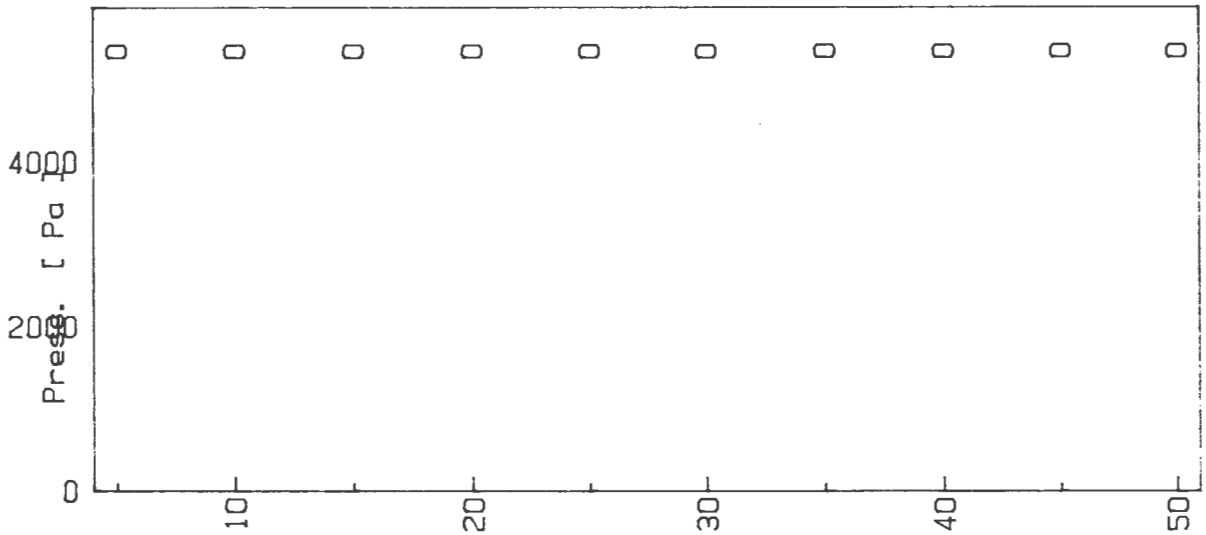

Fig. D.4 : Pressure vs. Time Graph for Point 2.

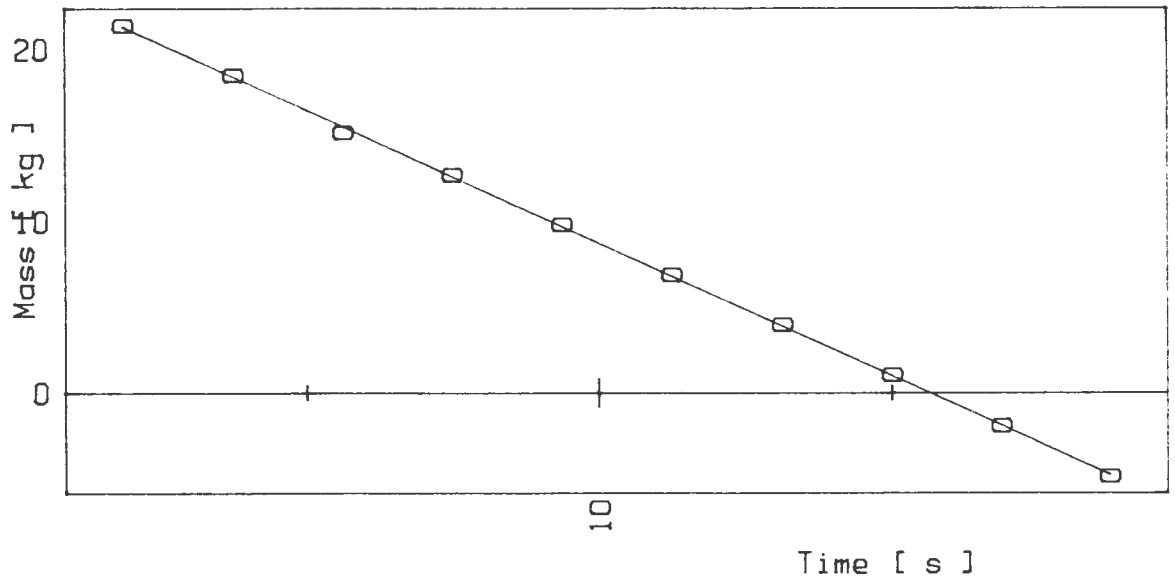

Fig. D.5 : Mass vs. Time Graph for Point 3.

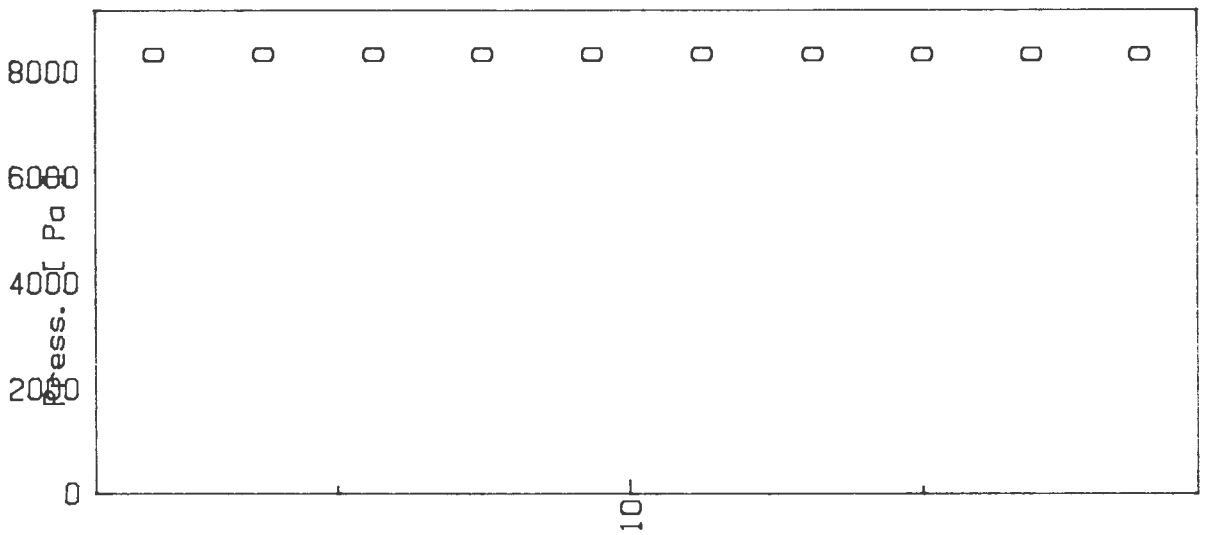

Fig. D.6 : Pressure vs. Time Graph for Point 3.

RESULTS FROM DATA FILE TS2103

LARGE TUBE

DIAM .03163
TEMP 20
Ss 2.4449
Sm 1.2559
Cv .1771
LOAD CELL CALIBRATION SLOPE -482414.24500000 CONST 940.58311000
D P CELL CALIBRATION SLOPE -1488877.22147000 CONST -60170.59070220
pH 7.00
Length Between Taps 4 m

No	Mass (kg)	Q (M^3/S)	v (m/s)	p (Pa)	P S V
1	9.717	2.312E-004	.294	2362	5.000
2	9.717	4.623E-004	.589	5340	5.000
3	9.717	1.233E-003	1.569	8318	5.000

RESULTS FROM DATA FILE TS2103

SMALL TUBE

DIAM .01337
TEMP 20
Ss 2.4449
Sm 1.2559
Cv .1771
LOAD CELL CALIBRATION SLOPE -482414.24500000 CONST 940.58311000
D P CELL CALIBRATION SLOPE -1488877.22147000 CONST -60170.59070220
pH 7.00
Length Between Taps 4 m

No	Mass (kg)	Q (M^3/S)	v (m/s)	p (Pa)	P S V
1	9.717	2.312E-004	1.646	2362	5.000
2	9.717	4.623E-004	3.293	5340	5.000
3	9.717	1.233E-003	8.781	8318	5.000

Fig. D.7 : Raw Data Processing Printouts.

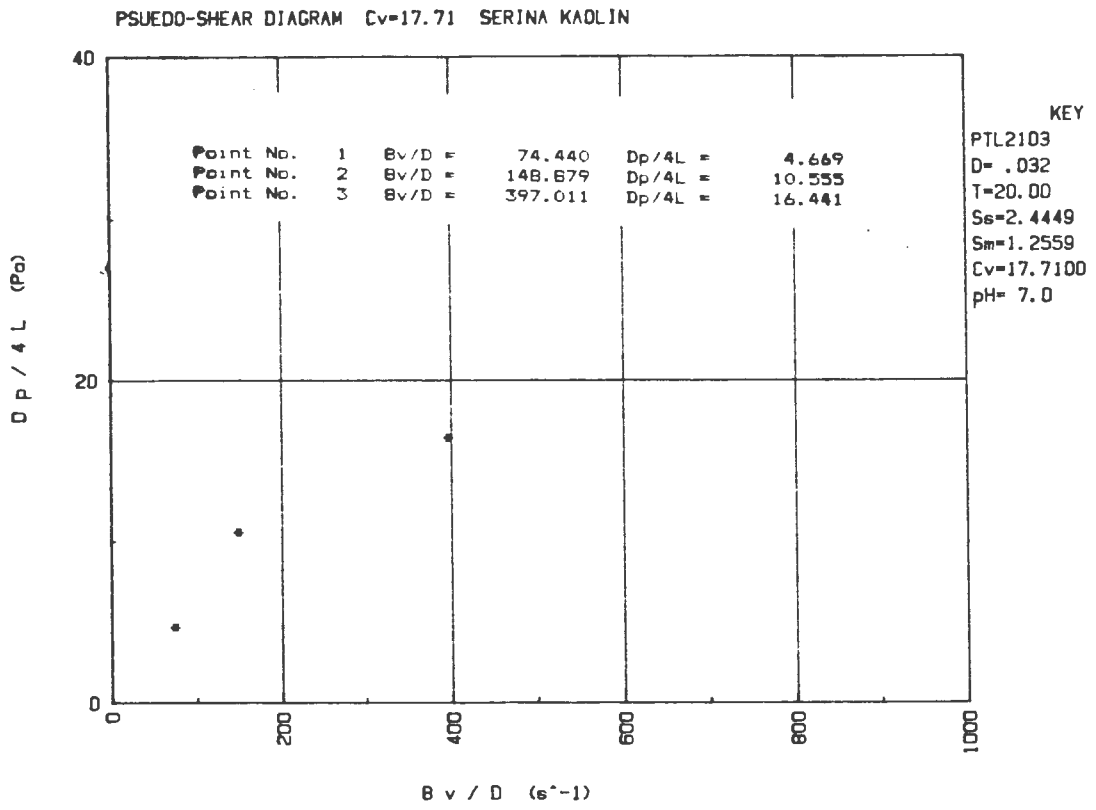

Fig. D.8 : Pseudo Shear Diagram - Large Tube.

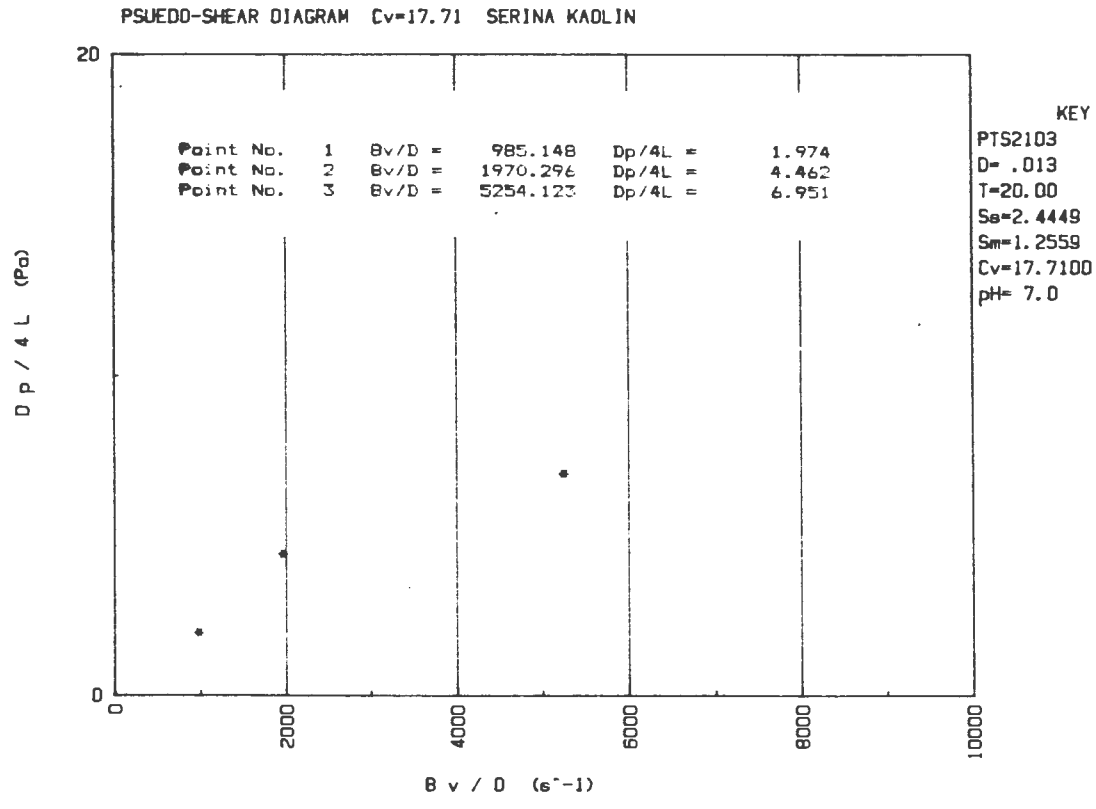

Fig. D.9 : Pseudo Shear Diagram - Small Tube.

APPENDIX E

ROTARY VISCOMETER

	Page
Calibration data	E.1 - E.2
Kaolin Results	E.3 - E.4
Uranium Tailings Results	E.5

APPENDIX E

ROTARY VISCOMETER

E.1 CALIBRATION

The readings for the absolute calibration (Ref. 23) are shown in Table E.1.

The constants supplied by the manufacturers is shown in Table E.2.

Switch Selling	Mass (g)	"S" (div)
500	200	90
500	100	45
500	50	23,5
500	30	14
500	20	9,5
50	20	85/88
50	10	41/45
50	5	20/24
50	3	11/15
50	2	6/10

Table E.1 : Absolute Calibration Results

ROTOR	Ø / L (mm)	f	c	B
NV	40,2 / 73	3,56	--	3140
MV I	40,08 / 60	6,55	--	1370
MV II	36,8 / 60	7,53	--	529
MV III	30,4 / 60	10,90	--	259
MV II prof.	36,8 / 60	7,53	--	514
SV I	20,2 / 60	25,1	--	529
SV II	20,2 / 20	75,3	--	529
SV II prof.	20,2 / 20	75,3	--	462
SV II FL	20,2 / 19,6	56,1	--	248
PK I	28	170	as indicated on calibrating certificate	
PK II	20	468		
PK III	12	2170		
T I	40,08/ 60	6,55	--	1370
T II	36,8/ 60	7,53	--	529
E 3	50 / 116	2,1	1,43	K = a x c
E 30	24 / 150	18,0	14,3	
E 100	16 / 35	60,0	47,8	
E 500	10 / 18	260,0	239,0	
E 1000	7 / 18	560,0	478,0	
FL 10	40 / 60	5,3	4,78	K = a x c
FL 100	22 / 16	55,0	47,8	A = a x f
FL 1000	10 / 9	439,0	478,0	

Table E.2 : Manufacturers Constants

HAAKE

ROTOVISKO RV 1

f. Nr. [redacted]
Datum: [redacted]
Kontr.: [redacted]

Berechnungsfaktoren / Calculation Factors

Prüfschein für Meßköpfe und Meßsysteme
Certificate for Measuring heads and Systems
Certificat pour têtes et systèmes de mesure

Meßkopf / Measuring Head / Tête de mesure

DMK [redacted] Nr.: [redacted] a = [redacted] $\left(\frac{N \cdot cm}{Skt}\right)$

DMK [redacted] Nr.: [redacted] a = [redacted] $\left(\frac{N \cdot cm}{Skt}\right)$

System	Rotor	f / L (mm)	Nr.	B ($_{\beta}$-1)	A $\left(\frac{Pa}{Skt}\right)$	K $\left(\frac{mPa \cdot s}{Skt}\right)$	A $\left(\frac{Pa}{Skt}\right)$	K $\left(\frac{mPa \cdot s}{Skt}\right)$
NV	NV	40.2 /60		2620				
MV	MV I	40.08/60		1139				
	MV II	36.8 /60		438				
	MV III	30.4 /60		214				
SV	SV I	20.2 /61.4		433	11,5	26,58	1,18	2,728
	SV II	20.2 /19.6		433				
SP	MV I P	40.08/60		872				
	MV II P	36.8 /60		498				
	SV II P	20.2 /19.6		379				
NORM	MV	38.7 /58.1		680				
	SV	21.3 /32		680				
HS [redacted]	HS I	19.95/15						
	HS II	19.6 /15						
PK [redacted]	PK I, 1°	28 /—						
	PK I, 0,3°	28 /—	7058	9401	79,2	8,425	8,13	0,8648
	PK II, 0,3°	20 /—						

HAAKE Mess-Technik GmbH u. Co. · Dieselstraße 8 · D-7500 Karlsruhe 41 · Telefon (0721) 40 69 53

HAAKE VISCOMETER TEST RESULTS : Kaolin

PARTICLE SIZE RANGE : Kaolin
VOLUMETRIC CONCENTRATION : 7.83 %

No	U	S	Shear Stress T [Pa]	Shear Rate dv/dy [1/s]
1	162.000	32.500	9.783	6.000
2	81.000	34.500	10.385	12.000
3	54.000	36.000	10.836	18.000
4	27.000	38.500	11.589	36.000
5	18.000	40.350	12.145	54.000
6	9.000	44.000	13.244	108.000
7	6.000	46.500	13.997	162.000
8	3.000	52.500	15.803	324.000
9	2.000	56.000	16.856	486.000
10	1.000	65.000	19.565	972.000

HAAKE VISCOMETER TEST RESULTS : Kaolin

PARTICLE SIZE RANGE : Kaolin
VOLUMETRIC CONCENTRATION : 12.08 %

No	U	S	Shear Stress T [Pa]	Shear Rate dv/dy [1/s]
1	162.000	11.000	30.580	6.000
2	81.000	12.000	33.360	12.000
3	54.000	12.500	34.750	18.000
4	27.000	13.400	37.252	36.000
5	18.000	14.000	38.920	54.000
6	9.000	14.500	40.310	108.000
7	6.000	15.000	41.700	162.000
8	3.000	16.000	44.480	324.000
9	2.000	17.500	48.650	486.000
10	1.000	19.500	54.210	972.000

HAAKE VISCOMETER TEST RESULTS : Kaolin

PARTICLE SIZE RANGE : Kaolin
VOLUMETRIC CONCENTRATION : 14.88 %

No	U	S	Shear Stress T [Pa]	Shear Rate dv/dy [1/s]
1	162.000	22.500	62.550	6.000
2	81.000	24.000	66.720	12.000
3	54.000	25.000	69.500	18.000
4	27.000	26.500	73.670	36.000
5	18.000	27.500	76.450	54.000
6	9.000	28.700	79.786	108.000
7	6.000	29.300	81.454	162.000
8	3.000	30.500	84.790	324.000
9	2.000	32.000	88.960	486.000
10	1.000	34.750	96.605	972.000

HAAKE VISCOMETER TEST RESULTS : Kaolin

PARTICLE SIZE RANGE : Kaolin
VOLUMETRIC CONCENTRATION : 17.71 %

No	U	S	Shear Stress T [Pa]	Shear Rate dv/dy [1/s]
1	162.000	40.500	112.590	6.000
2	81.000	43.000	119.540	12.000
3	54.000	45.500	126.490	18.000
4	27.000	50.000	139.000	36.000
5	18.000	52.000	144.560	54.000
6	9.000	55.500	154.290	108.000
7	6.000	57.500	159.850	162.000
8	3.000	60.500	168.190	324.000
9	2.000	62.000	172.360	486.000
10	1.000	68.000	189.040	972.000

HAAKE VISCOMETER TEST RESULTS : Slurry 1

PARTICLE SIZE RANGE : Slurry 1
VOLUMETRIC CONCENTRATION : 22.47 %

No	U	S	Shear Stress T [Pa]	Shear Rate dv/dy [1/s]
1	162.000	38.250	11.513	6.000
2	81.000	40.500	12.191	12.000
3	54.000	42.500	12.793	18.000
4	27.000	47.750	14.373	36.000
5	18.000	52.750	15.878	54.000
6	9.000	61.750	18.587	108.000
7	6.000	68.500	20.619	162.000
8	3.000	86.000	25.886	324.000
9	2.000	10.350	28.773	486.000
10	1.000	15.000	41.700	972.000

HAAKE VISCOMETER TEST RESULTS : Slurry 2

PARTICLE SIZE RANGE : Slurry 2
VOLUMETRIC CONCENTRATION : 28.59 %

No	U	S	Shear Stress T [Pa]	Shear Rate dv/dy [1/s]
1	162.000	46.000	13.846	6.000
2	81.000	46.000	13.846	12.000
3	54.000	49.500	14.900	18.000
4	27.000	54.000	16.254	36.000
5	18.000	57.000	17.157	54.000
6	9.000	65.000	19.565	108.000
7	6.000	74.000	22.274	162.000
8	3.000	91.000	27.391	324.000
9	2.000	10.800	30.024	486.000
10	1.000	16.500	45.870	972.000

APPENDIX F

LOG STANDARD ERROR DETERMINATIONS

APPENDIX F

LOG STANDARD ERROR DETERMINATIONS

Comparison of correlation errors was performed using the log standard error:

$$LSE = \sqrt{\frac{\sum_{1}^{n} \left[\log (i_{mo}) - \log (i_{mc})\right]^2}{(n - 1)}}$$

where LSE is the root mean square deviation of the log of observed points from the log of calculated points.

Calculations were performed using the equations in Chapter 2 for the yield-pseudoplastic model for laminar flow and the equation of Torrance for turbulent flow. The observed points were BBTV data points. The individual i_m values are presented in the following pages.

REFERENCE

Lazarus, J.H. and Neilson, I.D.; A generalised correlation for friction head losses of settling mixtures in horizontal smooth pipes; Hydrotransport 5; 1978.

KAOLIN Cv = 7.83 %
Ty = 6.00 Pa
K = .0270
n = .8200
V crit = 2.20 (SMALL TUBE)
V crit = 1.80 (LARGE TUBE)

No	V [m/s]	p [Pa]	imo [m/m]	imc [m/m]	% Error
1	.41	4206	.11	.11	-.41
2	1.08	4939	.13	.13	-3.82
3	2.54	8977	.23	.34	-31.35
4	3.19	14392	.37	.47	-21.71
5	3.92	20812	.54	.65	-17.85
6	4.12	22513	.58	.70	-17.77
7	4.47	28120	.72	.80	-9.77
8	4.91	33298	.86	.93	-8.18
9	5.12	37795	.97	1.00	-2.73
10	5.69	44836	1.15	1.18	-2.65
11	6.21	48845	1.26	1.37	-8.20
12	6.17	55754	1.43	1.35	6.07
13	5.58	61080	1.57	1.15	36.73
14	7.24	61908	1.59	1.76	-9.67
15	1.34	5205	.13	.14	-4.19
16	3.14	14673	.38	.46	-18.11
17	2.72	10531	.27	.37	-27.23
18	1.82	5989	.15	.21	-26.98
19	1.01	4820	.12	.13	-4.64
20	1.63	5723	.15	.15	-.52
21	.70	4510	.12	.12	-3.12
22	3.13	14366	.37	.46	-19.56
23	2.63	10068	.26	.35	-26.90
24	1.82	5989	.15	.21	-26.98
25	1.01	4820	.12	.13	-4.64
26	1.46	5490	.14	.14	-1.45
27	.55	4288	.11	.11	-3.40
28	2.92	38919	1.01	1.22	-17.28
29	2.47	27868	.72	.95	-24.25
30	2.18	21670	.56	.54	3.00
31	1.33	16788	.43	.44	-1.31
32	.84	14643	.38	.37	1.70
33	.18	10412	.27	.26	4.63
34	3.15	43890	1.14	1.36	-16.73
35	3.40	51138	1.32	1.54	-13.82
36	3.78	63077	1.63	1.81	-9.77
37	3.95	67145	1.74	1.94	-10.26
38	4.16	74039	1.92	2.09	-8.45
39	4.74	83240	2.15	2.57	-16.26
40	4.65	89749	2.32	2.49	-6.86
41	4.85	98166	2.54	2.67	-5.00
42	5.29	109572	2.83	3.06	-7.51
43	5.28	115090	2.98	3.06	-2.63
44	5.64	128715	3.33	3.40	-2.06
45	4.97	144366	3.74	2.78	34.58
46	6.20	156867	4.06	3.96	2.55
47	7.21	168183	4.35	5.06	-13.96
48	6.71	180358	4.67	4.50	3.73

LOG STANDARD ERROR = .071464

Fig. F.1 : Energy Gradient Calculations - Kaolin - C_v = 7,83% - BBTV Rheology

KAOLIN Cv = 7.83 %
Ty = 8.00 Pa
K = .9700
n = .3600
V crit = 2.20 (SMALL TUBE)
V crit = 1.80 (LARGE TUBE)

No	V [m/s]	p [Pa]	imo [m/m]	imc [m/m]	% Error
1	.41	4206	.11	.20	-44.55
2	1.08	4939	.13	.23	-44.27
3	2.54	8977	.23	.25	-6.24
4	3.19	14392	.37	.31	20.76
5	3.92	20812	.54	.38	39.72
6	4.12	22513	.58	.41	42.90
7	4.47	28120	.72	.45	62.27
8	4.91	33298	.86	.50	71.50
9	5.12	37795	.97	.53	84.69
10	5.69	44836	1.15	.60	92.12
11	6.21	48845	1.26	.67	86.84
12	6.17	55754	1.43	.67	115.33
13	5.58	61080	1.57	.59	168.02
14	7.24	61908	1.59	.82	93.34
15	1.34	5205	.13	.24	-43.46
16	3.14	14673	.38	.30	25.25
17	2.72	10531	.27	.26	3.27
18	1.82	5989	.15	.19	-18.61
19	1.01	4820	.12	.23	-45.00
20	1.63	5723	.15	.25	-40.06
21	.70	4510	.12	.21	-45.27
22	3.13	14366	.37	.30	22.90
23	2.63	10068	.26	.25	1.84
24	1.82	5989	.15	.19	-18.61
25	1.01	4820	.12	.23	-45.00
26	1.46	5490	.14	.24	-41.32
27	.55	4288	.11	.20	-45.90
28	2.92	38919	1.01	.74	35.32
29	2.47	27868	.72	.64	13.39
30	2.18	21670	.56	.73	-23.70
31	1.33	16788	.43	.66	-34.33
32	.84	14643	.38	.60	-37.18
33	.18	10412	.27	.46	-41.73
34	3.15	43890	1.14	.80	41.43
35	3.40	51138	1.32	.87	51.90
36	3.78	63077	1.63	.98	66.87
37	3.95	67145	1.74	1.03	69.14
38	4.16	74039	1.92	1.09	76.21
39	4.74	83240	2.15	1.27	69.84
40	4.65	89749	2.32	1.24	87.47
41	4.85	98166	2.54	1.31	94.48
42	5.29	109572	2.83	1.45	95.46
43	5.28	115090	2.98	1.45	105.67
44	5.64	128715	3.33	1.57	111.78
45	4.97	144366	3.74	1.34	177.96
46	6.20	156867	4.06	1.77	128.97
47	7.21	168183	4.35	2.16	101.58
48	6.71	180358	4.67	1.96	137.63

LOG STANDARD ERROR = .243955

Fig. F.2 : Energy Gradient Calculations - Kaolin - C_v = 7,83% - Rotary Viscometer Rheology

KAOLIN Cv = 12.08 %
Ty = 23.00 Pa
K = .5000
n = .5000
V crit = 4.40 (SMALL TUBE)
V crit = 4.00 (LARGE TUBE)

No	V [m/s]	p [Pa]	imo [m/m]	imc [m/m]	% Error
1	.41	15368	.40	.41	-4.04
2	2.12	20161	.52	.52	.24
3	4.60	26360	.68	.79	-13.92
4	4.90	31271	.80	.85	-5.15
5	5.35	40191	1.03	.94	9.61
6	6.07	50458	1.30	1.10	17.60
7	6.34	56124	1.44	1.17	23.50
8	6.88	66183	1.70	1.30	30.84
9	7.09	63654	1.64	1.35	20.86
10	7.48	73876	1.90	1.46	30.28
11	8.04	88664	2.28	1.61	41.76
12	5.00	31315	.81	.87	-7.14
13	4.27	24984	.64	.72	-11.32
14	3.88	24067	.62	.58	6.68
15	3.16	21862	.56	.56	1.00
16	2.79	21419	.55	.54	1.32
17	1.59	19155	.49	.49	-.13
18	.24	14924	.38	.39	-1.82
19	.68	16685	.43	.44	-1.74
20	1.48	18697	.48	.49	-1.32
21	2.95	22094	.57	.55	3.39
22	3.40	22691	.58	.56	3.29
23	3.83	23859	.61	.58	6.05
24	3.49	22868	.59	.57	3.57
25	4.38	25575	.66	.74	-11.70
26	3.11	23001	.59	.55	6.57
27	3.19	22291	.57	.56	2.76
28	.79	47277	1.22	1.20	2.23
29	1.38	53491	1.38	1.32	4.47
30	2.91	62633	1.62	1.56	4.12
31	4.25	65947	1.71	1.71	-.19
32	5.03	86568	2.24	2.38	-5.96
33	4.96	89355	2.31	2.34	-1.34
34	5.38	99158	2.57	2.59	-.81
35	3.26	62559	1.62	1.60	1.18
36	2.49	60029	1.55	1.50	3.47
37	1.00	50458	1.31	1.25	4.73
38	1.00	48135	1.25	1.25	-.07
39	.42	40428	1.05	1.08	-3.59
40	.75	46478	1.20	1.19	1.23
41	1.64	52174	1.35	1.37	-1.60
42	2.41	58165	1.50	1.49	.94
43	3.06	61745	1.60	1.58	1.36
44	3.68	66819	1.73	1.65	4.90
45	4.29	68816	1.78	1.71	3.89
46	4.68	78048	2.02	2.19	-7.63
47	4.80	83506	2.16	2.26	-4.22
48	5.11	88214	2.28	2.43	-6.11
49	5.80	107279	2.78	2.84	-2.31

LOG STANDARD ERROR = .043805

Fig. F.3 : Energy Gradient Calculations - C_v = 12,08% - BBTV Rheology

KAOLIN Cv = 12.08 %
Ty = 24.00 Pa
K = 5.6200
n = .2400
V crit = 4.40 (SMALL TUBE)
V crit = 4.00 (LARGE TUBE)

No	V [m/s]	p [Pa]	imo [m/m]	imc [m/m]	% Error
1	.41	15368	.40	.60	-34.09
2	2.12	20161	.52	.73	-28.56
3	4.60	26360	.68	.64	5.47
4	4.90	31271	.80	.67	19.58
5	5.35	40191	1.03	.72	43.74
6	6.07	50458	1.30	.80	62.84
7	6.34	56124	1.44	.83	74.27
8	6.88	66183	1.70	.89	90.95
9	7.09	63654	1.64	.92	78.56
10	7.48	73876	1.90	.97	96.71
11	8.04	88664	2.28	1.04	120.03
12	5.00	31315	.81	.68	18.07
13	4.27	24984	.64	.61	5.09
14	3.88	24067	.62	.79	-21.24
15	3.16	21862	.56	.76	-26.44
16	2.79	21419	.55	.75	-26.75
17	1.59	19155	.49	.70	-29.67
18	.24	14924	.38	.57	-32.45
19	.68	16685	.43	.63	-32.26
20	1.48	18697	.48	.69	-30.71
21	2.95	22094	.57	.76	-25.01
22	3.40	22691	.58	.77	-24.42
23	3.83	23859	.61	.78	-21.78
24	3.49	22868	.59	.77	-24.08
25	4.38	25575	.66	.62	5.82
26	3.11	23001	.59	.76	-22.46
27	3.19	22291	.57	.77	-25.11
28	.79	47277	1.22	1.69	-27.57
29	1.38	53491	1.38	1.82	-23.76
30	2.91	62633	1.62	2.01	-19.46
31	4.25	65947	1.71	2.13	-19.75
32	5.03	86568	2.24	1.75	27.86
33	4.96	89355	2.31	1.73	33.34
34	5.38	99158	2.57	1.85	38.91
35	3.26	62559	1.62	2.05	-20.86
36	2.49	60029	1.55	1.97	-21.08
37	1.00	50458	1.31	1.74	-24.97
38	1.00	48135	1.25	1.74	-28.41
39	.42	40428	1.05	1.56	-33.09
40	.75	46478	1.20	1.68	-28.40
41	1.64	52174	1.35	1.86	-27.35
42	2.41	58165	1.50	1.96	-23.21
43	3.06	61745	1.60	2.03	-21.20
44	3.68	66819	1.73	2.08	-16.95
45	4.29	68816	1.78	2.13	-16.38
46	4.68	78048	2.02	1.66	21.62
47	4.80	83506	2.16	1.69	27.62
48	5.11	88214	2.28	1.77	28.61
49	5.80	107279	2.78	1.96	41.30

LOG STANDARD ERROR = .151003

Fig. F.4 : Energy Gradient Calculations - C_v = 12,08% - Rotary Viscometer Rheology

KAOLIN Cv = 14.88 %
Ty = 44.00 Pa
K = 1.1700
n = .4900
V crit = 4.40 (SMALL TUBE)
V crit = 6.20 (LARGE TUBE)

No	V [m/s]	p [Pa]	imo [m/m]	imc [m/m]	% Error
1	.18	28874	.74	.75	-.71
2	.62	32395	.83	.86	-2.87
3	1.67	38816	1.00	1.00	.18
4	1.75	38742	1.00	1.00	-.79
5	3.53	43816	1.13	1.15	-1.99
6	4.01	45177	1.16	1.18	-1.67
7	4.34	46468	1.19	1.20	-.61
8	5.06	48195	1.24	1.24	-.44
9	5.46	49030	1.26	1.27	-.46
10	4.60	47366	1.22	1.22	.00
11	6.39	54393	1.40	1.66	-16.01
12	1.44	38579	.99	.97	2.15
13	2.49	40901	1.05	1.07	-1.84
14	4.16	46464	1.19	1.19	.28
15	4.06	45532	1.17	1.18	-1.18
16	4.98	49023	1.26	1.24	1.64
17	5.39	50010	1.29	1.26	1.82
18	6.28	55133	1.42	1.63	-13.31
19	6.77	56937	1.46	1.78	-17.96
20	6.89	66351	1.71	1.82	-6.36
21	7.28	73920	1.90	1.95	-2.41
22	7.53	85341	2.19	2.03	8.23
23	8.04	96288	2.48	2.20	12.39
24	6.12	24991	1.31	1.30	.71
25	6.02	22484	1.18	1.30	-9.05
26	4.92	23741	1.24	1.24	.67
27	4.89	23919	1.25	1.23	1.58
28	3.13	20706	1.09	1.12	-3.19
29	2.58	20319	1.07	1.08	-1.24
30	.55	16270	.85	.84	1.14
31	.80	16670	.87	.89	-1.60
32	1.63	19111	1.00	.99	1.04
33	1.91	19466	1.02	1.02	.05
34	4.05	22203	1.16	1.18	-1.67
35	4.42	22661	1.19	1.21	-1.56
36	5.47	24821	1.30	1.27	2.73
37	5.82	25250	1.32	1.29	2.99
38	6.36	26286	1.38	1.66	-16.88
39	6.27	27987	1.47	1.63	-10.08

LOG STANDARD ERROR = .029616

Fig. F.5 : Energy Gradient Calculations - C_v = 14,88% - BBTV Rheology

KAOLIN Cv = 14.88 %
Ty = 40.00 Pa
K = 19.8000
n = .1500
V crit = 4.40 (SMALL TUBE)
V crit = 6.20 (LARGE TUBE)

No	V [m/s]	p [Pa]	imo [m/m]	imc [m/m]	% Error
1	.18	28874	.74	1.07	-30.90
2	.62	32395	.83	1.18	-29.62
3	1.67	38816	1.00	1.28	-22.31
4	1.75	38742	1.00	1.29	-22.75
5	3.53	43816	1.13	1.37	-17.84
6	4.01	45177	1.16	1.39	-16.25
7	4.34	46468	1.19	1.40	-14.47
8	5.06	48195	1.24	1.42	-12.53
9	5.46	49030	1.26	1.43	-11.62
10	4.60	47366	1.22	1.40	-13.28
11	6.39	54393	1.40	.99	40.63
12	1.44	38579	.99	1.27	-21.78
13	2.49	40901	1.05	1.33	-20.90
14	4.16	46464	1.19	1.39	-14.16
15	4.06	45532	1.17	1.39	-15.69
16	4.98	49023	1.26	1.41	-10.89
17	5.39	50010	1.29	1.42	-9.75
18	6.28	55133	1.42	.99	43.68
19	6.77	56937	1.46	1.03	42.71
20	6.89	66351	1.71	1.04	64.73
21	7.28	73920	1.90	1.07	77.91
22	7.53	85341	2.19	1.09	101.50
23	8.04	96288	2.48	1.13	118.30
24	6.12	24991	1.31	1.44	-9.08
25	6.02	22484	1.18	1.44	-18.08
26	4.92	23741	1.24	1.41	-11.89
27	4.89	23919	1.25	1.41	-11.18
28	3.13	20706	1.09	1.36	-19.97
29	2.58	20319	1.07	1.33	-20.10
30	.55	16270	.85	1.17	-27.16
31	.80	16670	.87	1.21	-27.67
32	1.63	19111	1.00	1.28	-21.81
33	1.91	19466	1.02	1.30	-21.45
34	4.05	22203	1.16	1.39	-16.13
35	4.42	22661	1.19	1.40	-15.08
36	5.47	24821	1.30	1.43	-8.76
37	5.82	25250	1.32	1.43	-7.71
38	6.36	26286	1.38	.99	38.86
39	6.27	27987	1.47	.99	48.88

LOG STANDARD ERROR = .134175

Fig. F.6 : Energy Gradient Calculations - C_v = 14.88% - Rotary Viscometer Rheology

KAOLIN Cv = 17.71 %
Ty = 80.00 Pa
K = 2.2900
n = .4300
V crit = 7.00 (SMALL TUBE)
V crit = 6.00 (LARGE TUBE)

No	V [m/s]	p [Pa]	imo [m/m]	imc [m/m]	% Error
1	.13	47603	1.22	1.29	-5.08
2	2.00	65143	1.67	1.68	-.15
3	.75	56819	1.46	1.49	-2.04
4	.96	58949	1.52	1.53	-.99
5	.98	59926	1.54	1.54	.34
6	1.85	63935	1.64	1.66	-1.02
7	2.50	66553	1.71	1.73	-1.17
8	2.95	68654	1.77	1.77	-.48
9	3.34	70089	1.80	1.81	-.31
10	.37	49082	1.26	1.39	-9.45
11	.52	54644	1.40	1.44	-2.23
12	.74	56982	1.46	1.49	-1.52
13	1.09	61287	1.58	1.55	1.36
14	1.60	66272	1.70	1.63	4.60
15	3.02	69527	1.79	1.78	.45
16	3.66	70851	1.82	1.83	-.64
17	4.84	75751	1.95	1.92	1.51
18	5.08	77957	2.00	1.93	3.58
19	6.05	80059	2.06	1.86	10.36
20	6.29	82589	2.12	1.93	10.17
21	7.22	86458	2.22	2.18	1.99
22	7.79	89256	2.29	2.35	-2.25
23	8.59	109671	2.82	2.60	8.55
24	3.95	71967	1.85	1.86	-.28
25	.14	61523	3.23	3.26	-1.02
26	.49	70991	3.72	3.70	.63
27	.97	78099	4.10	4.05	1.29
28	1.71	85577	4.49	4.40	1.93
29	1.83	84438	4.43	4.46	-.60
30	2.50	92205	4.84	4.70	2.95
31	2.93	90903	4.77	4.83	-1.34
32	3.67	101066	5.30	5.04	5.15
33	4.35	98699	5.18	5.21	-.64
34	5.72	110815	5.81	5.51	5.46
35	6.62	105312	5.53	5.69	-2.84
36	1.26	82678	4.34	4.20	3.22
37	1.31	78136	4.10	4.23	-3.01
38	2.08	86702	4.55	4.55	-.08
39	2.84	90859	4.77	4.81	-.81
40	3.59	96913	5.08	5.02	1.27
41	4.42	98048	5.14	5.23	-1.64
42	5.09	105696	5.55	5.38	3.07
43	6.38	106584	5.59	5.64	-.89
44	5.93	109483	5.74	5.56	3.39
45	6.89	109262	5.73	5.74	-.08
46	7.80	116436	6.11	6.29	-2.85
47	8.46	117531	6.17	6.84	-9.89
48	9.07	122132	6.41	7.38	-13.16
49	9.61	139455	7.32	7.88	-7.15
50	8.99	136481	7.16	7.31	-2.02
51	9.08	147576	7.74	7.39	4.71
52	.12	45961	2.41	3.23	-25.37
53	.35	61583	3.23	3.56	-9.26
54	.80	68373	3.59	3.94	-8.87
55	.65	74689	3.92	3.83	2.23
56	1.00	85429	4.48	4.06	10.30
57	2.74	90277	4.74	4.78	-.85
58	2.30	94335	4.95	4.63	6.89
59	3.47	100134	5.25	4.99	5.30
60	4.34	105119	5.51	5.21	5.84
61	3.87	112486	5.90	5.09	15.85
62	6.84	112161	5.88	5.73	2.74
63	7.69	121081	6.35	6.19	2.61
64	7.83	117856	6.18	6.31	-2.04

LOG STANDARD ERROR = .027049

Fig. F.7 : Energy Gradient Calculations - C_v = 17,71% - BBTV Rheology

KAOLIN Cv = 17.71 %
Ty = 60.00 Pa
K = 49.0000
n = .1400
V crit = 7.00 (SMALL TUBE)
V crit = 6.00 (LARGE TUBE)

No	V [m/s]	p [Pa]	imo [m/m]	imc [m/m]	% Error
1	.13	47603	1.22	2.02	-39.41
2	2.00	65143	1.67	2.57	-34.73
3	.75	56819	1.46	2.34	-37.70
4	.96	58949	1.52	2.40	-36.75
5	.98	59926	1.54	2.40	-35.87
6	1.85	63935	1.64	2.55	-35.49
7	2.50	66553	1.71	2.62	-34.73
8	2.95	68654	1.77	2.66	-33.72
9	3.34	70089	1.80	2.70	-33.15
10	.37	49082	1.26	2.20	-42.71
11	.52	54644	1.40	2.27	-38.07
12	.74	56982	1.46	2.34	-37.39
13	1.09	61287	1.58	2.43	-35.05
14	1.60	66272	1.70	2.51	-32.20
15	3.02	69527	1.79	2.67	-33.02
16	3.66	70851	1.82	2.72	-33.01
17	4.84	75751	1.95	2.79	-30.29
18	5.08	77957	2.00	2.81	-28.61
19	6.05	80059	2.06	1.57	31.31
20	6.29	82589	2.12	1.59	33.23
21	7.22	86458	2.22	1.70	31.08
22	7.79	89256	2.29	1.76	30.28
23	8.59	109671	2.82	1.86	51.92
24	3.95	71967	1.85	2.74	-32.45
25	.14	61523	3.23	5.15	-37.38
26	.49	70991	3.72	5.77	-35.42
27	.97	78099	4.10	6.15	-33.38
28	1.71	85577	4.49	6.49	-30.85
29	1.83	84438	4.43	6.54	-32.25
30	2.50	92205	4.84	6.74	-28.24
31	2.93	90903	4.77	6.85	-30.35
32	3.67	101066	5.30	7.00	-24.29
33	4.35	98699	5.18	7.12	-27.31
34	5.72	110815	5.81	7.33	-20.63
35	6.62	105312	5.53	7.44	-25.69
36	1.26	82678	4.34	6.31	-31.21
37	1.31	78136	4.10	6.33	-35.23
38	2.08	86702	4.55	6.62	-31.30
39	2.84	90859	4.77	6.83	-30.16
40	3.59	96913	5.08	6.99	-27.24
41	4.42	98048	5.14	7.14	-27.92
42	5.09	105696	5.55	7.24	-23.39
43	6.38	106584	5.59	7.41	-24.51
44	5.93	109483	5.74	7.35	-21.88
45	6.89	109262	5.73	7.47	-23.22
46	7.80	116436	6.11	4.40	38.89
47	8.46	117531	6.17	4.59	34.23
48	9.07	122132	6.41	4.78	34.08
49	9.61	139455	7.32	4.95	47.82
50	8.99	136481	7.16	4.75	50.60
51	9.08	147576	7.74	4.78	61.83
52	.12	45961	2.41	5.10	-52.76
53	.35	61583	3.23	5.59	-42.20
54	.80	68373	3.59	6.04	-40.57
55	.65	74689	3.92	5.92	-33.83
56	1.00	85429	4.48	6.17	-27.35
57	2.74	90277	4.74	6.80	-30.38
58	2.30	94335	4.95	6.69	-25.97
59	3.47	100134	5.25	6.96	-24.57
60	4.34	105119	5.51	7.12	-22.58
61	3.87	112486	5.90	7.04	-16.18
62	6.84	112161	5.88	7.46	-21.13
63	7.69	121081	6.35	4.36	45.58
64	7.83	117856	6.18	4.41	40.31

LOG STANDARD ERROR = .168829

Fig. F.8 : Energy Gradient Calculations - C_v = 17,71% -

Rotary Viscometer Rheology

Slurry 1 Cv = 22.47 %
Ty = 17.00 Pa
K = .1800
n = .7400
V crit = 5.40 (SMALL TUBE)
V crit = 3.90 (LARGE TUBE)

No	V [m/s]	p [Pa]	imo [m/m]	imc [m/m]	% Error
1	.14	16833	.88	.78	13.82
2	.29	19540	1.03	.90	13.35
3	.72	24436	1.28	1.17	9.33
4	.97	29141	1.53	1.31	16.99
5	1.75	33579	1.76	1.66	5.86
6	2.07	38668	2.03	1.80	12.63
7	2.93	42381	2.22	2.13	4.19
8	3.36	47544	2.49	2.29	8.76
9	4.23	51686	2.71	2.60	4.49
10	5.17	61035	3.20	2.90	10.25
11	6.01	77352	4.06	6.13	-33.82
12	5.99	77175	4.05	6.10	-33.64
13	5.70	96199	5.05	5.67	-11.04
14	6.56	95163	4.99	6.98	-28.50
15	5.53	127724	6.70	5.41	23.75
16	.14	32292	.84	.78	7.12
17	.53	42055	1.09	1.07	2.15
18	1.02	51183	1.32	1.33	-.43
19	1.81	65015	1.68	1.69	-.63
20	2.23	71494	1.85	1.86	-.79
21	3.03	83669	2.16	2.17	-.34
22	3.44	89808	2.32	2.32	.09
23	4.52	106584	2.76	2.69	2.33
24	5.03	115208	2.98	2.86	4.21
25	6.11	130061	3.36	6.28	-46.45
26	5.79	145047	3.75	5.81	-35.37
27	5.26	173450	4.49	2.93	52.99

28	6.71	190374	4.93	7.22	-31.82
29	5.92	221232	5.72	5.99	-4.43
30	6.39	264991	6.86	6.72	2.08
31	6.05	295821	7.65	6.20	23.46
32	.10	10777	.28	.28	-.80
33	2.72	22291	.57	.59	-2.75
34	2.59	21721	.56	.58	-3.48
35	3.39	24540	.63	.65	-2.30
36	3.62	25723	.66	.66	-.40
37	4.21	27839	.72	1.23	-41.94
38	4.65	33593	.86	1.42	-39.34
39	4.57	45310	1.16	1.39	-16.13
40	4.84	46952	1.21	1.51	-20.06
41	4.73	55784	1.43	1.46	-1.93
42	5.09	61745	1.59	1.63	-2.65
43	5.24	66583	1.71	1.70	.58
44	5.62	74216	1.91	1.89	1.02
45	5.11	62662	1.61	1.64	-1.64
46	6.43	85237	2.19	2.32	-5.38
47	5.24	68639	1.76	1.70	3.83
48	4.95	59733	1.54	1.56	-1.76
49	4.74	46434	1.19	1.46	-18.49
50	4.19	40354	1.04	1.23	-15.52
51	4.56	31197	.80	1.38	-42.07
52	4.47	45184	1.16	1.35	-13.75
53	4.21	27380	.70	1.24	-43.08
54	3.48	24377	.63	.65	-3.96
55	3.30	23460	.60	.64	-5.43
56	2.35	19481	.50	.56	-10.08
57	1.73	16359	.42	.50	-15.60
58	1.46	15309	.39	.47	-16.53
59	.80	12898	.33	.40	-16.34
60	.37	10679	.27	.33	-17.85

61	.23	9998	.26	.31	-16.71
62	.16	9643	.25	.29	-15.77

LOG STANDARD ERROR = .098367

Fig. F.9 : Energy Gradient Calculations - Uranium Tailings - Slurry 1 - BBTV Rheology

61	.23	9998	.26	.24	6.88
62	.16	9643	.25	.22	11.79

LOG STANDARD ERROR = .110872

Slurry 1 Cv = 22.47 %
Ty = 8.00 Pa
K = 1.0600
n = .5000
V crit = 5.40 (SMALL TUBE)
V crit = 3.90 (LARGE TUBE)

No	V [m/s]	p [Pa]	imo [m/s]	imc [m/s]	% Error
1	.14	16833	.88	.63	40.89
2	.29	19540	1.03	.78	31.90
3	.72	24436	1.28	1.05	22.00
4	.97	29141	1.53	1.17	30.27
5	1.75	33579	1.76	1.47	19.82
6	2.07	38668	2.03	1.58	28.78
7	2.93	42381	2.22	1.82	22.49
8	3.36	47544	2.49	1.92	29.64
9	4.23	51686	2.71	2.12	27.85
10	5.17	61035	3.20	2.31	38.43
11	6.01	77352	4.06	4.08	-.52
12	5.99	77175	4.05	4.06	-.30
13	5.70	96199	5.05	3.80	32.83
14	6.56	95163	4.99	4.60	8.65
15	5.53	127724	6.70	3.64	84.05
16	.14	32292	.84	.63	32.23
17	.53	42055	1.09	.95	14.96
18	1.02	51183	1.32	1.19	10.90
19	1.81	65015	1.68	1.49	12.70
20	2.23	71494	1.85	1.62	14.01
21	3.03	83669	2.16	1.84	17.55
22	3.44	89808	2.32	1.94	19.61
23	4.52	106584	2.76	2.18	26.27
24	5.03	115208	2.98	2.29	30.37
25	6.11	130061	3.36	4.17	-19.34
26	5.79	145047	3.75	3.88	-3.31
27	5.26	173450	4.49	2.33	92.56
28	6.71	190374	4.93	4.74	3.88
29	5.92	221232	5.72	3.99	43.37
30	6.39	264991	6.86	4.43	54.62
31	6.05	295821	7.65	4.12	85.75
32	.10	10777	.28	.20	37.67
33	2.72	22291	.57	.53	8.48
34	2.59	21721	.56	.52	7.59
35	3.39	24540	.63	.58	9.64
36	3.62	25723	.66	.59	12.05
37	4.21	27839	.72	.90	-20.72
38	4.65	33593	.86	1.03	-16.18
39	4.57	45310	1.16	1.01	15.66
40	4.84	46952	1.21	1.09	11.02
41	4.73	55784	1.43	1.06	35.83
42	5.09	61745	1.59	1.17	36.06
43	5.24	66583	1.71	1.21	41.07
44	5.62	74216	1.91	1.34	42.92
45	5.11	62662	1.61	1.17	37.51
46	6.43	85237	2.19	1.61	36.12
47	5.24	68639	1.76	1.21	45.62
48	4.95	59733	1.54	1.12	36.81
49	4.74	46434	1.19	1.06	12.90
50	4.19	40354	1.04	.90	15.33
51	4.56	31197	.80	1.00	-20.13
52	4.47	45184	1.16	.98	18.64
53	4.21	27380	.70	.91	-22.25
54	3.48	24377	.63	.58	7.87
55	3.30	23460	.60	.57	6.02
56	2.35	19481	.50	.50	.13
57	1.73	16359	.42	.45	-5.84
58	1.46	15309	.39	.42	-6.52
59	.80	12898	.33	.34	-3.59
60	.37	10679	.27	.27	.72

Fig. F.10 : Energy Gradient Calculations - Uranium Tailings - Slurry 1 - Rotary Viscometer Rheology

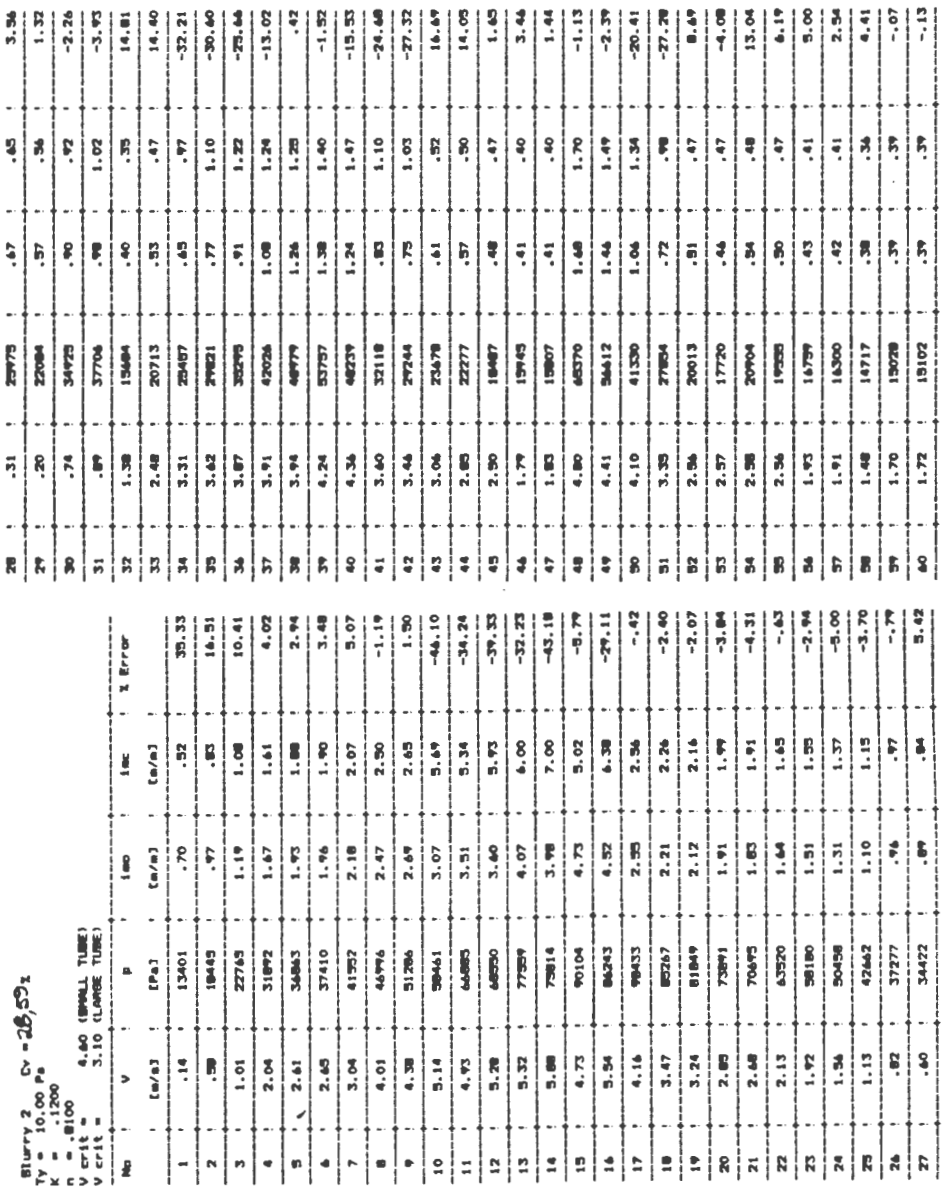

Slurry 2 Cv = 28.5%
Ty = 10.00 Pa
K = .1200
n = .8100
V crit = 4.60 (SMALL TUBE)
V crit = 3.10 (LARGE TUBE)

No	V [m/s]	p [Pa]	imo [m/s]	imc [m/s]	% Error
1	.14	13401	.70	.52	35.33
2	.58	19445	.97	.83	16.51
3	1.01	22765	1.19	1.08	10.41
4	2.04	31892	1.67	1.61	4.02
5	2.61	34883	1.93	1.88	2.94
6	2.65	37410	1.96	1.90	3.48
7	3.04	41557	2.18	2.07	5.07
8	4.01	46996	2.47	2.50	-1.19
9	4.38	51286	2.69	2.65	1.50
10	5.14	59461	3.07	5.69	-46.10
11	4.93	66885	3.51	5.34	-34.24
12	5.28	68550	3.60	5.93	-39.33
13	5.32	77529	4.07	6.00	-32.23
14	5.88	73814	3.98	7.00	-43.18
15	4.73	90104	4.73	5.02	-5.79
16	5.54	86243	4.52	6.38	-29.11
17	4.16	98433	2.93	2.96	-.42
18	3.47	85267	2.21	2.26	-2.40
19	3.24	81849	2.12	2.16	-2.07
20	2.85	73891	1.91	1.99	-3.84
21	2.68	70695	1.83	1.91	-4.31
22	2.13	63520	1.64	1.65	-.63
23	1.92	58180	1.51	1.55	-2.94
24	1.94	50458	1.51	1.57	-5.00
25	1.13	42662	1.10	1.15	-3.70
26	.82	37277	.96	.97	-.79
27	.60	34422	.89	.84	5.42
28	.31	25975	.67	.65	3.56
29	.20	22684	.57	.56	1.32
30	.74	34928	.90	.92	-2.26
31	.89	37706	.98	1.02	-3.93
32	1.38	15684	.40	.35	14.81
33	2.48	20713	.53	.47	14.40
34	3.31	25467	.65	.97	-32.21
35	3.62	29821	.77	1.10	-30.40
36	3.87	35295	.91	1.22	-25.44
37	3.91	42026	1.08	1.24	-13.02
38	3.94	48779	1.26	1.23	.42
39	4.24	53757	1.38	1.40	-1.52
40	4.36	48239	1.24	1.47	-15.53
41	3.60	32118	.83	1.10	-24.48
42	3.46	29244	.75	1.03	-27.32
43	3.06	23478	.61	.52	16.69
44	2.85	22277	.57	.50	14.05
45	2.50	18487	.48	.47	1.65
46	1.79	15945	.41	.40	3.46
47	1.83	15807	.41	.40	1.44
48	1.80	16370	1.48	1.70	-1.13
49	4.41	36412	1.44	1.49	-2.39
50	4.10	41330	1.06	1.34	-20.41
51	3.35	27854	.72	.98	-27.28
52	2.56	20013	.51	.47	8.69
53	2.57	17720	.46	.47	-4.08
54	2.58	20704	.54	.48	13.04
55	2.56	19333	.50	.47	6.19
56	1.93	16759	.43	.41	5.00
57	1.91	16300	.42	.41	2.54
58	1.48	14717	.38	.36	4.41
59	1.70	15028	.39	.39	-.07
60	1.72	15102	.39	.39	-.13
61	1.49	16044	.34	.36	-.41
62	.93	11773	.30	.30	1.26
63	.96	11581	.30	.30	-1.81
64	5.02	67603	1.74	1.83	-4.85
65	3.80	41301	1.06	1.19	-10.67
66	4.36	26226	.67	1.47	-54.02
67	3.01	21167	.54	.52	5.32
68	2.13	16625	.43	.43	-.92
69	1.27	12794	.33	.34	-2.98
70	1.75	14983	.39	.39	-1.62
71	1.21	12291	.32	.33	-5.05
72	.77	10412	.27	.28	-4.30
73	1.26	12868	.33	.34	-2.02
74	.91	9436	.24	.24	-.57
75	.23	7749	.20	.20	-1.12
76	.13	6877	.18	.18	-2.04
77	.97	11448	.29	.30	-3.42
78	.25	7698	.19	.20	-5.35
79	.39	8804	.22	.23	-3.83

LOG STANDARD ERROR = .082896

Fig. F.11 : Energy Gradient Calculations - Uranium Tailings - Slurry 2 - BBTV Rheology

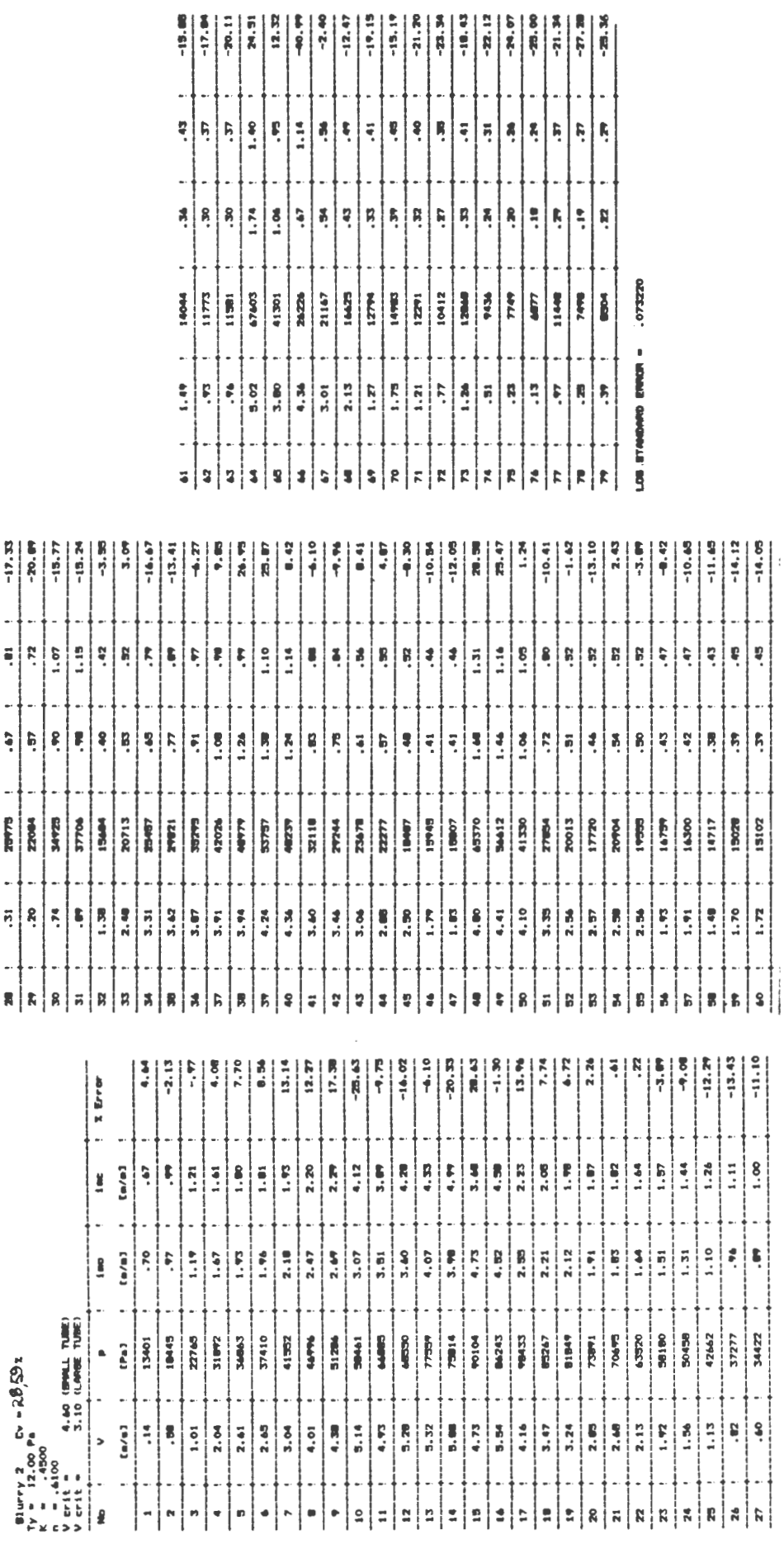

Slurry 2 Cv = 20.59%
Ty = 12.00 Pa
K = .4500
n = .4100
γ crit = 4.40 (SMALL TUBE)
γ crit = 3.10 (LARGE TUBE)

No	γ (s/s)	τ (Pa)	τ(s/s)	inc	τ(s/s)	% Error
1	.14	13401	.70	.67		4.64
2	.58	18445	.97	.99		-2.13
3	1.01	22765	1.19	1.21		-.97
4	2.04	31892	1.67	1.61		4.08
5	2.61	34863	1.93	1.80		7.70
6	2.85	37410	1.96	1.81		8.56
7	3.04	41552	2.18	1.93		13.14
8	4.01	44996	2.47	2.20		12.27
9	4.38	51286	2.69	2.29		17.38
10	5.14	58461	3.07	4.12		-25.43
11	4.93	64885	3.51	3.89		-9.73
12	5.28	68330	3.60	4.28		-16.02
13	5.32	77359	4.07	4.33		-6.10
14	5.88	75814	3.98	4.99		-20.33
15	4.73	90104	4.73	3.68		28.63
16	5.54	84243	4.52	4.58		-1.30
17	4.16	98433	2.35	2.23		13.96
18	3.47	85267	2.21	2.05		7.74
19	3.24	81849	2.12	1.98		6.72
20	2.85	73891	1.91	1.87		2.26
21	2.68	70695	1.83	1.82		.61
22	2.13	63520	1.64	1.64		.22
23	1.92	58180	1.51	1.57		-3.89
24	1.56	50458	1.31	1.44		-9.08
25	1.13	42662	1.10	1.26		-12.29
26	.82	37277	.96	1.11		-13.43
27	.60	34422	.89	1.00		-11.10

28	.31	29773	.67	.81	-17.33				
29	.20	22084	.57	.72	-20.69				
30	.74	34723	.90	1.07	-15.77				
31	.89	37706	.98	1.15	-15.24				
32	1.38	15484	.40	.42	-3.55				
33	2.48	20713	.53	.52	3.09				
34	3.31	25467	.65	.79	-16.67				
35	3.62	29821	.77	.89	-13.41				
36	3.87	35279	.91	.97	-6.27				
37	3.91	42026	1.08	.98	9.85				
38	3.94	48779	1.26	.99	26.93				
39	4.24	53757	1.38	1.10	25.87				
40	4.36	48239	1.24	1.14	8.42				
41	3.60	32118	.83	.88	-6.10				
42	3.46	29244	.75	.84	-9.96				
43	3.06	25678	.61	.56	8.41				
44	2.88	22277	.57	.55	4.87				
45	2.50	18987	.48	.52	-8.30				
46	1.79	15948	.41	.46	-10.84				
47	1.83	15807	.41	.46	-12.05				
48	4.80	65370	1.68	1.31	28.58				
49	4.41	58412	1.46	1.16	25.47				
50	4.10	41330	1.06	1.05	1.24				
51	3.33	27854	.72	.80	-10.41				
52	2.56	20013	.51	.52	-1.62				
53	2.57	17720	.46	.52	-13.10				
54	2.38	20904	.54	.52	2.43				
55	2.56	19588	.50	.52	-3.89				
56	1.93	16739	.43	.47	-8.42				
57	1.91	16300	.42	.47	-10.65				
58	1.48	14717	.38	.43	-11.65				
59	1.70	15028	.39	.45	-14.12				
60	1.72	15102	.39	.45	-14.05				

61	1.49	14044	.36	.43	-15.88				
62	.93	11773	.30	.37	-17.84				
63	.96	11581	.30	.37	-20.11				
64	5.02	67603	1.74	1.40	24.31				
65	3.80	41301	1.06	.95	12.32				
66	4.36	26226	.67	1.14	-40.99				
67	3.01	21167	.54	.56	-2.40				
68	2.13	16625	.43	.49	-12.47				
69	1.27	12794	.33	.41	-19.15				
70	1.75	14983	.39	.45	-15.19				
71	1.21	12291	.32	.40	-21.20				
72	.77	10412	.27	.38	-23.34				
73	1.26	12868	.33	.41	-18.43				
74	.51	9436	.24	.31	-22.12				
75	.23	7749	.20	.26	-24.07				
76	.13	6877	.18	.24	-25.00				
77	.97	11448	.29	.37	-21.34				
78	.25	7498	.19	.27	-27.38				
79	.39	8804	.22	.29	-25.36				

LOG STANDARD ERROR = .073220

Fig. F.12 : Energy Gradient Calculations - Uranium Tailings - Slurry 2 - Rotary Viscometer Rheology